U. S. DEPARTMENT OF COMMERCE
W. Averell Harriman, Secretary
NATIONAL BUREAU OF STANDARDS
E. U. Condon, Director

DECEMBER 1947
VOLUME 39
NUMBER 6

JOURNAL OF RESEARCH

of the

NATIONAL BUREAU OF STANDARDS

Contents

RP		Page
1842.	Sorption of nitrogen and water vapor on textile fibers. John W. Rowen and R. L. Blaine. (Price 10 cents)	479
1843.	Sieve tests of metal powders. Rolla E. Pollard. (Price 15 cents)	487
1844.	Table and Mollier chart of the thermodynamic properties of 1, 3-butadiene. Cyril H. Meyers, Carl S. Cragoe, and Eugene F. Mueller. (Price 20 cents)	507
1845.	Heats, equilibrium constants, and free energies of formation of the alkylcyclopentanes and alkylcyclohexanes. John E. Kilpatrick, Helene G. Werner, Charles W. Beckett, Kenneth S. Pitzer, and Frederick D. Rossini. (Price 15 cents)	523
1846.	Factors affecting operation of apparatus for counting alpha particles in an ion counting chamber. F. J. Davis. (Price 10 cents)	545
1847.	A statistical analysis of some mechanical properties of manila rope. Sanford B. Newman and J. H. Curtiss. (Price 10 cents)	551
1848.	Voltage anomalies of the glass electrode and the chemical durability of the glass. Donald Hubbard and Gerald F. Rynders. (Price 10 cents)	561
1849.	Instability of simply supported square plate with reinforced circular hole in edge compression. Samuel Levy, Ruth M. Woolley, and Wilhelmina D. Kroll. (Price 10 cents)	571
	Index to volume 39 (July to December 1947, Research Papers RP1807 to RP1849).	579

For sale by the Superintendent of Documents, U. S. Government Printing Office, Washington 25, D. C. · Price 60 cents
$4.50 per year on subscription

UNITED STATES GOVERNMENT PRINTING OFFICE, WASHINGTON : 1947

Sorp

Ther
textile
the fi
evidenc
phenon
loss of
moistu
various
surface
recogni
science
the pro

Seve
terpret
materia
a phen
If one
phenon
area a
from 1
several
value
DeWitt
ments
this ra
than th
et al., v
cellulos

In or
ments
measur

[1] This pa
Eng. Chem
[2] Figures
paper.

U. S. Department of Commerce
National Bureau of Standards

Research Paper RP1842
Volume 39, December 1947

Part of the Journal of Research of the National Bureau of Standards

Sorption of Nitrogen and Water Vapor on Textile Fibers[1]

By John W. Rowen and R. L. Blaine

Measurements were made of the adsorption of nitrogen and water vapor on six purified textile fibers and titanium dioxide. It was found that all of the fibers had a relatively low capacity for the adsorption of nitrogen as compared with the capacity for the adsorption of water vapor. The surface area values ranged from 0.31 square meter per gram for nylon to 0.98 square meter per gram for viscose rayon. The values of the free surface energies of adsorption as calculated by the Gibbs adsorption equation were the same for wool, cotton, silk, and rayon fibers but differed for the two synthetic polymers, nylon and acetate rayon.

I. Introduction

There is evidence that surface characteristics of textile fibers have some effect on the properties of the finished-textile fabrics. Examples of such evidence of surface properties are apparent in the phenomenon of water-repellency [1, 2],[2] in the loss of light-reflectance [3] and in the difference in moisture-sorption capacities of fabrics [4, 5] after various treatments. Although the importance of surface characteristics and properties has long been recognized in the technology of colloids and other sciences, the relation of these surface properties to the properties of fabrics is not well understood.

Several workers [6, 7, 8, 9, 10, 11, 12] have interpreted the adsorption of water by some textile materials (such as cellulose, wool, nylon, etc.) as a phenomenon in multimolecular [13] adsorption. If one assumes that the adsorption is a multilayer phenomenon, one may calculate that the surface area accessible to the first layer is in the range from 100 to 200 m^2/g. This range of values is several orders of magnitude greater than the value (0.60 m^2/g) calculated by Emmett and DeWitt [14] from nitrogen adsorption measurements on paper cellulose. On the other hand, this range of values is not appreciably greater than the value (53.0 m^2/g) reported by Purves [9] et al., working with nitrogen on a swollen cotton cellulose.

In order to obtain reliable surface area measurements of textile materials it is necessary to measure the surface area under conditions ensuring true physical adsorption. Brunauer, Emmett, and Teller [13] and Harkins and Jura [15] have shown that the adsorption isotherms of nitrogen, at −195°C (the boiling point of nitrogen, at which temperature nitrogen is physically adsorbed on solids) may be used to calculate the true surface areas of a great many crystalline and amorphous materials.

Knowledge of the molecular area or surface area [16] is believed necessary in order to evaluate such properties as the free surface energy [17] of adsorption and the work of adhesion [18] between the liquid and the solid phase. It therefore seemed highly desirable that the surface areas of the more common textile fibers—cotton, wool, viscose, silk, nylon, and cellulose acetate—be measured. It also seemed desirable to obtain the water adsorption isotherms of the same samples used in the nitrogen adsorption experiments. The work presented in the paper represents a portion of the preliminary work of a larger program sponsored and supported by the Office of the Quartermaster General, War Department.[3] It is intended to provide comparative data on the adsorption of the two vapors on six different purified textile materials.

II. Materials and Their Preparation

Six purified textile fibers and a sample of titanium dioxide (anatase) were used in this study. The four fibers, cotton, wool, silk, and rayon are from the samples studied by Wiegerink [19]. The titanium dioxide was employed as a reference standard. The cotton was purified by extracting

[1] This paper will also appear in the December 1947 issue of the J. Ind. and Eng. Chem.

[2] Figures in brackets indicate the literature references at the end of this paper.

[3] Permission to publish this paper was granted by the Office of the Quartermaster General.

with alcohol for 8 hours and with ether for 8 hours, followed by four washings in distilled water at 50° to 60°C. The wool was also extracted with ether and alcohol until the extracting liquid was free of residue traces. The wool was then washed at 50° to 60°C in distilled water. The raw silk was degummed in soap solution and then extracted with alcohol and ether. It was then thoroughly washed in distilled water. The viscose rayon was washed four times in a 1-percent water solution of ammonia at 50° to 60°C and then washed four times with distilled water at the same temperature.

The sample of nylon used in this study was 40 denier, 13 filament yarn, having one-half turn per inch of Z twist. The sample was supplied by the E. I. duPont de Nemours Co. It was extracted for 6 hours with ethyl ether. This length of time proved sufficient for the complete removal of the 0.4 percent of oil base lubricant applied during spinning. The acetate rayon was 150 denier, 46 filament yarn having 2½ turns per inch and was supplied by the American Viscose Co. The sample was washed four times in distilled water at 50° and 60°C.

III. Test Methods

The sorption of water by the textiles was determined gravimetrically using an analytical balance in conjunction with the conditioning apparatus described by Carson and Worthington [20]. In this apparatus the partial pressure of the water is maintained by means of saturated salt solutions, and the samples may be weighed without removal from the conditioned atmosphere. The moisture vapor pressures were obtained from wet and dry bulb temperatures and also by means of a Dunmore [21] electric hygrometer. The dry weights of the 5-gram samples of yarn were obtained by placing them over phosphorous pentoxide until constant weight was obtained. This constant weight was attained in about 5 days. It was observed that no loss of weight occurred from the fifth to the thirtieth day. After this drying period, the fibers were in equilibrium with an atmosphere whose relative water vapor partial pressure was less than 0.01. After the dry equilibrium point had been attained, the moisture content of the sample was determined at a series of increasing relative water vapor pressures. The rate of change of weight was plotted against time at each partial pressure, and the equilibrium value, usually attained within 24 to 48 hours, was indicated by the rate curve.

The adsorption of nitrogen was determined by a method similar to the one used by Brunauer and Emmett [22]. The saturation vapor pressure of the nitrogen was determined by use of a vapor pressure thermometer using the purified gas employed for the adsorption experiment.

The low temperature adsorption tests were made on 20- to 50-gram samples of the fibers. The sample bulb was packed as tightly as possible for each determination to reduce the dead space correction. For the experiments reported in this article, the textile fibers were evacuated for 16 to 20 hours at room temperature (about 25° C) to a pressure of about 10^{-6} mm of Hg. Other preliminary tests were made in which the temperature of evacuation was higher and one experiment was made of the cotton-fiber surface available to oxygen. For the low temperature adsorption of TiO_2, the temperature of evacuation was 200° C. Helium was used in evaluating the dead space in the sample bulb.

IV. Results and Discussion

1. Adsorption Measurements

As shown in figures 1, 2, and 3, the adsorption isotherms of both water vapor and nitrogen were found to be sigmoid-shaped, corresponding to the type II of the five types classified by Brunauer [23]. This type of adsorption curve is characteristic of physical adsorption on rigid solids with pore diameters larger than the molecular diameters of the adsorbed molecules [24]. However, this type of adsorption curve also occurs with nonrigid solids in which the adsorption sites are not restricted to the surface.

It may be noted from figure 1 that the millimoles of water vapor and nitrogen adsorbed by the TiO_2 differ only by a small percentage [25]. This is true despite the fact that the nitrogen was adsorbed after thorough evacuation, whereas water vapor was adsorbed from mixtures in air after drying the sample over P_2O_5. On the other hand, comparing the adsorption isotherms of the textile fibers in figures 2 and 3, and the data in table 1 reveals that the order of magnitude of adsorption capacity of nitrogen and water vapor are not the

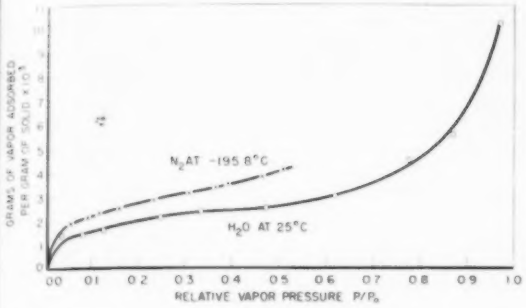

FIGURE 1.—*Adsorption isotherms of water and nitrogen on titanium dioxide.*

same. All the fibers had relatively low capacity for the adsorption of nitrogen as compared with the relatively high capacity for adsorption of water vapor.

The wool and viscose rayon fibers had slightly greater nitrogen adsorption capacities than silk and cotton, and the adsorption capacities of the acetate and nylon fibers were the lowest. In the adsorption of water vapor, the wool and viscose rayon fibers also had greater adsorption capacity

TABLE 1.—*Sorption of nitrogen and water vapors on textile fibers*

P/P_o	Wool	Viscose rayon	Silk	Cotton	Acetate	Nylon
MILLIMOLES OF WATER VAPOR (PER GRAM OF SOLID)						
0.034	1.3	1.2	0.7	0.7	.....	0.2
.081	1.9	1.8	1.1	1.1	.....	.4
.130	2.3	2.1	1.4	1.3	0.8	.6
.252	3.6	3.2	2.3	1.9	1.3	1.0
.335	4.6	4.0	2.9	2.4	1.7	1.3
.471	5.7	4.8	3.6	2.9	2.3	1.7
.620	7.1	6.2	4.6	3.7	3.2	2.1
.778	9.5	8.4	6.4	5.4	4.8	2.9
.866	11.6	10.8	8.3	6.4	6.0	3.5
.968	14.4	14.5	11.5	8.2	7.5	4.2
MILLIMOLES OF NITROGEN VAPOR×10³ (PER GRAM OF SOLID)						
0.05	1.1	1.4	0.7	0.8	0.3	0.3
.10	1.4	1.7	1.1	1.1	.4	.4
.15	1.7	2.0	1.4	1.3	.5	.5
.20	1.9	2.2	1.7	1.6	.6	.6
.25	2.2	2.5	2.0	1.8	.7	.7
.30	2.4	2.7	2.3	2.0	.8	.8
.35	2.7	2.9	2.7	2.3	.9	.9
.40	2.9	.....	2.9	2.6	1.1	1.1
.45	3.1	.....	3.6	.....	1.3	1.3
.50	3.4	.....	4.1	.....	1.4	1.4
.55	3.8	.....	4.6	.....	1.7	1.7

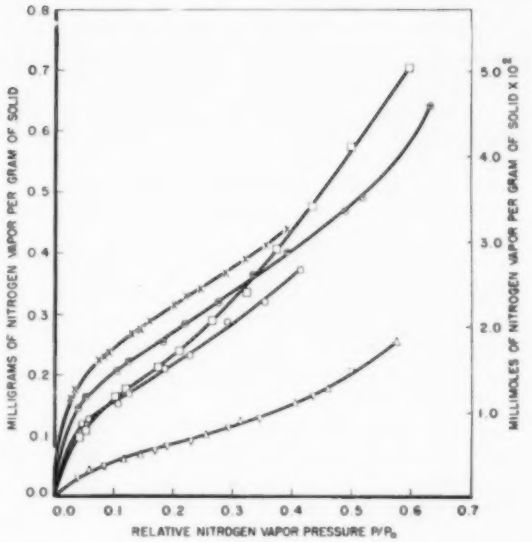
MILLIGRAMS OF NITROGEN VAPOR PER GRAM OF SOLID
MILLIMOLES OF NITROGEN VAPOR PER GRAM OF SOLID X 10³
RELATIVE NITROGEN VAPOR PRESSURE P/P₀

FIGURE 2.—*Adsorption isotherms of nitrogen on six textile fibers at −195° C.*

⊙, Wool; X, viscose; □, silk; ○, cotton; ▽, acetate; △, nylon.

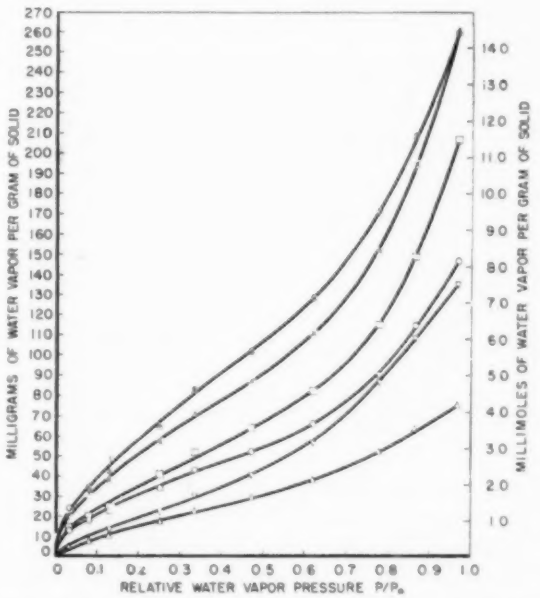
MILLIGRAMS OF WATER VAPOR PER GRAM OF SOLID
MILLIMOLES OF WATER VAPOR PER GRAM OF SOLID
RELATIVE WATER VAPOR PRESSURE P/P₀

FIGURE 3.—*Adsorption isotherms of water on six textile fibers at 25° C.*

⊙, Wool; X, viscose; □, silk; ○, cotton; ▽, acetate; △, nylon.

than silk and cotton, whereas the acetate and nylon also had the lowest capacities. There was, however, a certain lack of parallelism and shifting of relative position. Sufficient study has not been made to indicate the significance of these differences.

2. Calculated Quantities

(a) Surface Areas

The surface areas of the fibers available to the nitrogen vapor were calculated according to the BET equation [26], now commonly used for calculating the surface areas of solid materials. In evaluating the quantities of gas required for a monolayer on each of the textile fibers, the customary method of plotting P/V (P_0-P) versus P/P_0 was employed [26]. The plot is presented in figure 4. The calculated surface area values are presented in table 2. All of the surface areas were less than 1 m^2/g. The value obtained for cotton cellulose—0.72 m^2/g—compares favorably with the 0.60 m^2/g value reported by Emmett and DeWitt [14]. However, it differs markedly from the value of 53.0 [9] reported by Purves for a sample of swollen cotton cellulose. It is pointed out that the surface area available to the nitrogen vapor may be greatly dependent upon the source and treatment as the comparison with Purves' experimental value suggests. The surface area of cotton cellulose thus appears to vary from at least 0.60 to 53.0 m^2/g, depending upon its history. The value for cellulose of 0.60 m^2/g is only slightly larger than values (0.1—0.3 m^2/g) obtained by estimation of areas observed with the microscope and reported by Stamm and Millett [6] and Howell and Jackson [27]. It is likely, therefore, that the surface area, as determined with nitrogen, represents a lower limit.

TABLE 2.—*Surface areas of textile fibers*

Material	Area available to nitrogen molecule at −195° C (m^2/g)
Wool	0.96
Viscose rayon	.98
Silk	.76
Cotton	.72
Acetate rayon	.38
Nylon	.31
Titanium dioxide (TiO_2)	7.90

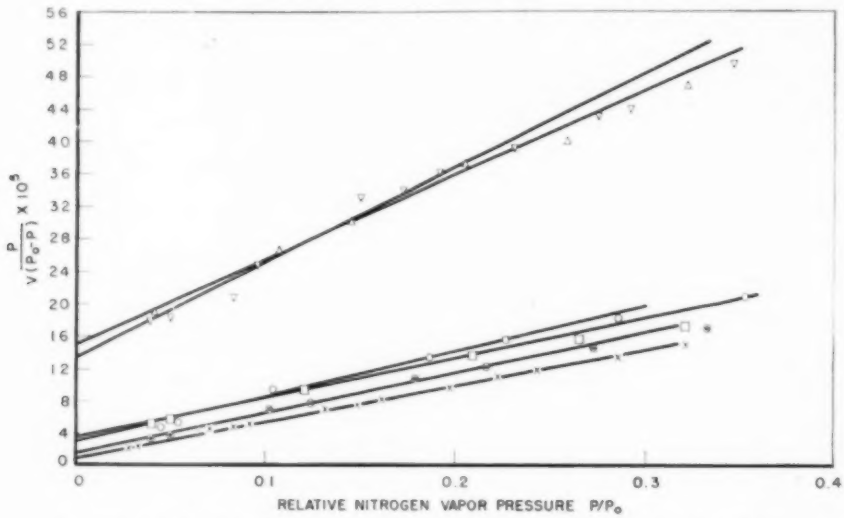

FIGURE 4.—*BET plots used for obtaining surface areas accessible to nitrogen.*

⊙, Wool; X, viscose; □, silk; ○, cotton; ▽, acetate; △, nylon.

In view of the large differences between the adsorption capacities observed in the water isotherm and the nitrogen isotherm, it was of interest to calculate the "water" areas of the same samples. This calculation was carried out

even though the authors were aware of the possibility that the data could be interpreted from another point of view. The plot of $P/V(P_0-P)$ versus P/P_0 is shown in figure 5, and the areas that may be calculated from them, by assuming all adsorbing sites were on a free surface, are tabulated in table 3. It may be noted in this table that the calculated surface areas of the

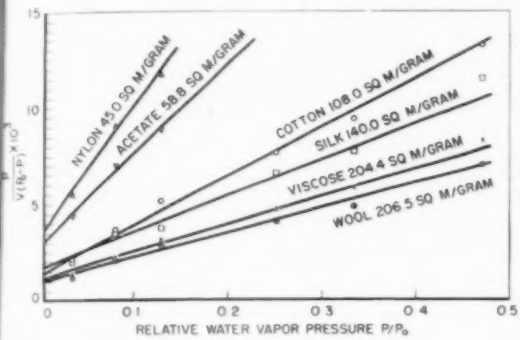
NYLON 45.0 SQ M/GRAM
ACETATE 58.8 SQ M/GRAM
COTTON 108.0 SQ M/GRAM
SILK 140.0 SQ M/GRAM
VISCOSE 204.4 SQ M/GRAM
WOOL 206.5 SQ M/GRAM
RELATIVE WATER VAPOR PRESSURE P/P₀

FIGURE 5.—*BET plots used for obtaining surface areas accessible to water vapor.*

textile fibers were from 150 to 200 times as great when determined by water adsorption as they were when determined by nitrogen adsorption.

TABLE 3.—*Calculated surface areas accessible to water vapor and nitrogen vapor*

Material	Area (I) available to water molecules at 25° C.	Area (II) available to nitrogen molecule at −195° C.	Ratio of area I to area II
	m^2/g	m^2/g	
Wool	206	0.96	215
Viscose rayon	204	.98	208
Silk	140	.76	184
Cotton	108	.72	150
Acetate rayon	58.8	.38	154
Nylon	45.0	.31	145
Titanium dioxide (TiO_2)	7.0	7.9	0.9

This apparent discrepancy may be explained in a number of ways:

1. The sites that adsorb water are not restricted to a free surface.

2. If the water adsorbing sites are restricted to a surface, there may be an additional internal surface specific to certain adsorbates as well as an external surface.

3. The internal surface within the fibrous structure exists only in the presence of a swelling agent such as water.

4. The smaller diameter and the polarity of the water molecule enables it to penetrate into capillaries not accessible to the nitrogen molecule.

Stamm and Millett [6], after a careful consideration of various adsorption data on cellulose (including selective adsorption from solution and heats of swelling) concluded that all the estimated values in the literature for the surface areas of cellulose fell into two groups. The first group was about 0.2 m^2/g—"the microscopically visible surface"—and the other group was about 300 m^2/g—"the surface of the transient capillary structure created within the cell walls by the swelling agents".

It is pointed out by the present authors that all four of the above factors may operate to account for the apparent discrepancy. There is insufficient evidence at present for evaluating the relative merit of the four hypotheses suggested above.

Plotting the nitrogen and water vapor adsorption data according to the method suggested by Harkins and Jura [28] resulted in a line or series of lines concave to the X axis rather than convex as usually found for other materials. In the two instances somewhat lower surface area values were obtained using this method of plotting.

(b) Free Energy of Adsorption

In view of the possibility that we are here dealing with an internal as well as an external surface, it seemed of interest to attempt to treat both systems as heterogeneous systems and to apply the relationship of J. Willard Gibbs [29]. This equation is applicable to interfaces between solid surfaces and vapors; it was written by Gibbs as follows:

$$\sigma=\epsilon_s-tn_s-\mu_1\Gamma_1-\mu_2\Gamma_2. \quad (1)$$

Where:

σ = the work spent in forming a square centimeter of clean new surface,
ϵ_s = surface total energy,
t = temperature
n = surface entropy,
μ_1 = chemical potential of the solid at boundary,
μ_2 = chemical potential of the vapor at boundary,

Γ_1 = surface concentration of the solid, and
Γ_2 = surface concentration of the vapor.

Under isothermal conditions [30] and under conditions in which Γ_1 is set at zero (by choosing the Gibbs boundary so that the surface concentration of the solid is zero) eq (1) reduces to:

$$d\sigma = -\Gamma_2 d\mu_2. \tag{2}$$

Under appropriate conditions $d\mu_2$ may be replaced by its equivalent $d\,(RT \ln P)$ where P is the vapor pressure, and we have:

$$d\sigma/d(RT \ln P) = -\Gamma_2, \tag{3}$$

or

$$\int_0^\sigma d\sigma = RT \int_0^P \Gamma_2 d \ln P, \tag{4}$$

and

$$\int_0^\sigma d\sigma = RT/MS \int_0^P q d \ln P. \tag{5}$$

Where Gibbs' surface concentration Γ_2 is expressed [32, 33] as the number of moles of vapor adsorbed per square centimeter:

$$\Gamma_2 = q/MS. \tag{6}$$

q = grams of absorbate,
M = its molecular weight, and
S = total surface area

As σ is the work required to form a square centimeter of surface, it is also the free surface energy, therefore, covering the surface with a vapor lowers the value of σ. This change of the free surface energy, which accompanies adsorption is referred to here as the free energy change of adsorption and designated ΔF as follows:

$$\Delta F = RT/MS \int_0^P q/p \, dp \tag{7}$$

The ΔF of eq (7) may be evaluated after experimental determination of S, q and P. The integral $\int q/p \, dp$ can be obtained by graphical integration. This is done by estimating the area under the curve that is obtained when one plots values of q/p vs P. Plots of the data of figures 2 and 3 in this manner are shown in figures 6 and 7. (See also [8]). As the plots do not lend themselves easily to extrapolation, the method used by Boyd and Livingston [32] was employed in obtaining the areas. The ΔF values thus obtained were in turn plotted against the relative vapor pressure, P/P_0, and the resulting curves are shown in figure 8.

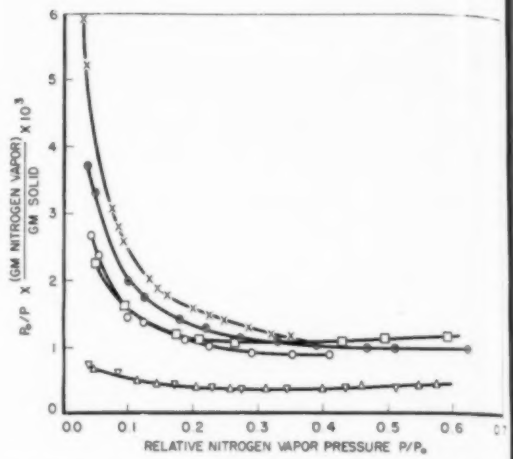

FIGURE 6.— *Plot of nitrogen adsorption data in accordance with a modified Gibbs equation.*

⊙, Wool; ×, viscose; □, silk; ○, cotton; ▽, acetate; △, nylon.

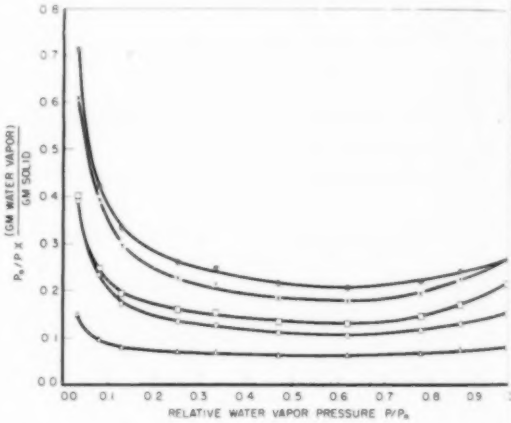

FIGURE 7.— *Plot of water adsorption data in accordance with a modified Gibbs equation.*

⊙, Wool; ×, viscose; □, silk; ○, cotton; △, nylon.

It is noted that the free energy of adsorption of water is the same at all relative vapor pressures for wool, silk, viscose, and cotton. The free energies of the two synthetic polymers, nylon, and acetate, did not fall on the common curve. As was the case in the surface area measurements, the free energy of adsorption of these two fibers was in a separate class (see table 4). With the

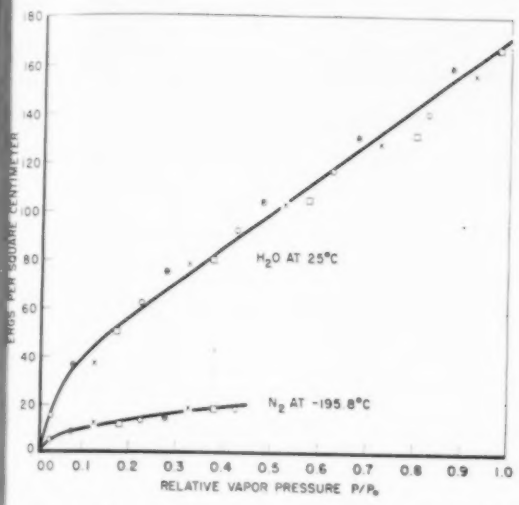

FIGURE 8.—*Free surface energy of adsorption as a function of relative vapor pressure.*

⊙, Wool; ×, viscose; □, silk; ○, cotton.

exception of nylon and cellulose acetate, whose fiber-water contact angles are greater than zero, the free energy of adsorption appears to be insensitive to the chemical nature of the adsorbent. It is possible that the bonding between the water and the four fibrous materials may be a hydrogen bond type. If such bonds existed in the four cases, the average value of a variety of hydrogen bond energies might very well be the same for the four materials.

TABLE 4.—*Free energy of adsorption of water and nitrogen on textile polymeric materials*

Material	Water		Nitrogen	
	P/P_0=0.40	P/P_0=1.0	P/P_0=0.40	P/P_0=1.0
	e/cm²	*e/cm²*	*e/cm²*	*e/cm²*
Wool	89	170	20	
Viscose rayon	89	170	20	
Silk	89	170	20	
Cotton	89	170	20	
Acetate rayon	114	247	14	
Nylon	113	223	12	

V. Summary

1. The sorption isotherms of water and nitrogen on six important textile materials have been determined.

2. The fiber surface areas available to the nitrogen have been computed with the aid of the theory of multilayer adsorption. The surface areas of the textile fibers were found to vary between 0.31 and 0.96 m^2/g. These values are of the same order of magnitude as the reported areas estimated with the aid of the microscope.

3. The water and nitrogen isotherms on samples of the same textile fibers showed marked differences in sorptive capacities.

4. The free energy of adsorption of nitrogen on the six fibrous materials have been calculated.

5. The implications of these calculations are discussed.

Acknowledgment is made for some of the laboratory measurements made by Lee A. Dunlap and H. J. Valis.

VI. References

[1] S. Baxter and A. B. D. Cassie, J. Textile Inst. **36,** 167 (1945).
[2] J. W. Rowen and D. Gagliardi, J. Research NBS **38,** 103 (1947). RP1762
[3] J. G. Wiegerink, J. Research NBS **25,** 435 (1940). RP1337.
[4] J. W. McBain, The sorption of gases and vapours by solids, (George Routledge & Sons, London, 1932).
[5] M. Harris, J. Research NBS **12,** 475 (1934) RP673; **23,** 299, (1939). RP1234
[6] A. J. Stamm and M. A. Millet, J. Phys. Chem. **45,** 43 (1941).
[7] J. D. Babbitt; Can. J. Research **20,** 143 (1942).
[8] H. B. Bull; J. Am. Chem. Soc. **66,** 1499 (1944).
[9] A. C. Assaf, P. H. Haas, and C. B. Purves, J. Am. Chem. Soc. **66,** 66 (1944).
[10] T. M. Shaw, J. Chem. Phys. **12,** 391 (1944).
[11] L. Pauling, J. Am. Chem. Soc. **67,** 555 (1945).
[12] G. Pickett, J. Am. Chem. Soc. **67,** 1958 (1945).
[13] S. Brunauer, P. H. Emmett, and E. Teller, J. Am. Chem. Soc. **60,** 309 (1938).
[14] P. H. Emmett and T. DeWitt, Ind. & Eng. Chem. Anal. Ed. **13,** No. 1, 28 (1941).
[15] W. D. Harkins and G. Jura, J. Am. Chem. Soc. **66,** 1366 (1944).
[16] G. E. Boyd, Surface chemistry, AAAS publication No. 21, 55 (Science Press Printing Co. 1943).
[17] D. H. Bangham, Trans. Farad. Soc. 33, part 1 and part 2 (1937).
[18] W. D. Harkins; Surface chemistry, AAAS publication No. 21, 55 (Science Press Printing Co. 1943).
[19] J. G. Wiegerink; J. Research NBS **24,** 645 (1940). RP1304
[20] NBS Circular C 453 (1946).
[21] Bulletin 2140, American Instrument Co., Silver Spring, Md. (April 1946).

[22] P. H. Emmett, A new method for measuring the surface areas of finely divided materials and for determining the size of particles. Symposium on New Methods for Particle Size Determination in the Subsieve Range, ASTM (1941).
[23] S. Brunauer, The adsorption of gases and vapors, p. 149 (Princeton Univ. Press, Princeton, N. J., 1943). Symposium on New Methods for Particle Size Determination in the Subsieve Range, ASTM (1941).
[24] P. H. Emmett and M. Cines, J. Am. Chem. Soc. **68,** 2535 (1946).
[25] P. H. Emmett, J. Am. Chem. Soc. **68,** 1784 (1946).
[26] S. Brunauer, The adsorption of gases and vapors (Princeton Univ. Press, Princeton, N. J., 1943).
[27] R. Howell and A. Jackson, J. Chem. Soc. (London) 979 (1937).
[28] W. D. Harkins and G. Jura, J. Am. Chem. Soc. **66,** 1366 (1944).
[29] J. W. Gibbs, Collected works **1,** 92 and 315 (Longmans, Green and Co., New York, N. Y. 1928).
[30] D. H. Bangham, Trans. Farad. Soc. **33,** part 1 (1937).
[31] D. H. Bangham and R. K. Razouk, Trans. Farad. Soc. **33,** part 2, 1463 (1937).
[32] G. E. Boyd and H. K. Livingston, J. Am. Chem. Soc. **64,** 2383 (1942).

WASHINGTON, June 17, 1947.

U. S. Department of Commerce
National Bureau of Standards

Research Paper RP1843
Volume 39, December 1947

Part of the Journal of Research of the National Bureau of Standards

Sieve Test of Metal Powders

By Rolla E. Pollard

Reproducible results were obtained in sieve tests of sponge iron, electrolytic iron, electrolytic copper, and nickel when certain variables affecting the sieving characteristics of the powders were eliminated or controlled. One of these was a cumulative sampling error resulting from repeated riffle cutting of limited powder supplies. Another was the effect of exposure of the powder to humid atmospheres. The effects of both variables were demonstrated in tests with sponge iron. Variations of considerable magnitude were observed when either variable was uncontrolled.

Significant variations also were noted when the same powders were sieved with different sets of certified sieves. These differences were reduced considerably in magnitude when comparisons were made on the basis of the size of the average opening as determined during the certification tests instead of the nominal sieve opening.

Development of more effective methods for controlling these variables or evaluating their effects would improve the reproducibility of sieve tests.

I. Introduction

In most arts and industries producing or using powdered material, close control of the size distribution of particles is necessary. Sieving is the most rapid and convenient method of size analysis, but it is limited to particles that are retained on a 325 mesh screen, having a nominal opening of 44 μ. Manufacturing difficulties have prevented production of sieves of smaller mesh, hence the size distribution of finer materials must be determined by other means.

Two standard sieve series, with specified dimensions and permissible variations, have been widely used in this country for many years. The Tyler Standard Scale introduced in 1910 is based on the size of the average opening, 0.0029 in., in 200 mesh wire cloth. The openings of the other sieves in the series vary by the fixed ratio of the square root of two. The U. S. Standard sieve series, proposed by the National Bureau of Standards in 1919, is based on a 1 mm (0.0394 in.) opening in the No. 18 sieve. In general, the sieve sizes vary in the same ratios as the Tyler Series and there is little difference between corresponding sieves. The U. S. Standard Sieve Series has been adopted by the U. S. Government [1],[1] by the National Bureau of Standards [2], by the American Society for Testing Materials [3], and by the American Standards Association [4]. A calibration service is available at the National Bureau of Standards where, for a small fee, sieves may be tested and, if acceptable, certified to conform to the requirements of these specifications.

Standard methods have been adopted by the American Society for Testing Materials and other technical organizations for sieve analyses of particular materials such as ores [4], refractories [5], fine and coarse aggregates [6], pigments [7], powdered coal [8], soap [9], cement [10], and roofing materials [11, 12]. Three of these specifications, namely those for powdered coal [8] and roofing materials [11] and [12] include criteria for the reproducibility of sieving tests by these standard methods. All three require that duplicate determinations by the same operator, using the same sieves, shall check within 1 percent of the total weight of the sample on all sieves. The standard method for coal [8] requires that duplicate determinations by different operators using different sieves shall check within 3 percent on the material sieved on the No. 200 sieve.

[1] Figures in brackets indicate the literature references at the end of this paper.

Tentative standard procedures for sieve analysis of granular metal powders have recently been proposed by the American Society for Testing Materials (B214–46T) and the Metal Powder Association (5–46T). Considerable information on sieving is available in the literature, but most of it is concerned with materials other than metal powders. Investigators generally agree that the sieving characteristics of different materials vary considerably. In particular, the rate of sieving, sharpness of separation, and average particle size of sieve fractions are influenced by the shape of the particles and their size distribution. The diversity of methods used in the manufacture of metal powders causes wide variations in particle shape and particle size distribution. Consequently different metal powders or powders of the same composition made by different processes, might be expected to display variations in sieving characteristics.

It is generally agreed that satisfactorily reproducible sieving results can be obtained for a given material when a single set of sieves and a standard method of testing are used. If the sieving conditions are not closely controlled, or if different sets of sieves are used, variations considerably greater than those cited as criteria for reproducibility may be obtained. For example, in cooperative tests of standard samples of cement, Wig and Pearson [13] found differences as high as 13 percent in the values reported from 80 different laboratories, all using standard sieves. Similar differences have been reported for cooperative tests of foundry sand [14], powdered coal [15] and road building materials [16]. Weber and Moran [21] in tests with granular and powdered sodium bicarbonate obtained differences of as much as 12 percent in sieving, values obtained with diffe- standard sieves in the same laboratory.

In beginning an investigation of the basic p- ciples of powder metallurgy at the Nati- Bureau of Standards, one of the first object- was to determine the effects of particle size d- tribution on the properties of metal powders a- the compacts made from them. In the proces- accumulating supplies of sieved fractions f- various powders for these studies, signific- variations in sieve analyses were noted w- samples of the same powder were sieved a- different times with the same sieves. Variati- of considerable magnitude also were obtai- when different sets of certified sieves were u- for the same powder.

Therefore, further study of the problems c- nected with the sieve analysis of these powd- seemed desirable. The results presented her- are those obtained in preliminary studies of t- effect of variation in sieving time, the reprodu- bility of sieve analyses and the particle size d- tribution within the sieve fractions.

II. Materials

The character and properties of metal powd- used in obtaining the data presented herein a- given in table 1. Four different methods of pr- duction are represented; reduction (iron), electr- ysis (iron and copper), pulverization (nickel), an- atomization (zinc, tin, and lead).

The size distribution of the sponge iron, electr- lytic iron, copper and nickel powders was fou- to be such that several fractions of substanti- size could be obtained by sieving. These powder-

TABLE 1.—*Properties of the metal powders*

Material	Method of production	Fineness (approximate)	Apparent density	Flow rate
			gm/cc	*sec*
Sponge iron	Reduced mill scale pulverized, screened and annealed.	32 to 40 percent through 325 mesh	2.51	
Electrolytic iron	Electrodeposit in sheet form pulverized, screened, annealed, and again screened.	37 to 46 percent through 325 mesh	2.28	
Electrolytic copper	Electrolytic "Grade B"	51 to 59 percent through 325 mesh	2.70	
Nickel	Mechanical pulverization	68 to 73 percent through 325 mesh	3.65	
Zinc	Atomization	99 percent through 325 mesh	2.02	No flo-
Tin	do	89 percent through 325 mesh	4.19	No flo-
Lead	do	84 percent through 325 mesh	5.61	No flo-

[a] Hall Standard Flowmeter—50-gram sample.

fore, were suitable for studies of the effect of ng time and the reproducibility of sieve yses. The atomized powders on hand at the were not suitable for such studies because the ders were extremely fine and sieving produced one or two small fractions. However, micro- ic measurements of accumulated fractions useful information on particle size distribu- within fractions.

Microscopic examination revealed that the nge iron, which had been prepared by reduc- of millscale, was composed of irregular plate- particles as shown in figure 1. The thickness these particles appeared to be considerably less an either of the other two dimensions as in- ated by the relatively small adjustment re- ired to change the focus from the top to the ttom of the particle. Many of the larger rticles consisted of several plates apparently ld together by oxide (fig. 2). The pearlite as frequently observed indicated the presence carbon in the metal.

The electrolytic iron was similar to the sponge iron in shape of particle and oxide content, but the plates were more distorted and there was no microscopic evidence of carbon in the iron (figs. 3 and 4).

The electrolytic copper powder was composed of two distinctly different types of particles. One was plate-like, and the other was irregular and tree-like in shape, as shown in figure 5, 6, and 7. Many of the spaces between the branches in the tree-like particles appeared to be filled with light blue or dark blue oxide.

The nickel particles (figs. 8, 9, and 10) were roughly rectangular or elliptical in shape. Plate-like particles were prevalent, and the larger particles often consisted of two or more plates apparently cemented by oxide.

The zinc, tin, and lead powders, produced by atomization were composed of globular particles, all dimensions being of the same order of magnitude. These particles appeared to be largely solid metal with little porosity and few inclusions (figs. 11 to 16, inclusive).

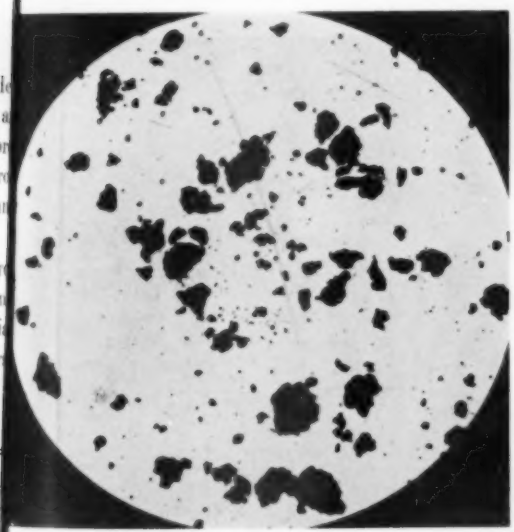

FIGURE 1.—*Sponge iron powder particles, as received.* ×50.

FIGURE 2.—*Areas of pearlite are visible in sections of sponge iron particles.*

Some particles appear to be composed of several plates cemented together with oxide. Etched with nital. ×500.

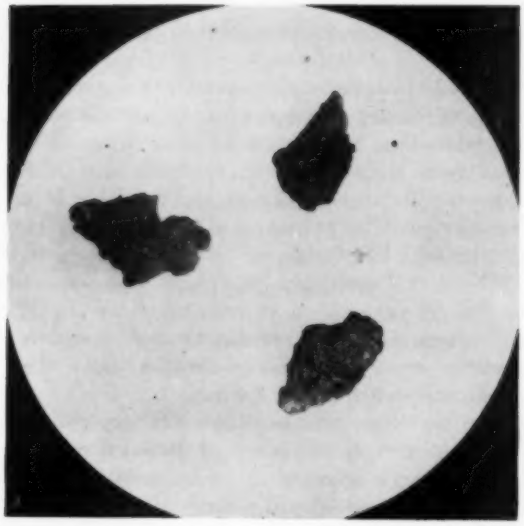

FIGURE 3.—*Electrolytic iron particles retained on 140 mesh sieve.* ×50.

FIGURE 5.—*Electrolytic copper particles retained on* [illegible] *mesh sieve.* ×50.

FIGURE 4.—*Sections of electrolytic iron particles which show distortion as a result of pulverization.*

Some particles consist of plates held together by oxide. Etched with nital. ×500

FIGURE 6.—*Sections of irregular, tree-like copper particles.*

Some of the spaces between branches apparently are filled with oxide. Etched with ammonium hydroxide and hydrogen peroxide. ×500.

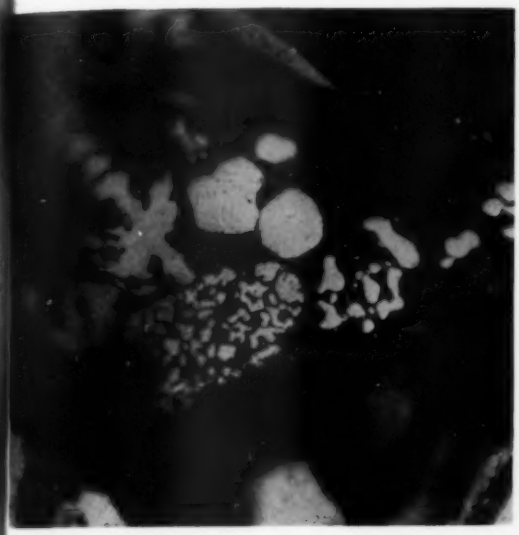

FIGURE 7.—*Spaces between branches of tree-like, electrolytic copper are filled with oxide.*

Same etchant as figure 6. ×500.

FIGURE 9.—*Sections of plate-like nickel particles.*

Some of the particles were distorted during pulverization and the interspaces apparently filled with oxide. Etched with nitric and acetic acids in acetone. ×500.

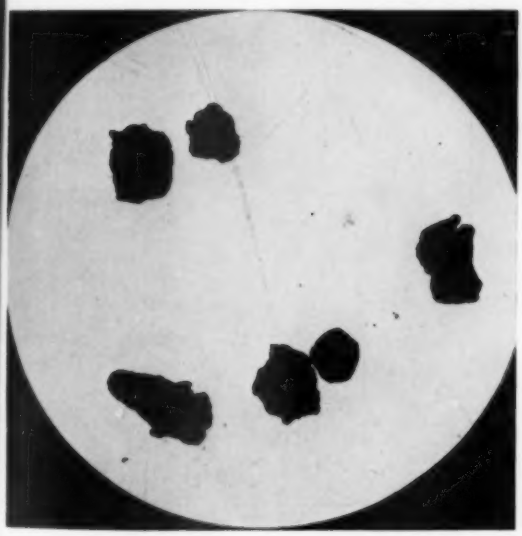

FIGURE 8.—*Nickel powder particles retained on 140 mesh sieve.* ×50.

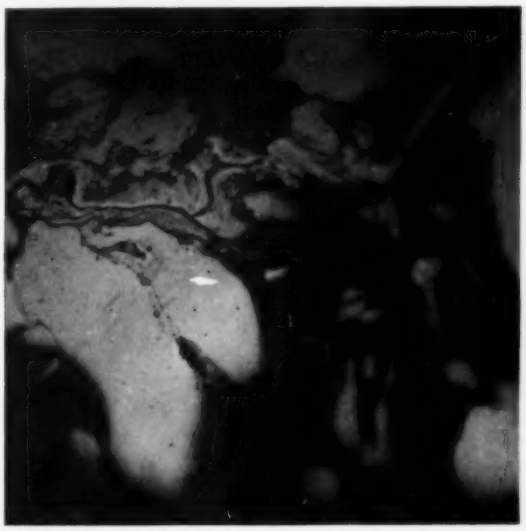

FIGURE 10.—*Section of nickel particle that apparently consists of several plates cemented together with oxide.*

Same etchant as figure 9. ×500.

which were selected from the following six sieves of the U. S. Standard Series:

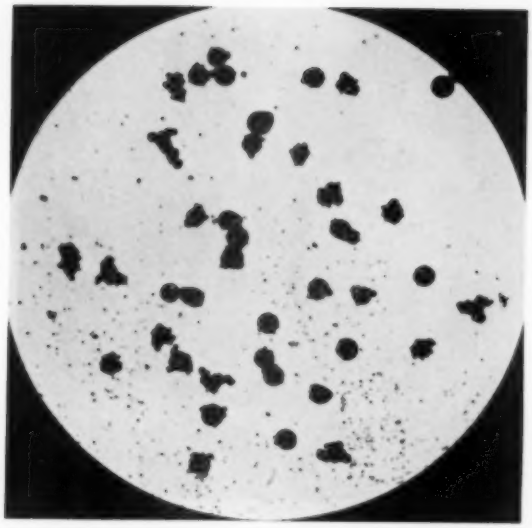

FIGURE 11.—*Particles of atomized zinc powder retained on 325 mesh sieve.* ×50.

FIGURE 12.—*Sections of globular zinc particles show few voids or inclusions.*

Etched with nitric acid in amyl alcohol. ×500.

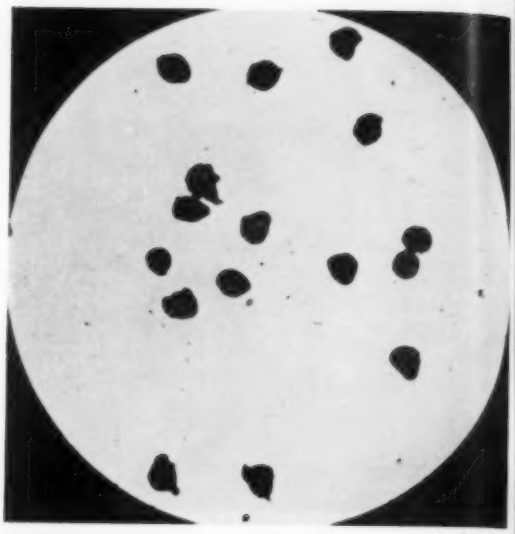

FIGURE 13. *Particles of atomized tin powder retained on 200 mesh sieve.* ×50.

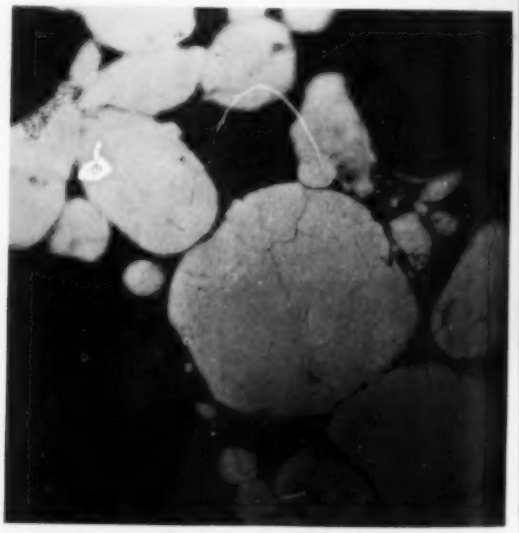

FIGURE 14. *The globular particles of tin contain few voids or inclusions.*

The sections were etched with nitric and acetic acids in glycerol. ×500.

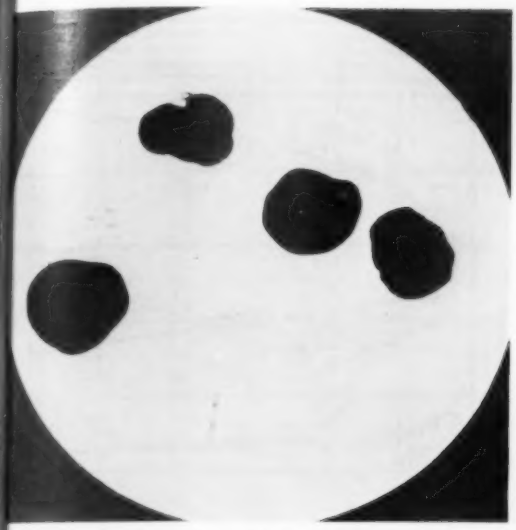

FIGURE 15. *Particles of atomized lead powder retained on 80 mesh sieve.* ×50.

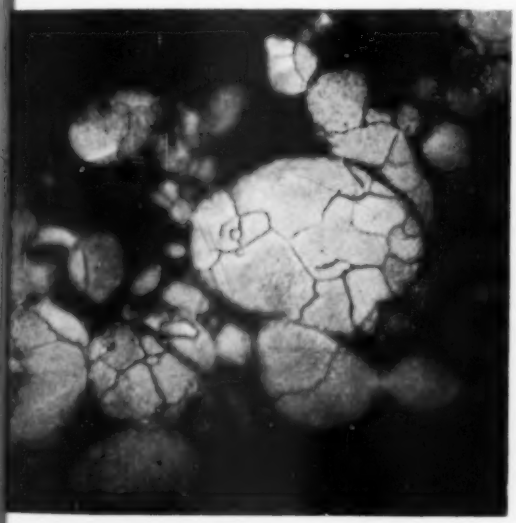

FIGURE 16. *Lead particles are roughly spherical with few voids or inclusions.*

Sections etched with nitric and acetic acids in glycerol. ×500.

III. Method of Testing

A Tyler RO-Tap shaker provided with an automatic time switch was used in making the sieve tests as specified in ASTM B–46T and MPA4–45T Standards. The machine was adjusted to accommodate a set of five tested sieves, which were selected from the following six sieves of the U. S. Standard Series:

Sieve No.	Average sieve opening	Permissible variation in average opening	Maximum permissible opening microns	Permissible dimension, which not more than 5 percent of the opening are permitted to exceed
	μ	μ±		
80	177	11	247	212
100	149	9	208	179
140	105	6	147	126
200	74	5	118	96
230	62	4	117	90
325	44	3	83.6	64

Two sets of sieves, designated as set I and set II were used for most of the tests. The No. 230 sieve was omitted from both of these sets. In later tests set No. III was used, which omitted the No. 80 but included a No. 230 sieve. All sieves were tested at the National Bureau of Standards and certified to conform to ASTM Specification E11–9 and Federal Specification RR–S366a.

The sieves were brushed with a stiff bristle brush after each test. At frequent intervals, for instance at the beginning of a series of tests or when a different material was to be sieved, the sieves were cleaned in hot soapy water with stiff bristle brushes, rinsed with alcohol and dried in an oven at 110° C.

The sampling procedure included the use of a riffle-type sample splitter, to reduce the entire supply of each metal powder (50 to 100 lb in most cases) to a "sample supply" that could be stored in one to five 1-pint Mason jars (3 to 15 lb). Smaller samples for individual tests were taken from these jars, after thorough shaking, by means of a curved spatula ("scoopula"), which reached to the bottom of the container.

IV. Time of Sieving

To determine the effect of shaking time on sieving, 25, 50, 100, and 150 gram samples of sponge iron powder (3 samples of each weight) were sieved for various periods of time, using Sieve set I. Two series of tests were made, one in March, the other in July 1946. The schedules of sieving time periods for both series are given in table 2.

To obtain information on possible differences caused by sampling, each of the three samples of

765484—47——2

TABLE 2.—*Schedules of sieving time for two series of sieve tests of sponge iron—Sieve Set I*

Weight of sample	Number of samples	Time of sieving and resieving
		SERIES I
g		*minutes*
25	3	10, 20, 30, 40, 10.
50	3	5, 10, 20, 30, 40, 60, 20.
100	3	5, 10, 20, 30, 40, 60, 80, 30.
150	3	5, 10, 20, 30, 40, 60, 80, 100, 40.
		SERIES II
25	3	5, 10, 20, 30, 40, 60, 80, 100, 120, 10.
50	3	5, 10, 20, 30, 40, 60, 80, 100, 120, 20.
100	3	5, 10, 20, 30, 40, 60, 80, 100, 120, 30.
150	3	5, 10, 20, 30, 40, 60, 80, 100, 120, 40.

each weight was resieved through the selected range of time periods. After each period the weighed sieve fractions were thoroughly mixed and resieved for the next time period. The total weight added to the top sieve at the beginning of each period was used in calculating the percentage by weight retained by the sieves during that period.

The last time period in each series of the schedule was selected as a duplication of one of the earlier periods for the purpose of determining to what extent disintegration of particles had occurred as a result of grinding or abrasion during prolonged sieving. The total time of sieving, including the last or duplicate periods ranged from 110 to 505 minutes.

The results of two series of sieve tests on sponge iron are shown in figures 17, 18, 19, and 20. The sieving rate was greatest during the initial period, decreased rapidly for periods up to 15 to 30 minutes, and then decreased slowly with continued sieving time. Appreciable amounts of material continued to pass through the sieves after sieving periods up to 120 minutes. It is evident, therefore, that for practical purposes at least, there is no definite time of sieving at which complete separation can be said to have occurred.

The period of high sieving rate or rapid change in weight distribution represents the time required for the definitely undersized particles to pass through the sieve openings. The period of slowly diminishing sieving rate represents the continued separation of the so-called "difficult" particles

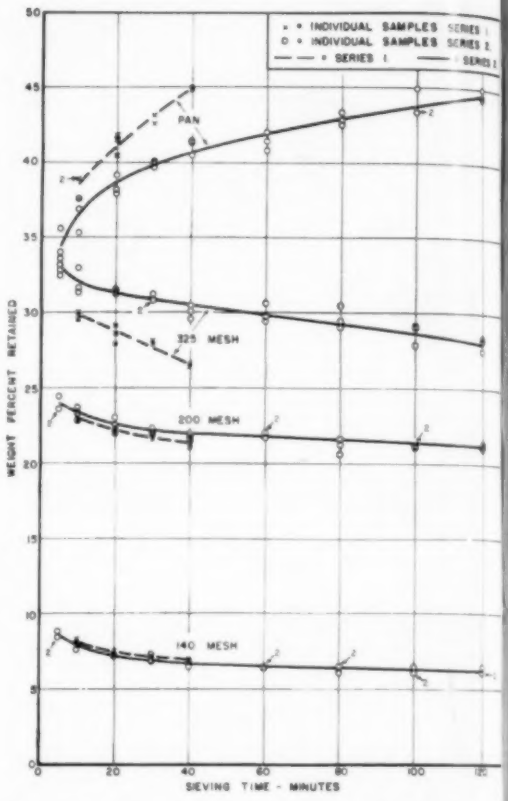

FIGURE 17.—*Sieve tests of 25-gram samples of sponge iron made at different times using sieving schedule given in table 2.*

Series I was made in March, Series II in July.

(particles whose controlling dimensions are close to those of the sieve openings or which, because of their shape, pass through the openings with difficulty) or the continued passage of large particles through oversize openings.

The values for the duplicate time periods, given in table 3, indicate that the continuous change in weight distribution during prolonged sieving was not caused by disintegration of the particles. The values agree within the range of difference between samples, although the sieving time between duplicate periods was as much as 45 minutes (see sieving schedule, table 2). Evidently disintegration of these sponge-iron particles as a result of grinding or abrasion, during prolonged sieving, is negligible.

The average total sieve losses during the sieving

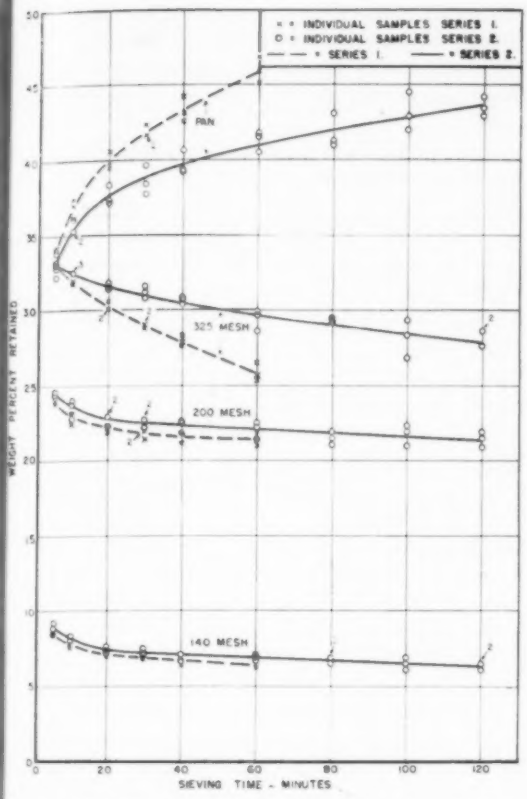

FIGURE 18.—*Sieve tests of 50-gram samples of sponge iron.*

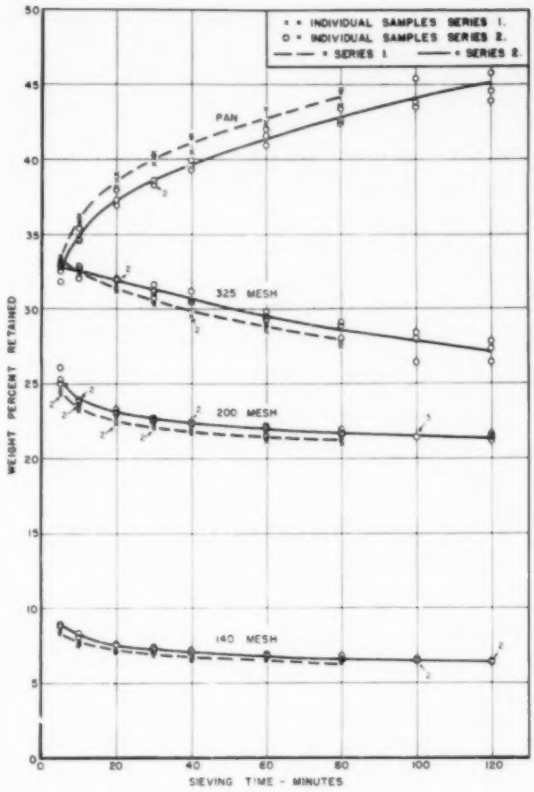

FIGURE 19.—*Sieve tests of 100-gram samples of sponge iron.*

schedules, for the 25, 50, 100, and 150 gram samples, respectively, were 1.0, 1.5, 1.2, and 1.0 percent for Series I and 2.0, 1.9, 1.3, and 0.8 for Series II. Each of these values represents the accumulative losses over as many as 10 different sieving periods, hence these losses are not considered to be excessive. As the total losses decreased appreciably with increase in weight of sample, particularly in Series II where the sieving schedules were approximately equal, they probably resulted from repeated handling rather than from formation of appreciable amounts of dust.

V. Reproducibility

The curves of figures 17, 18, 19, and 20, which represent the change in sieving rate with increasing sieving time are noticeably different for Series I and Series II. This difference is particularly marked for the pan fractions that are measures of the material passing all of the sieves. The difference between the pan fractions of the two series, therefore, represents the algebraic sum of the differences between the corresponding sieve fractions. The values for the corresponding samples of the two series fall into definitely separate groups after the initial 5-minute sieving period. With increased sieving time the mean values for the two series are separated by an amount greater than the difference between individual samples of either series.

The results obtained for Series I show differences between individual samples of the same weight, sieved for the same length of time, ranging from 0 to a maximum of 1.9 percent of the total weight of the sample. In Series II the differences between corresponding samples range from 0 to a maximum of 2.4 percent. The differences between the average values for the two series vary from 0 to a maximum of 4.6 percent. It should be noted that these differences are con-

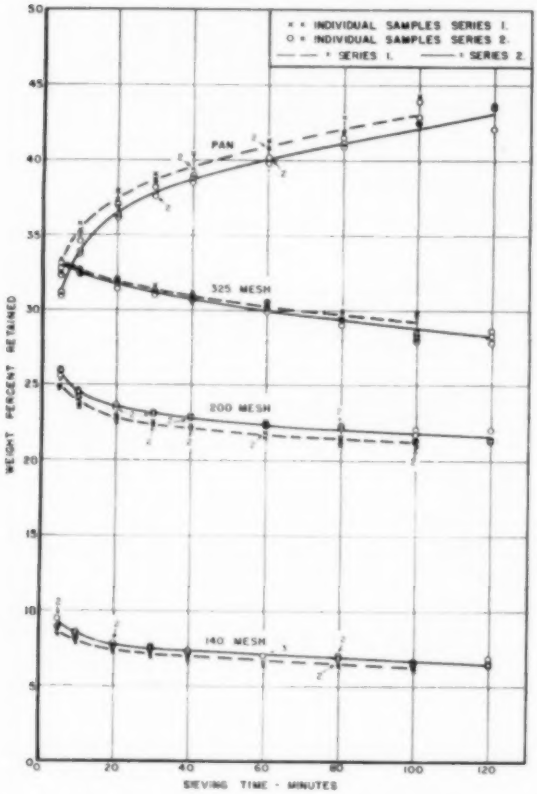

FIGURE 20.—*Sieve tests of 150-gram samples of sponge iron.*

sistently in the same direction. In other words, there is no overlapping of results between the two series, and the maximum scatter of corresponding values for both series considered together (5.3 percent) is more than twice as great as that of either series alone (1.9 to 2.4 percent).

The close grouping of the values for the samples of each series and the fact that smooth curves can be drawn through the points representing them indicate that testing conditions were relatively stable during each series of tests. The separation of the curves by an amount greater than the scatter between the samples indicates that testing conditions or the sieving characteristics of the powder were different for the two series. The differences between the corresponding fractions of the same series are comparatively small and can be attributed chiefly to the sampling error inherent in the method used in selecting the samples from the "sample supply". The differences between the two series are much greater in magnitude and are consistently in the same direction. It must be concluded, therefore, that they were caused by other uncontrolled variables.

One of these variables would be an additional sampling error resulting from the use of a sample splitter to cut the powder supply, originally 100 lb, to the two different "sample supplies" of 3 to 15 lb from which the samples for the two series were taken. This error, being produced by a mechanical operation, would be expected to be smaller than that resulting from the manual method used in selecting samples from the "sample supply".

Another possible variable is suggested by the different seasons of the year in which the tests were made, one in March, the other in July 1946. The physical condition or sieving characteristics of the powder may have been changed by exposure to different atmospheric conditions. A change in size distribution, for instance, could be produced under oxidizing or corrosive conditions such as would prevail with high humidities, by the formation of additional composite particles similar to those previously described as being composed of two or more smaller particles cemented together by oxide (see figs. 2, 4, 6, 9, and 10). Variations in humidity might also affect the sieving characteristics of the powder by changing the tendency of particles to agglomerate, or by modifying the static charges accumulated during handling or sieving.

To test the effect of these and other possible variables such as clogging of sieves or changes in sieve motion, additional sieve tests were made in November and December 1946, and January and February 1947. For these tests sieve set No. III was used.

A new hard maple plug was placed in the RO-Tap machine, and the sieve motion was checked at frequent intervals over the 4-month period by counting the number of hammer blows per minute. The rate of hammer blows was found to average 154 per minute with variations no greater than ± 1 blow per minute. This fixed the speed of rotary motion of the sieves at 289 ± 2 revolutions per minute.

Samples of sponge iron 25, 50, and 100 grams in weight, all taken from the same freshly riffle cut "sample supply", were sieves for periods of

TABLE 3.—*Effect of prolonged sieving of sponge iron*

[Samples were seived and resieved to schedules given in table 2, Sieve Set I]

Sieve No.	Weight percent retained															
	25-gram samples				50-gram samples				100-gram samples				150-gram samples			
	First 10-min period		Last 10-min period		First 20-min period		Last 20-min period		First 30-min period		Last 30-min period		First 40-min period		Last 40-min period	
	Mean 3 samples	Deviation from mean	Mean 3 samples	Deviation from mean	Mean 3 samples	Deviation from mean	Mean 3 samples	Deviation from mean	Mean 3 samples	Deviation from mean	Mean 3 samples	Deviation from mean	Mean 3 samples	Deviation from mean	Mean 3 samples	Deviation from mean
SERIES I																
80	Trace		Trace		Trace		Trace		Trace		Trace		Trace		Trace	
100	Trace		Trace		Trace		Trace		Trace		Trace		Trace		Trace	
140	8.1	±0.2	7.9	±0.1-0.2	7.1	±0.1	7.2	±0.1-0.3	6.9	±0.1	6.8	±0.1-0	6.9	+0.1-0.2	6.8	±0.2
200	23.0	+.4-0.2	22.8	+.1-.2	22.2	+.1-0.3	22.3	+.2-.3	22.1	±.1	22.0	±.4	22.2	±.1	21.8	±.2
325	29.8	+.2-.3	30.0	+.2-.3	30.2	+.4-.1	30.3	±.1	30.6	+.3-0.2	30.6	+.3-0.4	30.9	+.3-.5	30.8	+.4-0.7
Pan	38.5	+.4-.9	39.1	+.2-.3	40.0	+.6-.2	39.9	+.6-.4	40.1	+.3-.4	39.8	+.3-.4	39.7	+.7-.3	39.8	+.4-.2
SERIES II																
80	Trace		Trace		Trace		Trace		Trace		Trace		Trace		Trace	
100	Trace		Trace		Trace		Trace		Trace		Trace		Trace		Trace	
140	7.9	+0.1-0.3	7.9	+0.2-0.1	7.4	±0.2	7.5	±0.2	7.3	+0.1-0.2	7.2	0	7.2	+0.1-0	7.3	+0.3-0.2
200	23.3	+.4-.5	23.1	±.2	22.7	+.2-0.4	23.0	+.4-0.7	22.6	±.1	22.7	+0.3-0.6	22.8	+.1-0	22.4	+.4-.2
325	31.9	+1.0-.6	31.7	±.5	31.6	±.2	30.7	±.5	31.2	+.4-.5	29.8	+.2-.5	30.8	±.1	30.4	+.2-.3
Pan	36.6	+1.0-1.3	37.2	+.5-.4	37.7	+.7-.5	38.3	+.4-.6	38.4	+.2-.1	40.0	+.4-.5	38.8	+.2-0.3	39.5	+.6-.8

5, 10, 15, 20, 30, 40, and 60 minutes after the following treatments of the powder:

Series III—3 samples of each weight for each time period were oven dried for 1 hour at 110° C. prior to sieving.

Series IV—3 samples of each weight for each time period were exposed for 64 to 72 hours to a very humid atmosphere in a closed vessel (a desiccator) over water in which wicks were dipped to increase the evaporating surface.

Series V—The humidified samples of Series IV after sieving were mixed, dried for 5 hours at 110° C. and resieved.

The results are illustrated by the curves of figure 21, representing the pan fractions of the 100 gram samples. Similar results were obtained with the 25 and 50 gram samples. The value for the humidified samples, Series IV, are consistently lower than those of the dried material, Series III, by amounts corresponding to 3.5 to 6.5 percent of the original weight of the sample. Part of

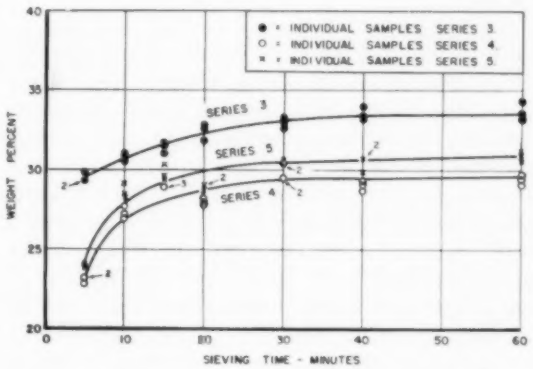

FIGURE 21.—*Three series of sieve tests of sponge iron made with 100-gram samples all from the same "sample supply" after the following treatments of the powder: Series III, dried; Series IV, humidified; Series V, samples of Series IV dried and resieved.*

this difference (approximately one-fourth) was recovered when the humidified samples were dried and resieved as shown by the position of the values for Series V. It will be noted that the values for individual samples of Series III are all quite close to the curve. The values for the

Series IV are more scattered, and the irregularities are matched by similar deviations in Series V.

The relative humidity in the humidification chamber undoubtedly was very high, probably saturated at times due to overnight or week-end changes in room temperature. Exposure to this atmosphere for 64 to 72 hours produced no change in the appearance of the powder except for a slight tendency to cake and to retain the shape of the dish in which the samples were contained. The gain in weight of the 100 gram samples, due largely to the presence of absorbed or condensed moisture, was 0.4 to 1.3 percent, average 0.8 percent. A large part of this weight increase was lost when the humidified samples were dried prior to resieving. The oxide content of the humidified samples after drying and resieving, as measured by the percentage loss in weight in hydrogen according to Metal Powder Association Tentative Standard 2–45T, was 1.2 percent. The hydrogen loss of samples taken from the original "sample supply" was 0.9 percent, indicating that the reducible oxide content of the powder was increased by 0.3 percent of the original weight of the sample during humidifying, sieving, drying and resieving.

All samples of the three series for each sieving period were taken from the same "sample supply" at the same time. The sieving for the three series was done concurrently, that is, all samples for each time period were sieved within the 72 to 96 hours required to humidify, sieve, dry, and resieve the samples of Series IV and V. These precautions eliminated the consideration of such variables, as the sampling error resulting from riffle splitting clogging of sieves or changes in sieve motion as major factors in causing the differences observed between the three series of tests. It must be concluded, therefore, that these differences resulted only from the exposure of the powder to a humid atmosphere.

Two additional series of sieve tests of sponge iron were made about 1 month after Series III, IV, and V were completed. The same sieves were used, but the samples, 25, 50, and 100 grams in weight, were taken from two different "sample supplies" riffle split within the same week. The samples were dried for 1 hour at 110° C and sieved for periods of 5, 10, 15, 20, 30, 40, and 60 minutes.

The pan fractions of the 100 gram samples are shown in figure 22 in comparison with those of

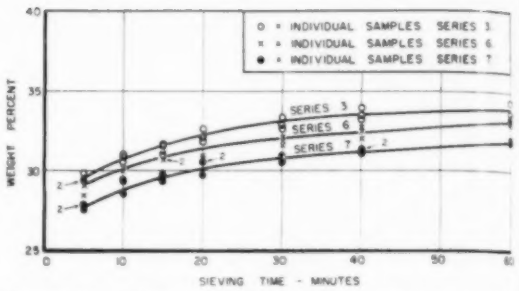

FIGURE 22.—*Three series of sieve tests of 100-gram samples taken from three different "sample supplies" riffle cut from the same lot of sponge iron powder in the order Series III, Series VI, Series VII.*

Series III. The difference between each succeeding series, in the order in which they were riffle-cut, amounts to about 1 percent of the original weight of the sample. The sampling, handling, and sieving for all of these tests were done in a heated laboratory during the winter months when the humidity was low and relatively constant. Changes in sieving characteristics resulting from exposure to such atmospheres should be small. It is believed, therefore, that the differences between Series III, VI, and VII resulted chiefly from sampling errors produced by repeated riffle cutting.

Variations similar to those obtained with sponge iron have been observed with electrolytic iron, electrolytic copper, and nickel in sieve tests made over extended periods of time. When a series of sieve tests of any of these powders was made on the same day or over a short period of time, the results for individual samples usually agreed within about 1 percent of the original weight of the sample. A similar series of tests made at another time using the same sieves and the same source of powder, again usually showed good agreement between the individual samples, but the average results often differed from those of the previous series by as much as 4 to 8 percent.

The variations observed in the sieve tests of these powders, extending over periods of 1 week to 8 months, are given in table 4. The maximum differences between corresponding fractions of electrolytic iron were as high as 5.6 percent with Sieve Set I (column 2) and 4.4 percent with Sieve Set 2 (column 4). With electrolytic copper, the differences were 7.8 percent (column 6) and 7.1 percent (column 8), respectively.

TABLE 4.—*Sieve tests of electrolytic iron, electrolytic copper, and nickel powders showing variation of results*

[100-gram samples, sieved 30 min.]

Sieve No.	Weight percent retained											
	Electrolytic iron				Electrolytic copper				Nickel			
	Sieve Set I (25 tests)		Sieve Set II (20 tests)		Sieve Set I (33 tests)		Sieve Set II (48 tests)		Sieve Set I (7 tests)[a]		Sieve Set II (16 tests)	
	Mean	Deviation from mean	Mean	Deviation from mean	Mean	Deviation from mean	Mean	Deviation from mean	Mean	Deviation from mean	Mean	Deviation from mean
	(1)	(2)	(3)	(4)	(5)	(6)	(7)	(8)	(9)	(10)	(11)	(12)
80	Trace	.....	Trace	.....	Trace	.....	Trace	.....	.....	.....	.....	.....
100	1.2	±0.1	1.3	+0.2-0.3	Trace	.....	Trace	.....	.....	.....	.....	.....
140	12.7	+ .6-0.7	10.5	+ .6- .7	6.2	+0.8-0.7	4.3	+0.9-0.8	2.3	+0 -0.1	1.4	+0.6-0.3
200	21.3	+1.3-1.0	24.4	+ .8- .6	16.4	+ .9- .8	19.1	+1.8-2.6	11.4	±0.1	12.5	+ .4- .7
325	20.3	+1.5- .7	23.9	+ .8- .6	20.6	+3.8-1.8	22.9	+3.0-2.4	12.5	± .3	15.4	+3.5-2.4
pan	44.0	+2.1-3.5	39.4	+2.4-2.0	56.1	+2.8-5.0	52.8	+4.8-2.3	73.4	± .2	70.3	+2.8-3.7

[a] These seven tests were made over a period of 1 week. All other tests covered periods of 6 to 8 months.

The data for nickel illustrate the agreement that may be expected in sieving tests made over a short space of time as well as the lack of agreement among tests made at different times. The results of seven tests with sieve Set I made over a period of about 1 week agree within 1 percent (column 10). The three series of tests with sieve Set II, using 6, 4, and 6 samples respectively, were made at different times over a period of about 8 months. The values within each series of tests made over a period of a few days, agreed within 1 percent, whereas differences between the series were as much as 6.5 percent.

Much of the data given in table 4 were obtained during the spring and summer seasons of the year. It is possible, therefore, that variations in the atmospheric conditions to which the powders were exposed may have contributed to the variations noted in the sieve test results. A sampling error built up by several repetitions of riffle cutting might also account for part of the differences observed. Further work will be required under better controlled conditions, particularly with respect to sampling and humidity, before the relative effects of the two variables can be determined with certainty.

The average values of a large number of tests of electrolytic iron, electrolytic copper, and nickel, made with two different sets of certified sieves over long periods of time, are given in table 4. The differences between these averages (calculated to the third decimal place) are compared in table 5.

TABLE 5. *Sieve tests of electrolytic iron, electrolytic copper, and nickel powders showing differences in results obtained with two different sets of certified sieves* [a]

[100-gram samples, sieved 30 minutes]

Sieve No.	Weight percent retained															
	Sponge iron				Electrolytic iron				Electrolytic copper				Nickel			
	Mean, Sieve Set I (3 tests)	Mean, Sieve Set II (3 tests)	Difference of 2 means	Estimated standard error of difference	Mean, Sieve Set I (25 tests)	Mean, Sieve Set II (20 tests)	Difference of means	Estimated standard error of difference	Mean, Sieve Set I (33 tests)	Mean, Sieve Set II (48 tests)	Difference of 2 means	Estimated standard error of difference	Mean, Sieve Set I (7 tests)	Mean, Sieve Set II (16 tests)	Difference of 2 means	Estimated standard error of difference
	(1)	(2)	(3)	(4)	(5)	(6)	(7)	(8)	(9)	(10)	(11)	(12)	(13)	(14)	(15)	(16)
80	Trace	Trace	.....	.....	Trace	Trace	.....	.....	Trace	Trace	.....	.....	Trace	Trace	.....	.....
100	Trace	Trace	.....	.....	1.172	1.260	0.088	.0.05	Trace	Trace	.....	.....	Trace	Trace	.....	.....
140	7.267	4.400	2.867	0.35	12.700	10.495	2.205	.12	6.152	4.294	1.858	0.09	2.286	1.431	0.855	0.10
200	22.600	24.400	1.800	.35	21.280	24.380	3.100	.22	16.352	19.065	2.713	.23	11.429	12.484	1.055	.10
325	31.167	33.000	1.833	.27	20.260	23.860	3.600	.17	20.630	22.927	2.297	.29	12.514	15.356	2.842	.77
Pan	38.400	37.867	.533	.11	45.956	39.425	4.531	.30	56.103	52.821	3.282	.43	73.371	70.314	3.057	.88

[a] The tests on nickel with Sieve Set I were made over a period of 1 week, tests on sponge iron over a period of 4 weeks, all others over periods of 6 to 8 months.

Included also are the averages of a few tests on sponge iron made with both sets of sieves within an interval of 4 weeks on samples from the same "sample supply". The maximum difference of the means for the two sets of sieves ranges from 2.9 to 4.5 percent and, although the same fractions are consistently larger or smaller for a given sieve mesh, the magnitude of difference varies with the different materials.

The standard error or standard deviation of the difference of the means, σ_D, given in columns 4, 8, 12, and 16 was estimated according to the formula

$$\sigma_D=(1/n+1/m)^{1/2}(\Sigma X^2+\Sigma Y^2/n+m-2)^{1/2},$$

where

n = the number of tests with sieve Set I
m = the number of tests with sieve Set II
$\Sigma X^2=\Sigma X^2-n\overline{X}^2$
$\Sigma Y^2=\Sigma Y^2-m\overline{Y}^2$
ΣX^2 = the sum of the squares of the observations for sieve Set I at a given mesh
ΣY^2 = the sum of the squares of the observations for sieve Set II at a given mesh
$\overline{X}$ = the arithmetic mean of the observations for sieve Set I at a given mesh
$\overline{Y}$ = the arithmetic mean of the observations for sieve Set II at a given mesh

The small magnitude of the estimated standard error in comparison to the difference of the means indicates that the difference between sieve sets was significant in spite of the wide scatter in individual values for tests made at different times.

Two new 325 mesh sieves were obtained from the manufacturer of Sieve Set I for use in either of the original sets if replacements should be necessary. These sieves were tested and certified by the National Bureau of Standards to conform to all specification requirements except material. The screen wire cloth was of monel metal instead of bronze, the latter being unavailable at the time of purchase. The differences in sieving results obtained when the new sieves were substituted in each of the original sets are shown in table 6. The tests with the new sieves (columns 3 and 6) were made on the same day. Those with the original Sieve Set I and Sieve Set II (column 1) were made 2 weeks before and 2 weeks later.

TABLE 6.—*Sieve tests of sponge iron showing variations due to use of different sieves in same set*

[The tests were made over a period of about 4 weeks in July. Average of 3 tests on 100-gram samples sieved 30 minutes]

Sieve No.	Weight percent retained								
	With original 325 mesh sieve		With new 325 mesh sieve (NBS No. 8887)		Difference from original (3)−(1)	With new 325 mesh sieve (NBS No. 8888)		Difference from original (6)−(1)	Difference between new sieves (6)−(3)
	Mean	Deviation from mean	Mean	Deviation from mean		Mean	Deviation from mean		
	(1)	(2)	(3)	(4)	(5)	(6)	(7)	(8)	(9)
SIEVE SET I									
80	Trace	.....	Trace	.....	.....	Trace	.....	.....	.....
100	Trace	.....	Trace	.....	.....	Trace	.....	.....	.....
140	7.3	+0.1-0.2	7.0	+0.1-0.2	−0.3	6.9	+0.1-0	−0.4	.....
200	22.6	±.1	22.4	+.2-.4	−.2	22.6	±.1	0	.....
325	31.2	+.4-.5	38.2	±.1	+7.0	41.0	+.4-.2	+9.8	+2.8
Pan	38.4	+.2-.1	32.0	+.2-.1	−6.4	28.9	±.3	−9.5	−3.1
SIEVE SET II									
80	Trace	.....	Trace	.....	.....	Trace	.....	.....	.....
100	Trace	.....	Trace	.....	.....	Trace	.....	.....	.....
140	4.4	±0.6	5.2	+0.1-0	+0.8	5.1	0	+0.7	.....
200	24.4	±.6	23.5	+.1-0.3	−.9	23.3	±0.1	−1.1	.....
325	33.0	±.2	38.6	+.3-.2	+5.6	40.8	+.1-0	+7.8	+2.2
Pan	37.9	±.2	32.2	±.1	−4.7	30.2	±.1	−7.7	−2.2

respectively. All samples were taken from the same "sample supply". It will be noted that the fractions larger than 200 mesh agreed within 1.2 percent with any given sieve assembly. The new 325 mesh sieves retained 7.0 and 9.8 percent more material, respectively, than the sieve they replaced in Sieve Set I. With Sieve Set II, the differences were 5.6 percent and 7.8 percent with corresponding changes in the pan fraction. The amounts retained by the two new sieves differed by 2.8 percent when used with Sieve Set I and 2.2 percent with Sieve Set II.

In connection with these differences it is interesting to compare the average openings of the several sieves. These sieve openings, as measured during the certification tests, are given in table 7.

The variation in the average opening permitted in 325 mesh sieves by ASTM Specification E–11 is 44 microns$\pm$7 percent, or from 41 to 47 μ inclusive. The average openings of the four 325 mesh sieves range, in the order given in table 7, from a value near the upper limit to one at the lower limit. The weight of the fractions retained by these sieves vary in the reverse order, as would be expected, the sieve with the largest average opening retaining the smallest quantity, the sieve with the smallest average opening retaining the largest quantity. The effect of seemingly negligible differences in sieve aperture on sieve tests is illustrated by the results obtained with sieves 8887 and 8888. Although the sieves differ by only 1 μ between the shoot wires, the fractions retained by Sieve 8888, with the smaller aperture, were 2.2 to 2.8 percent greater than those retained by the other sieve.

Variations of such magnitude in sieving results with different sieves are not peculiar to metal powders; similar variations observed by many workers with nonmetallic powders were mentioned in the introduction to this paper.

TABLE 7.—*Average opening of sieves as measured in certification tests*

Sieve No.	NBS Certification No.	Average opening [a]	
		Between warp wires	Between shoot wires
ORIGINAL SIEVE SET I			
		μ	μ
80	8805	186	174
100	8806	143	148
140	8807	107	102
200	8808	78	75
325	8809	46	46
ORIGINAL SIEVE SET II			
80	8889	185	174
100	8890	144	140
140	8891	104	107
200	8892	77	73
325	8893	43	45
NEW NO. 325 SIEVES			
325	8887	41	43
325	8888	41	42

[a] These measurements were made under the supervision of L. V. Judson of the Metrology Division of the National Bureau of Standards who states that the measurements were made with an accuracy sufficient to determine whether or not the openings were within the limits permitted by specifications. It is not likely that the errors are in excess of about 1 μ.

VI. Size Distribution within Fractions

The particle size distribution of the fractions retained on the several sieves was determined by microscopic measurement. Xylene containing a few drops of cedar wood oil was used as a dispersing agent in making the slides. Measurements were made on the image of the particles projected upon the ground glass of a camera at a magnification of $\times$50. The projected dimension measured was the one which, in the opinion of the observer, would control the passage of the particle through a sieve opening.

The controlling dimension was easily determined when, as was usually the case, the projected image was circular, roughly rectangular or elliptical. However, when very irregular particles, such as the "tree-shaped" electrolytic copper particles shown in figure 5, were measured, selection of the controlling dimension was difficult. In such cases the branches were considered a part of the dimension when they were small or close together, as at *A* and *B* (fig. 5). When the branches were widely separated, as at *C*, the dimension was measured from the fork of the branch. The controlling dimensions obtained for the three particles by this procedure (between 5 and 6 mm at $\times$50 magnification) are in line with the dimensions of the other particles of the sample.

The particle size distribution of the five sieve fractions of sponge iron larger than 325 mesh is shown in figure 23. The fractions retained by the

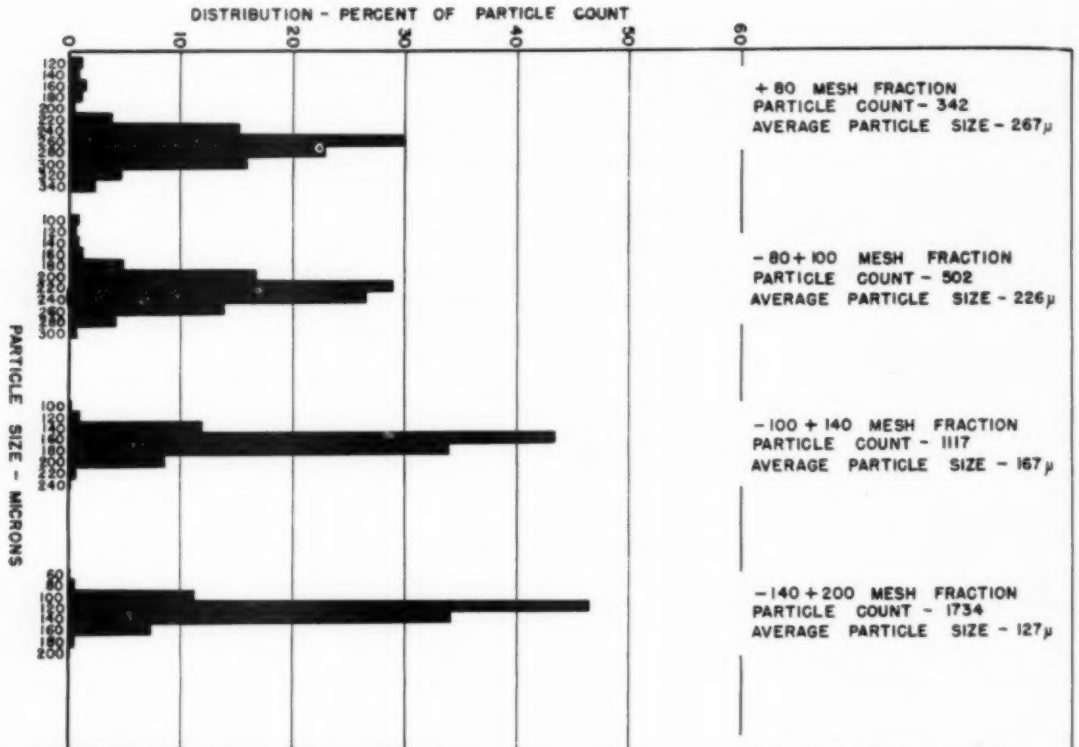

FIGURE 23.—*Particle size distribution of sieve fractions of sponge iron measured microscopically at a magnification of ×50 (accuracy ±10 microns).*

80 and 100 mesh sieves contain particles ranging in size from class mark 100 to class mark 340μ. The range in size distribution decreases considerably with the finer sieves. However, even in the −200+325 mesh fraction the range in particle size is over 80μ (from class mark 60 to class mark 140μ) with over 50 percent of the particles between 90 and 110μ.

The average particle size of a sieve fraction is often described in the literature as the mean of the nominal openings of the sieves which retained, and which just passed the fraction. The average particle size of sieved fractions of the metal powders listed in table 1, and the mean apertures of the passing-retaining sieves are given in table 8. Measurements were made at magnifications of ×50 and ×100, with accuracies of ±10 and ±5μ, respectively. The average particle size of the fractions vary greatly with the different materials. The values for the atomized powders, zinc, tin, and lead, composed of roughly spherical particles with

TABLE 8.—*Average particle size of sieve fractions of metal powders as measured microscopically at magnifications of ×50 and ×100 with accuracies of ±10 and ±5 microns respectively*

Sieve fraction	Mean aperture of passing-retaining sieves	Average particle size, controlling dimension						
		Sponge iron	Electrolytic iron	Electrolytic copper	Nickel	Zinc [a]	Tin	Lead
	μ	μ	μ	μ	μ	μ	μ	μ
+80		267	278	271	246	219		228
−80+100	163	226	238	186	228	157	194	190
−100+140	127	167	173	136	178	129	142	128
−140+200	89	127	134	112	124	92	90	98
−200+325	59	95	96	86	86	63	64	68

[a] Measured at ×100. All other measurements made at ×50 magnification.

the three dimensions approximately equal, are close to the mean of the sieve apertures. The plate-like or very irregularly shaped particles of electrolytic iron, sponge iron, copper, and nickel have controlling dimensions considerably greater than the mean of the apertures. This tendency for the projected dimensions of particles, particularly irregularly shaped particles, to exceed the average aperture of the passing-retaining sieves has been noted by other investigators [17, 18, 19, 20].

VII. Discussion of Results

The results of the sieving tests indicate that the sieving rates of metal powders vary considerably with different sieves and with different materials, that appreciable variations in results may be obtained when the same powder is sieved at different times with the same sieves and that sharp or complete separation into fractions cannot be attained by sieving, at least in a reasonable length of time. Hence, selection of the proper sieving time for a given material would appear difficult. However, the results also show that reproducible values can be obtained when certain sampling errors and other variables affecting the physical condition of the powder, such as exposure to high humidities, can be eliminated or controlled. Under these conditions the scatter in values for samples of the same weight sieved for the same time apparently is independent of the time of sieving (see figs. 17 to 22). Any time between 5 minutes and 2 hours could be selected without seriously affecting the reproducibility, provided the other conditions are fixed. As prolonged sieving would increase the proportion of particles passed by oversized openings, it would seem advisable to select a sieving time near the end of the period of rapid sieving rate, that is, after the separation of the definitely undersized particles. The time required for sponge iron would be 15 to 30 minutes, depending upon sample size and other conditions.

Two variables seemed to cause the most serious differences observed in the results of sieve tests made at different times with the same sieves and the same powder. One of these was a sampling error produced in riffle cutting, the other the result of exposure of the powder to high humidity. The sample error in riffle cutting can be attributed largely to the loss of fines as dust during the operation. Evidently this is not a good method to use for sampling limited supplies of metal powders, particularly if the cutting operation is to be repeated, for then the sampling error becomes cumulative. A noncumulative method, possibly the use of a sample thief, might improve the reproducibility.

The effect of exposure to humid atmospheres on the sieving characteristics of some metal powders as demonstrated by the tests on sponge iron and suggested by the results on electrolytic iron, electrolytic copper, and nickel, poses difficult problems of storage and handling. With wrought metals it is known that at ordinary temperatures and low humidity corrosion is very slow or nonexistant. Polished samples of sheet steel, for instance, have been stored for many years in an atmosphere of about 50 percent relative humidity (over a saturated solution of calcium nitrate) without evidence of rust. However, with finely divided metal powders oxidization or corrosion may proceed at much lower humidities. Relatively small temperature changes also may have an effect. For example, it has been noted that some very fine powders, notably electrolytic copper and tin (89 to 91 percent through 325 mesh) change color when heated at 110° C for drying.

The problem posed by the differences in results obtained with different certified sieves also is difficult. There seems to be little hope that sieves can be manufactured, by present methods at least, to tolerances sufficiently close to eliminate the differences caused by minute variations in the dimensions of the average openings. The long continued and successful use of sieve analyses in the production and utilization of powdered substances shows that present manufacturing tolerances and calibration methods are adequate for control purposes at least. For research work, a more accurate method of evaluating the differences obtained with sieves that vary within specification tolerances would be desirable.

It should be pointed out that the variations in results obtained with different sieves are not as great as is indicated by comparison of values on the basis of the nominal opening. For example, in figure 24, cumulative curves of the data given in table 6 are shown in which the percentage by weight passing the several sieves is plotted against the size of the average openings as determined during the certification tests. It will be noted

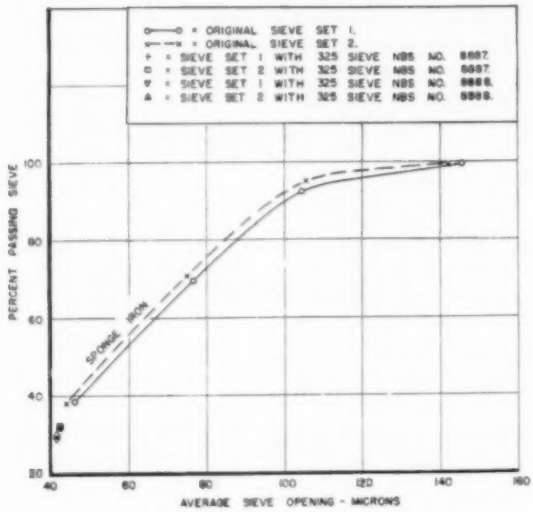

FIGURE 24.—*Cumulative weight distribution curves for sponge iron using the actual size of the average opening of the different certified sieves instead of the nominal opening as the bases of comparison.*

100-gram samples sieved for 30 minutes.

that the differences between sieves are considerably less than they would be if the comparison were made on the basis of the nominal openings.

Possibly still closer agreement would be found if the variations in size of sieve openings were taken into consideration after the method of Weber and Moran [21]. This method consists in measuring random openings microscopically. Two sieves are said to be identical if the average openings and the standard deviations are the same. The percentage standard deviation or coefficient of variance $V=100\ \sigma/\bar{X}$, where σ is the standard deviation and $\bar{X}$ the average opening, is used as the measure of sieve equivalence. An empirical formula based on the sieving time and the coefficient of variation has been applied to evaluate the effective openings of different sieves used in sieve analyses of soda ash and sodium bicarbonate.

In the cement industry, the No. 200 sieves used in accordance with ASTM Standard C184–44 for fineness tests of hydraulic cement [10] are calibrated against a standard sample of cement prepared by the National Bureau of Standards.

Hatch [17], using crushed limestone, measured the dimensions of sieved particles microscopically and, by statistical methods, calculated the size distribution by weight. The calibrated size of a sieve was taken as the median or geometric average size by weight of the material retained on the sieve.

Fagerholt [22], working with ground sand and feldspar, found that the particle size to which a result obtained by sieving in the time, t, should be referred in determining the cumulative weight distribution is the average particle size of the fraction passing the sieve by continued sieving under the same conditions to the time $3t$. The particle size is determined by counting the number of particles in a weighed portion of the fraction obtained during the interval t to $3t$.

It is possible that these or similar methods of calibration could be applied to sieve analyses of metal powders. Because of the wide variations in particle shape and particle size distribution resulting from many different production methods it is not to be expected that any one formula or standard material or calibration factor can be devised that will be equally applicable to all metal powders. However, even limited application to a powder from a given source or possibly to restricted classes of powders, such as iron made from reduced mill scale or electrolytic copper or atomized zinc, would be of value. These applications and limitations must be determined by further investigation that should include further study of the effect of humidity.

VIII. Summary

In sieve tests of sponge iron, electrolytic iron, electrolytic copper, and nickel, reproducible results were obtained only when certain variables were controlled. One factor was a cumulative sampling error resulting from repeated riffle cutting of limited powder supplies. Another variable affecting the sieving characteristics of the powders was exposure to different atmospheric conditions.

The effects of these variables was demonstrated by tests on sponge iron. Differences obtained on successive riffle cut samples were of the order of 1 percent of the original weight of the sample. The effects of humidity were considerably greater, differences of 3 to 6 percent being observed between sieve tests of dried samples and samples exposed to high humidities.

Variations of considerable magnitude were observed in the results of sieve tests of the same metal powder when sieved under comparable

conditions with different sets of certified sieves. With sponge iron, these differences were as high as 9.8 percent when comparisons were made on the basis of the nominal sieve opening. When compared on the basis of the actual size of the average opening as measured during the certification tests, the differences were reduced considerably.

Further investigation of possible methods of eliminating, controlling, or evaluating the effects of all of these variables is desirable.

Grateful acknowledgment is made to Louis V. Judson for his constructive criticism of testing methods and interpretation of results; to C. M. Saeger who was formerly connected with the investigation; to W. Earl Lindlief who assisted in the preparation of graphs; and to Eleanor M. Crook, Ruth K. Kimble, and Mary E. Steinbaugh who assisted in the sieve testing and microscopic work.

VIII. References

[1] Sieves; Standard, Testing, Federal Specification RR-S-366a.

[2] NBS Letter Circular LC854 (March 1940).

[3] Standard Specifications for Sieves for Testing Purposes (E11–39), 1946 Book of ASTM Standards (II) 1237.

[4] American Recommended Practice for Methods for Screen Testing of Ores, American Standards Association, Min. & Met. **13,** 447 (July 6, 1932).

[5] Standard Method of Test for Sieve Analysis and Water Content of Refractory Materials (C92–46), 1946 Book of ASTM Standards (II) 325.

[6] Standard Method of Test for Sieve Analysis of Fine and Coarse Aggregates (C136–46), 1946 Book of ASTM Standards (II) 467.

[7] Standard Method of Test for Coarse Particles in Pigments, Pastes, and Paints (D185–37), 1946 Book of ASTM Standards (II) 988.

[8] Standard Method of Sampling and Fineness Test of Powdered Coal (D197–30), 1944 Book of ASTM Standards (III) 41.

[9] Standard Method of Test for Particle Size of Soaps and other Detergents (D502–39), 1944 Book of ASTM Standards (III) 967.

[10] Standard Method of Test for Fineness of Hydraulic Cement by the No. 200 Sieve (C184–44), 1946 Book of ASTM Standards (II) 59.

[11] Standard Method of Test for Sieve Analysis of Granular Mineral Surfacing for Asphalt Roofing and Shingles (D451–40), 1946 Book of ASTM Standards (II) 740.

[12] Standard Method of Test for Sieve Analysis of Nongranular Mineral Surfacing for Asphalt Roofing and Shingles (D452–40), 1946 Book of ASTM Standards (II) 743.

[13] R. J. Wig and J. C. Pearson, Techn. Pap. BS (1914) T42.

[14] S. Walker, Trans. A. F. A. **49,** 789 (1941).

[15] H. Heyward, Inst. Min. & Met. Bulletin 476 (March 1946).

[16] A. H. C. Marwich, A. R. Lee, and W. H. Glanville, J. Soc. Chem. Ind. **58,** 1931 (1939).

[17] T. Hatch, J. Franklin Inst. **215,** 27 (1933).

[18] F. D. DeVaney and W. H. Coghill, Trans. AIMME **134,** 282 (1939).

[19] R. Schumann, Jr., Powder Metallurgy, ASM **186** (1942).

[20] J. M. Dallevalle, Micromeritics (Pitman Publishing Co., New York, N. Y., 1943).

[21] M. Weber, Jr., and Raymond F. Moran, Ind. Eng. Chem., Anal. Ed. **10,** 180 (1938).

[22] G. Fagerhold, Particle Size Distributing of Products Ground in Tube Mill, English translation of Thesis for Doctor Degree, G. E. C. Gads Forlag-Copenhagen, Denmark (1945).

Washington, August 20, 1947.

U. S. Department of Commerce
National Bureau of Standards

Research Paper RP1844
Volume 39, December 1947

Part of the Journal of Research of the National Bureau of Standards

Table and Mollier Chart of the Thermodynamic Properties of 1, 3-Butadiene*

By Cyril H. Meyers, Carl S. Cragoe, and Eugene F. Mueller

This paper contains a working table and Mollier chart of the thermodynamic properties of 1, 3-butadiene in engineering units, for which the data were calculated from a set of empirical equations. These equations have been published elsewhere and shown to be consistent with exact thermodynamic relations and to represent the observed data within the limits of the experimental accuracy. The table covers the properties of the saturated fluid over the temperature range extending from the triple point (−164.05 °F) to within 20 degrees of the critical temperature (305.6 °F). Examples are solved to illustrate the use of the table and Mollier chart (log P versus H). Several other charts are also presented.

I. Introduction

The extensive use of butadiene in the production of synthetic rubber led to a need for more complete and more accurate data on the properties of this substance than were available when it acquired commercial and military importance. Letter Circular LC710, a collection of the available data at the time, was published in December 1942. Further need developed for tables of liquid densities of butadiene and other C_4 hydrocarbons found in commercial C_4 mixtures, for the purpose of computing, from observed volumes, the quantities of materials bought or sold. This problem was brought to the National Bureau of Standards in July 1943, by representatives of the Rubber Reserve Company. Letter Circular LC 736, containing tables of liquid densities of eleven hydrocarbons found in commercial C_4 mixtures, was prepared from data available in the literature and issued in November 1943. The need for more extensive tables of the thermodynamic properties of butadiene led to a program of experimental work at the National Bureau of Standards to supply the data. The results of these measurements were published in 1945 in Research Papers RP1640 and RP1661. The present paper gives the data in the customary engineering units in the more useful form of an extensive table and a Mollier chart.

II. Experimental Data

The experimental data upon which these tables are based are those given in two recent publications [7, 8] [1]. These publications describe the results of measurements made on butadiene at the National Bureau of Standards, compare them with the relatively small amount of data available from other laboratories, and develop empirical equations that are consistent with exact thermodynamic relations and that represent the observed data within the limit of experimental accuracy, which for P-V-T data on the vapor is one to three parts per thousand, for density of the liquid a very few parts in ten thousand, and for the excess of the enthalpy or entropy over that for the solid at the triple point is approximately one part per thousand. This limit is probably as small as is practicable in view of the rather unstable character of the material that polymerizes to some extent, even while observations are in progress.

Other publications [1, 2] were consulted, and the data they contained were used for comparison and verification, but not to any considerable extent as source data for the tables. The temperature of the triple point was taken as −164.05°F (−108.92°C), that of the boiling point as 24.06°F (−4.41°C), and that of the critical point as 305.6°F (152°C). The value for the critical point is believed to be reliable to one or two °C. Poly-

* This paper was also published as a Technical Report to the Office of Rubber Reserve, June 30, 1947.

[1] Figures in brackets indicate the literature references at the end of this paper.

merization occurring before and during the observations limited the accuracy of the determination of the critical temperature.

III. Notation

In general, the abbreviations approved as American Tentative Standard (ASA Z101-1932) have been used, with the exception that in giving numerical values of temperatures, the degree sign (°) has been retained. The units and symbols used are listed in table 1.

TABLE 1.—*Units and notation*

Quantity	Unit	Symbol	Formula
Pressure	lb/in.^{2}	P	
Specific volume	ft^3/lb	v	
Temperature	°F	t	
Absolute temperature	°R	T	$T=t+459.688$.
Heat added	Btu/lb	q	
Internal energy	do	u	$^a du=dq-pdv$.
Enthalpy (heat content)	do	h	$^a h=u+pv$.
Entropy	Btu/lb°R	s	$ds=dq/T$.
Latent heat of vaporization	Btu/lb	h_{fg}	$h_{fg}=h_g-h_f$.

SUBSCRIPTS

Property of liquid	f
Property of vapor	g
Transition from liquid to vapor	fg

[a] The factor 1 (ft^3) (lb/in.^{2}) =0.185052 Btu is necessary for numerical calculations in engineering units.

IV. Fundamental Units and Constants

1. Temperature Scale

The Fahrenheit scale used in these tables is derived from the international temperature scale [3] of 1927 by means of the relation:

$$\text{Fahrenheit temperature} = 1.8 \times \text{centigrade temperature} + 32.$$

It is not expected that any changes that may be made when the pending revision of the scale of 1927 is adopted, will require any material change in the numerical values of temperatures as given in these tables.

Temperatures on the absolute Fahrenheit scale were obtained by adding 459.688° to the temperatures as defined above.

2. Heat Units

All of the calorimetric measurements were made in terms of the international joule, which was therefore the fundamental heat unit. It is based upon the standards of resistance and electromotive force maintained at the Bureau and upon the mean solar second. The relation between the international joule and the corresponding cgs units, according to the most recent data [4] is:

1 international joule = 1.00017 absolute joules.

In the thermodynamic equations relations occur between quantities of energy, some of which were measured in international joules, whereas others such as the product of pressure and volume each expressed in appropriate units, were measured directly in mechanical units, that is, absolute joules. Although the difference might be considered of negligible importance, it was taken into account where it could have any appreciable effect on the results obtained.

As secondary heat units the calorie and the British thermal unit (Btu) have been used. The calorie is the International Table (IT) calorie, widely used in engineering tables of the properties of steam. It was officially adopted by the second International Steam Table conference [5] held in London in 1929, and is *defined* as 3,600/860 (approximately 4.1860) international joules. In this way the mechanical equivalent of heat, so significant in earlier tables, loses its importance as it becomes a defined rather than an experimental constant and therefore is in no way dependent upon the results of past or future measurements of the properties of water.

The Btu used is derivable from the calorie by use of relations that depend only upon the relative sizes of the centigrade and Fahrenheit degrees, and the relation between the kilogram and the pound thus,

$$1 \text{ Btu} = 453.592 \times \frac{5}{9} = 251.996 \text{ IT calories} = 1054.866 \text{ int joules.}$$

This method of defining the Btu retains the convenient relation

1 calorie per gram = 1.8 Btu per pound.

3. Relations Between Energy Units

The relation between the Btu defined above, and the standard foot-pound is 1 Btu = 1054.866 int joules $\times \frac{10^7 \times 0.3937}{980.665 \times 453.592 \times 12} = 778.160$ ft lb.

In using the tables, quantities of heat or work that are given in Btu may be converted into foot-pounds by multiplying by the factor 778.160. In cases where the reverse conversion is desired, the relation may be written,

$$1 \text{ ft-lb} = 0.00128508 \text{ Btu}.$$

As volumes are given in ft^3 and pressures in $lb/in.^2$, the relation $1\ (ft^3)\ (lb/in.^2) = 144\ (0.00128508) = 0.185052$ Btu becomes necessary wherever numerical values are given in an equation involving both energy in Btu and the product pe in British engineering units.

4. Units of Pressure

In the British system the unit of force is the pound weight, which becomes definite when the value of the acceleration due to gravity is specified. The value used here is 980.665 cm/sec^{-2}.[2]

The unit of pressure used in this publication is one standard pound weight per sq in. absolute. The lower pressures have been expressed also in inches of mercury with use of the factor,

$$1 \text{ lb/in.}^2 = 2.03601 \text{ in Hg}.$$

[2] In 1901 the International Committee of Weights and Measures recommended the adoption of an experimental value 980.665 cm/sec² (32.174 ft/sec²) as the value of gravity at latitude 45° and sea level [5]. Since then, those who have occasion to use a standard value for g have been divided into two groups, one of which uses the current "best" value for g at latitude 45° and sea level. The current value is about 980.62 cm/sec². The other group has loyally followed the lead of the international committee in using 980.665 cm/sec². The value 980.665 cm/sec² has been used in computing these tables.

5. Units of Volume and Density

The volumetric apparatus was calibrated either with water or with mercury. The volume unit was defined by the relations:

One cm^3 of water at 4° C under 1 atm pressure has a mass of 0.999973 g. One ml of water at 4° C under 1 atm pressure has a mass of 1.000000 grams. One cm^3 of mercury at 0° C under 1 atm pressure has a mass of 13.5951 g. Densities measured in g/ml were converted by means of the relation [4],

$$1 \text{ g/ml} = 62.42658 \text{ lb/ft}^3.$$

V. Description of Table

Only the properties of the saturated fluid have been tabulated. These are presented in table 2, which uses the notation described in the preceding section and in which the argument is temperature. The table covers the whole temperature range from the triple point −164.05° F to the critical temperature 305.6° F. Values are given every degree Fahrenheit in the temperature range 0° to 200° F and at less frequent intervals outside this range. Such arrangement gives a table with an ample number of entries in the portion most used, and keeps the table within a reasonable size. The pressures are absolute and for the lower temperatures are given in two units, namely $lb/in.^2$ and inches Hg at 32° F. The next two columns are devoted to the specific volume of liquid and vapor respectively in ft^3/lb. In that portion of the table where only one column of pressures is given, a column of densities of the vapor in lb/ft^3 has been inserted so that the table contains the same number of columns throughout.

765484—47——3

TABLE 2.—*Properties of saturated 1, 3-butadiene*

Temperature, t	Abs. pressure		Specific volume		Enthalpy			Entropy		Temperature, t
	p	p	Liquid, v_f	Vapor, v_g	Liquid, h_f	Evap., h_{fg}	Vapor, h_g	Liquid, s_f	Vapor, s_g	
°F	lb/in.²	in. Hg	ft³/lb	ft³/lb	Btu/lb	Btu/lb	Btu/lb	Btu/lb°R	Btu/lb°R	°F
Triple	0.010	Solid		5,706	59.14	282.7	341.8	0.3757	1.3317	−164.05
point	.010	Liquid	0.020972	5,706	122.61	219.2	341.8	.5904	1.3317	−164.05
−160	.013	0.027	.021036	4,504	124.44	218.3	342.7	.5973	1.3256	−160
−155	.018	.037	.021117	3,310	126.71	217.1	343.8	.6048	1.3174	−155
−150	.025	.051	.021198	2,461	128.98	216.0	345.0	.6122	1.3096	−150
−145	.034	.069	.021279	1,850	131.26	214.8	346.1	.6195	1.3023	−145
−140	.045	.092	.021362	1,406	133.55	213.7	347.3	.6267	1.2953	−140
−135	.060	.121	.021446	1,079.6	135.83	212.6	348.4	.6338	1.2886	−135
−130	.078	.159	.021530	836.8	138.13	211.5	349.6	.6408	1.2823	−130
−125	.101	.206	.021615	654.6	140.42	210.4	350.8	.6478	1.2764	−125
−120	.130	.265	.021701	516.5	142.72	209.3	352.0	.6546	1.2707	−120
−115	.166	.338	.021787	411.0	145.03	208.2	353.2	.6613	1.2654	−115
−110	.210	.428	.021876	329.6	147.33	207.1	354.5	.6680	1.2603	−110
−105	.264	.537	.021964	266.3	149.65	206.1	355.7	.6745	1.2555	−105
−100	.329	.669	.022054	216.7	151.96	205.0	356.9	.6810	1.2509	−100
−95	.407	.828	.022144	177.6	154.29	203.9	358.2	.6874	1.2466	−95
−90	.500	1.017	.022236	146.4	156.61	202.9	359.5	.6938	1.2425	−90
−85	.610	1.242	.022328	121.52	158.95	201.8	360.8	.7000	1.2386	−85
−80	.740	1.507	.022420	101.44	161.29	200.8	362.0	.7062	1.2350	−80
−75	.893	1.817	.022511	85.16	163.63	199.7	363.3	.7124	1.2315	−75
−70	1.071	2.180	.022606	71.88	165.99	198.7	364.7	.7184	1.2283	−70
−65	1.277	2.600	.022702	60.98	168.35	197.6	366.0	.7245	1.2252	−65
−60	1.516	3.086	.022799	52.00	170.72	196.6	367.3	.7304	1.2223	−60
−58	1.621	3.300	.022838	48.85	171.67	196.2	367.8	.7328	1.2212	−58
−56	1.732	3.526	.022878	45.93	172.62	195.8	368.4	.7352	1.2201	−56
−54	1.849	3.765	.022917	43.21	173.57	195.3	368.9	.7375	1.2190	−54
−52	1.973	4.017	.022957	40.68	174.53	194.9	369.5	.7399	1.2180	−52
−50	2.103	4.283	.022997	38.33	175.49	194.5	370.0	.7422	1.2170	−50
−48	2.241	4.563	.023037	36.14	176.44	194.1	370.5	.7445	1.2160	−48
−46	2.386	4.857	.023077	34.10	177.40	193.7	371.1	.7469	1.2150	−46
−44	2.538	5.167	.023118	32.19	178.36	193.3	371.6	.7492	1.2141	−44
−42	2.698	5.494	.023158	30.41	179.33	192.8	372.2	.7515	1.2132	−42
−40	2.867	5.836	.023199	28.75	180.29	192.4	372.7	.7538	1.2123	−40
−38	3.043	6.196	.023240	27.20	181.26	192.0	373.3	.7561	1.2114	−38
−36	3.229	6.574	.023281	25.74	182.23	191.6	373.8	.7584	1.2105	−36
−34	3.423	6.970	.023323	24.38	183.19	191.2	374.4	.7606	1.2097	−34
−32	3.627	7.386	.023364	23.10	184.16	190.7	374.9	.7629	1.2089	−32
−30	3.841	7.821	.023406	21.91	185.14	190.3	375.5	.7652	1.2081	−30
−28	4.065	8.277	.023448	20.79	186.11	189.9	376.0	.7674	1.2074	−28
−26	4.299	8.754	.023491	19.73	187.09	189.5	376.6	.7697	1.2066	−26
−24	4.544	9.252	.023533	18.74	188.06	189.1	377.1	.7719	1.2059	−24
−22	4.801	9.774	.023576	17.81	189.04	188.6	377.7	.7742	1.2052	−22
−20	5.068	10.319	.023619	16.94	190.02	188.2	378.2	.7764	1.2045	−20
−18	5.348	10.888	.023662	16.11	191.01	187.8	378.8	.7786	1.2038	−18
−16	5.639	11.482	.023705	15.34	191.99	187.4	379.4	.7809	1.2032	−16
−14	5.944	12.102	.023749	14.61	192.98	186.9	379.9	.7831	1.2025	−14
−12	6.261	12.748	.023793	13.92	193.97	186.5	380.5	.7853	1.2019	−12
−10	6.592	13.421	.023837	13.27	194.96	186.1	381.0	.7875	1.2013	−10
−8	6.937	14.123	.023882	12.66	195.95	185.7	381.6	.7897	1.2007	−8
−6	7.295	14.854	.023926	12.08	196.94	185.2	382.2	.7919	1.2002	−6
−4	7.669	15.614	.023971	11.53	197.94	184.8	382.7	.7941	1.1996	−4
−2	8.057	16.405	.024016	11.01	198.94	184.4	383.3	.7963	1.1991	−2
0	8.461	17.23	.024062	10.525	199.94	183.9	383.9	.7984	1.1985	0
1	8.669	17.65	.024084	10.290	200.44	183.7	384.2	.7995	1.1983	1
2	8.881	18.08	.024107	10.062	200.94	183.5	384.4	.8006	1.1980	2
3	9.097	18.52	.024130	9.839	201.44	183.3	384.7	.8017	1.1978	3
4	9.317	18.97	.024153	9.623	201.94	183.1	385.0	.8028	1.1976	4

TABLE 2.—*Properties of saturated 1, 3-butadiene*—Continued

Temperature, t	Abs. pressure		Specific volume		Enthalpy			Entropy		Temperature, t
	p	p	Liquid, v_f	Vapor, v_g	Liquid, h_f	Evap., h_{fg}	Vapor, h_g	Liquid, s_f	Vapor, s_g	
°F	lb/in.²	in. Hg	ft³/lb	ft³/lb	Btu/lb	Btu/lb	Btu/lb	Btu/lb°R	Btu/lb°R	°F
5	9.542	19.43	0.024176	9.413	202.44	182.8	385.3	0.8038	1.1973	5
6	9.770	19.89	.024199	9.208	202.95	182.6	385.6	.8049	1.1971	6
7	10.003	20.37	.024223	9.008	203.45	182.4	385.9	.8060	1.1969	7
8	10.241	20.85	.024246	8.814	203.96	182.2	386.1	.8071	1.1966	8
9	10.482	21.34	.024269	8.625	204.47	182.0	386.4	.8082	1.1964	9
10	10.728	21.84	.024293	8.441	204.97	181.7	386.7	.8092	1.1962	10
11	10.979	22.35	.024316	8.261	205.48	181.5	387.0	.8103	1.1960	11
12	11.234	22.87	.024340	8.087	205.98	181.3	387.3	.8114	1.1957	12
13	11.494	23.40	.024363	7.917	206.49	181.1	387.6	.8125	1.1955	13
14	11.759	23.94	.024387	7.751	207.00	180.9	387.9	.8135	1.1953	14
15	12.029	24.49	.024411	7.589	207.50	180.6	388.1	.8146	1.1951	15
16	12.303	25.05	.024435	7.431	208.01	180.4	388.4	.8157	1.1949	16
17	12.582	25.62	.024459	7.278	208.52	180.2	388.7	.8167	1.1947	17
18	12.866	26.20	.024483	7.128	209.03	180.0	389.0	.8178	1.1945	18
19	13.155	26.78	.024507	6.982	209.54	179.7	389.3	.8189	1.1943	19
20	13.45	27.38	.024531	6.840	210.05	179.5	389.6	.8199	1.1942	20
21	13.75	27.99	.024555	6.701	210.57	179.3	389.9	.8210	1.1940	21
22	14.05	28.61	.024579	6.566	211.08	179.1	390.1	.8220	1.1938	22
23	14.36	29.24	.024604	6.434	211.59	178.8	390.4	.8231	1.1936	23
24	14.68	29.88	.024628	6.305	212.10	178.6	390.7	.8242	1.1934	24
25	15.00	30.54	.024653	6.179	212.62	178.4	391.0	.8252	1.1933	25
26	15.32	31.20	.024677	6.057	213.13	178.2	391.3	.8263	1.1931	26
27	15.66	31.87	.024702	5.937	213.65	177.9	391.6	.8273	1.1929	27
28	15.99	32.56	.024727	5.820	214.16	117.7	391.9	.8284	1.1928	28
29	16.34	33.26	.024752	5.706	214.68	177.5	392.2	.8294	1.1926	29
30	16.68	33.97	.024777	5.595	215.19	177.2	392.4	.8305	1.1925	30
31	17.04	34.69	.024802	5.487	215.71	177.0	392.7	.8316	1.1923	31
32	17.40	35.42	.024827	5.381	216.23	176.8	393.0	.8326	1.1921	32
33	17.76	36.17	.024852	5.277	216.75	176.6	393.3	.8337	1.1920	33
34	18.13	36.92	.024877	5.176	217.27	176.3	393.6	.8347	1.1919	34
35	18.51	37.69	.024903	5.077	217.79	176.1	393.9	.8357	1.1917	35
36	18.90	38.47	.024928	4.981	218.31	175.9	394.2	.8368	1.1916	36
37	19.29	39.27	.024954	4.887	218.83	175.6	394.5	.8378	1.1914	37
38	19.68	40.07	.024979	4.795	219.35	175.4	394.7	.8389	1.1913	38
39	20.08	40.89	.025005	4.705	219.87	175.2	395.0	.8399	1.1912	39
40	20.49	41.72	.025031	4.617	220.40	174.9	395.3	.8410	1.1910	40
41	20.91	42.57	.025057	4.531	220.92	174.7	395.6	.8420	1.1909	41
42	21.33	43.43	.025083	4.447	221.44	174.4	395.9	.8431	1.1908	42
43	21.76	44.30	.025109	4.365	221.97	174.2	396.2	.8441	1.1907	43
44	22.19	45.19	.025135	4.285	222.50	174.0	396.5	.8451	1.1905	44
45	22.63	46.08	.025161	4.207	223.02	173.7	396.8	.8462	1.1904	45
46	23.08	47.00	.025188	4.130	223.55	173.5	397.0	.8472	1.1903	46
47	23.54	47.92	.025214	4.055	224.08	173.3	397.3	.8483	1.1902	47
48	24.00	48.86	.025241	3.982	224.61	173.0	397.6	.8493	1.1901	48
49	24.47	49.82	.025267	3.911	225.13	172.8	397.9	.8503	1.1900	49

TABLE 2.—*Properties of saturated 1, 3-butadiene*—Continued

Temperature, t	Abs. pressure	Specific volume		Density vapor $1/v_g$	Enthalpy			Entropy		Temperature, t
		v_f	v_g		Liquid h_f	Evap. h_{fg}	Vapor h_g	Liquid s_f	Vapor s_g	
°F	lb/in.²	ft³/lb	ft³/lb	lb/ft³	Btu/lb	Btu/lb	Btu/lb	Btu/lb°R	Btu/lb°R	°F
50	24.94	0.025294	3.840	0.2604	225.66	172.5	398.2	0.8514	1.1899	50
51	25.43	.025321	3.772	.2651	226.19	172.3	398.5	.8524	1.1898	51
52	25.92	.025348	3.705	.2699	226.72	172.1	398.8	.8534	1.1897	52
53	26.42	.025375	3.639	.2748	227.26	171.8	399.1	.8545	1.1896	53
54	26.92	.025402	3.575	.2797	227.79	171.6	399.4	.8555	1.1895	54
55	27.43	.025429	3.512	.2847	228.32	171.3	399.6	.8565	1.1894	55
56	27.95	.025456	3.451	.2898	228.85	171.1	399.9	.8575	1.1893	56
57	28.48	.025484	3.391	.2949	229.39	170.8	400.2	.8586	1.1892	57
58	29.01	.025511	3.332	.3001	229.93	170.6	400.5	.8596	1.1891	58
59	29.56	.025539	3.275	.3054	230.46	170.3	400.8	.8607	1.1891	59
60	30.11	.025567	3.218	.3107	231.00	170.1	401.1	.8617	1.1890	60
61	30.66	.025595	3.163	.3162	231.53	169.8	401.4	.8627	1.1889	61
62	31.23	.025623	3.109	.3217	232.07	169.6	401.7	.8637	1.1888	62
63	31.80	.025651	3.056	.3272	232.61	169.3	401.9	.8648	1.1887	63
64	32.39	.025679	3.004	.3329	233.15	169.1	402.2	.8658	1.1887	64
65	32.97	.025707	2.954	.3386	233.69	168.8	402.5	.8668	1.1886	65
66	33.57	.025736	2.904	.3444	234.23	168.6	402.8	.8678	1.1885	66
67	34.18	.025764	2.855	.3502	234.77	168.3	403.1	.8689	1.1885	67
68	34.79	.025793	2.808	.3562	235.31	168.1	403.4	.8699	1.1884	68
69	35.42	.025821	2.761	.3622	235.85	167.8	403.7	.8709	1.1883	69
70	36.05	.025850	2.715	.3683	236.40	167.6	404.0	.8719	1.1883	70
71	36.69	.025879	2.670	.3745	236.94	167.3	404.2	.8730	1.1882	71
72	37.34	.025908	2.626	.3808	237.49	167.0	404.5	.8740	1.1882	72
73	37.99	.025938	2.583	.3871	238.03	166.8	404.8	.8750	1.1881	73
74	38.66	.025967	2.541	.3935	238.58	166.5	405.1	.8760	1.1880	74
75	39.33	.025996	2.500	.4001	239.13	166.3	405.4	.8770	1.1880	75
76	40.02	.026026	2.459	.4066	239.68	166.0	405.7	.8780	1.1879	76
77	40.71	.026056	2.419	.4133	240.23	165.7	406.0	.8791	1.1879	77
78	41.41	.026085	2.380	.4201	240.77	165.5	406.3	.8801	1.1879	78
79	42.12	.026115	2.342	.4269	241.32	165.2	406.5	.8811	1.1878	79
80	42.84	.026145	2.305	.4339	241.88	165.0	406.8	.8821	1.1878	80
81	43.57	.026176	2.268	.4409	242.43	164.7	407.1	.8831	1.1877	81
82	44.31	.026206	2.232	.4480	242.98	164.4	407.4	.8841	1.1877	82
83	45.06	.026236	2.197	.4552	243.53	164.2	407.7	.8852	1.1876	83
84	45.82	.026267	2.162	.4625	244.09	163.9	408.0	.8862	1.1876	84
85	46.59	.026298	2.128	.4699	244.64	163.6	408.3	.8872	1.1876	85
86	47.36	.026328	2.095	.4773	245.20	163.4	408.5	.8882	1.1875	86
87	48.15	.026359	2.062	.4849	245.75	163.1	408.8	.8892	1.1875	87
88	48.95	.026391	2.030	.4926	246.31	162.8	409.1	.8902	1.1875	88
89	49.75	.026422	1.999	.5003	246.87	162.5	409.4	.8912	1.1875	89
90	50.57	.026453	1.968	.5082	247.43	162.3	409.7	.8922	1.1874	90
91	51.40	.026485	1.938	.5161	247.99	162.0	410.0	.8933	1.1874	91
92	52.23	.026516	1.908	.5242	248.55	161.7	410.3	.8943	1.1874	92
93	53.08	.026548	1.879	.5323	249.11	161.4	410.5	.8953	1.1874	93
94	53.94	.026580	1.850	.5405	249.67	161.2	410.8	.8963	1.1873	94
95	54.81	.026612	1.822	.5489	250.23	160.9	411.1	.8973	1.1873	95
96	55.68	.026644	1.794	.5573	250.80	160.6	411.4	.8983	1.1873	96
97	56.57	.026677	1.767	.5658	251.36	160.3	411.7	.8993	1.1873	97
98	57.47	.026709	1.741	.5745	251.93	160.0	412.0	.9003	1.1873	98
99	58.38	.026742	1.715	.5832	252.49	159.8	412.3	.9013	1.1873	99
100	59.30	.026775	1.689	.5921	253.0	159.5	412.5	.9023	1.1872	100
101	60.24	.026808	1.664	.6010	253.6	159.2	412.8	.9033	1.1872	101
102	61.18	.026841	1.639	.6101	254.2	158.9	413.1	.9043	1.1872	102
103	62.13	.026874	1.615	.6193	254.8	158.6	413.4	.9053	1.1872	103
104	67.10	.026908	1.591	.6285	255.4	158.3	413.7	.9063	1.1872	104

TABLE 2.—*Properties of saturated 1, 3-butadiene*—Continued

Temperature, t	Abs. pressure	Specific volume		Density vapor $1/v_g$	Enthalpy			Entropy		Temperature, t
		v_f	v_g		Liquid h_f	Evap. h_{fg}	Vapor h_g	Liquid s_f	Vapor s_g	
°F	lb/in.²	ft³/lb	ft³/lb	lb/ft³	Btu/lb	Btu/lb	Btu/lb	Btu/lb°R	Btu/lb°R	°F
105	64.07	0.020941	1.568	0.6379	256.0	158.0	414.0	0.9073	1.1872	105
106	65.06	.020975	1.545	.6474	256.4	157.8	414.2	.9083	1.1872	106
107	66.06	.021009	1.522	.6570	257.0	157.5	414.5	.9093	1.1872	107
108	67.07	.021043	1.500	.6668	257.6	157.2	414.8	.9103	1.1872	108
109	68.09	.021077	1.478	.6766	258.2	156.9	415.1	.9113	1.1872	109
110	69.12	.021112	1.457	.6865	258.8	156.6	415.4	.9123	1.1872	110
111	70.17	.021146	1.436	.6966	259.3	156.3	415.6	.9133	1.1872	111
112	71.23	.021181	1.415	.7068	259.9	156.0	415.9	.9143	1.1872	112
113	72.29	.021216	1.395	.7171	260.5	155.7	416.2	.9153	1.1872	113
114	73.37	.021251	1.375	.7275	261.1	155.4	416.5	.9163	1.1872	114
115	74.47	.021286	1.355	.7380	261.7	155.1	416.8	.9173	1.1872	115
116	75.57	.021322	1.336	.7487	262.2	154.8	417.0	.9183	1.1872	116
117	76.69	.021358	1.317	.7595	262.8	154.5	417.3	.9193	1.1872	117
118	77.82	.021393	1.298	.7704	263.4	154.2	417.6	.9203	1.1872	118
119	78.96	.021429	1.280	.7814	264.0	153.9	417.9	.9213	1.1873	119
120	80.11	.021466	1.262	.7926	264.6	153.6	418.2	.9223	1.1873	120
121	81.28	.021502	1.244	.8039	265.1	153.3	418.4	.9233	1.1873	121
122	82.46	.021538	1.227	.8153	265.7	153.0	418.7	.9243	1.1873	122
123	83.65	.021575	1.209	.8268	266.3	152.7	419.0	.9253	1.1873	123
124	84.85	.021612	1.193	.8385	267.0	152.3	419.3	.9263	1.1873	124
125	86.07	.021649	1.176	.8503	267.5	152.0	419.5	.9273	1.1873	125
126	87.30	.021687	1.160	.8623	268.1	151.7	419.8	.9283	1.1874	126
127	88.54	.021724	1.144	.8743	268.7	151.4	420.1	.9293	1.1874	127
128	89.80	.021762	1.128	.8865	269.3	151.1	420.4	.9303	1.1874	128
129	91.07	.021800	1.112	.8989	269.8	150.8	420.6	.9313	1.1874	129
130	92.35	.021838	1.097	.9114	270.4	150.5	420.9	.9323	1.1874	130
131	93.65	.021877	1.082	.9240	271.1	150.1	421.2	.9333	1.1875	131
132	94.96	.021915	1.067	.9368	271.7	149.8	421.5	.9343	1.1875	132
133	96.28	.021954	1.053	.9497	272.2	149.5	421.7	.9353	1.1875	133
134	97.62	.021993	1.039	.9628	272.8	149.2	422.0	.9363	1.1875	134
135	98.97	.022032	1.0246	.9760	273.5	148.8	422.3	.9373	1.1875	135
136	100.33	.022072	1.0108	.9893	274.0	148.5	422.5	.9383	1.1876	136
137	101.71	.022111	.9972	1.0028	274.6	148.2	422.8	.9392	1.1876	137
138	103.10	.022151	.9838	1.0165	275.2	147.9	423.1	.9402	1.1876	138
139	104.51	.022191	.9706	1.0303	275.9	147.5	423.4	.9412	1.1876	139
140	105.93	.022232	.9576	1.044	276.4	147.2	423.6	.9422	1.1877	140
141	107.36	.022272	.9449	1.058	277.0	146.9	423.9	.9432	1.1877	141
142	108.81	.022313	.9323	1.073	277.7	146.5	424.2	.9442	1.1877	142
143	110.27	.022354	.9199	1.087	278.2	146.2	424.4	.9452	1.1878	143
144	111.75	.022395	.9077	1.102	278.8	145.9	424.7	.9462	1.1878	144
145	113.24	.022437	.8957	1.116	279.5	145.5	425.0	.9472	1.1878	145
146	114.75	.022479	.8839	1.131	280.0	145.2	425.2	.9482	1.1878	146
147	116.27	.022521	.8723	1.146	280.7	144.8	425.5	.9492	1.1879	147
148	117.81	.022563	.8608	1.162	281.3	144.5	425.8	.9501	1.1879	148
149	119.36	.022606	.8496	1.177	281.9	144.1	426.0	.9511	1.1879	149
150	120.9	.022648	.8385	1.193	282.5	143.8	426.3	.9521	1.1880	150
151	122.5	.022691	.8275	1.208	283.1	143.5	426.6	.9531	1.1880	151
152	124.1	.022735	.8167	1.224	283.7	143.1	426.8	.9541	1.1880	152
153	125.7	.022778	.8061	1.240	284.4	142.7	427.1	.9551	1.1881	153
154	127.3	.022822	.7957	1.257	285.0	142.4	427.4	.9561	1.1881	154
155	129.0	.022866	.7854	1.273	285.6	142.0	427.6	.9571	1.1881	155
156	130.6	.022911	.7753	1.290	286.2	141.7	427.9	.9581	1.1882	156
157	132.3	.022956	.7653	1.307	286.8	141.3	428.1	.9590	1.1882	157
158	134.0	.023001	.7554	1.324	287.4	141.0	428.4	.9600	1.1883	158
159	135.7	.023046	.7458	1.341	288.0	140.6	428.6	.9610	1.1883	159

TABLE 2.—*Properties of saturated 1, 3-butadiene*—Continued

Temperature, t	Abs. pressure	Specific volume		Density vapor $1/v_g$	Enthalpy			Entropy		Temperature, t
		v_f	v_g		Liquid h_f	Evap. h_{fg}	Vapor h_g	Liquid s_f	Vapor s_g	
°F	lb/in.²	ft³/lb	ft³/lb	lb/ft³	Btu/lb	Btu/lb	Btu/lb	Btu/lb°R	Btu/lb°R	°F
160	137.4	0.029092	0.7362	1.358	288.6	140.3	428.9	0.9620	1.1883	160
161	139.2	.029138	.7268	1.376	289.3	139.9	429.2	.9630	1.1884	161
162	140.9	.029184	.7175	1.394	289.9	139.5	429.4	.9640	1.1884	162
163	142.7	.029230	.7084	1.412	290.5	139.2	429.7	.9650	1.1884	163
164	144.5	.029277	.6994	1.430	291.1	138.8	429.9	.9659	1.1885	164
165	146.3	0.29324	.6905	1.448	291.8	138.4	430.2	.9669	1.1885	165
166	148.1	.029372	.6818	1.467	292.3	138.1	430.4	.9679	1.1885	166
167	149.9	.029419	.6731	1.486	293.0	137.7	430.7	.9689	1.1886	167
168	151.8	.029467	.6646	1.505	293.7	137.3	431.0	.9699	1.1886	168
169	153.7	.029516	.6563	1.524	294.3	136.9	431.2	.9709	1.1887	169
170	155.5	.029565	.6480	1.543	294.9	136.5	431.4	.9719	1.1887	170
171	157.5	.029614	.6399	1.563	295.5	136.2	431.7	.9728	1.1887	171
172	159.4	.029665	.6318	1.583	296.2	135.8	432.0	.9738	1.1888	172
173	161.3	.029713	.6239	1.603	296.8	135.4	432.2	.9748	1.1888	173
174	163.3	.029763	.6161	1.623	297.4	135.0	432.4	.9758	1.1888	174
175	165.2	.029814	.6084	1.644	298.1	134.6	432.7	.9768	1.1889	175
176	167.2	.029865	.6008	1.664	298.8	134.2	433.0	.9778	1.1889	176
177	169.2	.029916	.5934	1.685	299.4	133.8	433.2	.9787	1.1890	177
178	171.3	.029968	.5860	1.707	300.0	133.4	433.4	.9797	1.1890	178
179	173.3	.030020	.5787	1.728	300.6	133.1	433.7	.9807	1.1890	179
180	175.4	.030072	.5715	1.750	301.3	132.6	433.9	.9817	1.1891	180
181	177.4	.030125	.5644	1.772	301.9	132.3	434.2	.9827	1.1891	181
182	179.5	.030178	.5575	1.794	302.5	131.9	434.4	.9837	1.1891	182
183	181.7	.030232	.5506	1.816	303.2	131.4	434.6	.9846	1.1892	183
184	183.8	.030286	.5438	1.839	303.9	131.0	434.9	.9856	1.1892	184
185	185.9	.030340	.5371	1.862	304.5	130.6	435.1	.9866	1.1892	185
186	188.1	.030395	.5305	1.885	305.2	130.2	435.4	.9876	1.1893	186
187	190.3	.030450	.5239	1.909	305.8	129.8	435.6	.9886	1.1893	187
188	192.5	.030506	.5175	1.932	306.4	129.4	435.8	.9896	1.1894	188
189	194.7	.030562	.5112	1.956	307.1	129.0	436.1	.9906	1.1894	189
190	197.0	.030619	.5049	1.981	307.7	128.6	436.3	.9915	1.1894	190
191	199.2	.030676	.4987	2.005	308.3	128.2	436.5	.9925	1.1895	191
192	201.5	.030734	.4926	2.030	309.1	127.7	436.8	.9935	1.1895	192
193	203.8	.030792	.4866	2.055	309.7	127.3	437.0	.9945	1.1895	193
194	206.1	.030850	.4806	2.081	310.3	126.9	437.2	.9955	1.1895	194
195	208.5	.030909	.4748	2.106	311.0	126.4	437.4	.9964	1.1896	195
196	210.9	.030969	.4690	2.132	311.7	126.0	437.7	.9974	1.1896	196
197	213.2	.031029	.4632	2.159	312.3	125.6	437.9	.9984	1.1896	197
198	215.6	.031090	.4576	2.185	313.0	125.1	438.1	.9994	1.1897	198
199	218.1	.031151	.4520	2.212	313.6	124.7	438.3	1.0004	1.1897	199
200	220.5	.031213	.4465	2.240	315	124	439	1.001	1.190	200
202	225.4	.031337	.4357	2.295	316	123	439	1.003	1.190	202
204	230.5	.031464	.4252	2.352	317	122	439	1.005	1.190	204
206	235.6	.031594	.4149	2.410	318	122	440	1.007	1.190	206
208	240.8	.031726	.4049	2.470	319	121	440	1.009	1.190	208
210	246.0	.031861	.3951	2.531	321	120	441	1.011	1.190	210
212	251.4	.031998	.3856	2.594	322	119	441	1.013	1.190	212
214	256.8	.032138	.3763	2.658	323	118	441	1.015	1.190	214
216	262.4	.032281	.3672	2.732	325	117	442	1.017	1.190	216
218	268.0	.012427	.3583	2.791	326	116	442	1.019	1.190	218
220	273.7	.032576	.3496	2.860	328	115	443	1.021	1.190	220
222	279.5	.012728	.3411	2.931	329	114	443	1.023	1.190	222
224	285.4	.032884	.3329	3.004	330	113	443	1.025	1.190	224
226	291.4	.033044	.3248	3.079	332	112	444	1.027	1.190	226
228	297.5	.033207	.3168	3.156	333	111	444	1.029	1.190	228

TABLE 2.—*Properties of saturated 1, 3-butadiene*—Continued

Temperature, t	Abs. pressure	Specific volume		Density vapor $1/v_g$	Enthalpy			Entropy		Temperature, t
		v_f	v_g		Liquid h_f	Evap. h_{fg}	Vapor h_g	Liquid s_f	Vapor s_g	
°F	lb/in.²	ft³/lb	ft³/lb	lb/ft³	Btu/lb	Btu/lb	Btu/lb	Btu/lb°R	Btu/lb°R	°F
230	303.7	0.03337	0.3091	3.235	334	110	444	1.031	1.190	230
232	310.0	.03354	.3015	3.317	336	109	445	1.033	1.190	232
234	316.3	.03372	.2941	3.400	338	107	445	1.035	1.190	234
236	322.8	.03390	.2868	3.487	339	106	445	1.037	1.190	236
238	329.4	.03408	.2797	3.575	341	105	446	1.039	1.190	238
240	336.1	.03427	.2727	3.667	342	104	446	1.041	1.190	240
242	342.9	.03447	.2659	3.761	343	103	446	1.043	1.190	242
244	349.8	.03467	.2592	3.858	344	102	446	1.045	1.189	244
246	356.8	.03488	.2526	3.959	347	100	447	1.047	1.189	246
248	363.9	.03509	.2462	4.062	348	99	447	1.049	1.189	248
250	371.1	.03531	.2398	4.170	349	98	447	1.051	1.189	250
252	378.5	.03554	.2336	4.281	351	96	447	1.053	1.189	252
254	385.9	.03578	.2274	4.397	352	95	447	1.055	1.189	254
256	393.5	.03603	.2214	4.517	354	94	448	1.057	1.188	256
258	401.2	.03628	.2155	4.640	356	92	448	1.059	1.188	258
260	409	.0365	.2097	4.770	357	91	448	1.062	1.188	260
262	417	.0368	.2039	4.904	359	89	448	1.064	1.187	262
264	425	.0371	.1982	5.045	360	88	448	1.066	1.187	264
266	433	.0374	.1926	5.192	362	86	448	1.068	1.187	266
268	441	.0377	.1870	5.347	364	84	448	1.070	1.186	268
270	450	.0381	.1815	5.51	365	83	448	1.073	1.186	270
272	459	.0384	.1761	5.68	367	81	448	1.075	1.185	272
274	467	.0388	.1707	5.86	369	79	448	1.077	1.185	274
276	476	.0392	.1653	6.05	370	77	447	1.079	1.184	276
278	485	.0396	.1599	6.25	372	75	447	1.082	1.183	278
280	494	.0401	.155	6.47	375	72	447	1.084	1.182	280
282	504	.0406	.149	6.71	376	70	446	1.087	1.181	282
284	513	.0411	.144	6.96	379	67	446	1.090	1.180	284
286	523	.0417	.138	7.24	380	65	445	1.092	1.179	286
288	533	.0424	.132	7.55	382	62	444	1.095	1.178	288

The values of enthalpy for the liquid have been given to hundredths of a Btu/lb where they were well supported by experimental data. In consequence of the rounding off of the values for the vapor and for evaporation, the latter may differ by one in the last place from the difference between the enthalpy of vapor and of liquid.

The values in the table and chart were calculated by methods described in a previous publication [8] after first converting the four empirical equations given in that publication to engineering units.

In computing the figures in the table from the empirical equations, all calculations were carried two digits beyond the number to be finally retained in the table. The values have been checked by differences.

The number of empirical equations used has been kept to a minimum, and exact thermodynamic relations have been used whenever possible. In consequence, the values given in the table are thermodynamically consistent.

In consideration of the large size of tables for superheated vapor and of the fact that the data for 1,3-butadiene can be represented on a chart nearly within the accuracy of the observed data, the properties of the superheated vapor are presented only in graphical form.

VI. Description of the Mollier Chart

Five properties, namely, temperature, pressure, specific volume, enthalpy, and entropy are useful in solving thermodynamic problems. These properties may be presented either in a table or on a chart such as first designed by Mollier [9]. Any two of the properties may be plotted as coordinates, but enthalpy usually is chosen as one coordinate as it is the property for which numerical values are of most interest. Any one of the other

four properties or a function thereof may be used for the other coordinate, depending upon the nature of the problems to be solved and the individual preference of the user. In the present instance, the use of the logarithm of pressure gives a constant percentage accuracy in reading the pressure and utilizes the rectangular paper efficiently. Usually all five properties are included, but for the sake of clarity, the constant volume lines have been omitted from the present Mollier chart. Values for the volume may be derived from figures 3, 4, and 5.

The logarithms of pressures from 3 to 300 lb/in.^{2} have been plotted as ordinates. Two scales along the abscissa have been used to represent enthalpies, the one at the left for the liquid, and the one at the right for the vapor. The curves representing the saturated vapor and the saturated liquid are so marked. The area to the left of the curve for saturated liquid represents the subcooled liquid for which no data are available. It should be noted that data for other substances indicate that the constant temperature lines are practically vertical over this area. The area between the curves for saturated liquid and for saturated vapor represents mixtures of vapor and liquid. It has not been charted and the distance between the two saturation lines has no physical significance. The area at the right represents superheated vapor up to 300° F.

The chart as originally drawn is 80 by 98 cm (approximately 31½ x 38½ in.). The mid points of each coordinate line were located by means of a beam compass and an accurate scale, and the coordinate lines drawn in by means of a parallel straight edge. Various checks indicate that the coordinates are drawn with an accuracy of 0.2 or 0.3 mm, corresponding to about 0.05 Btu/lb and to about two parts in 1,000 of the pressure.

Over 600 points were plotted so that each curve was drawn through a considerable number of suitably chosen points by means of a spline and weights. Errors in plotting larger than 0.2 or 0.3 mm became evident due to the difficulty of fitting the spline to the points with a reasonable number of weights. This estimate of the accuracy of plotting is supported by the fact that out of values read from 20 points on the original drawing, the largest discrepancy between the chart and calculated values was 0.05 Btu/lb (0.3 mm) and 0.0008 Btu/lb °R in entropy unit (0.3 mm).

VII. Use of Tables and Charts

The usefulness of the table and Mollier char is based largely on three properties of the therm dynamic function enthalpy (sometimes called hea content). The three properties referred to ar (1) In any process that occurs at constant pres sure the increase in enthalpy is equal to the hea added; (2) in adiabatic compression—that is, a constant entropy—the work done by the com pressor is equal to the change in enthalpy of th fluid between intake and discharge; and (3) in a throttling process, such as occurs at an expansio valve, the increase in enthalpy is equal to th heat added. Therefore, when no heat is adde the enthalpy is constant.

Two problems that illustrate the application o the three principles mentioned above, through us of the chart, will now be discussed.

Problem 1. Butadiene is admitted into a di tillation unit as liquid under an absolute pressur of about 80 lb/in.^{2} and at a temperature of 70° F It is to be converted under the same pressure t gas at 120° F. How much heat must be added pe pound of butadiene?

Due to lack of experimental data, the chart doe not give values of enthalpy for the subcoole liquid; but from data on other substances it may be inferred that the change of enthalpy with pressure for subcooled liquid butadiene at constan temperature is so small that for all practica purposes the value at 80 lb/in.^{2} absolute and 70° F is the same as the value 236.5 Btu/lb for satu rated liquid at 70° F. The chart indicates tha vapor leaving the still at 80 lb/in.^{2} absolut pressure and 120° F is practically saturated vapo and that its enthalpy is 418.2 Btu/lb. Th difference 418.2−236.5=181.7 Btu per lb mus be supplied to the butadiene. The answer shoul be affected only slightly by the presence of appreci able amounts of other C_4 hydrocarbons, as they have properties very similar to butadiene, but th presence of dissimilar compounds renders the answer unreliable in such problems. The heat of solution is involved in evaporation of mixtures that for dissimilar substances may differ appreci ably from the heat of evaporation for butadiene.

Although correct answers can be obtained only when these data are applied to the pure monomer

of 1,3-butadiene, yet in many of the problems to be solved, mixtures of the monomer with polymer or with other compounds are encountered. In some cases if the composition of the mixture is known, a judicious use of the chart may lead to a sufficiently approximate answer.

In the following problem, which involves such a mixture, the results of two methods of calculation with the use of the chart are compared with the results of a third method of calculation in which data are used from tables or charts appropriate for each component of the mixture.

The correct answer to this problem could be obtained only from measurements made on the mixture itself. Such data are rarely available, but the results obtained by the third method are believed to approach the correct answer most closely.

Problem 2. In some processes a gaseous mixture saturated with water vapor and containing about 90 percent of butadiene and 8 percent of ammonia is encountered. The initial temperature and pressure of this mixture will be assumed to be 78° F and 25 lb/in.^{2}, respectively. In actual practive the pressure of this mixture is increased only a few pounds per square inch through compression. We will assume for the present problem, however, a compression ratio of two, i. e. a discharge pressure of 50 lb/in.^{2}, for the sake of sizable differences on the Mollier chart that may be read with sufficient accuracy for the comparison of three methods of calculation. The problem will consist in finding (1) the work performed by the compressor (2) the temperature of the discharged gas and (3) the increase in work of compression caused by pressure drop through valves or other constrictions.

In the first method, the procedure is to calculate the results for pure butadiene as a rough approximation to the results for the mixture.

The initial condition is represented on the Mollier chart by the intersection between the pressure ordinate 25 lb/in.^{2} and the constant temperature 78° F interpolated between the dotted curves for 70° F and for 80° F. This intersection corresponds to an enthalpy of 408.0 Btu/lb and an entropy of 1.209. The intersection of this value for entropy with the pressure ordinate 50 lb/in.^{2} is at an enthalpy of 421.5 Btu/lb and a temperature of 120° F. Then for pure butadiene (1) the work of compression is 421.5—408.0=13.5 Btu/lb and (2) the discharge temperature is 120° F.

A second method, which gives a better estimate of the work of compression, uses the chart by taking account of the fact that for equal compression ratios with the same inlet temperature, the work of compression per mole varies only 10 or 20 percent from substance to substance, whereas the work per unit mass varies over a wide range. On the molar basis the calculation is as follows:

0.9 lb butadiene = 0.9/54 = 0.01665 lb mole.
0.08 lb ammonia = 0.08/17 = 0.00471 lb mole.
0.02 lb water = 0.02/18 = 0.00111 lb mole.

Total ..... 0.02247 lb mole.

1 lb butadiene = 1/54 = 0.01852 mole.

Work of compression for 1 lb of mixture is

$$13.5 \times 0.02247/0.01852 = 16.4 \text{ Btu/lb.}$$

The third and probably the best method for estimating the work of compression is to sum up the work for compressing the various components separately through the same compression ratio from their initial partial pressures. Fortunately, such procedure is possible for the mixture presented in this problem, as tables of the properties of ammonia [10] and of steam [11] are both available.

The partial pressures are for butadiene 22.5 lb/in.^{2}, for ammonia 2.0 lb/in.^{2}, and for water the saturation pressure at 78° F, which is given by Keenan and Keyes in their table 1 as 0.4747 lb/in.^{2} Using the same procedure as before for butadiene at 25 lb/in.^{2} initial pressure, and the same initial temperature 78° F and compression ratio, two, one finds the same values for the work and the discharge temperature, for example, 13.5 Btu/lb and 120° F, respectively.

The ammonia tables mentioned do not include pressures below 5 lb/in.^{2} but the work of compression for a compression ratio of 2 and initial temperature 78° F is nearly independent of initial pressure. For initial pressures of 5 and10 lb/in.^{2}, the work of compression is respectively 46.8 and 46.7 Btu/lb, the discharge temperature in both cases being 170.5° F. One may assume the work of compression to be 46.8 Btu/lb for an initial pressure of 2 lb/in.^{2}, and the discharge temperature 170° F.

The steam tables by Keenan and Keyes give

for the enthalpy and entropy of saturated steam at 78° F, respectively 1,095.8 Btu/lb and 2.0416 Btu/lb °R. The discharge pressure is 2 x 0.4747 = 0.95 lb/in.². For convenience we will use the rounded pressure 1 lb/in.². The enthalpy and temperature corresponding to an entropy of 2.0416 and a pressure of 1 lb/in.² are 1144.1 Btu/lb and 186° F, respectively. The work is then 1144.1 − 1095.8 = 48.3 Btu/lb.

The work of compression for the mixture is then,

$$(0.9\times 13.5)+(0.08\times 46.8)+(0.02\times 48.3)=$$
$$16.8 \text{ Btu/lb},$$

and the discharge temperature is,

$$(0.9\times(120-78))+(0.08\times(170-78))+$$
$$(0.02\times(186-78))+78=125^\circ \text{ F}.$$

We now have three values calculated for the work of compression, namely:

(1) For pure butadiene, 13.5 Btu/lb.

(2) For the mixture, using the chart for butadiene together with the assumption that the work of compression per mole is the same for different substances, 16.4 Btu/lb.

(3) For the mixture using the appropriate chart or table for each component of the mixture, 16.8 Btu/lb.

This last method would be expected to give the nearest to the correct answer, but cannot always be used as data may be lacking on some of the components.

The discharge temperature (120° F) for pure butadiene is in this case lower than that (125° F) for the mixture. This is due to the fact that the molar specific heats of ammonia and steam are less than that for butadiene.

The additional work that the compressor must perform in consequence of a pressure drop due to throttling through valves or other constrictions may be estimated by employing the third property previously mentioned for enthalpy, i. e. the constancy of enthalpy during a throttling process when no heat is added or removed. The loss is very nearly proportional to the pressure drop and may be calculated by multiplying the work per (lb/in.²) by the pressure drop. If on the Mollier chart we follow from the point representing intake conditions (78° F and 25 lb/in.²) downward along the constant enthalpy abscissa (408.0 Btu/lb) to 24 lb/in.,² the new entropy is 1.210. If this constant entropy line is followed back to 25 lb/in.² an enthalpy of (409.0 Btu/lb) is obtained. The additional work that the compressor must perform in consequence of a 1 lb/in.² pressure drop in the suction line is 409 − 408 = 1 Btu/lb. By a similar process one finds that 1 lb/in.² pressure drop on the discharge side where the pressure is 50 lb/in.² causes the compressor to perform extra work amounting to 0.5 Btu/lb. In the case where the total compression amounts to only a few pounds, losses due to pressure drop may become an important portion of the whole.

VIII. Graphs of Certain Properties of 1, 3-Butadiene

A number of smaller graphs of the properties of butadiene are presented in this publication (1) to furnish data not readable directly from the Mollier chart and (2) to give the reader a clearer picture of the basis for, and relationships between these data. Figure 1 in which enthalpy (Btu/lb) is plotted vs temperature (°F) is especially in the latter class.

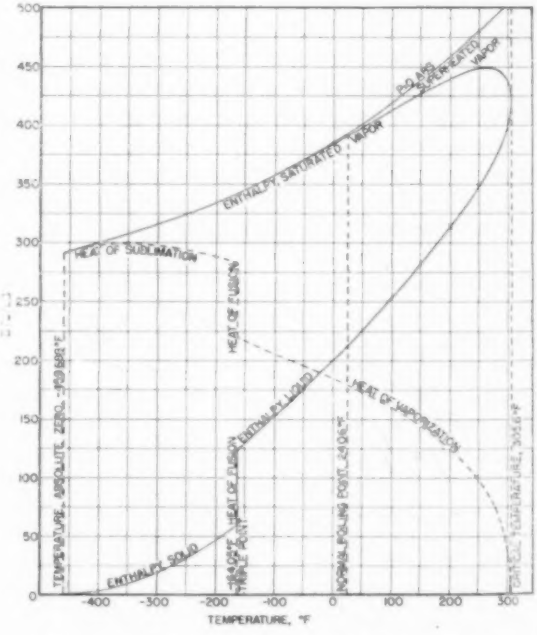

FIGURE 1.—*Enthalpy of saturated 1, 3-butadiene.*

As will be noted in this figure, the value for the enthalpy of the crystalline solid has been taken as zero. This has been done for two reasons, namely, (1) except in problems involving chemical reactions no negative numbers are encountered with such choice (2) as many of the theoretical calculations of thermodynamics are based on the theorem that the entropy of crystalline substances is zero at the absolute zero of temperature, the zero for entropy was chosen for this state, and it seemed appropriate to assume the same state for the zero of enthalpy.

This choice of zero state is satisfactory for all the problems for which this publication was designed. A value for the heat of formation from the elements [12] may be added to the enthalpies used here, but its assignment was considered beyond the scope of this publication. As illustrated by the continuous curve in the lower left hand corner of figure 1, the enthalpy for solid butadiene gradually increases with temperature up to the triple point (—164.05° F) then increases through fusion to liquid without any change in temperature. When the liquid is warmed, the enthalpy again changes with temperature at a rate that gradually increases. The normal boiling point is reached at 24.06° F, in other words the vapor pressure has increased to one standard atmosphere. With further warming of the liquid, the enthalpy continued to increase at a rate that becomes infinite at the critical temperature 305.6° F, although the enthalpy itself is finite (about 421 Btu/lb).

The heat of vaporization is zero at the critical temperature, but increases to finite values as the temperature is decreased (see dotted curve fig. 1). The rate of increase at the critical is infinite but finite at lower temperatures. At the triple point the heat of sublimation exceeds the heat of vaporization by an amount equal to the heat of fusion. At lower temperatures the heat of sublimation increases to a maximum and then decreases. As near as can be deduced from values of $C_p°$ from this formulation [8] together with the assumption that $C_p°$ for the vapor approaches asymptotically toward $4R$ at absolute zero, the enthalpy of the vapor and consequently the heat of sublimation at absolute zero is about 287 Btu/lb. The enthalpy of the saturated vapor is the sum of the enthalpy for the solid and heat of sublimation, or at higher temperatures the sum of the enthalpy for the liquid and the heat of vaporization. The enthalpy of saturated vapor increases with temperature without any break at the triple point, passes through a maximum at about 265° F and joins up with the enthalpy of the liquid at the critical temperature. The enthalpy of the vapor at zero pressure, which is the same as that at the standard state (ideal gas at 1 atmos), is not distinguishable from the enthalpy of the saturated vapor at low temperatures, but at higher temperatures the difference calculated from the equation of state increases so that the enthalpy at $p=0$ increases steadily with temperature without any peculiar turn at the critical temperature as exhibited for the saturated vapor.

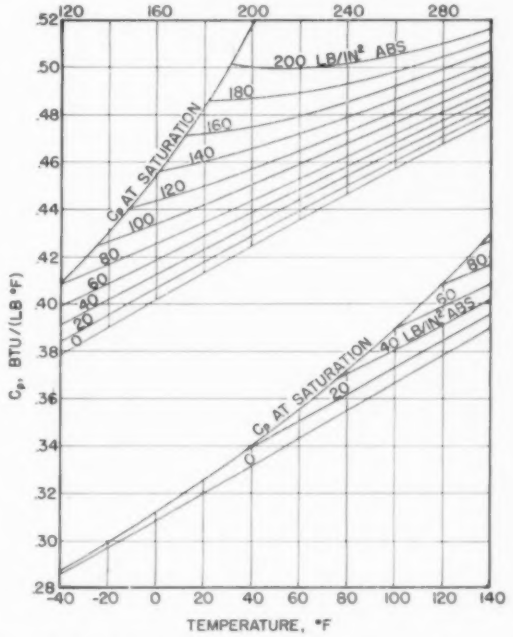

FIGURE 2.—*Specific heat at constant pressure of gaseous 1, 3-butadiene.*

Figure 2 is a plot of C_p the specific heat of the vapor at various pressures from 0 absolute to 200 lb/in.² abs as a function of temperature expressed in degrees F. The values of C_p at zero pressure are calculable from spectroscopic data but were actually calculated from an empirical equation [8] and the values at other pressures can be deduced from these by using the equation of state. The temperatures at the bottom of the graph apply to the lower set of curves, those at the

top to the upper set, with the two sets overlapping in the range 120° to 140° F. The curve for 200 lb/in.^{2} shows a minimum in C_p for the vapor, and if the curves were computed for higher pressures, these minimums would be more pronounced.

Figure 3 shows values of the quantity Pv/RT (which is unity for an ideal gas) as a function of pressure for saturated vapor and for superheated vapor at various temperatures. It may be noted that at the highest pressure plotted, 120 lbs/in^2 the value of Pv for saturated vapor is more than 16 percent less than the value for an ideal gas, but that at low pressure, the values of Pv approach RT, the approach being closer for the higher temperatures.

Figure 4 is a plot of the quantity $\frac{1-Pv/RT}{P(lbs/in^2)}10^4$

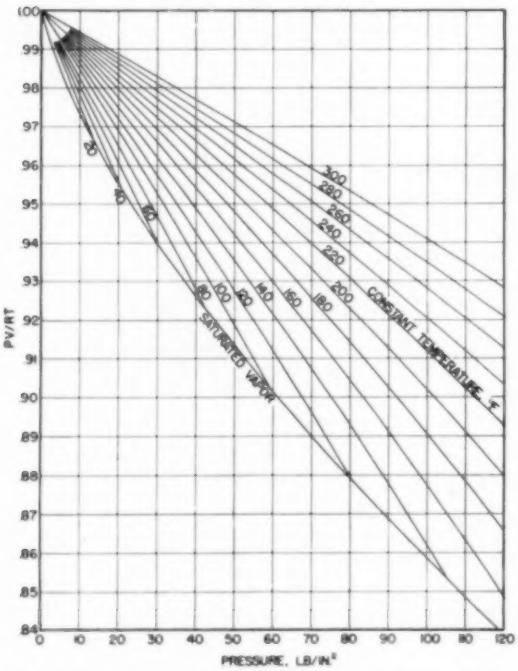

FIGURE 3.—*Pressure-volume-temperature relations for gaseous 1, 3-butadiene.*

(which is equal to zero for an ideal gas) for the vapor, as a function of the absolute pressure for various temperatures from −40° to 180° F. The quantity plotted never reaches the value for an ideal gas, but approaches it as the pressure is decreased or as the temperature is raised.

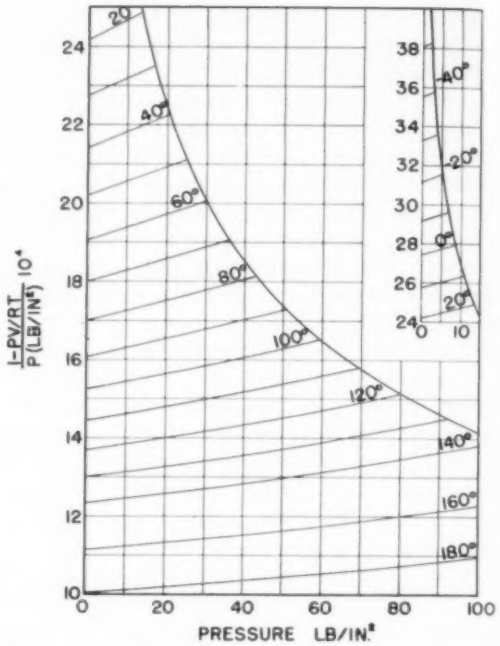

FIGURE 4.—*Pressure-volume-temperature relations for gaseous 1, 3-butadiene.*

For use at higher pressures and temperatures the coordinates used in figure 4 require too large a page for accurate presentation of the data. This difficulty is overcome in figure 5 by plotting the product $\frac{1-Pv/RT}{P(\text{lb/in.}^2)}\left(\frac{T}{100}\right)^3$ as ordinate vs pressure as abscissa. Through the use of these coordinates accurate values of Pv/RT may be obtained over the whole pressure and temperature range although more calculation is involved than in using figure 4. The isotherms cross each other as well as the saturation curve at low pressures and temperatures. In this region the isotherms have been omitted and the use of figure 4 will be less ambiguous.

An acknowledgment with thanks is given to Martin T. Wechsler for calculating the values appearing in the table and to Robert E. McCoskey for calculating the data needed for the Mollier chart and for drawing this chart.

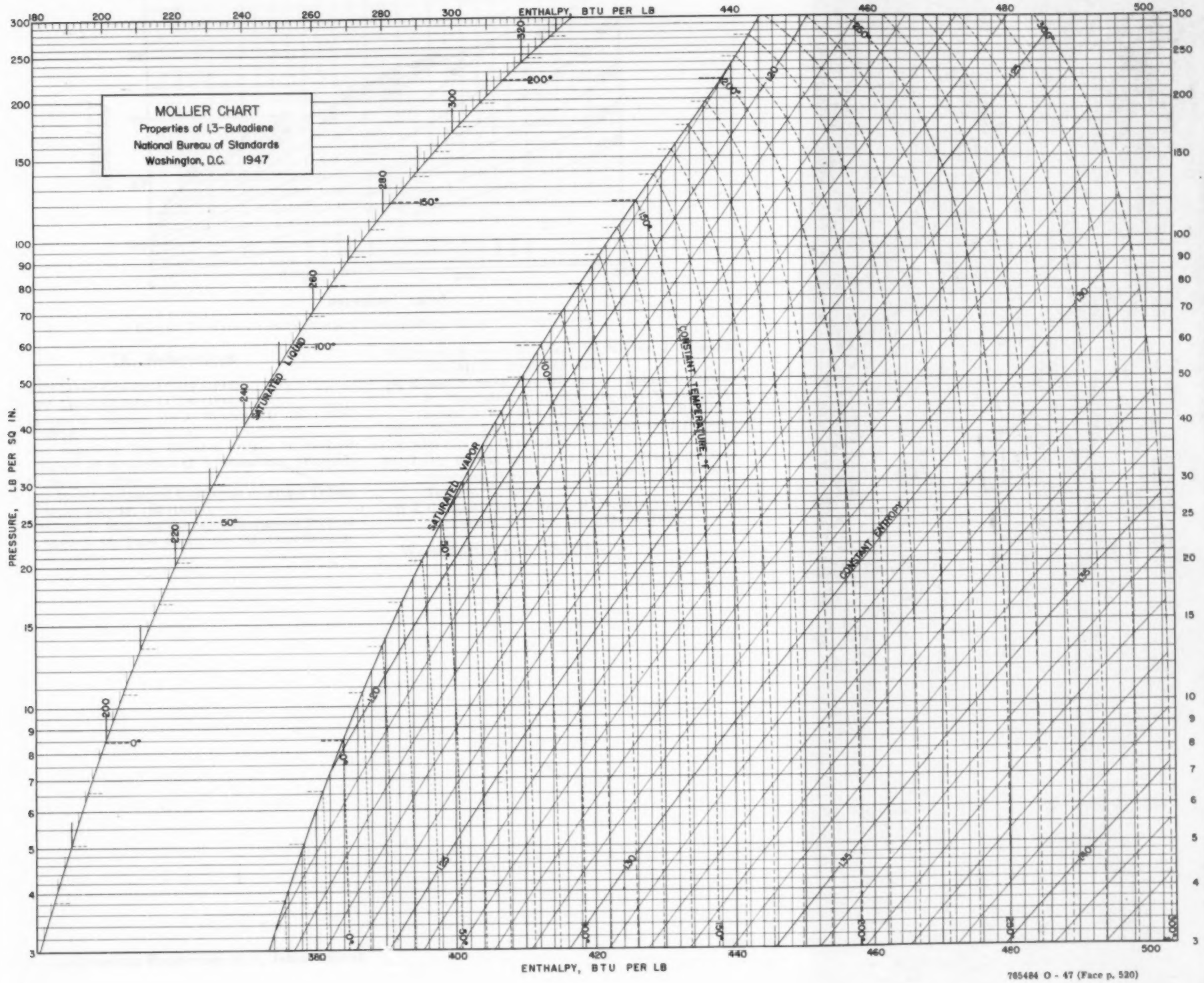

765484 O - 47 (Face p. 520)

[1] N
[2] N
[3] C
[4] A
[5] T
[6] T

The

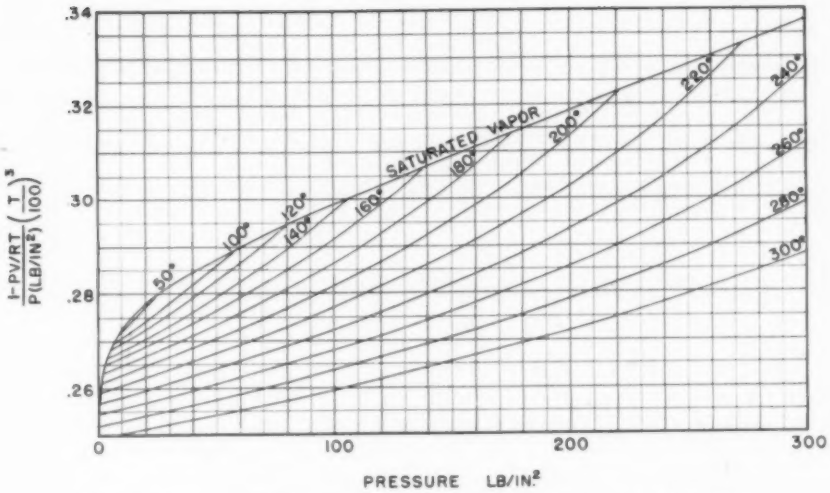

FIGURE 5.—*Pressure-volume-temperature relations for gaseous 1, 3-butadiene.*

IX. References

[1] NBS Letter Circular LC710 (1942).

[2] NBS Letter Circular LC736 (1943).

[3] George K. Burgess, BS J. Research **1,** 635 (1928) RP22.

[4] Am. Petroleum Inst. Research Project 44, Selected values of properties of hydrocarbons (Revised, March 31, 1945).

[5] The First International Conference on Steam Tables, Mech. Eng. **52,** 120 (1930).

[6] Travaux at Memories Bureau International Poids et Mesures **12,** Third Conference Int. Committee, p. 66 (1902).

[7] Russell B. Scott and Jane W. Mellors, J. Research NBS **34,** 243 (1945) RP1640.

[8] Russell B. Scott, Cyril H. Meyers, Robert D. Rands, Jr., Ferdinand G. Brickwedde, and Norman Bekkedahl, J. Research NBS **35,** 39 (1945) RP1661.

[9] R. Mollier, Zts. d Ver. Deutscher Ing. **48,** 271 (1904).

[10] NBS Circular C142 (1923).

[11] J. H. Keenan and F. G. Keyes, Thermodynamic properties of steam (John Wiley and Sons, New York, N. Y., 1936).

[12] J. G. Aston, George Szasz, H. W. Woolley, and F. G. Brickwedde, J. Chem. Phys. **14,** 67 (1946).

WASHINGTON, July 28, 1947.

U. S. Department of Commerce
National Bureau of Standards

Research Paper RP1845
Volume 39, December 1947

Part of the Journal of Research of the National Bureau of Standards.

Heats, Equilibrium Constants, and Free Energies of Formation of the Alkylcyclopentanes and Alkylcyclohexanes*[1]

By John E. Kilpatrick,[2] Helene G. Werner,[2] Charles W. Beckett,[3] Kenneth S. Pitzer,[4] and Frederick D. Rossini [5]

For cyclopentane, cyclohexane, the seven dimethylcyclohexanes, and the normal alkylcyclopentanes and alkylcyclohexanes, values are presented for the following thermodynamic properties to 1,000° or 1,500°K: The heat of formation from the elements; the free energy of formation from the elements; and the logarithm of the equilibrium constant of formation from the elements. For cyclopentane, cyclohexane, and the normal alkylcyclopentanes and alkylcyclohexanes, values are also given to 1,500°K, for the following properties: The heat-content function; the free-energy function; the entropy; the heat content; and the heat capacity.

Equilibrium constants and concentrations are given in tabular and graphical form for some reactions of isomerization, hydrogenation, and cyclization.

I. Introduction

As a part of the work of the American Petroleum Institute Research Project 44 at the National Bureau of Standards and the University of California, values have been calculated for the heat-content function, free-energy function, entropy, heat content and heat capacity of the normal alkylcyclopentanes and the normal alkylcyclohexanes above ethylcyclohexane, in the gaseous state to 1,500° K. These data, together with previously published data on cyclopentane, cyclohexane, methylcyclohexane, and ethylcyclohexane, have been combined with values of the heats of formation at 25° C to calculate values of the heats, free energies, and equilibrium constants of formation of 17 alkylcyclopentanes and 24 alkylcyclohexanes. The free energies and equilibrium constants of a number of reactions involving these compounds have been calculated.

II. Fundamental Constants

The unit of energy, atomic weights, and values of the fundamental constants used in this report are the same as those previously used [5, 13][6].

III. Heat-Content Function, Free-Energy Function, Entropy, Heat Content, and Heat Capacity

1. Method and Data Used in the Calculations

For cyclopentane, cyclohexane, methylcyclohexane, ethylcyclohexane, and the seven dimethylcyclohexanes, the values were taken from references [1, 2].

For methylcyclopentane, the thermodynamic functions were calculated by means of the following relation:

$$[\text{methylcyclopentane}] = [\text{cyclopentane}] + [\text{methyl}] + [\text{restricted rotation of ring puckering}] + (R \ln 10). \quad (1)$$

The terms written in brackets represent a given thermodynamic function of the indicated sub-

* Presented before the Division of Physical and Inorganic Chemistry of the American Chemical Society at New York, N. Y., Sept. 1947.

[1] This investigation was performed as a part of the work of the American Petroleum Institute Research Project 44 at the National Bureau of Standards.

[2] Research Associate on the American Petroleum Institute Research Project 44 at the National Bureau of Standards.

[3] Research Associate on the American Petroleum Research Project 44 at the University of California at Berkeley, Calif.

[4] Associate Director of the American Petroleum Institute Research Project 44; Professor of Chemistry at the University of California, Berkeley, Calif.

[5] Director of the American Petroleum Institute Research Project 44 at the National Bureau of Standards.

[6] Figures in brackets indicate the literature references at the end of the paper.

stance. In eq 1, the term [methyl] represents the contribution (vibration and restricted rotation) of the methyl group and was calculated by the following relation:

$$[\text{methyl}] = [\text{methylcyclohexane}] - [\text{steric factor}] - [\text{cyclohexane}] - (R \ln 6). \quad (2)$$

In eq 2, the term [steric factor] is the contribution of the equatorial-polar tautomerism of methylcyclohexane to its thermodynamic functions. The term [methyl] is therefore the difference between the functions of methylcyclohexane and cyclohexane, without the inclusion of the effects of tautomerism and of symmetry number. The symmetry number corrections, which are written in parentheses, are to be used for the negative of the free-energy function, $-(F-H_0^\circ)/T$, and for the entropy, S°, but not for the other functions.

The term [restricted rotation of ring puckering] is the contribution arising from a restricting barrier of 750 cal/mole from the asymmetry induced by the presence of the methyl group on the ring. See reference [1] for details. A classical partition function was used.

The thermodynamic functions of ethylcyclopentane were calculated from the following relation:

$$[\text{ethylcyclopentane}] = [\text{methylcyclopentane}] + [\text{2-methylbutane}] - [\text{2-methylpropane}] - (R \ln 3). \quad (3)$$

For normal propylcyclopentane and each of the higher normal alkylcyclopentanes, the following relation, with the appropriate number of CH_2 groups, was used to calculate the thermodynamic functions:

$$[\text{normal alkylcyclopentane}] = [\text{ethylcyclopentane}] + n\ [\text{CH}_2]. \quad (4)$$

The thermodynamic functions of normal propylcyclohexane were calculated from the following relation:

$$[\text{normal propylcyclohexane}] = [\text{ethylcyclohexane}] + [\text{2-methylpentane}] - [\text{2-methylbutane}]. \quad (5)$$

In the case of normal butylcyclohexane and the higher normal alkylcyclohexanes, a relation similar to eq 4 was used:

$$[\text{normal alkylcyclohexane}] = [\text{normal propylcyclohexane}] + n\ [\text{CH}_2]. \quad (6)$$

The thermodynamic functions of the paraffin hydrocarbons and of the CH_2 increment that are used in eq 3 to 6 are taken from reference [14].

2. Results

The resulting values of the thermodynamic properties for the normal alkylcyclopentanes and alkylcyclohexanes are presented in tables 1 to 10, which give values of the following properties: Heat-content function, $(H^\circ-H_0^\circ)/T$; free-energy function, $(F^\circ-H_0^\circ)/T$; entropy, S°; heat content, $H^\circ-H_0^\circ$; and heat capacity, C_p°.

TABLE 1.—*Values of the heat content function, for the ideal gaseous state, to 1,500° K, for the normal alkylcyclopentanes*

Compound (gas)	Formula	Temperature in °K														
		0	298.16	300	400	500	600	700	800	900	1,000	1,100	1,200	1,300	1,400	1,500
		Heat content function $(H°-H°_0)/T$, in cal/deg mole														
Cyclopentane	C_5H_{10}	0	12.07	12.12	15.12	18.52	21.98	25.29	28.40	31.29	33.97	36.46	38.75	40.87	42.83	44.65
Methylcyclopentane	C_6H_{12}	0	16.01	16.09	19.88	24.03	28.17	32.09	35.75	39.15	42.28	45.18	47.87	50.34	52.62	54.74
Ethylcyclopentane	C_7H_{14}	0	18.91	19.01	23.70	28.66	33.55	38.16	42.43	46.38	50.00	53.36	56.47	59.32	61.96	64.40
n-Propylcyclopentane	C_8H_{16}	0	22.34	22.46	27.9	33.6	39.1	44.4	49.2	53.7	57.8	61.6	65.1	68.3	71.3	74.1
n-Butylcyclopentane	C_9H_{18}	0	25.77	25.90	32.1	38.5	44.7	50.6	56.0	61.0	65.6	69.8	73.7	77.3	80.6	83.7
n-Pentylcyclopentane	$C_{10}H_{20}$	0	29.20	29.35	36.3	43.4	50.3	56.8	62.8	68.3	73.3	78.0	82.3	86.3	90.0	93.4
n-Hexylcyclopentane	$C_{11}H_{22}$	0	32.63	32.80	40.5	48.3	55.9	63.0	69.5	75.6	81.1	86.2	91.0	95.3	99.4	103.0
n-Heptylcyclopentane	$C_{12}H_{24}$	0	36.06	36.24	44.8	53.2	61.5	69.2	76.3	82.8	88.9	94.4	99.6	104.3	108.7	112.7
n-Octylcyclopentane	$C_{13}H_{26}$	0	39.49	39.69	49.0	58.2	67.1	75.4	83.1	90.1	96.6	102.6	108.2	113.3	118.0	122.4
n-Nonylcyclopentane	$C_{14}H_{28}$	0	42.92	43.14	53.2	63.1	72.7	81.6	89.9	97.4	104.4	110.8	116.8	122.3	127.4	132.0
n-Decylcyclopentane	$C_{15}H_{30}$	0	46.35	46.59	57.4	68.0	78.2	87.9	96.6	104.7	112.2	119.1	125.4	131.3	136.7	141.7
n-Undecylcyclopentane	$C_{16}H_{32}$	0	49.78	50.03	61.6	72.9	83.8	94.1	103.4	112.0	120.0	127.3	134.0	140.3	146.1	151.3
n-Dodecylcyclopentane	$C_{17}H_{34}$	0	53.21	53.48	65.8	77.8	89.4	100.3	110.2	119.3	127.7	135.5	142.7	149.3	155.4	161.0
n-Tridecylcyclopentane	$C_{18}H_{36}$	0	56.64	56.93	70.0	82.8	95.0	106.5	117.0	126.6	135.5	143.7	151.3	158.3	164.8	170.7
n-Tetradecylcyclopentane	$C_{19}H_{38}$	0	60.07	60.37	74.2	87.7	100.6	112.7	123.8	133.9	143.3	151.9	159.9	167.3	174.1	180.3
n-Pentadecylcyclopentane	$C_{20}H_{40}$	0	63.50	63.82	78.4	92.6	106.2	118.9	130.5	141.2	151.0	160.1	168.5	176.3	183.5	190.0
n-Hexadecylcyclopentane	$C_{21}H_{42}$	0	66.93	67.27	82.6	97.5	111.8	125.1	137.3	148.5	158.8	168.3	177.2	185.3	192.8	199.6
Increment per CH_2 group	.....	0	3.430	3.447	4.21	4.92	5.59	6.21	6.78	7.29	7.77	8.21	8.62	9.00	9.35	9.66

TABLE 2.—*Values of the heat content function, for the ideal gaseous state, to 1,500° K, for the normal alkylcyclohexanes*

Compound (gas)	Formula	Temperature in °K														
		0	298.16	300	400	500	600	700	800	900	1,000	1,100	1,200	1,300	1,400	1,500
		Heat content function $(H°-H°_0)/T$, in cal/deg mole														
Cyclohexane	C_6H_{12}	0	14.21	14.28	18.38	22.85	27.34	31.64	35.67	39.40	42.85	46.0	48.9	51.6	54.0	56.3
Methylcyclohexane	C_7H_{14}	0	17.55	17.66	22.84	28.26	33.53	38.53	43.16	47.42	51.33	54.9	58.2	61.2	64.0	66.5
Ethylcyclohexane	C_8H_{16}	0	20.45	20.58	26.7	32.9	38.9	44.6	49.9	54.7	59.1	63.1	66.8	70.2	73.3	76.2
n-Propylcyclohexane	C_9H_{18}	0	23.66	23.81	30.6	37.7	44.3	50.6	56.4	61.8	66.7	71.3	75.4	79.2	82.6	85.9
n-Butylcyclohexane	$C_{10}H_{20}$	0	27.09	27.26	34.8	42.6	50.0	56.8	63.2	69.1	74.5	79.5	84.0	88.2	92.0	95.5
n-Pentylcyclohexane	$C_{11}H_{22}$	0	30.52	30.70	39.0	47.5	55.5	63.0	70.0	76.4	82.2	87.7	92.7	97.2	101.3	105.2
n-Hexylcyclohexane	$C_{12}H_{24}$	0	33.95	34.15	43.2	52.5	61.1	69.2	76.7	83.7	90.0	96.0	101.3	106.2	110.7	114.8
n-Heptylcyclohexane	$C_{13}H_{26}$	0	37.38	37.60	47.4	57.4	66.6	75.5	83.5	91.0	97.8	104.2	109.9	115.2	120.0	124.5
n-Octylcyclohexane	$C_{14}H_{28}$	0	40.81	41.05	51.6	62.3	72.2	81.7	90.3	98.3	105.6	112.4	118.5	124.2	129.4	134.2
n-Nonylcyclohexane	$C_{15}H_{30}$	0	44.24	44.49	55.9	67.2	77.8	87.9	97.1	105.6	113.3	120.6	127.1	133.2	138.7	143.8
n-Decylcyclohexane	$C_{16}H_{32}$	0	47.67	47.94	60.1	72.1	83.4	94.1	103.8	112.9	121.1	128.8	135.8	142.2	148.1	153.5
n-Undecylcyclohexane	$C_{17}H_{34}$	0	51.10	51.39	64.3	77.0	89.0	100.3	110.6	120.1	128.9	137.0	144.4	151.2	157.4	163.1
n-Dodecylcyclohexane	$C_{18}H_{36}$	0	54.53	54.83	68.5	82.0	94.6	106.5	117.4	127.4	136.7	145.2	153.0	160.2	166.8	172.8
n-Tridecylcyclohexane	$C_{19}H_{38}$	0	57.96	58.28	72.7	86.9	100.2	112.7	124.2	134.7	144.4	153.4	161.6	169.2	176.1	182.5
n-Tetradecylcyclohexane	$C_{20}H_{40}$	0	61.39	61.73	76.9	91.8	105.8	118.9	130.9	142.0	152.2	161.7	170.2	178.2	185.5	192.1
n-Pentadecylcyclohexane	$C_{21}H_{42}$	0	64.82	65.17	81.1	96.7	111.3	125.2	137.7	149.3	160.0	169.9	178.9	187.2	194.8	201.8
n-Hexadecylcyclohexane	$C_{22}H_{44}$	0	68.25	68.62	85.3	101.6	116.9	131.4	144.5	156.6	167.7	178.1	187.5	196.2	204.2	211.4
Increment per CH_2 group	.....	0	3.430	3.447	4.21	4.92	5.59	6.21	6.78	7.29	7.77	8.21	8.62	9.00	9.35	9.66

765484—47——4

TABLE 3.—*Values of the free energy function, for the ideal gaseous state, to 1,500° K, for the normal alkylcyclopentanes*

Compound (gas)	Formula	Temperature in ° K														
		0	298.16	300	400	500	600	700	800	900	1,000	1,100	1,200	1,300	1,400	1,500
		Free energy function $(F^\circ - H^\circ_0)/T$, in cal/deg mole														
Cyclopentane	C_5H_{10}	0	−57.93	−58.00	−61.88	−65.62	−69.30	−72.95	−76.52	−80.04	−83.48	−86.84	−90.13	−93.31	−96.40	−99.42
Methylcyclopentane	C_6H_{12}	0	−65.23	−65.33	−70.45	−75.33	−80.07	−84.72	−89.26	−93.68	−97.97	−102.13	−106.18	−110.08	−113.89	−117.63
Ethylcyclopentane	C_7H_{14}	0	−71.71	−71.83	−77.90	−83.72	−89.34	−94.89	−100.30	−105.53	−110.62	−115.54	−120.32	−124.97	−129.41	−133.79
n-Propylcyclopentane	C_8H_{16}	0	−77.46	−77.61	−84.8	−91.6	−98.2	−104.6	−110.9	−117.0	−122.9	−128.6	−134.1	−139.4	−144.5	−149.6
n-Butylcyclopentane	C_9H_{18}	0	−83.22	−83.38	−91.6	−99.5	−107.0	−114.4	−121.6	−128.4	−135.1	−141.6	−147.8	−153.9	−159.7	−165.3
n-Pentylcyclopentane	$C_{10}H_{20}$	0	−88.97	−89.16	−98.5	−107.4	−115.9	−124.2	−132.2	−139.9	−147.4	−154.6	−161.6	−168.4	−174.8	−181.1
n-Hexylcyclopentane	$C_{11}H_{22}$	0	−94.72	−94.94	−105.4	−115.3	−124.7	−133.9	−142.8	−151.4	−159.6	−167.6	−175.4	−182.8	−189.9	−196.9
n-Heptylcyclopentane	$C_{12}H_{24}$	0	−100.48	−100.72	−112.2	−123.2	−133.6	−143.7	−153.4	−162.8	−171.9	−180.7	−189.1	−197.3	−205.1	−212.6
n-Octylcyclopentane	$C_{13}H_{26}$	0	−106.23	−106.49	−119.1	−131.0	−142.4	−153.4	−164.1	−174.3	−184.2	−193.7	−202.9	−211.8	−220.2	−228.4
n-Nonylcyclopentane	$C_{14}H_{28}$	0	−111.98	−112.27	−126.0	−138.9	−151.2	−163.2	−174.7	−185.8	−196.4	−206.7	−216.6	−226.2	−235.3	−244.2
n-Decylcyclopentane	$C_{15}H_{30}$	0	−117.73	−118.05	−132.8	−146.8	−160.1	−172.9	−185.3	−197.2	−208.7	−219.7	−230.4	−240.7	−250.5	−259.9
n-Undecylcyclopentane	$C_{16}H_{32}$	0	−123.49	−123.82	−139.7	−154.7	−168.9	−182.7	−195.9	−208.7	−220.9	−232.8	−244.2	−255.1	−265.6	−275.7
n-Dodecylcyclopentane	$C_{17}H_{34}$	0	−129.24	−129.60	−146.6	−162.6	−177.8	−192.4	−206.6	−220.1	−233.2	−245.8	−257.9	−269.6	−280.7	−291.5
n-Tridecylcyclopentane	$C_{18}H_{36}$	0	−134.99	−135.38	−153.4	−170.5	−186.6	−202.2	−217.2	−231.6	−245.4	−258.8	−271.7	−284.1	−295.9	−307.2
n-Tetradecylcyclopentane	$C_{19}H_{38}$	0	−140.75	−141.15	−160.3	−178.4	−195.5	−211.9	−227.8	−243.0	−257.7	−271.8	−285.4	−298.5	−311.0	−323.0
n-Pentadecylcyclopentane	$C_{20}H_{40}$	0	−146.50	−146.93	−167.2	−186.2	−204.3	−221.7	−238.4	−254.5	−270.0	−284.8	−299.2	−313.0	−326.1	−338.8
n-Hexadecylcyclopentane	$C_{21}H_{42}$	0	−152.25	−152.71	−174.0	−194.1	−213.1	−231.4	−249.1	−266.0	−282.2	−297.9	−313.0	−327.4	−341.3	−354.5
Increment per CH_2 group		0	−5.753	−5.777	−6.87	−7.89	−8.84	−9.75	−10.63	−11.46	−12.26	−13.02	−13.76	−14.46	−15.13	−15.77

TABLE 4.—*Values of the free energy function, for the ideal gaseous state, to 1,500° K, for the normal alkylcyclohexanes*

Compound (gas)	Formula	Temperature in ° K														
		0	298.16	300	400	500	600	700	800	900	1,000	1,100	1,200	1,300	1,400	1,500
		Free energy function $(F^\circ - H^\circ_0)/T$, in cal/deg mole														
Cyclohexane	C_6H_{12}	0	−57.07	−57.16	−61.80	−66.39	−70.96	−75.50	−79.98	−84.40	−88.74	−93.0	−97.1	−101.1	−105.0	−108.8
Methylcyclohexane	C_7H_{14}	0	−64.51	−64.62	−70.38	−76.06	−81.68	−87.24	−92.70	−98.04	−103.24	−108.3	−113.2	−118.0	−122.6	−127.1
Ethylcyclohexane	C_8H_{16}	0	−70.99	−71.12	−77.8	−84.5	−91.0	−97.4	−103.7	−109.9	−115.9	−121.7	−127.3	−132.8	−138.1	−143.3
n-Propylcyclohexane	C_9H_{18}	0	−76.45	−76.62	−84.4	−91.9	−99.4	−106.7	−113.9	−120.9	−127.7	−134.2	−140.5	−146.8	−152.7	−158.5
n-Butylcyclohexane	$C_{10}H_{20}$	0	−82.20	−82.40	−91.3	−99.8	−108.2	−116.5	−124.5	−132.4	−140.0	−147.2	−154.3	−161.3	−167.8	−174.3
n-Pentylcyclohexane	$C_{11}H_{22}$	0	−87.96	−88.17	−98.1	−107.7	−117.1	−126.2	−135.2	−143.8	−152.2	−160.2	−168.0	−175.7	−183.0	−190.0
n-Hexylcyclohexane	$C_{12}H_{24}$	0	−93.71	−93.95	−105.0	−115.6	−125.9	−136.0	−145.8	−155.3	−164.5	−173.3	−181.8	−190.2	−198.1	−205.8
n-Heptylcyclohexane	$C_{13}H_{26}$	0	−99.46	−99.73	−111.9	−123.4	−134.8	−145.7	−156.4	−166.7	−176.7	−186.3	−195.5	−204.7	−213.2	−221.6
n-Octylcyclohexane	$C_{14}H_{28}$	0	−105.22	−105.51	−118.7	−131.3	−143.6	−155.5	−167.0	−178.2	−189.0	−199.3	−209.3	−219.1	−228.4	−237.3
n-Nonylcyclohexane	$C_{15}H_{30}$	0	−110.97	−111.28	−125.6	−139.2	−152.5	−165.2	−177.7	−189.7	−201.2	−212.3	−223.1	−233.6	−243.5	−253.1
n-Decylcyclohexane	$C_{16}H_{32}$	0	−116.72	−117.06	−132.5	−147.1	−161.3	−175.0	−188.3	−201.1	−213.5	−225.4	−236.8	−248.0	−258.6	−268.9
n-Undecylcyclohexane	$C_{17}H_{34}$	0	−122.47	−122.84	−139.3	−155.0	−170.1	−184.7	−198.9	−212.6	−225.8	−238.4	−250.6	−262.5	−273.8	−284.6
n-Dodecylcyclohexane	$C_{18}H_{36}$	0	−128.23	−128.61	−146.2	−162.9	−179.0	−194.5	−209.5	−224.0	−238.0	−251.4	−264.3	−277.0	−288.9	−300.4
n-Tridecylcyclohexane	$C_{19}H_{38}$	0	−133.98	−134.39	−153.1	−170.8	−187.8	−204.2	−220.2	−235.5	−250.3	−264.4	−278.1	−291.4	−304.0	−316.2
n-Tetradecylcyclohexane	$C_{20}H_{40}$	0	−139.73	−140.17	−159.9	−178.7	−196.7	−214.0	−230.8	−247.0	−262.5	−277.5	−291.8	−305.9	−319.2	−331.9
n-Pentadecylcyclohexane	$C_{21}H_{42}$	0	−145.49	−145.94	−166.8	−186.5	−205.5	−223.7	−241.4	−258.4	−274.8	−290.5	−305.6	−320.4	−334.3	−347.7
n-Hexadecylcyclohexane	$C_{22}H_{44}$	0	−151.24	−151.72	−173.7	−194.4	−214.4	−233.5	−252.1	−269.9	−287.0	−303.5	−319.4	−334.8	−349.4	−363.5
Increment per CH_2 group		0	−5.753	−5.777	−6.87	−7.89	−8.84	−9.75	−10.63	−11.46	−12.26	−13.02	−13.76	−14.46	−15.13	−15.77

TABLE 5.—*Values of the entropy, for the ideal gaseous state, to 1,500° K, for the normal alkylcyclopentanes*

Compound (gas)	Formula	Temperature in ° K														
		0	298.16	300	400	500	600	700	800	900	1,000	1,100	1,200	1,300	1,400	1,500
		Entropy, $S°$, in cal/deg mole														
Cyclopentane	C_5H_{10}	0	70.00	70.12	77.00	84.14	91.28	98.24	104.92	111.33	117.45	123.30	128.88	134.18	139.23	144.07
Methylcyclopentane	C_6H_{12}	0	81.24	81.42	90.33	99.36	108.24	116.81	125.01	132.83	140.25	147.31	154.05	160.42	166.51	172.37
Ethylcyclopentane	C_7H_{14}	0	90.62	90.84	101.60	112.38	122.89	133.05	142.73	151.91	160.62	168.90	176.79	184.29	191.37	198.19
n-Propylcyclopentane	C_8H_{16}	0	99.80	100.06	112.7	125.2	137.3	149.0	160.1	170.7	180.6	190.1	199.2	207.8	215.8	223.6
n-Butylcyclopentane	C_9H_{18}	0	108.99	109.29	123.8	138.0	151.8	165.0	177.5	189.4	200.7	211.4	221.6	231.2	240.3	249.0
n-Pentylcyclopentane	$C_{10}H_{20}$	0	118.17	118.51	134.8	150.8	166.2	181.0	194.9	208.2	220.7	232.6	243.9	254.7	264.8	274.5
n-Hexylcyclopentane	$C_{11}H_{22}$	0	127.35	127.74	145.9	163.6	180.6	196.9	212.4	226.9	240.7	253.8	266.3	278.1	289.3	299.9
n-Heptylcyclopentane	$C_{12}H_{24}$	0	136.54	136.96	157.0	176.4	195.0	212.9	229.8	245.7	260.8	275.1	288.7	301.6	313.8	325.3
n-Octylcyclopentane	$C_{13}H_{26}$	0	145.72	146.18	168.1	189.2	209.5	228.8	247.2	264.4	280.8	296.3	311.1	325.0	338.2	350.8
n-Nonylcyclopentane	$C_{14}H_{28}$	0	154.90	155.41	179.1	202.0	223.9	244.8	264.6	283.2	300.8	317.6	333.4	348.5	362.7	376.2
n-Decylcyclopentane	$C_{15}H_{30}$	0	164.08	164.63	190.2	214.8	238.3	260.8	282.0	301.9	320.9	338.8	355.8	372.0	387.2	401.6
n-Undecylcyclopentane	$C_{16}H_{32}$	0	173.27	173.86	201.3	227.6	252.8	276.7	299.4	320.7	340.9	360.0	378.2	395.4	411.7	427.0
n-Dodecylcyclopentane	$C_{17}H_{34}$	0	182.45	183.08	212.4	240.4	267.2	292.7	316.8	339.4	360.9	381.3	400.6	418.9	436.2	452.5
n-Tridecylcyclopentane	$C_{18}H_{36}$	0	191.63	192.30	223.4	253.2	281.6	308.7	334.2	358.2	381.0	402.5	423.0	442.4	460.6	477.9
n-Tetradecylcyclopentane	$C_{19}H_{38}$	0	200.82	201.53	234.5	266.0	296.0	324.6	351.6	377.0	401.0	423.7	445.3	465.8	485.1	503.3
n-Pentadecylcyclopentane	$C_{20}H_{40}$	0	210.00	210.75	245.6	278.8	310.5	340.6	369.0	395.7	421.0	445.0	467.7	489.3	509.6	528.7
n-Hexadecylcyclopentane	$C_{21}H_{42}$	0	219.18	219.98	256.7	291.6	324.9	356.6	386.4	414.4	441.0	466.2	490.1	512.7	534.1	554.2
Increment per CH_2 group	.....	0	9.183	9.224	11.08	12.80	14.43	15.97	17.40	18.75	20.03	21.24	22.38	23.46	24.48	25.43

TABLE 6.—*Values of the entropy, for the ideal gaseous state, to, 1500° K, for the normal alkylcyclohexanes*

Compound (gas)	Formula	Temperature in ° K														
		0	298.16	300	400	500	600	700	800	900	1,000	1,100	1,200	1,300	1,400	1,500
		Entropy, $S°$, in cal/deg mole														
Cyclohexane	C_6H_{12}	0	71.28	71.44	80.18	89.24	98.30	107.14	115.65	123.80	131.59	139.0	146.0	152.7	159.0	165.1
Methylcyclohexane	C_7H_{14}	0	82.06	82.28	93.22	104.32	115.21	125.77	135.86	145.46	154.57	163.2	171.4	179.2	186.6	193.7
Ethylcyclohexane	C_8H_{16}	0	91.44	91.70	104.5	117.3	129.9	142.0	153.6	164.5	174.9	184.8	194.2	203.0	211.4	219.5
n-Propylcyclohexane	C_9H_{18}	0	100.11	100.43	115.0	129.6	143.7	157.3	170.4	182.7	194.3	205.5	215.9	226.0	235.3	244.4
n-Butylcyclohexane	$C_{10}H_{20}$	0	109.29	109.66	126.1	142.4	158.1	173.3	187.8	201.5	214.3	226.7	238.3	249.5	259.8	269.8
n-Pentylcyclohexane	$C_{11}H_{22}$	0	118.48	118.87	137.2	155.2	172.6	189.2	205.2	220.2	234.4	248.0	260.7	272.9	284.3	295.3
n-Hexylcyclohexane	$C_{12}H_{24}$	0	127.66	128.10	148.2	168.0	187.0	205.2	222.6	239.0	254.4	269.2	283.0	296.4	308.7	320.7
n-Heptylcyclohexane	$C_{13}H_{26}$	0	136.84	137.33	159.3	180.8	201.4	221.2	240.0	257.7	274.4	290.4	305.4	319.8	333.2	346.1
n-Octylcyclohexane	$C_{14}H_{28}$	0	146.03	146.56	170.4	193.6	215.8	237.1	257.4	276.5	294.4	311.7	327.8	343.3	357.7	371.5
n-Nonylcyclohexane	$C_{15}H_{30}$	0	155.21	155.77	181.5	206.4	230.3	253.1	274.8	295.2	314.5	332.9	350.2	366.8	382.2	397.0
n-Decylcyclohexane	$C_{16}H_{32}$	0	164.39	165.00	192.5	219.2	244.7	269.1	292.2	314.0	334.5	354.2	372.6	390.2	406.7	422.4
n-Undecylcyclohexane	$C_{17}H_{34}$	0	173.57	174.23	203.6	232.0	259.1	285.0	309.6	332.7	354.5	375.4	394.9	413.7	431.1	447.8
n-Dodecylcyclohexane	$C_{18}H_{36}$	0	182.76	183.44	214.7	244.8	273.6	301.0	327.0	351.5	374.6	396.6	417.3	437.1	455.6	473.2
n-Tridecylcyclohexane	$C_{19}H_{38}$	0	191.94	192.67	225.8	257.6	288.0	317.0	344.4	370.2	394.6	417.9	439.7	460.6	480.1	498.7
n-Tetradecylcyclohexane	$C_{20}H_{40}$	0	201.12	201.90	236.8	270.4	302.4	332.9	361.8	389.0	414.6	439.1	462.1	484.1	504.6	524.1
n-Pentadecylcyclohexane	$C_{21}H_{42}$	0	210.31	211.11	247.9	283.2	316.9	348.9	379.2	407.7	434.7	460.3	484.4	507.5	529.1	549.5
n-Hexadecylcyclohexane	$C_{22}H_{44}$	0	219.49	220.34	259.0	296.1	331.3	364.9	396.7	426.5	454.7	481.6	506.8	531.0	553.5	575.0
Increment per CH_2 group	.....	0	9.183	9.224	11.08	12.80	14.43	15.97	17.40	18.75	20.03	21.24	22.38	23.46	24.48	25.43

TABLE 7.—*Values of the heat content, for the ideal gaseous state, to 1,500° K, for the normal alkylcyclopentanes*

Compound (gas)	Formula	Temperature in ° K														
		0	298.16	300	400	500	600	700	800	900	1,000	1,100	1,200	1,300	1,400	1,5
		Heat content ($H°-H°_0$), in cal/mole														
Cyclopentane	C_5H_{10}	0	3,599	3,636	6,048	9,200	13,188	17,703	22,720	28,161	33,970	40,110	46,500	53,130	59,960	66,9
Methylcyclopentane	C_6H_{12}	0	4,774	4,827	7,952	12,015	16,902	22,463	28,600	35,235	42,280	49,700	57,440	65,440	73,670	82,1
Ethylcyclopentane	C_7H_{14}	0	5,638	5,703	9,480	14,330	20,100	26,700	33,900	41,700	50,000	58,700	67,800	77,109	86,700	96,6
n-Propylcyclopentane	C_8H_{16}	0	6,661	6,737	11,160	16,790	23,500	31,100	39,400	48,300	57,800	67,700	78,100	88,800	99,800	111,1
n-Butylcyclopentane	C_9H_{18}	0	7,683	7,771	12,850	19,250	26,800	35,400	44,800	54,900	65,500	76,800	88,400	100,500	112,900	125,5
n-Pentylcyclopentane	$C_{10}H_{20}$	0	8,706	8,805	14,530	21,710	30,200	39,800	50,200	61,400	73,300	85,800	98,800	112,200	126,000	140,2
n-Hexylcyclopentane	$C_{11}H_{22}$	0	9,729	9,839	16,220	24,160	33,500	44,100	55,600	68,000	81,100	94,800	109,100	123,900	139,100	154,6
n-Heptylcyclopentane	$C_{12}H_{24}$	0	10,752	10,874	17,900	26,620	36,900	48,500	61,100	74,600	88,900	103,800	119,500	135,600	152,200	169,2
n-Octylcyclopentane	$C_{13}H_{26}$	0	11,774	11,908	19,580	29,080	40,200	52,800	66,500	81,100	96,600	112,900	129,800	147,300	165,300	183,8
n-Nonylcyclopentane	$C_{14}H_{28}$	0	12,797	12,942	21,270	31,540	43,600	57,200	71,900	87,700	104,400	121,900	140,100	159,000	178,400	198,4
n-Decylcyclopentane	$C_{15}H_{30}$	0	13,820	13,976	22,950	34,000	46,900	61,500	77,300	94,300	112,200	130,900	150,500	170,700	191,500	212,9
n-Undecylcyclopentane	$C_{16}H_{32}$	0	14,842	15,010	24,640	36,460	50,300	65,900	82,700	100,800	120,000	140,000	160,800	182,400	204,600	227,3
n-Dodecylcyclopentane	$C_{17}H_{34}$	0	15,865	16,044	26,320	38,920	53,600	70,200	88,200	107,400	127,700	149,000	171,200	194,100	217,600	241,7
n-Tridecylcyclopentane	$C_{18}H_{36}$	0	16,888	17,078	28,000	41,370	57,000	74,600	93,600	113,900	135,500	158,000	181,500	205,800	230,700	256,2
n-Tetradecylcyclopentane	$C_{19}H_{38}$	0	17,910	18,112	29,680	43,830	60,400	78,900	99,000	120,500	143,300	167,000	191,800	217,500	243,800	270,8
n-Pentadecylcyclopentane	$C_{20}H_{40}$	0	18,933	19,146	31,370	46,290	63,700	83,300	104,400	127,100	151,000	176,100	202,300	229,200	256,900	285,4
n-Hexadecylcyclopentane	$C_{21}H_{42}$	0	19,956	20,180	33,060	48,750	67,100	87,600	109,900	133,600	158,800	185,100	212,500	240,900	270,000	299,9
Increment per CH_2 group	.....	0	1,022.7	1,034.1	1,684	2,458	3,350	4,350	5,420	6,560	7,770	9,030	10,340	11,700	13,090	14,5

TABLE 8.—*Values of the heat content, for the ideal gaseous state, to 1,500° K, for the normal alkylcyclohexanes*

Compound (gas)	Formula	Temperature in ° K														
		0	298.16	300	400	500	600	700	800	900	1,000	1,100	1,200	1,300	1,400	1,5
		Heat content ($H°-H°_0$), in cal/mole														
Cyclohexane	C_6H_{12}	0	4,237	4,284	7,352	11,435	16,404	22,148	28,536	35,460	42,850	50,600	58,680	67,080	75,690	84,6
Methylcyclohexane	C_7H_{14}	0	5,233	5,298	9,136	14,130	20,118	26,971	34,528	42,678	51,330	60,390	69,840	79,560	89,600	99,9
Ethylcyclohexane	C_8H_{16}	0	6,097	6,174	10,680	16,450	23,300	31,200	39,900	49,200	59,100	69,400	80,200	91,300	102,600	114,2
n-Propylcyclohexane	C_9H_{18}	0	7,054	7,143	12,240	18,850	26,600	35,400	45,100	55,600	66,700	78,400	90,500	103,000	115,700	128,6
n-Butylcyclohexane	$C_{10}H_{20}$	0	8,077	8,177	13,920	21,310	29,900	39,800	50,500	62,200	74,500	87,500	100,800	114,700	128,800	143,2
n-Pentylcyclohexane	$C_{11}H_{22}$	0	9,100	9,211	15,610	23,770	33,300	44,100	56,000	68,700	82,200	96,500	111,200	126,400	141,900	157,6
n-Hexylcyclohexane	$C_{12}H_{24}$	0	10,123	10,245	17,290	26,230	[illegible]	48,500	61,400	75,300	90,000	105,500	121,500	138,100	155,000	172,2
n-Heptylcyclohexane	$C_{13}H_{26}$	0	11,145	11,279	18,980	28,680	[illegible]	52,800	66,800	81,900	97,800	114,600	131,900	149,800	168,100	186,9
n-Octylcyclohexane	$C_{14}H_{28}$	0	12,168	12,313	20,660	31,140	43,300	57,200	72,200	88,400	105,600	123,600	142,200	161,500	181,200	201,3
n-Nonylcyclohexane	$C_{15}H_{30}$	0	13,191	13,348	22,340	33,600	46,700	61,500	77,700	95,000	113,300	132,600	152,500	173,200	194,200	215,7
n-Decylcyclohexane	$C_{16}H_{32}$	0	14,213	14,382	24,030	36,060	50,000	65,900	83,100	101,600	121,100	141,600	162,900	184,900	207,300	230,3
n-Undecylcyclohexane	$C_{17}H_{34}$	0	15,236	15,416	25,710	38,520	53,400	70,200	88,500	108,100	128,900	150,700	173,200	196,600	220,400	244,9
n-Dodecylcyclohexane	$C_{18}H_{36}$	0	16,259	16,450	27,400	40,980	56,700	74,600	93,900	114,700	136,700	159,700	183,600	208,300	233,500	259,4
n-Tridecylcyclohexane	$C_{19}H_{38}$	0	17,282	17,484	29,080	43,440	60,100	78,900	99,300	121,300	144,400	168,700	193,900	220,000	246,600	273,8
n-Tetradecylcyclohexane	$C_{20}H_{40}$	0	18,304	18,518	30,760	45,890	63,500	83,300	104,800	127,800	152,200	177,800	204,200	231,700	259,700	288,4
n-Pentadecylcyclohexane	$C_{21}H_{42}$	0	19,327	19,552	32,430	48,350	66,800	87,600	110,200	134,400	160,000	186,800	214,600	243,400	272,800	302,9
n-Hexadecylcyclohexane	$C_{22}H_{44}$	0	20,350	20,586	34,130	50,810	70,200	92,000	115,600	141,000	167,700	195,800	224,900	255,100	285,800	317,5
Increment per CH_2 group	.....	0	1,022.7	1,034.1	1,684	2,458	3,350	4,350	5,420	6,560	7,770	9,030	10,340	11,700	13,090	14,5

TABLE 9.—*Values of the heat capacity, for the ideal gaseous state, to 1,500° K, for the normal alkylcyclopentanes*

Compound (gas)	Formula	Temperature in ° K														
		0	298.16	300	400	500	600	700	800	900	1,000	1,100	1,200	1,300	1,400	1,500
		Heat capacity, C_p°, in cal/deg mole														
Cyclopentane	C_5H_{10}	0	19.82	19.98	28.24	35.86	42.36	47.81	52.44	56.37	59.75	62.68	65.18	67.36	69.24	70.89
Methylcyclopentane	C_6H_{12}	0	26.24	26.46	36.11	44.94	52.43	58.68	64.00	68.53	72.44	75.82	78.72	81.24	83.43	85.35
Ethylcyclopentane	C_7H_{14}	0	31.93	32.18	43.39	53.55	62.09	69.24	75.31	80.48	84.94	88.81	92.12	95.00	97.51	99.69
n-Propylcyclopentane	C_8H_{16}	0	37.69	37.99	50.5	62.0	71.6	79.6	86.4	92.3	97.3	101.7	105.4	108.7	111.5	113.9
n-Butylcyclopentane	C_9H_{18}	0	43.45	43.80	57.7	70.4	81.0	90.0	97.6	104.1	109.7	114.5	118.7	122.3	125.5	128.2
n-Pentylcyclopentane	$C_{10}H_{20}$	0	49.21	49.61	64.8	78.9	90.5	100.3	108.7	115.9	122.0	127.4	132.0	136.0	139.5	142.4
n-Hexylcyclopentane	$C_{11}H_{22}$	0	54.97	55.42	71.9	87.3	100.0	110.7	119.9	127.6	134.4	140.2	145.3	149.7	153.5	156.7
n-Heptylcyclopentane	$C_{12}H_{24}$	0	60.73	61.23	79.1	95.7	109.4	121.1	131.0	139.4	146.8	153.1	158.6	163.4	167.4	171.0
n-Octylcyclopentane	$C_{13}H_{26}$	0	66.49	67.04	86.2	104.2	118.9	131.4	142.2	151.2	159.2	166.0	171.9	177.0	181.4	185.2
n-Nonylcyclopentane	$C_{14}H_{28}$	0	72.25	72.85	93.3	112.6	128.4	141.8	153.3	163.0	171.5	178.8	185.2	190.7	195.4	199.5
n-Decylcyclopentane	$C_{15}H_{30}$	0	78.01	78.66	100.4	121.0	137.8	152.2	164.4	174.8	183.9	191.7	198.4	204.4	209.4	213.7
n-Undecylcyclopentane	$C_{16}H_{32}$	0	83.77	84.47	107.6	129.5	147.3	162.5	175.6	186.6	196.3	204.6	211.7	218.0	223.4	228.0
n-Dodecylcyclopentane	$C_{17}H_{34}$	0	89.53	90.28	114.7	137.9	156.8	172.9	186.7	198.4	208.6	217.4	225.0	231.7	237.4	242.2
n-Tridecylcyclopentane	$C_{18}H_{36}$	0	95.29	96.09	121.8	146.4	166.2	183.3	197.8	210.2	221.0	230.3	238.3	245.4	251.4	256.5
n-Tetradecylcyclopentane	$C_{19}H_{38}$	0	101.05	101.90	129.0	154.8	175.7	193.6	209.0	222.0	233.4	243.1	251.6	259.0	265.4	270.7
n-Pentadecylcyclopentane	$C_{20}H_{40}$	0	106.81	107.71	136.1	163.2	185.2	204.0	220.1	233.8	245.8	256.0	264.9	272.7	279.3	285.0
n-Hexadecylcyclopentane	$C_{21}H_{42}$	0	112.57	113.52	143.2	171.7	194.6	214.4	231.3	245.6	258.1	268.8	278.2	286.4	293.3	299.2
Increment per CH_2 group	.....	0	5.760	5.810	7.13	8.44	9.47	10.37	11.14	11.79	12.37	12.86	13.29	13.67	13.99	14.25

TABLE 10.—*Values of the heat capacity, for the ideal gaseous state to 1,500° K, for the normal alkylcyclohexanes*

Compound (gas)	Formula	Temperature in ° K														
		0	298.16	300	400	500	600	700	800	900	1,000	1,100	1,200	1,300	1,400	1,500
		Heat capacity, C_p°, in cal/deg mole														
Cyclohexane	C_6H_{12}	0	25.40	25.58	35.82	45.47	53.83	60.87	66.76	71.68	75.80	79.3	82.2	84.7	86.8	88.6
Methylcyclohexane	C_7H_{14}	0	32.27	32.51	44.35	55.21	64.46	72.23	78.74	84.20	88.79	92.7	96.0	98.8	101.2	103.2
Ethylcyclohexane	C_8H_{16}	0	37.96	38.23	51.6	63.8	74.1	82.8	90.1	96.2	101.3	105.7	109.4	112.5	115.3	117.6
n-Propylcyclohexane	C_9H_{18}	0	43.59	43.89	58.6	72.1	83.5	93.1	101.1	107.9	113.6	118.6	122.7	126.2	129.3	131.9
n-Butylcyclohexane	$C_{10}H_{20}$	0	49.35	49.70	65.7	80.5	93.0	103.5	112.2	119.7	126.0	131.4	136.0	139.8	143.3	146.1
n-Pentylcyclohexane	$C_{11}H_{22}$	0	55.11	55.51	72.9	89.0	102.4	113.8	123.4	131.5	138.3	144.3	149.3	153.5	157.3	160.4
n-Hexylcyclohexane	$C_{12}H_{24}$	0	60.87	61.32	80.0	97.4	111.9	124.2	134.5	143.3	150.7	157.1	162.6	167.2	171.2	174.6
n-Heptylcyclohexane	$C_{13}H_{26}$	0	66.63	67.13	87.1	105.8	121.4	134.6	145.7	155.1	163.1	170.0	175.8	180.8	185.2	188.9
n-Octylcyclohexane	$C_{14}H_{28}$	0	72.39	72.94	94.3	114.3	130.8	144.9	156.8	166.9	175.4	182.9	189.1	194.5	199.2	203.1
n-Nonylcyclohexane	$C_{15}H_{30}$	0	78.15	78.75	101.4	122.7	140.3	155.3	167.9	178.7	187.8	195.7	202.4	208.2	213.2	217.4
n-Decylcyclohexane	$C_{16}H_{32}$	0	83.91	84.56	108.5	131.2	149.8	165.7	179.1	190.5	200.2	208.6	215.7	221.9	227.2	231.6
n-Undecylcyclohexane	$C_{17}H_{34}$	0	89.67	90.37	115.7	139.6	159.2	176.0	190.2	202.2	212.6	221.4	229.0	235.5	241.2	245.9
n-Dodecylcyclohexane	$C_{18}H_{36}$	0	95.43	96.18	122.8	148.0	168.7	186.4	201.4	214.0	224.9	234.3	242.3	249.2	255.2	260.1
n-Tridecylcyclohexane	$C_{19}H_{38}$	0	101.19	101.99	129.9	156.5	178.2	196.8	212.5	225.8	237.3	247.2	255.6	262.9	269.2	274.4
n-Tetradecylcyclohexane	$C_{20}H_{40}$	0	106.95	107.80	137.1	164.9	187.6	207.1	223.6	237.6	249.7	260.0	268.9	276.5	283.1	288.6
n-Pentadecylcyclohexane	$C_{21}H_{42}$	0	112.71	113.61	144.2	173.3	197.1	217.5	234.8	249.4	262.0	272.9	282.2	290.2	297.1	302.9
n-Hexadecylcyclohexane	$C_{22}H_{44}$	0	118.47	119.42	151.3	181.8	206.6	227.9	245.9	261.2	274.4	285.7	295.5	303.9	311.1	317.1
Increment per CH_2 group	.....	0	5.760	5.810	7.13	8.44	9.47	10.37	11.14	11.79	12.37	12.86	13.29	13.67	13.99	14.25

IV. Heat of Formation, Free Energy of Formation, and Equilibrium Constant of Formation

1. Method and Data Used in the Calculations

The same method of calculation was used as described in section IV, 1 of reference [5].

For the heats of formation at 25° C of the cyclopentane and cyclohexane derivatives treated in this report, the values given in references [3, 4] were used.

2. Results

The resulting values of the thermodynamic properties for the formation of cyclopentane, cyclohexane, the seven dimethylcyclohexanes and the normal alkylcyclopentanes and alkylcyclohexanes, in the gaseous state, from the elements carbon (solid, graphite) and hydrogen (gaseous), are presented in tables 11 to 19, which give values of the following properties, to 1,000° K or 1,500° K: heat of formation, ΔHf°; free energy of formation, ΔFf°; and the logarithm of the equilibrium constant of formation, $\log_{10}Kf$.

TABLE 11.—*Values of the heat of formation, for the ideal gaseous state, to 1,500° K, for the normal alkylcyclopentanes*

Compound (gas)	Formula	Temperature in ° K														
		0	298.16	300	400	500	600	700	800	900	1,000	1,100	1,200	1,300	1,400	1,500
		Heat of formation, $\Delta Hf°$, in kcal/mole														
Cyclopentane	C_5H_{10}	−10.68	−18.46	−18.50	−20.80	−22.67	−24.12	−25.25	−26.06	−26.61	−26.91	−27.01	−26.97	−26.81	−26.57	−26.25
Methylcyclopentane	C_6H_{12}	−16.62	−25.50	−25.54	−28.07	−30.11	−31.68	−32.88	−33.74	−34.29	−34.58	−34.65	−34.52	−34.30	−33.97	−33.56
Ethylcyclopentane	C_7H_{14}	−20.80	−30.37	−30.42	−33.24	−35.50	−37.24	−38.54	−39.47	−40.06	−40.36	−40.40	−40.22	−39.94	−39.53	−39.04
n-Propylcyclopentane	C_8H_{16}	−23.85	−35.39	−35.44	−38.6	−41.1	−43.0	−44.4	−45.4	−46.1	−46.4	−46.4	−46.2	−45.9	−45.4	−44.8
n-Butylcyclopentane	C_9H_{18}	−27.43	−40.22	−40.28	−43.7	−46.4	−48.5	−50.1	−51.2	−51.9	−52.2	−52.2	−52.0	−51.6	−51.0	−50.4
n-Pentylcyclopentane	$C_{10}H_{20}$	−31.10	−45.15	−45.21	−48.9	−51.9	−54.2	−55.9	−57.1	−57.8	−58.2	−58.2	−57.9	−57.4	−56.8	−56.1
n-Hexylcyclopentane	$C_{11}H_{22}$	−34.77	−50.07	−50.14	−54.1	−57.4	−59.8	−61.6	−63.0	−63.8	−64.1	−64.1	−63.8	−63.3	−62.6	−61.8
n-Heptylcyclopentane	$C_{12}H_{24}$	−38.44	−55.00	−55.08	−59.4	−62.8	−65.5	−67.4	−68.8	−69.7	−70.1	−70.0	−69.6	−69.1	−68.3	−67.5
n-Octylcyclopentane	$C_{13}H_{26}$	−42.12	−59.92	−60.01	−64.6	−68.3	−71.1	−73.2	−74.7	−75.6	−76.0	−76.0	−75.5	−74.9	−74.1	−73.2
n-Nonylcyclopentane	$C_{14}H_{28}$	−45.79	−64.85	−64.94	−69.8	−73.8	−76.8	−79.0	−80.6	−81.6	−82.0	−81.9	−81.4	−80.8	−79.8	−78.9
n-Decylcyclopentane	$C_{15}H_{30}$	−49.46	−69.78	−69.87	−75.0	−79.2	−82.4	−84.8	−86.4	−87.5	−87.9	−87.8	−87.3	−86.6	−85.6	−84.6
n-Undecylcyclopentane	$C_{16}H_{32}$	−53.14	−74.70	−74.80	−80.2	−84.7	−88.1	−90.5	−92.3	−93.4	−93.8	−93.7	−93.2	−92.4	−91.4	−90.3
n-Dodecylcyclopentane	$C_{17}H_{34}$	−56.81	−79.63	−79.73	−85.5	−90.2	−93.7	−96.3	−98.2	−99.3	−99.8	−99.7	−99.1	−98.2	−97.1	−96.0
n-Tridecylcyclopentane	$C_{18}H_{36}$	−60.48	−84.55	−84.66	−90.7	−95.6	−99.4	−102.1	−104.0	−105.3	−105.7	−105.6	−105.0	−104.1	−102.9	−101.6
n-Tetradecylcyclopentane	$C_{19}H_{38}$	−64.16	−89.48	−89.59	−95.9	−101.1	−105.0	−107.9	−109.9	−111.2	−111.6	−111.5	−110.8	−109.9	−108.6	−107.3
n-Pentadecylcyclopentane	$C_{20}H_{40}$	−67.83	−94.41	−94.52	−101.1	−106.5	−110.7	−113.6	−115.8	−117.1	−117.6	−117.4	−116.7	−115.7	−114.4	−113.0
n-Hexadecylcyclopentane	$C_{21}H_{42}$	−71.50	−99.33	−99.45	−106.4	−112.0	−116.3	−119.4	−121.6	−123.0	−123.5	−123.4	−122.6	−121.6	−120.1	−118.7
Increment per CH_2 group		−3.673	−4.926	−4.931	−5.22	−5.46	−5.65	−5.78	−5.87	−5.93	−5.94	−5.93	−5.89	−5.83	−5.76	−5.69

TABLE 12.—*Values of the heat of formation, for the ideal gaseous state, to 1,500° K, for the normal alkylcyclohexanes*

Compound (gas)	Formula	Temperature in ° K														
		0	298.16	300	400	500	600	700	800	900	1,000	1,100	1,200	1,300	1,400	1,500
		Heat of formation, $\Delta Hf°$, in kcal/mole														
Cyclohexane	C_6H_{12}	−20.01	−29.43	−29.48	−31.70	−34.08	−35.57	−36.59	−37.19	−37.46	−37.41	−37.14	−36.68	−36.05	−35.44	−34.61
Methylcyclohexane	C_7H_{14}	−26.30	−36.99	−37.04	−39.79	−41.92	−43.46	−44.50	−45.10	−45.34	−45.25	−44.92	−44.36	−43.71	−42.89	−42.10
Ethylcyclohexane	C_8H_{16}	−28.94	−41.05	−41.10	−44.13	−46.50	−48.22	−49.35	−49.98	−50.25	−50.17	−49.84	−49.25	−48.51	−47.69	−46.71
n-Propylcyclohexane	C_9H_{18}	−32.79	−46.20	−46.27	−49.6	−52.2	−54.2	−55.4	−56.2	−56.5	−56.4	−56.0	−55.3	−54.5	−53.7	−52.5
n-Butylcyclohexane	$C_{10}H_{20}$	−36.29	−50.95	−51.02	−54.7	−57.5	−59.6	−61.0	−61.9	−62.3	−62.2	−61.7	−61.0	−60.2	−59.3	−58.0
n-Pentylcyclohexane	$C_{11}H_{22}$	−39.96	−55.88	−55.95	−59.9	−62.9	−65.3	−66.8	−67.8	−68.2	−68.2	−67.6	−66.9	−66.0	−65.0	−63.7
n-Hexylcyclohexane	$C_{12}H_{24}$	−43.64	−60.80	−60.88	−65.2	−68.4	−70.9	−72.6	−73.7	−74.1	−74.1	−73.6	−72.8	−71.8	−70.8	−69.4
n-Heptylcyclohexane	$C_{13}H_{26}$	−47.31	−65.73	−65.81	−70.4	−73.9	−76.6	−78.4	−79.6	−80.1	−80.0	−79.5	−78.7	−77.6	−76.5	−75.1
n-Octylcyclohexane	$C_{14}H_{28}$	−50.98	−70.65	−70.74	−75.6	−79.3	−82.2	−84.2	−85.4	−86.0	−86.0	−85.4	−84.6	−83.5	−82.3	−80.8
n-Nonylcyclohexane	$C_{15}H_{30}$	−54.66	−75.58	−75.68	−80.8	−84.8	−87.9	−89.9	−91.3	−91.9	−91.9	−91.3	−90.5	−89.3	−88.0	−86.5
n-Decylcyclohexane	$C_{16}H_{32}$	−58.33	−80.51	−80.61	−86.0	−90.3	−93.5	−95.7	−97.2	−97.8	−97.9	−97.3	−96.4	−95.1	−93.8	−92.2
n-Undecylcyclohexane	$C_{17}H_{34}$	−62.00	−85.43	−85.54	−91.3	−95.7	−99.2	−101.5	−103.0	−103.8	−103.8	−103.2	−102.2	−101.0	−99.6	−97.9
n-Dodecylcyclohexane	$C_{18}H_{36}$	−65.67	−90.36	−90.47	−96.5	−101.2	−104.8	−107.3	−108.9	−109.7	−109.8	−109.1	−108.1	−106.8	−105.3	−103.6
n-Tridecylcyclohexane	$C_{19}H_{38}$	−69.35	−95.28	−95.40	−101.7	−106.7	−110.4	−113.0	−114.8	−115.6	−115.7	−115.0	−114.0	−112.6	−111.1	−109.3
n-Tetradecylcyclohexane	$C_{20}H_{40}$	−73.02	−100.21	−100.33	−106.9	−112.1	−116.1	−118.8	−120.6	−121.6	−121.6	−121.0	−119.9	−118.5	−116.8	−115.0
*n*Pentadecylcyclohexane	$C_{21}H_{42}$	−76.69	−105.14	−105.26	−112.2	−117.6	−121.8	−124.6	−126.5	−127.5	−127.6	−126.9	−125.8	−124.3	−122.6	−120.6
n-Hexadecylcyclohexane	$C_{22}H_{44}$	−80.37	−110.06	−110.19	−117.4	−123.1	−127.4	−130.4	−132.4	−133.4	−133.5	−132.8	−131.7	−130.1	−128.4	−126.3
Increment per CH_2 group		−3.673	−4.926	−4.931	−5.22	−5.46	−5.65	−5.78	−5.87	−5.93	−5.94	−5.93	−5.89	−5.83	−5.76	−5.69

TABLE 13.—*Values of the heat of formation, for the ideal gaseous state, to 1,500° K, for the 7 dimethylcyclohexanes*

Compound (gas)	Formula	Temperature in ° K														
		0	298.16	300	400	500	600	700	800	900	1,000	1,100	1,200	1,300	1,400	1,500
		Heat of formation, $\Delta Hf°$, in kcal/mole														
1,1-Dimethylcyclohexane	C_8H_{16}	−30.93	−43.26	−43.31	−46.4	−48.9	−50.6	−51.8	−52.4	−52.5	−52.4	−51.9	−51.2	−50.4	−49.4	−48.4
cis-1,2-Dimethylcyclohexane	C_8H_{16}	−28.95	−41.15	−41.20	−44.3	−46.7	−48.4	−49.6	−50.2	−50.5	−50.4	−50.0	−49.4	−48.6	−47.4	−46.9
trans-1,2-Dimethylcyclohexane	C_8H_{16}	−30.91	−43.02	−43.07	−46.1	−48.4	−50.1	−51.2	−51.9	−52.0	−51.9	−51.5	−50.9	−50.1	−49.2	−48.2
cis-1,3-Dimethylcyclohexane[a]	C_8H_{16}	−32.02	−44.16	−44.21	−47.3	−49.7	−51.4	−52.5	−53.1	−53.3	−53.2	−52.8	−52.1	−51.2	−50.4	−49.3
trans-1,3-Dimethylcyclohexane[a]	C_8H_{16}	−30.06	−42.20	−42.25	−45.3	−47.7	−49.5	−50.7	−51.3	−51.6	−51.6	−51.2	−50.6	−49.9	−49.1	−48.1
cis-1,4-Dimethylcyclohexane	C_8H_{16}	−30.08	−42.22	−42.27	−45.4	−47.7	−49.5	−50.7	−51.4	−51.7	−51.6	−51.2	−50.6	−49.9	−49.1	−48.2
trans-1,4-Dimethylcyclohexane	C_8H_{16}	−31.99	−44.12	−44.17	−47.2	−49.6	−51.3	−52.3	−53.0	−53.2	−53.0	−52.6	−51.9	−51.2	−50.3	−49.3

[a] See footnotes a and b of table 22.

TABLE 14.—*Values of the free energy of formation, for the ideal gaseous state, to 1,500° K, for the normal alkylcyclopentanes*

Compound (gas)	Formula	Temperature in ° K														
		0	298.16	300	400	500	600	700	800	900	1,000	1,100	1,200	1,300	1,400	1,500
		Free energy of formation, $\Delta Ff°$, in kcal/mole														
Cyclopentane	C_5H_{10}	−10.68	+9.23	9.40	19.06	29.25	39.78	50.52	61.40	72.37	83.38	94.41	105.43	116.47	127.48	138.47
Methylcyclopentane	C_6H_{12}	−16.62	+8.55	8.76	20.59	33.00	45.78	58.79	71.93	85.17	98.46	111.77	125.08	138.41	151.68	164.87
Ethylcyclopentane	C_7H_{14}	−20.08	+10.59	10.84	25.05	39.99	55.17	70.66	86.29	102.06	117.86	133.68	149.50	165.29	181.11	196.83
n-Propylcyclopentane	C_8H_{16}	−23.85	+12.54	12.84	29.4	46.7	64.5	82.5	100.7	119.0	137.4	155.7	174.1	192.4	210.8	229.1
n-Butylcyclopentane	C_9H_{18}	−27.43	+14.69	15.02	34.0	53.8	74.0	94.6	115.3	136.1	157.0	177.9	198.8	219.7	240.6	261.5
n-Pentylcyclopentane	$C_{10}H_{20}$	−31.10	+16.73	17.11	38.5	60.7	83.4	106.5	129.7	153.2	176.6	200.0	223.5	246.9	270.4	293.8
n-Hexylcyclopentane	$C_{11}H_{22}$	−34.77	+18.78	19.20	43.0	67.6	92.9	118.5	144.2	170.2	196.2	222.2	248.2	274.2	300.2	326.2
n-Heptylcyclopentane	$C_{12}H_{24}$	−38.44	+20.83	21.29	47.4	74.6	102.3	130.4	158.7	187.2	215.8	244.3	272.8	301.4	329.9	358.5
n-Octylcyclopentane	$C_{13}H_{26}$	−42.12	+22.88	23.38	51.9	81.5	111.7	142.4	173.2	204.2	235.3	266.4	297.5	328.6	359.7	390.8
n-Nonylcyclopentane	$C_{14}H_{28}$	−45.79	+24.93	25.47	56.4	88.4	121.2	154.3	187.7	221.3	254.9	288.6	322.2	355.8	389.5	423.2
n-Decylcyclopentane	$C_{15}H_{30}$	−49.46	+26.97	27.56	60.9	95.4	130.6	166.3	202.2	238.3	274.5	310.7	346.8	383.0	419.2	455.5
n-Undecylcyclopentane	$C_{16}H_{32}$	−53.14	+29.02	29.65	65.4	102.3	140.0	178.2	216.6	255.3	294.1	332.8	371.5	410.2	449.0	487.8
n-Dodecylcyclopentane	$C_{17}H_{34}$	−56.81	+31.07	31.74	69.8	109.2	149.4	190.2	231.1	272.4	313.6	354.9	396.2	437.4	478.8	520.1
n-Tridecylcyclopentane	$C_{18}H_{36}$	−60.48	+33.12	33.83	74.3	116.1	158.9	202.1	245.6	289.4	333.2	377.0	420.8	464.7	508.5	552.5
n-Tetradecylcyclopentane	$C_{19}H_{38}$	−64.16	+35.17	35.92	78.8	123.1	168.3	214.1	260.1	306.4	352.8	399.2	445.5	491.9	538.3	584.8
n-Pentadecylcyclopentane	$C_{20}H_{40}$	−67.83	+37.21	38.01	83.3	130.0	177.7	226.0	274.6	323.4	372.4	421.3	470.2	519.1	568.0	617.1
n-Hexadecylcyclopentane	$C_{21}H_{42}$	−71.50	+39.26	40.10	87.8	136.9	187.2	238.0	289.1	340.5	392.0	443.4	494.8	546.3	597.8	649.5
Increment per CH_2 group		−3.673	+2.048	2.090	4.48	6.93	9.43	11.95	14.48	17.03	19.58	22.12	24.67	27.22	29.76	32.33

TABLE 15.—*Values of the free energy of formation, for the ideal gaseous state, to 1,500° K, for the normal alkylcyclohexanes*

Compound (gas)	Formula	Temperature in ° K														
		0	298.16	300	400	500	600	700	800	900	1,000	1,100	1,200	1,300	1,400	1,500
		Free energy of formation, $\Delta Ff°$, in kcal/mole														
Cyclohexane	C_6H_{12}	−20.01	+7.59	7.81	20.66	34.07	47.86	61.85	75.96	90.13	104.30	118.42	132.58	146.69	160.73	174.72
Methylcyclohexane	C_7H_{14}	−26.30	+6.52	6.79	21.84	37.51	53.55	69.80	86.16	102.59	119.03	135.43	151.83	168.13	184.43	200.65
Ethylcyclohexane	C_8H_{16}	−28.94	+9.38	9.69	27.12	45.19	63.72	82.50	101.37	120.28	139.23	158.17	177.11	195.93	214.71	233.36
n-Propylcyclohexane	C_9H_{18}	−32.79	+11.33	11.70	31.5	52.2	73.2	94.6	116.0	137.6	159.1	180.7	202.3	223.6	245.0	266.4
n-Butylcyclohexane	$C_{10}H_{20}$	−36.29	+13.55	13.97	36.2	59.3	82.8	106.7	130.7	154.8	178.8	203.0	227.1	251.0	275.0	298.9
n-Pentylcyclohexane	$C_{11}H_{22}$	−39.96	+15.60	16.06	40.7	66.2	92.3	118.7	145.2	171.8	198.4	225.1	251.8	278.2	304.8	331.2
n-Hexylcyclohexane	$C_{12}H_{24}$	−43.64	+17.65	18.15	45.2	73.2	101.7	130.6	159.6	188.8	218.0	247.2	276.5	305.4	334.5	363.5
n-Heptylcyclohexane	$C_{13}H_{26}$	−47.31	+19.69	20.24	49.6	80.1	111.1	142.6	174.1	205.8	237.6	269.4	301.1	332.6	364.3	395.9
n-Octylcyclohexane	$C_{14}H_{28}$	−50.98	+21.74	22.33	54.1	87.0	120.6	154.5	188.6	222.9	257.2	291.5	325.8	359.8	394.0	428.2
n-Nonylcyclohexane	$C_{15}H_{30}$	−54.66	+23.79	24.42	58.6	94.0	130.0	166.5	203.1	239.9	276.7	313.6	350.5	387.0	423.8	460.7
n-Decylcyclohexane	$C_{16}H_{32}$	−58.33	+25.84	26.51	63.1	100.9	139.4	178.4	217.6	256.9	296.3	335.7	375.1	414.3	453.6	492.9
n-Undecylcyclohexane	$C_{17}H_{34}$	−62.00	+27.89	28.60	67.6	107.8	148.8	190.4	232.1	274.0	315.9	357.9	399.8	441.5	483.3	525.2
n-Dodecylcyclohexane	$C_{18}H_{36}$	−65.67	+29.93	30.69	72.0	114.8	158.3	202.3	246.6	291.0	335.5	380.0	424.5	468.7	513.1	557.5
n-Tridecylcyclohexane	$C_{19}H_{38}$	−69.35	+31.98	32.78	76.5	121.7	167.7	214.3	261.0	308.0	355.0	402.1	449.1	495.9	542.9	589.9
n-Tetradecylcyclohexane	$C_{20}H_{40}$	−73.02	+34.03	34.87	81.0	128.6	177.1	226.2	275.5	325.0	374.6	424.2	473.8	523.1	572.6	622.2
n-Pentadecylcyclohexane	$C_{21}H_{42}$	−76.69	+36.08	36.96	85.5	135.5	186.6	238.2	290.0	342.1	394.2	446.4	498.5	550.3	602.4	654.5
n-Hexadecylcyclohexane	$C_{22}H_{44}$	−80.37	+38.13	39.05	90.0	142.5	196.0	250.1	304.5	359.1	413.8	468.5	523.1	577.6	632.2	686.8
Increment per CH_2 group		−3.673	+2.048	2.090	4.48	6.93	9.43	11.95	14.48	17.03	19.58	22.12	24.67	27.22	29.76	32.31

TABLE 16.—*Values of the free energy of formation, for the ideal gaseous state, to 1,500° K, for the seven dimethylcyclohexanes*

Compound (gas)	Formula	Temperature in ° K														
		0	298.16	300	400	500	600	700	800	900	1,000	1,100	1,200	1,300	1,400	1,500
		Free energy of formation, $\Delta Ff°$, in kcal/mole														
1,1-Dimethylcyclohexane	C_8H_{16}	−30.93	+8.42	8.74	26.6	45.2	64.1	83.4	102.7	122.1	141.4	160.8	180.2	199.5	218.4	237.1
cis-1,2-Dimethylcyclohexane	C_8H_{16}	−28.95	+9.85	10.17	27.8	46.1	64.8	83.8	102.9	122.1	141.2	160.4	179.5	198.6	217.4	236.0
trans-1,2-Dimethylcyclohexane	C_8H_{16}	−30.91	+8.24	8.55	26.2	44.6	63.4	82.4	101.5	120.6	139.9	159.1	178.1	197.3	216.1	234.9
cis-1,3-Dimethylcyclohexane [a]	C_8H_{16}	−32.02	+7.13	7.44	25.2	43.6	62.4	81.4	100.6	119.8	139.0	158.3	177.5	196.6	215.6	234.5
trans-1,3-Dimethylcyclohexane [a]	C_8H_{16}	−30.06	+8.68	8.99	26.6	44.8	63.6	82.5	101.5	120.6	139.8	158.9	178.0	197.2	216.0	234.7
cis-1,4-Dimethylcyclohexane	C_8H_{16}	−30.08	+9.07	9.38	27.1	45.5	64.3	83.4	102.6	121.8	141.2	160.4	179.7	190.0	217.8	236.5
trans-1,4-Dimethycyclohexane	C_8H_{16}	−31.99	+7.58	7.89	25.8	44.3	63.2	82.4	101.6	121.0	140.3	159.6	179.0	198.2	217.2	235.9

[a] See footnotes *a* and *b* of table 22.

TABLE 17.—*Values of the logarithm of the equilibrium constant of formation, for the ideal gaseous state, at 1 atm, K, for the*

Compound (gas)	Formula	Temperature in ° K														
		0	298.16	300	400	500	600	700	800	900	1,000	1,100	1,200	1,300	1,400	1,500
		Logarithm of equilibrium constant of formation, $\log_{10} K$														
Cyclopentane	C_5H_{10}	Infinite	−6.7643	−6.8490	−10.4144	−12.7851	−14.4897	−15.7722	−16.7736	−17.5731	−18.2228	−18.7571	−19.2005	−19.5796	−19.9002	−20.1753
Methylcyclopentane	C_6H_{12}	do	−6.2649	−6.3801	−11.2501	−14.4250	−16.6770	−18.3549	−19.6492	−20.6813	−21.5189	−22.2067	−22.7795	−23.2694	−23.6775	−24.0218
Ethylcyclopentane	C_7H_{14}	do	−7.7632	−7.8999	−13.6861	−17.4379	−20.0959	−22.0620	−23.5741	−24.7831	−25.7585	−26.5600	−27.2278	−27.7871	−28.2725	−28.6778
n-Propylcyclopentane	C_8H_{16}	do	−9.195	−9.351	−16.082	−20.429	−23.495	−25.763	−27.504	−28.896	−30.016	−30.936	−31.703	−32.347	−32.904	−33.375
n-Butylcyclopentane	C_9H_{18}	do	−10.768	−10.942	−18.582	−23.498	−26.965	−29.523	−31.487	−33.054	−34.316	−35.351	−36.213	−36.938	−37.565	−38.099
n-Pentylcyclopentane	$C_{10}H_{20}$	do	−12.269	−12.465	−21.029	−26.528	−30.399	−33.254	−35.444	−37.189	−38.595	−39.746	−40.706	−41.513	−42.212	−42.809
n-Hexylcyclopentane	$C_{11}H_{22}$	do	−13.770	−13.987	−23.476	−29.557	−33.833	−36.985	−39.401	−41.325	−42.874	−44.140	−45.199	−46.088	−46.858	−47.520
n-Heptylcyclopentane	$C_{12}H_{24}$	do	−15.271	−15.510	−25.924	−32.587	−37.268	−40.716	−43.358	−45.460	−47.153	−48.534	−49.691	−50.664	−51.504	−52.231
n-Octylcyclopentane	$C_{13}H_{26}$	do	−16.772	−17.032	−28.371	−35.616	−40.702	−44.448	−47.314	−49.595	−51.432	−52.929	−54.184	−55.239	−56.150	−56.941
n-Nonylcyclopentane	$C_{14}H_{28}$	do	−18.274	−18.555	−30.818	−38.646	−44.136	−48.179	−51.271	−53.730	−55.711	−57.323	−58.676	−59.814	−60.797	−61.652
n-Decylcyclopentane	$C_{15}H_{30}$	do	−19.775	−20.078	−33.265	−41.675	−47.570	−51.910	−55.228	−57.865	−59.990	−61.718	−63.169	−64.389	−65.443	−66.362
n-Undecylcyclopentane	$C_{16}H_{32}$	do	−21.276	−21.600	−35.712	−44.705	−51.004	−55.641	−59.185	−62.001	−64.269	−66.112	−67.662	−68.964	−70.089	−71.073
n-Dodecylcyclopentane	$C_{17}H_{34}$	do	−22.777	−23.123	−38.160	−47.734	−54.438	−59.372	−63.142	−66.136	−68.548	−70.506	−72.154	−77.540	−74.736	−75.784
n-Tridecylcyclopentane	$C_{18}H_{36}$	do	−24.278	−24.645	−40.607	−50.764	−57.872	−63.104	−67.098	−70.271	−72.827	−74.901	−76.647	−78.115	−79.382	−80.494
n-Tetradecylcyclopentane	$C_{19}H_{38}$	do	−25.780	−26.168	−43.054	−53.793	−61.306	−66.835	−71.055	−74.406	−77.106	−79.295	−81.139	−82.690	−84.028	−85.205
n-Pentadecylcyclopentane	$C_{20}H_{40}$	do	−27.281	−27.691	−45.501	−56.823	−64.740	−70.566	−75.012	−78.541	−81.385	−83.690	−85.632	−87.265	−88.675	−89.915
n-Hexadecylcyclopentane	$C_{21}H_{42}$	do	−28.782	−29.213	−47.948	−59.852	−68.174	−74.297	−78.969	−82.677	−85.664	−88.084	−90.125	−91.840	−93.321	−94.626
Increment per CH_2 group		do	−1.5012	−1.5226	−2.4472	−3.0295	−3.4341	−3.7312	−3.9568	−4.1352	−4.2790	−4.3944	−4.4926	−4.5752	−4.6463	−4.7106

TABLE 18.—*Values of the logarithm of the equilibrium constant of formation, for the ideal gaseous state, to 1,500° K, for the normal alkylcyclohexanes*

Compound (gas)	Formula	Temperature in ° K													
		0	298.16	300	400	500	600	700	800	900	1,000	1,100	1,200	1,300	1,400	1,500
		Logarithm of equilibrium constant of formation, $\log_{10} K_f$														
Cyclohexane	C_6H_{12}	Infinite	−5.5905	−5.6031	−11.2861	−14.8832	−17.4318	−19.3103	−20.7501	−21.8852	−22.7943	−23.5277	−24.1478	−24.6613	−25.0805	−25.4571
Methylcyclohexane	C_7H_{14}	do	−4.7819	−4.9487	−11.9344	−16.3959	−19.5095	−21.7967	−23.5374	−24.9110	−26.0133	−26.9077	−27.6521	−28.2657	−28.7908	−29.2345
Ethylcyclohexane	C_8H_{16}	do	−6.8744	−7.0592	−14.8200	−19.7522	−23.2697	−25.7561	−27.6926	−29.2075	−30.4279	−31.4243	−32.2567	−32.9394	−33.5168	−33.9669
n-Propylcyclohexane	C_9H_{18}	do	−8.304	−8.522	−17.232	−22.814	−26.679	−29.534	−31.686	−33.402	−34.770	−35.900	−36.841	−37.587	−38.253	−38.810
n-Butylcyclohexane	$C_{10}H_{20}$	do	−9.935	−10.174	−19.776	−25.918	−30.176	−33.318	−35.700	−37.579	−39.086	−40.330	−41.365	−42.192	−42.928	−43.546
n-Pentylcyclohexane	$C_{11}H_{22}$	do	−11.436	−11.697	−22.223	−28.948	−33.610	−37.050	−39.657	−41.715	−43.365	−44.724	−45.857	−46.767	−47.574	−48.257
n-Hexylcyclohexane	$C_{12}H_{24}$	do	−12.937	−13.219	−24.670	−31.978	−37.044	−40.781	−43.613	−45.850	−47.644	−49.119	−50.350	−51.342	−52.220	−52.967
n-Heptylcyclohexane	$C_{13}H_{26}$	do	−14.438	−14.742	−27.118	−35.007	−40.478	−44.512	−47.570	−49.985	−51.923	−53.513	−54.842	−55.917	−56.866	−57.678
n-Octylcyclohexane	$C_{14}H_{28}$	do	−15.940	−16.264	−29.565	−38.036	−43.912	−48.243	−51.527	−54.120	−56.202	−57.908	−59.335	−60.492	−61.513	−62.388
n-Nonylcyclohexane	$C_{15}H_{30}$	do	−17.441	−17.787	−32.012	−41.066	−47.346	−51.974	−55.484	−58.255	−60.481	−62.302	−63.828	−65.068	−66.159	−67.099
n-Decylcyclohexane	$C_{16}H_{32}$	do	−18.942	−19.310	−34.459	−44.096	−50.780	−55.706	−59.441	−62.391	−64.760	−66.696	−68.320	−69.643	−70.805	−71.810
n-Undecylcyclohexane	$C_{17}H_{34}$	do	−20.443	−20.852	−36.906	−47.125	−54.214	−59.437	−63.397	−66.526	−69.039	−71.091	−72.813	−74.218	−75.452	−76.520
n-Dodecylcyclohexane	$C_{18}H_{36}$	do	−21.944	−22.355	−39.354	−50.154	−57.648	−63.168	−67.354	−70.661	−73.318	−75.485	−77.305	−78.793	−80.098	−81.231
n-Tridecylcyclohexane	$C_{19}H_{38}$	do	−23.446	−23.878	−41.801	−53.184	−61.083	−66.899	−71.311	−74.796	−77.597	−79.880	−81.798	−83.398	−84.744	−85.941
n-Tetradecylcyclohexane	$C_{20}H_{40}$	do	−24.947	−25.400	−44.248	−56.214	−64.517	−70.630	−75.268	−78.931	−81.876	−84.274	−86.291	−87.944	−89.390	−90.652
n-Pentadecylcyclohexane	$C_{21}H_{42}$	do	−26.448	−26.923	−46.695	−59.243	−67.951	−74.362	−79.225	−83.067	−86.155	−88.668	−90.783	−92.519	−94.037	−95.363
n-Hexadecylcyclohexane	$C_{22}H_{44}$	do	−27.949	−28.445	−49.142	−62.272	−71.385	−78.093	−83.181	−87.202	−90.434	−93.063	−95.276	−97.094	−98.683	−100.073
Increment per CH_2 group		do	−1.5012	−1.5226	−2.4472	−3.0295	−3.4341	−3.7312	−3.9568	−4.1352	−4.2790	−4.3944	−4.4926	−4.5752	−4.6463	−4.7106

TABLE 19.—*Values of the logarithm of the equilibrium constant of formation, for the ideal gaseous state, to 1,500° K, for the 7 dimethylcyclohexanes*

Compound (gas)	Formula	Temperature in ° K													
		0	298.16	300	400	500	600	700	800	900	1,000	1,100	1,200	1,300	1,400	1,500
		Logarithm of equilibrium constant of formation, $\log_{10} K_f$														
1,1-Dimethylcyclohexane	C_8H_{16}	Infinite	−6.174	−6.363	−14.541	−19.735	−23.359	−26.031	−28.045	−29.642	−30.911	−31.947	−32.813	−33.544	−34.146	−34.628
cis-1,2-Dimethylcyclohexane	C_8H_{16}	do	−7.225	−7.408	−15.186	−20.163	−23.622	−26.108	−28.105	−29.642	−30.863	−31.859	−32.692	−33.396	−33.974	−34.435
trans-1,2-Dimethylcyclohexane	C_8H_{16}	do	−6.038	−6.227	−14.334	−19.503	−23.083	−25.731	−27.723	−29.298	−30.566	−31.601	−32.445	−33.176	−33.755	−34.259
cis-1,3-Dimethylcyclohexane [a]	C_8H_{16}	do	−5.228	−5.424	−13.749	−19.040	−22.722	−25.428	−27.485	−29.094	−30.389	−31.446	−32.339	−33.055	−33.670	−34.185
trans-1,3-Dimethylcyclohexane [a]	C_8H_{16}	do	−6.363	−6.549	−14.510	−19.760	−23.152	−25.756	−27.737	−29.286	−30.555	−31.573	−32.425	−33.144	−33.736	−34.230
cis-1,4-Dimethylcyclohexane	C_8H_{16}	do	−6.650	−6.836	−14.831	−19.867	−23.429	−26.034	−27.994	−29.586	−30.856	−31.875	−32.727	−33.447	−34.038	−34.533
trans-1,4-Dimethylcyclohexane	C_8H_{16}	do	−5.552	−5.746	−14.071	−19.359	−23.039	−25.722	−27.756	−29.384	−30.657	−31.714	−32.597	−33.322	−33.937	−34.430

[a] See footnotes a and b of table 22.

Figures 1 and 2 show the thermodynamic stability of the normal alkylcyclopentanes and alkylcyclohexanes in the gaseous state as a function of the temperature, in the form of a plot of the standard free energy of formation, per carbon atom, divided by the absolute temperature $(\Delta f^\circ/n)/T$.

V. Free Energies and Equilibria of Some Reactions of Isomerization, Cyclization, and Hydrogenation Involving Alkylcyclopentanes and Alkylcyclohexanes

In figures 3 and 4 are plotted, as a function of temperature, values of the logarithm of the equilibrium constant for the reaction of cyclization of a given normal paraffin to a normal alkylcyclopentane or a normal alkylcyclohexane.

In figure 5 are plotted, as a function of temperature, values of the logarithm of the equilibrium constant for the reaction of isomerization of a given normal alkylcyclohexane to a normal alkylcyclopentane.

Values of the logarithm of the equilibrium constant for the reactions of hydrogenation of the normal alkylbenzenes [17] to normal alkylcyclopentanes and alkylcyclohexanes, as a function of temperatures, are plotted in figures 6 and 7.

Figures 8 and 9 show the logarithms of the equilibrium constants of the reactions of cyclization of normal l-alkenes [18] to normal alkylcyclopentanes and alkylcyclohexanes, as a function of the temperature.

In figure 10 are plotted, as a function of the temperature, the values of $\Delta F^\circ/T$ for the isomerization of ethylcyclohexane into each of the seven dimethylcyclohexanes. The corresponding numerical values are given in table 20.

In figure 11 are plotted, as a function of the temperature, for the C_8H_{16} alkylcyclohexanes, the amounts, in mole fraction, of each of the isomers present at equilibrium with its other isomers in the gas phase. The corresponding numerical values are given in table 21.

TABLE 20.—*Free energies and equilibrium constants for the isomerization of ethylcyclohexane to the isomeric dimethylcyclohexanes in the ideal gaseous state to 1,500° K*

Temperature	Ethylcyclohexane = 1,1-dimethylcyclohexane		Ethylcyclohexane = *cis*-1,2-dimethylcyclohexane		Ethylcyclohexane = *trans*-1,2-dimethylcyclohexane	
°K	$\Delta F^\circ/T$	K	$\Delta F^\circ/T$	K	$\Delta F^\circ/T$	K
200	6.65	28.4	−1.55	0.46	7.05	34.8
298.16	3.20	5.01	−1.61	.446	3.83	6.85
300	3.18	4.97	−1.60	.446	3.81	6.79
400	1.28	1.90	−1.68	.431	2.23	3.06
500	0.08	1.04	−1.88	.398	1.14	1.77
600	−.68	0.710	−1.88	.398	0.58	1.34
700	−1.26	.531	−1.80	.398	.11	1.06
800	−1.61	.445	−1.89	.398	−.14	0.933
900	−1.99	.367	−1.99	.367	−.41	.813
1,000	−2.21	.329	−1.99	.367	−.63	.728
1,100	−2.39	.300	−1.99	.367	−.81	.665
1,200	−2.54	.278	−1.99	.367	−.86	.649
1,300	−2.77	.248	−2.09	.349	−1.09	.579
1,400	−2.88	.235	−2.09	.349	−1.09	.579
1,500	−2.87	.236	−1.99	.367	−1.19	.551

	Ethylcyclohexane = *cis*-1,3-dimethylcyclohexane [a]		Ethylcyclohexane = *trans*-1,3-dimethylcyclohexane [a]		Ethylcyclohexane = *cis*-1,4-dimethylcyclohexane		Ethylcyclohexane = *trans*-1,4-dimethylcyclohexane	
	$\Delta F^\circ/T$	K	$\Delta F^\circ/T$	K	$\Delta F^\circ/T$	K	$\Delta F^\circ/T$	K
200	12.60	568.	4.2	8.28	2.9	4.31	11.15	274.
298.16	7.53	44.3	2.34	3.24	1.02	1.68	6.05	21.0
300	7.49	43.2	2.33	3.24	1.02	1.67	6.01	20.6
400	4.90	11.8	1.40	2.04	−0.05	0.975	3.43	5.61
500	3.26	5.15	0.74	1.45	−.62	.733	1.80	2.47
600	2.23	3.08	.27	1.14	−1.00	.604	0.78	1.48
700	1.50	2.13	.00	1.00	−1.27	.527	.16	1.08
800	0.95	1.61	−.20	0.904	−1.47	.500	−.29	0.865
900	.52	1.30	−.36	.836	−1.73	.418	−.81	.665
1,000	.18	1.09	−.58	.747	−1.96	.373	−1.05	.590
1,100	−.10	0.951	−.68	.710	−2.06	.354	−1.33	.513
1,200	−.33	.845	−.77	.679	−2.15	.339	−1.56	.457
1,300	−.53	.766	−.94	.624	−2.32	.310	−1.75	.414
1,400	−.70	.703	−1.00	.604	−2.39	.301	−1.92	.380
1,500	−.85	.653	−1.05	.589	−2.44	.293	−1.97	.372

[a] See footnotes a and b of table 22.

TABLE 21.—*Equilibrium concentrations of the* C_8H_{16} *alkylcyclohexanes in the ideal gaseous state to 1,500° K.*

Temperature	Composition, in mole fraction, of equilibrium mixture of isomers							
	Ethylcyclohexane	Dimethylcyclohexanes [a]						
		1,1	*cis*-1,2	*trans*-1,2	*cis*-1,3	*trans*-1,3	*cis*-1,4	*trans*-1,4
°K								
200	0.0011	0.0309	0.0005	0.0379	0.6179	0.0690	0.0047	0.2081
298.16	.0120	.0600	.0053	.0820	.5304	.0388	.0201	.2514
300	.0122	.0607	.0055	.0829	.5273	.0386	.0204	.2515
400	.0373	.0709	.0161	.1141	.4400	.0761	.0364	.2092
500	.0719	.0743	.0277	.1264	.3678	.1036	.0524	.1764
600	.1027	.0729	.0397	.1376	.3162	.1170	.0620	.1519
700	.1296	.0688	.0502	.1374	.2761	.1286	.0683	.1400
800	.1505	.0670	.0582	.1404	.2423	.1361	.0753	.1302
900	.1734	.0636	.0636	.1410	.2255	.1450	.0725	.1153
1,000	.1914	.0630	.0703	.1394	.2087	.1430	.0714	.1129
1,100	.2058	.0617	.0755	.1368	.1957	.1461	.0728	.1056
1,200	.2167	.0603	.0795	.1407	.1831	.1472	.0735	.0980
1,300	.2331	.0578	.0814	.1350	.1786	.1455	.0723	.0965
1,400	.2410	.0566	.0841	.1393	.1694	.1455	.0725	.0916
1,500	.2462	.0581	.0804	.1357	.1608	.1450	.0721	.0916

[a] See footnotes a and b of table 22.

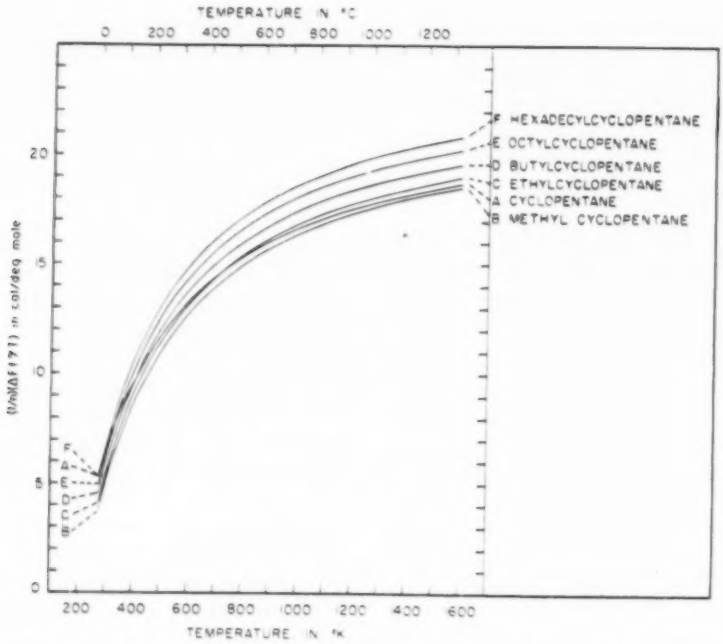

FIGURE 1.—*Thermodynamic stability of the n-alkylcyclopentanes in gaseous state as of a function of the temperature.*

The scale of ordinates gives the value of $(1/n)$ $(\Delta F^\circ/T)$ in calories per degree mole, where n is the number of carbon atoms per molecule, T is the absolute temperature in degrees Kelvin, and ΔF° is the standard free energy of formation of the hydrocarbon from the elements, solid carbon (graphite) and gaseous hydrogen, all at the given temperature. The scale of abscissas gives the temperature in degrees Kelvin.

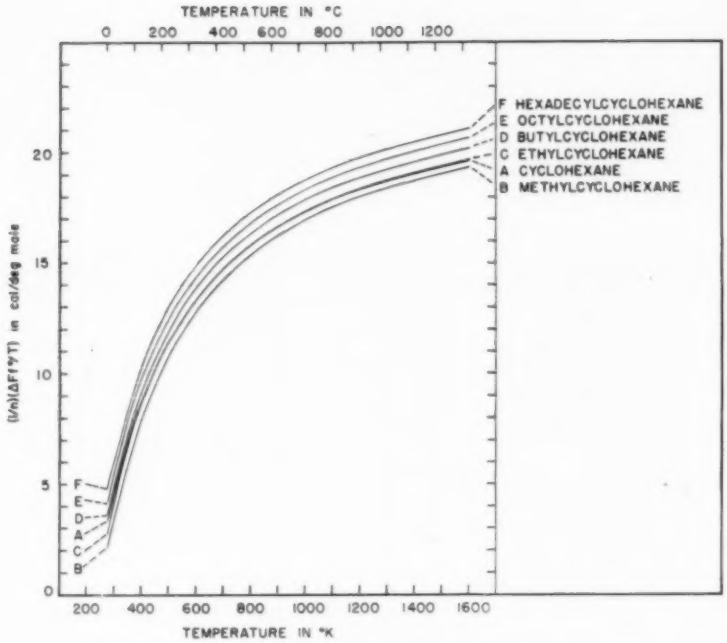

FIGURE 2.—*Thermodynamic stability of the n-alkylcyclohexanes in the gaseous state as a function of the temperature.*

The scale of ordinates gives the value of $(1/n)\ (\Delta F_T^\circ/T)$ in calories per degree mole, where n is the number of carbon atoms per molecule, T is the absolute temperature in degrees Kelvin, and ΔF_T° is the standard free energy of formation of the hydrocarbon from the elements, solid carbon (graphite) and gaseous hydrogen, all at the given temperature. The scale of abscissas gives the temperature in degrees Kelvin.

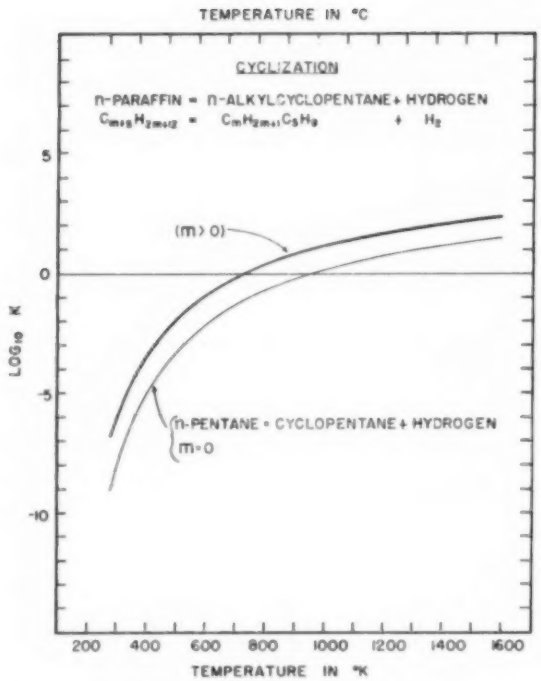

FIGURE 3.—*Logarithm of the equilibrium constant for the reaction of cyclization of n-paraffins to n-alkylcyclopentanes.*

The scale of ordinates gives the value of the logarithm (to the base 10) of the equilibrium constant for the reaction of cyclization of a given *n*-paraffin to the corresponding *n*-alkylcyclopentane, in the gaseous state. The scale of abscissas gives the temperature in degrees Kelvin. The values calculated for methylcyclopentane, ethylcyclopentane, and the higher *n*-alkylcyclopentanes all fall within the width of the heavy line indicated.

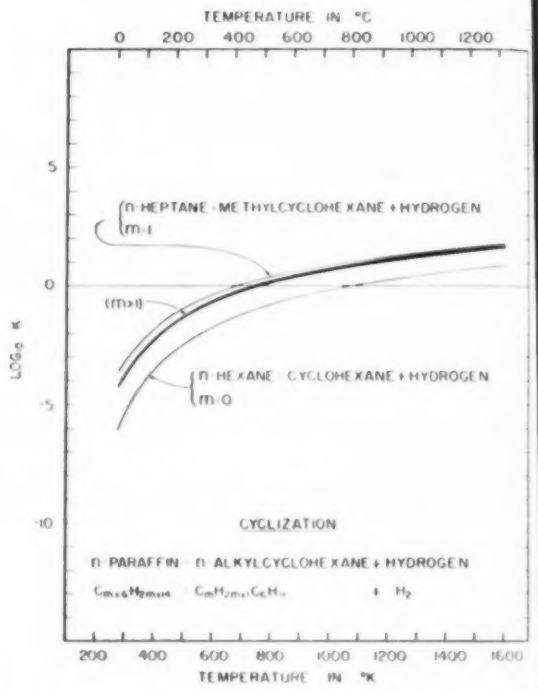

FIGURE 4.—*Logarithm of the equilibrium constant for the reaction of cyclization of n-paraffins to n-alkylcyclohexanes.*

The scale of ordinates gives the value of the logarithm (to the base 10) of the equilibrium constant for the reaction of cyclization of a given *n*-paraffin to the corresponding *n*-alkylcyclohexane, in the gaseous state. The scale of abscissas gives the temperature in degrees Kelvin. The values calculated for ethylcyclohexane, *n*-propylcyclohexane, and the higher *n*-alkylcyclohexanes all fall within the width of the heavy line indicated.

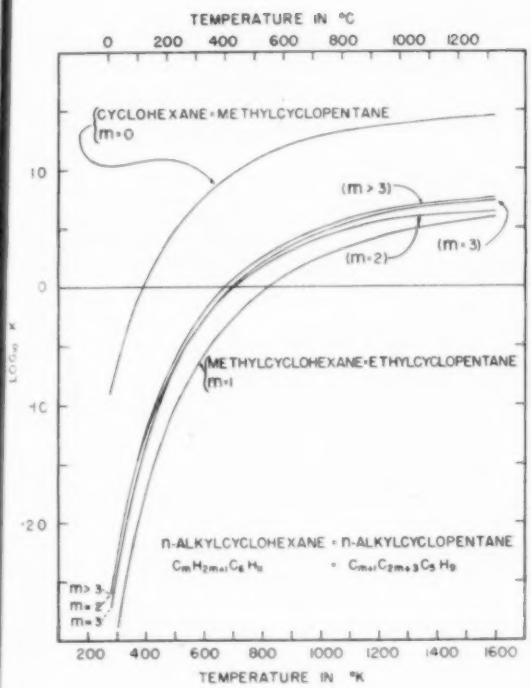

FIGURE 5.—*Logarithm of the equilibrium constant for the reaction of conversion of n-alkylcyclohexanes to n-alkylcyclopentanes.*

The scale of ordinates gives the value of the logarithm (to the base 10) of the equilibrium constant for the reaction of conversion of a given *n*-alkylcyclohexane to the corresponding *n*-alkylcyclopentane, in the gaseous state. The scale of abscissas gives the temperature in degrees Kelvin.

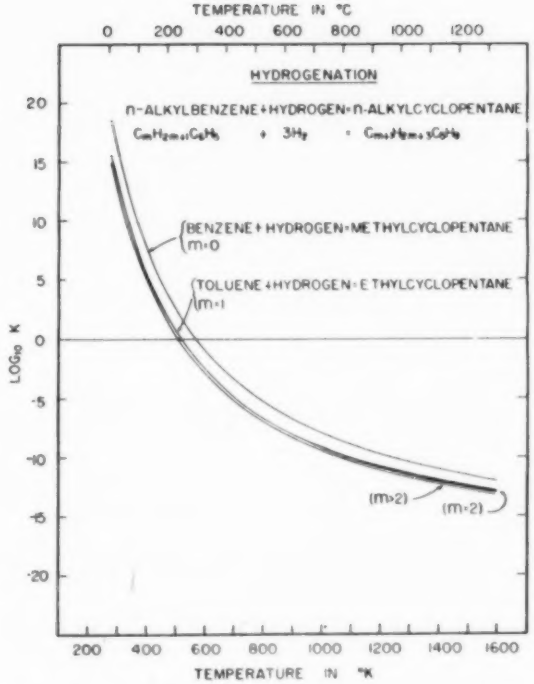

FIGURE 6.—*Logarithm of the equilibrium constant for the reaction of hydrogenation of n-alkylbenzenes to n-alkylcyclopentanes.*

The scale of ordinates gives the value of the logarithm (to the base 10) of the equilibrium constant for the reaction of hydrogenation of a given *n*-alkylbenzene to the corresponding *n*-alkylcyclopentane, in the gaseous state. The scale of abscissas gives the temperature in degrees Kelvin.

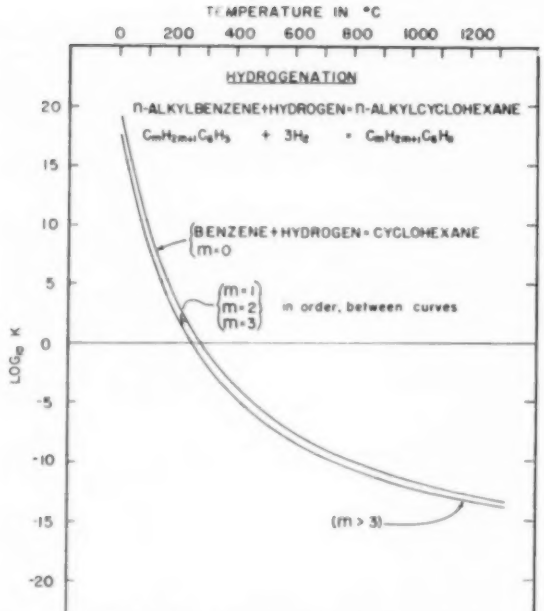

FIGURE 7.—*Logarithm of the equilibrium constant for the reaction of hydrogenation of n-alkylbenzenes to n-alkylcyclohexanes.*

The scale of ordinates gives the value of the logarithm (to the base 10) of the equilibrium constant for the reaction of hydrogenation of a given *n*-alkylbenzene to the corresponding *n*-alkylcyclohexane, in the gaseous state. The scale of abscissas gives the temperature in degrees Kelvin. The upper curve is that for the hydrogenation of benzene and the lower curve is for the hydrogenation of butylbenzene, *n*-pentylbenzene and the higher *n*-alkylbenzenes. The curves for toluene, ethylbenzene, and *n*-propylbenzene lie, in order, between the two curves.

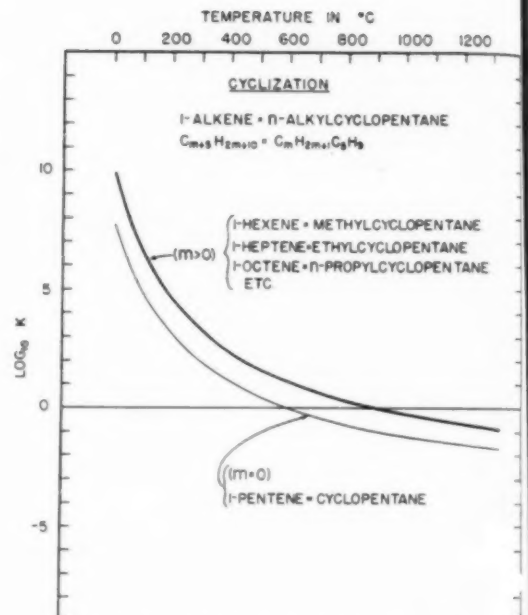

FIGURE 8.—*Logarithm of the equilibrium constant for th reaction of cyclization of 1-olefins to n-alkylcyclopentanes.*

The scale of ordinates gives the value of the logarithm (to the base 10) of th equilibrium constant for the reaction of cyclization of a given 1-olefin t the corresponding *n*-alkylcyclopentane, in the gaseous state. The scal of abscissas gives the temperature in degrees Kelvin. The values for th formation of methylcyclopentane, ethylcyclopentane, and higher *n*-alkyl cyclopentanes all fall within the width of the heavy line indicated.

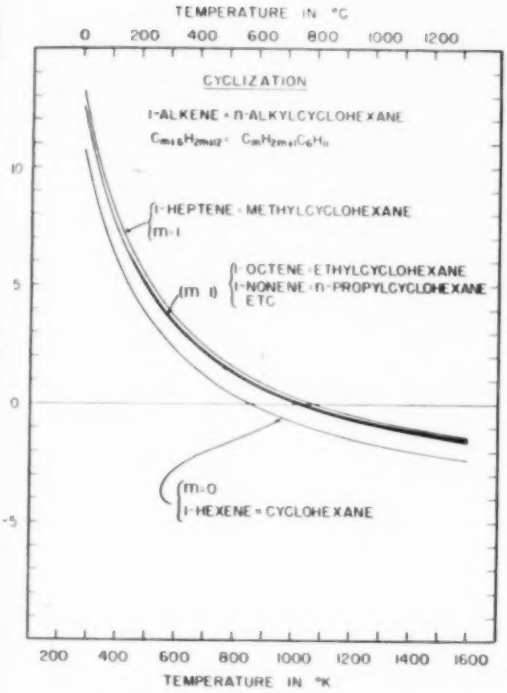

FIGURE 9.—*Logarithms of the equilibrium constant for the reaction of cyclization of 1-olefins to n-alkylcyclohexanes.*

The scale of ordinates gives the value of the logarithm (to the base 10) of the equilibrium constant for the reaction of cyclization of a given 1-olefin to the corresponding *n* alkylcyclohexane, in the gaseous state. The scale of abscissas gives the temperature in degrees Kelvin. The values calculated for ethylcyclohexane, propylcyclohexane and the higher *n*-alkylcyclohexanes all fall within the width of the heavy line indicated.

Figure 12 shows, for the equilibrium between cyclohexane and methylcyclopentane, a comparison of the values derived from this report with values reported experimentally by Schuit, Hoog, and Verheus [9], Glasebrook and Lovell [10], Shell Development Co. [11], and Mizusima, Morino, and Fujisiro [12].

Table 22 gives, for the relative amounts of the *cis* and *trans* isomers of 1,2-dimethylcyclohexane, 1,3-dimethylcyclohexane, and 1,4-dimethylcyclohexane, a comparison of the values derived from this report with experimental values reported by Boord, Greenlee, et al. [15].

TABLE 22.—*Comparison of the calculated and experimental values for the relative amounts at equilibrium of some pairs of isomeric (cis and trans) dimethylcyclohexanes*

Compounds	Temperature	Relative amounts at equilibrium	
		Calculated (liquid)	Experimental [c] (liquid)
	°C		
cis-1,2-Dimethylcyclohexane	250	21	35
trans-1,2-Dimethylcyclohexane	.....	79	65
cis-1,3-Dimethylcyclohexane [a]	225	77	78
trans-1,3-Dimethylcyclohexane [b]	.....	23	22
cis-1,4-Dimethylcyclohexane	200	22	37
trans-1,4-Dimethylcyclohexane	.....	78	63

[a] This isomer, formerly labeled "*trans*", has the following properties [16]: Boiling point at 1 atm, 120.09° C; refractive index, n_D at 25° C, 1.4206; density at 25° C, 07620 g/ml.

[b] This isomer, formerly labeled "*cis*", has the following properties [16]: Boiling point at 1 atm, 124.45° C; refractive index, n_D at 25° C, 1.4284; density, at 25° C, 0.7806 g/ml.

[c] From reference [15].

765484—47——5

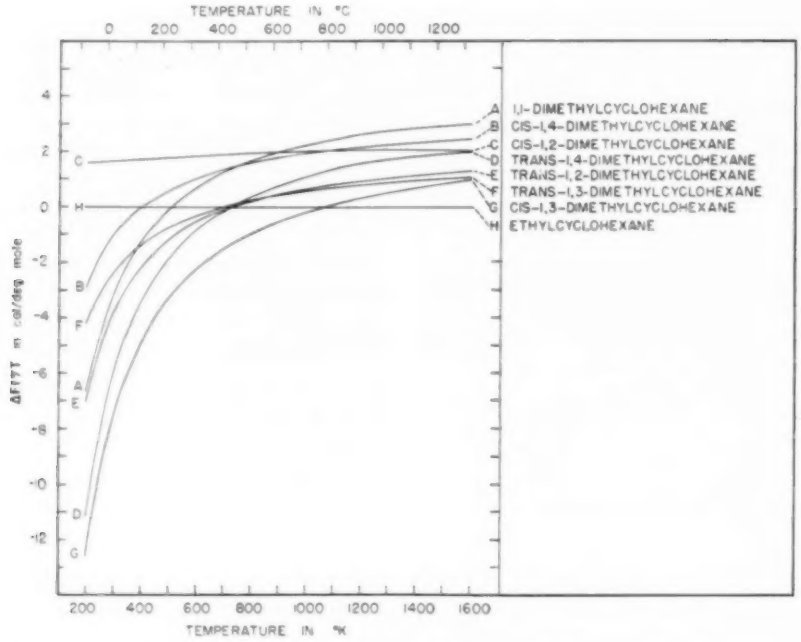

FIGURE 10.—*Free energy of isomerization of the eight* C_8H_{16} *alkylcyclohexanes.*

The scale of ordinates gives the value of $\Delta F°/T$, in calories per degree mole, for the isomerization of ethylcyclohexane into the other isomers, in the gaseous state, as indicated. The scale of abscissas gives the temperature in degrees Kelvin. See reference [16] for identification of the dimethylcyclohexanes.

VI. References

[1] J. E. Kilpatrick, K. S. Pitzer, and R. Spitzer, J. Am. Chem. Soc. **69**, 2488 (1947)

[2] C. W. Beckett, K. S. Pitzer, and R. Spitzer, J. Am. Chem. Soc., **69**, 2488 (1947)

[3] E. J. Prosen, W. H. Johnson, and F. D. Rossini, J. Research NBS **37,** 1 (1946) RP1728.

[4] E. J. Prosen, W. H. Johnson, and F. D. Rossini, J. Research NBS **39,** 173 (1947) RP1821.

[5] D. D. Wagman, J. E. Kilpatrick, W. J. Taylor, K. S. Pitzer, and F. D. Rossini, J. Research NBS, **34,** 143 (1945) RP1634.

[6] K. S. Pitzer and J. E. Kilpatrick, Chem. Rev. **39,** 435 (1946).

[7] K. S. Pitzer, Ind. Eng. Chem. **36,** 829 (1944).

[8] K. S. Pitzer and C. W. Beckett, J. Am. Chem. Soc., **69,** 977 (1947).

[9] G. C. A. Schuit, H. Hoog, and J. Verheus, Rec. Trav. Chem. Pay-bas, **59,** 793 (1940).

[10] A. L. Glasebrook and W. G. Lovell, J. Am. Chem. Soc. **61,** 1717 (1939).

[11] Shell Development Co., Emeryville, Calif. Unpublished data.

[12] S. Mizusima, Y. Morino, and R. Fujisiro, Sci. Papers Inst. Phys. Chem. Research, **38,** No. 1034, 40 (1941).

[13] American Petroleum Institute Research Project 44 at the National Bureau of Standards. Selected Values of Properties of Hydrocarbons. Table ... Values of constants.

[14] American Petroleum Institute Research Project 44 at the National Bureau of Standards. Selected Values of Properties of Hydrocarbons. Tables 1, 2, 5, 20, and 24, *r*, *s*, and *v*. Heat-content function, Free-energy function, and Heat capacity.

[15] C. E. Boord, K. W. Greenlee, et al., American Petroleum Institute Research Project 45. Ohio State University. Unpublished data.

[16] American Petroleum Institute Research Project 44 at the National Bureau of Standards. Selected Values of Properties of Hydrocarbons. Table 7a. Boiling point, refractive index, density, and freezing point.

[17] W. J. Taylor, D. D. Wagman, M. G. Williams, K. S. Pitzer, and F. D. Rossini, J. Research NBS **37,** 95 (1946) RP1732.

[18] J. E. Kilpatrick, E. J. Prosen, K. S. Pitzer, and F. D. Rossini, J. Research NBS **36,** 559 (1946) RP1722.

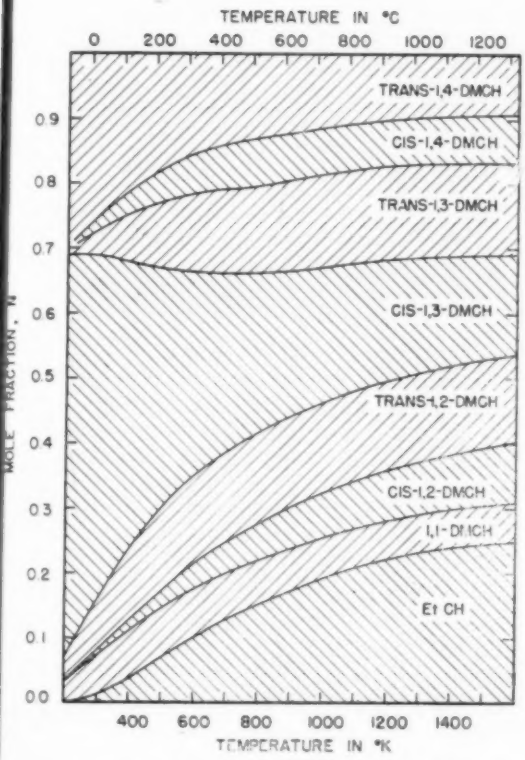

FIGURE 11.—*Equilibrium concentrations of the eight C_8H_{16} alkylcyclohexanes.*

The scale of ordinates measures the amount in mole fraction, and the scale of abscissas gives the temperature in degrees Kelvin and degrees centigrade. The vertical width of a band at a given temperature measures the mole fraction of the given isomer present when at equilibrium with all of its other isomers, in the gas phase. See reference [16] for identification of the dimethylcyclohexanes.

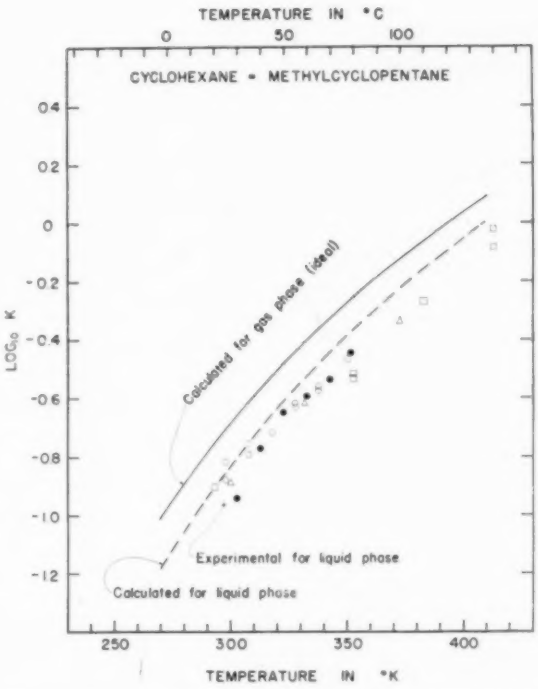

FIGURE 12.—*Comparison of calculated and experimental data on the equilibrium between cyclohexane and methylcyclopentane.*

The scale of ordinates gives the value of the logarithm (to the base 10) of the equilibrium constant for the reaction of isomerization of cyclohexane to methylcyclopentane. The scale of abscissas gives the temperature in degrees Kelvin. The solid line refers to the reaction with both components in the liquid phase. The experimental data refer to the liquid phase and are from the following investigations: □, Schuit, Hoog, and Verheus [9]; ○, Glasebrook and Lovell [10]; △, Shell Development Company [11]; ●, Mizusima, Morino and Fujisiro [12]. The dotted line refers to the reaction with both components in the ideal gaseous phase.

WASHINGTON, July 18, 1947.

U. S. Department of Commerce
National Bureau of Standards

Research Paper RP1846
Volume 39, December 1947

Part of the Journal of Research of the National Bureau of Standards

Factors Affecting Operation of Apparatus for Counting Alpha Particles in an Ion Counting Chamber

By F. J. Davis

The resolving times of two amplifier circuits for the counting of alpha particles in a cylindrical ion chamber is discussed. The original circuit, using a floating grid on the first stage of the amplifier, gave a resolving time of 2.5×10^{-3} second. An improved circuit using a 1-megohm grid resistor on the first stage lowered the resolving time to 1.4×10^{-4} second

The effect on the counting rate of the presence of small amounts of CO, CO_2, H_2O and HCl in the ion chamber was found to be negligible. The presence of 1 percent of air, however, reduces the counting efficiency by 20 percent.

A method whereby the collection time of radon in radium solutions may be of the order of ½ hour is given. Experiments show that boiling and bubbling nitrogen through 200 ml radium solutions for 17 minutes removes 99.99 percent of the radon. The absorption of radon by small neoprene meteorlogical balloons was found to be approximatly (0.03%/min)/100 cm^2.

I. Introduction

In the operation of the alpha particle counting apparatus for the determination of radium by the radon method [1] two problems that have been investigated are (1) the resolution of the electronic pulses resulting from the alpha particles and (2) the quantitative transfer of the radon representing the radium.

Factors contributing to the first problem are the resolving time of the electronic circuit and the composition of the gas. Pulses occuring within an interval less than the resolving time are recorded as a single pulse. This affects the calibration constant so that it is a function of counting rate as well as resolving time. The electronic pulses are essentially produced by the collection of electrons on the center electrode of the ion chamber. In the presence of gases such as oxygen, which have a high affinity for electrons, the electrons are captured with the formation of heavy negative ions of low mobility. As a result, the pulses are broadened and reduced in height so that many pulses fail to reach the threshold pulse height that will just activate the pulse discriminator and thus fail to be recorded.

Factors involved in the second problem (transfer of radon) are (1) deemanation time, (2) collection time, and (3) absorption of radon. The deemanation time or the time required to extract the radon from the solution should be sufficient to transfer all radon from the solution to the chamber, and it will depend on the volume of the ion chamber as well as on the amount of solution. The collection time, that is, the time allowed for the growth of radon in the radium solution, should be sufficiently well defined so that the amount of radon produced may serve as a measure of the radium present. This is especially critical when this time interval is short. The absorption of radon in rubber is important in the taking of breath samples that are usually obtained by the inflation of a balloon.

II. Resolving Time

The resolving time used in this paper is defined by the relation $N=N_0e^{-ft}$, where N is the count per hour per 10^{-12} curie, t the resolving time, f the

[1] L. F. Curtiss and F. J. Davis, J. Research NBS 31, 181 (1943) RP1557.

actual count per hour and N_o is the count per hour per 10^{-12} curie for $f=0$.

The calibration constant N becomes smaller the larger the resolving time. The immediate advantage of a short resolving time, seen from the formula, is that larger samples may be measured without having to apply a large correction to allow for unresolved pulses. As the statistical error of a random count is determined by the square root of its total count, a further advantage gained by a higher counting rate is that greater accuracy is obtained in a given time of measurement.

If the apparatus used is an ion chamber with an amplifying device, such as a FP–54 circuit with a galvanometer, the resolving time may be of the order of 1 second, thus limiting the radon from the sample measured to the order of 10^{-12} curie. With this limitation, samples that must be fused in a vacuum furnace may require quantities of the order of milligrams or less, thereby introducing sampling errors.

In figure 1 is shown the calibration or count per hour per 10^{-12} curie for different counting

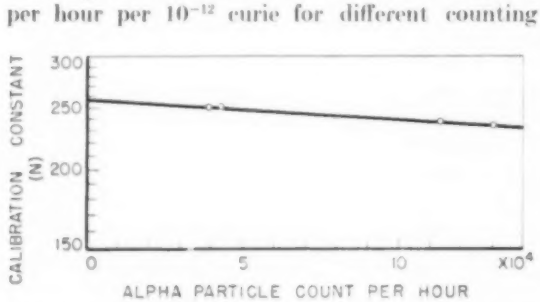

FIGURE 1.—*Variation of calibration count per hour per 10^{-12} curie with counting rate for the original circuit.*

Resolving time calculated from slope of curve equals 2.5×10^{-3} sec.

rates for the apparatus as described in a previous paper.[2] The count per hour per 10^{-12} curie is plotted as the ordinate on a logarithmic scale and the counting rate as the abscissa on a linear scale. It is to be noted that the calibration constant N drops from 257 counts/hr per 10^{-12} curie for small counts, to 239 for a counting rate of 100,000 counts/hr, which is the equivalent of 4.2×10^{-10} curie.

Calculating t from the slope of the line in figure 1 gives $t=2.5\times10^{-3}$ sec. Although this resolving time is adequate for breath samples and room air samples where the amount of radon rarely exceeds 5×10^{-11} curie, it requires the use of the calibration curve for samples over this value.

In the amplifier used to secure the data shown in figure 1, no grid leak was used on the first amplification stage (type 38 tube). To shorten the resolving time for this circuit, the obvious method was the placing of a 1-megohm grid leak between the grid of the 38 tube and ground. The effect of this is shown in figure 2. The

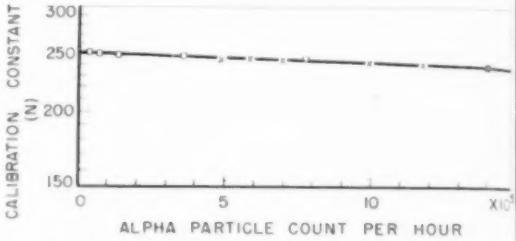

FIG. 2.—*Variation of calibration count per hour per 10^{-12} curie with the counting rate for short resolving time circuit.*

Resolving time calculated from slope of curve equals 1.4×10^{-4} sec. The circles represent independent samples of radon. The crosses represent different recounts of a single sample while decaying during a period of 1 week.

calibration count per hour per 10^{-12} curie drops from 252 for small counting rates to 238 for a counting rate of 1,400,000 counts/hr. It is to be noted that the counting rate in figure 2 covers a tenfold range of that shown in figure 1. Calculating the resolving time from the slope of the line gives $t=1.4\times10^{-4}$ sec.

These two curves are for the same chamber, 38 tube and amplifier. For the first curve, the circuit for the 38 tube and amplifier was as suggested by Waddell.[3] In our amplifier a coupling condenser of 500 $\mu\mu$f was used for the plate of the 38 tube to the grid of the following stage. For the second curve the changes made in the circuit of the 38 tube were (1) replacing the 500-$\mu\mu$f coupling condenser on the plate with a 100-$\mu\mu$f condenser, (2) connecting a 1-megohm grid leak to the ground, (3) limiting the cathode emission by placing a resistor of about 30 ohms in parallel with the heater, and (4) the 38 tube was connected as a triode, that is, with the screen grid and plate connected together.

The original circuit with the longer resolving time has a greater efficiency of counting at slow

[2] See footnote 1.

[3] R. C. Waddell, Rev. Sci. Instruments **10**, 311 (1939).

ates as shown by comparing figures 1 and 2. This increased efficiency is probably due to a better signal to noise ratio, which is somewhat higher for the original circuit. As the number of pulses that are below the threshold pulse height in either circuit is small, the difference in the efficiency of counting by the two circuits amounts to only 2 perent.

In figure 2 the calibration curve for the short resolving time circuit shows both circles and crosses. The circles are independent fillings of the chambers from two different standards, one containing 10^{-9} g Ra for the lower counting rates and the other 1.077×10^{-8} g Ra for the higher counting rate. The crosses are all from a single filling and represent different recounts, beginning on the right and proceeding to the left, as the radon decayed in the chamber. The value used for λ, the decay constant of radon was 0.00755/hr. The decay of the radon was followed for 1 week, and each cross was the average of a 12-hour run with 24 hours between the beginning of each run, except between the third and fourth crosses from the right, when it was 48 hours.

A side tube containing water was sealed on a chamber and the temperature of the water controlled. No effect on the counting rate was noted for temperatures below room temperature. At room temperature spurious pulses occurred, probably due to leakage across insulators in the chamber. A single drying trap using $CaCl_2$ removes water vapor sufficiently for satisfactory operation.

Hydrogen chloride of the amount driven off from deemanating a 5-percent HCl solution has no effect on the counting rate. However, if strong HCl solutions such as constant boiling mixtures are used, the counting rate is reduced. A trap filled with Ascarite followed by a drying trap can be used to remove the hydrogen chloride.

The CO and CO_2 were taken from commercial gas cylinders and passed through the purification system described in a previous paper,[4] which removed the oxygen and water vapor. In the case of CO, an additional trap of Ascarite plus a drying agent was used to remove any CO_2 present.

[4] See footnote 1.

III. Effect of Composition of Gas

The effect on the calibration constant of the presence of carbon monoxide, carbon dioxide, air, and water vapor was determined. Considerable quantities of CO are formed by a carbon-crucible vacuum-furnace when oxygen is liberated from the samples fused. The effect of using CO in place of nitrogen in the ion chamber was to lower the calibration constant by only 1 percent.

A small amount of CO_2 seems to decrease the resolving time of the apparatus. The effect of the addition of CO_2 is shown in figure 3. The ordinate represents the resolving time in 10^{-4} sec, and the abscissa represents the percent by volume of CO_2 in the chamber. The resolving time falls to a minimum near 10 percent of CO_2, whereas at 20 percent of CO_2 it is about the same as pure nitrogen and at greater percentages the resolving time rises. The effect of CO_2 on the calibration constant for concentrations less than 20 percent at a counting rate of 250,000 counts/hr is less than ½ percent.

The effect of air in the chambers is very marked; 1 percent of air reduces the counting efficiency at 30,000 counts/hr by approximately 20 percent.

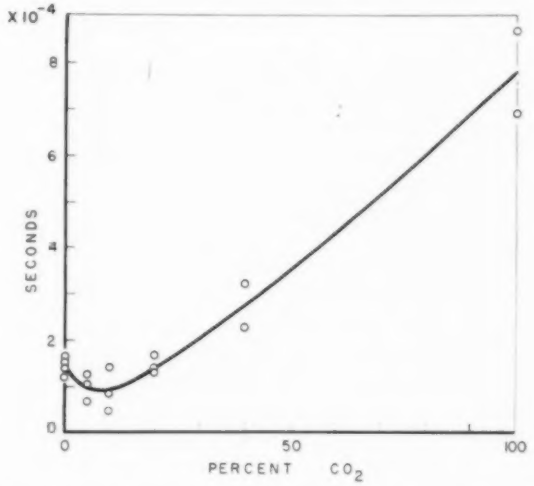

FIGURE 3.—*Curve showing effect of* CO_2 *on resolving time.*

The circles represent observations made by using the short resolving time circuit.

IV. Deemanation Time

The method used for deemanating solutions is to boil the solutions under reduced pressure of approximately 1/2 atmosphere in a reflux condenser while bubbling N_2 through it as the transfer agent to carry the radon into the chamber. As the chamber is filled to atmospheric pressure, the pressure and boiling temperature in the condenser rises accordingly. The time required to fill the chamber is usually 16 to 18 minutes in order to efficiently remove O_2.

A test was made to measure the efficiency of transferring the radon from a 200-ml solution for various deemanation times into a 3.6-liter chamber. This was accomplished by filling a chamber in a specified time and immediately on completion reboiling the same solution and filling a second chamber to measure any radon remaining in the solution. For a 17-minute deemanation time, no radon was found in the solution in excess of that amount that would grow from the radium in the solution in the short time between the two runs. The efficiency of the above test was such that one-hundredth of a percent would have been detected. For a 10.5-minute run, 0.020 $\pm$0.003 percent of the radon remained in the solution. For a run of 6 minutes 1.01 percent of the radon remained.

The results of a slightly different experiment to determine the amount of radon transferred during a normal run of 16 minutes is shown in figure 4, where the amount of radon removed from a solution containing 1.62×10^{-10} curie of radon is plotted against the time from the start of the deemanation. In this case, the flow of nitrogen through the solution was adjusted to a rate that would normally fill a chamber to atmospheric pressure in 16 minutes. It was then allowed to flow for the first minute into chamber number one; for the second minute into chamber number two; for the next 2 minutes into chamber number three; the next 4 minutes into chamber number four, and the remaining 8 minutes into chamber number five. After the deemanation was completed, the chambers were filled to atmospheric pressure with N_2. The amount of radon transferred at the termination of the filling of any one chamber would then be the sum of the amount of radon in the chamber and the preceding chambers filled.

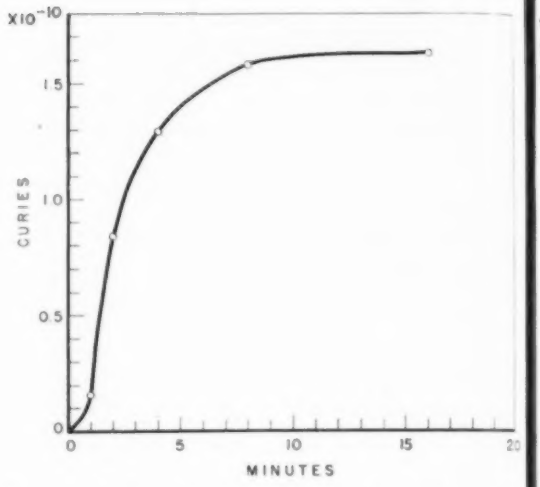

FIGURE 4.—*Curve showing radon transferred from reflux condenser to ion chamber during deemanation.*

Total amount of radon transferred 1.62×10^{-10} curie

During the first minute of deemanation the stopcocks are being adjusted, consequently the first point may vary considerably for different runs. According to the curve in figure 4 the radon transferred in the first 6 minutes is 92 percent. As only a portion of the nitrogen has passed through the solution to fill a chamber, less radon is transferred than when all the nitrogen passes through the solution to fill a chamber as in the earlier experiment.

V. Collection Time

The time allowed for the collection of the radon from a sample is the interval between a preliminary deemanation and the filling of the chamber by a second deemanation process. This interval is measured from the instant when the stopcocks are closed on the reflux condenser at the end of the first deemanation to the exact instant during the subsequent filling of the ion chamber when all the radon destined to enter the chamber has been removed from the solution. The collection time terminates before the ionization chamber stopcock is closed, as it takes some time for the radon to pass through the purification system. The effective point of termination of the collection is fixed according to the following consideration. Suppose first that the ionization chamber is filled to atmospheric pressure and the purifying

system evacuated. If then the stopcock T_3 in figure 5 is opened, the mercury manometer will come to a level B depending on the relative volumes of the ionization chamber and the purifying system. Vice versa, in our actual operation, when the manometer reaches the level B, we know that all the radon contained in the purifying system and that radon alone will be swept into the ionization chamber when this is filled up to atmospheric pressure. All that is necessary to determine the time of the second deemanation is to record the time when the mercury crosses the mark B while filling the chamber. The radon accumulated in the additional time of filling fails to reach the chamber.

Using this interval for short time collections proved to be accurate within the statistical error of 0.3 percent, even for a collection time of 30 minutes.

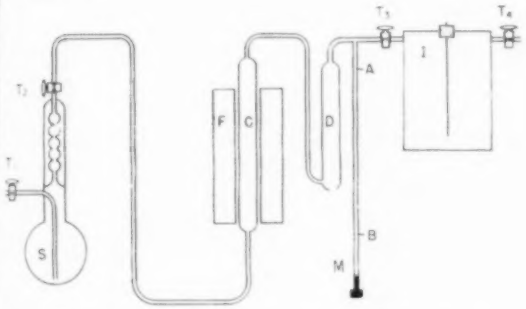

FIGURE 5.—*Diagram of apparatus for filling chambers.*

F, Furnace; *C*, quartz tube containing reduced copper gauze; *D*, drying tube; *M*, mercury manometer; *I*, ion chamber; *S*, reflux condenser containing radium solution or standard.

VI. Absorption of Radon

The absorption of radon by small neoprene meteorological balloons, such as are sometimes used in transferring samples, is shown in figure 6. The percent absorption of radon is plotted against time of contact with the neoprene. The area of the balloon used was about 2,500 cm². Using this value, the amount of absorption is approximately (0.03%/min)/100 cm². The absorption was measured by placing a known amount of radon in a balloon, allowing it to stand for the period of time under consideration, and then measuring the remaining radon. The amount of radon lost under these conditions would be due not only to absorption but also to transmission through the neoprene.

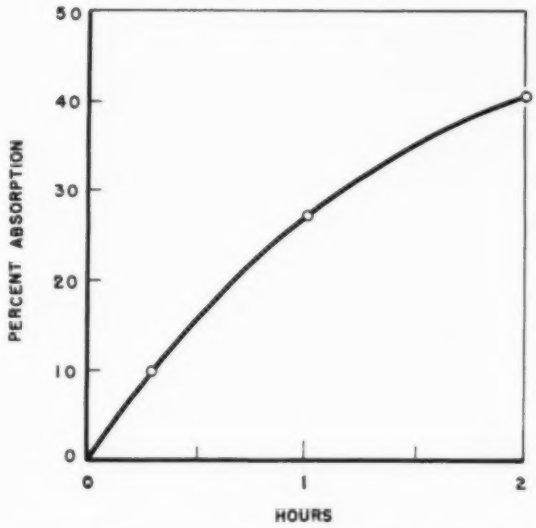

FIGURE 6.—*Percentage absorption of radon by neoprene balloon during time in contact*

Area of balloon 2,500 cm².

VII. Additional Remarks

A satisfactory arrangement when a sufficient number of chambers are available is to reserve some chambers for large samples and use the short resolving time circuit. The remaining chambers, if reserved for small samples, can be used either with the short or long resolving time circuit. A sample of 10^{-8} curie was used to calibrate one chamber connected to a short resolving time circuit and its value was found to fall on the same line of calibration points used for smaller rates of counting with this arrangement. This indicates that quantities of this order can be readily measured within the same limits of error as smaller samples.

The writer acknowledges the helpful criticism of L. F. Curtiss and the assistance in measurements by Christine Shaffer and Sarah Culpepper

WASHINGTON, July 28, 1947.

U. S. Department of Commerce
National Bureau of Standards

Research Paper RP1847
Volume 39, December 1947

Part of the Journal of Research of the National Bureau of Standards

A Statistical Analysis of Some Mechanical Properties of Manila Rope

By Sanford B. Newman and J. H. Curtiss

Breaking strength, weight, and circumference are three important qualities that are determined when fiber ropes are submitted for test.

These properties are all subject to some variation because of differences in fiber quality, method of fabrication, and previous treatment. The results of tests on more than 800 samples of 3-strand manila ropes ranging in size from $^3/_{16}$ in. to 3 in. in diameter are tabulated and analyzed by the methods of modern mathematical statistics. Considerable emphasis is placed on the rationale and details of the methods of analysis, as they are considered to be applicable to a broad variety of similar projects.

I. Introduction

Strength, weight, and size are usually determined for samples of fiber rope submitted to the Bureau for acceptance tests. These properties have been found to be subject to some variation in manila rope by Stang and Strickenberg [1].[1] This variation would appear to be caused by differences in fiber quality and in the mode of fabrication of the rope.

In many applications of fiber rope where even small economies in weight are important, i. e., in use of ropes on cargo airplanes, a knowledge of the probable strength of a set of ropes can result in an increase of the pay load. For other applications where ropes pass over sheaves and through eyes, the probable range of size is an important design consideration.

The manila ropes discussed in this paper were submitted for test by a Government agency from 1938 to 1941. They represent material supplied by rope works and rope contractors in the 3 years just prior to the loss of sources of manila fiber in World War II. This accounts for the heterogeneous sizes of the samples available for the various nominal diameters, as the smaller sizes and the integral multiples of ¼ in. in diameter are ordered more frequently than other sizes. Although some data were available for 4-strand manila rope, they were not of sufficient quantity to allow statistical treatment and consequently are not discussed here. In general, the requirements for 4-strand rope in the Federal Specification [2] will yield a basis for comparison with the 3-strand ropes treated in this paper.

The methods of test described are those found in the Federal Specification for manila rope [2], but the data are applicable to many situations where the conditions may be somewhat different. Whittemore [3] found that the speed of the moving head of the testing machine between 1 and 4 in./min had little effect on the observed strength of the rope. It has also been noted [4] that measurements of circumference with increasing loads on the specimen yielded decreasing changes in circumference for equal increments of load up to loads equal in pounds to 300 times the diameter in inches squared.

II. Methods of Test

1. Circumference and Weight

Both weight and circumference of manila ropes were determined on an unspliced sample that had been conditioned in an atmosphere of 65 ± 2 percent relative humidity and $70° \pm 2°$ F for at least 72 hours preceding the test. The samples were

[1] Figures in brackets indicate the literature references at the end of this paper.

long enough to provide the minimum free length specified in table 1.

TABLE 1*.—*Length of weight—circumference specimens*

Circumference	Minimum free length
In.	*Ft.*
Below 3	10
3 to 6, incl	5
Over 6	3

* Values from Table III of Federal Specification for Rope, Manila.

The rope was placed in a horizontal testing machine and a tensile load $P=200\ D^2$ lb (where D is the nominal diameter of the rope in inches) was applied. A single fiber was passed snugly around the rope, near the middle of the sample, and cut where it overlapped. The cut length of fiber was measured and the circumference recorded to the nearest $\frac{1}{16}$ in.

With the load, P, still applied to the rope, a length as specified in table 1 was marked off on the free length, and the load was then removed. The marked length was cut from the sample and weighed, and the weight in pounds per foot was computed.

2. Breaking Strength

A breaking strength sample had an eye splice at each end and measured from 5 to 6 ft between the inner ends of the splices. The samples were conditioned in the same fashion as the circumference-weight samples. The ropes were then removed from the conditioning room and the splices were immersed in water for 15 minutes in order to minimize the possibility of a failure in the splice.

Ropes with breaking strengths over 2,000 lb were loaded to failure in a horizontal hydraulic testing machine, and all others were tested using a horizontal, pendulum, screw testing machine. The ropes were loaded by means of 3-in. diameter steel pins passed through the eyes at each end of the sample. The speed of the moving head of the testing machine was 3 in./min during the tests. The tensile load was increased, until at the maximum load the rope failed in one or more strands.

III. Methods of Statistical Analysis

Four fundamental relationships were studied: (1) Circumference as a function of nominal diameter, (2) weight as a function of nominal diameter, (3) strength as a function of nominal diameter, and (4) strength as a function of weight. The first three are useful in preparing specifications and predicting the characteristics of individual ropes purchased under a contract or order. It was therefore considered desirable in these cases to furnish careful predictions of the dispersions encountered in practice, as well as of the mean values, so that realistic tolerances for individual ropes can be set up. The fourth relationship is important as a measure of innate characteristics of the material. Central tendency, rather than the dispersion, seemed to be of paramount interest in this case.

Observations on 863 ropes were available for this study. With truly random sampling and a clearly defined and homogenous universe or population, such a large sample, if properly handled, should provide close estimates of the underlying frequency distributions and relationships of the variables. In such circumstances the use of empirical equations containing, if necessary, several parameters would be justified. In the present instance, no direct control could be exercised over the sampling, and the universe, which presumably consists of the entire National output of manila rope of the relevant nominal sizes during the period from 1938 to 1941, was far from homogeneous. The data, as might be expected, contained certain anomalies that are more or less directly attributable to the composite nature of this universe, or to the nonrandom sampling.

In spite of these shortcomings, the observations appeared to exhibit a sufficient amount of internal consistency to warrant the use of mathematical methods, provided that the description of the underlying causal situation attempted thereby should not be too elaborate.

The mean values of the dependent variable were represented in each case by a curve of the general form

$$\overline{Y}=kX^b, \qquad (1)$$

where $\overline{Y}$ designates the (arithmetic) mean value of the dependent variable and X the independent variable. The parameters k and b were adjusted to the data, except in the case of the circumference-diameter relationship, where b was arbitrarily taken as unity.

The curves were fitted by the following general process: All data were first transformed to logarithms (to the base ten), and then a regression equation of the form

$$\log Y = a + b \log X, \tag{2}$$

was fitted by the standard unweighted least squares method to the logarithmic data. At the same time the standard error of estimate s (that is, the root-mean-square deviation of the data about the regression line) was also determined. The resulting equation (2) yielded an optimum estimate of the mean log Y for each log X, provided that it can be assumed that the true relation between mean log Y and log X is exactly linear and that the standard deviation of the variable log Y for a given log X is a constant independent of X. As the antilog of the mean of a set of logarithms of Y is not the arithmetic mean of Y itself,[2] it was necessary to add a correction of some sort to (2) in transforming back to the form (1). The correction chosen in this case was $1.15129s^2$, which is based on the further assumption that log Y is normally distributed for each value of log X (see [5], pp. 120–121). Thus in terms of the notation used in connection with (2), formula (1) becomes

$$\overline{Y} = 10^{a+1.15129s^2} X^b. \tag{3}$$

The calculations involved in the curve-fitting process were carried out almost entirely on punched-card machinery at the Computation Laboratory of the Bureau. The logarithmic transformation was accomplished automatically by the use of master logarithm cards in conjunction with a collater that simultaneously punched both the logarithms and their squares onto the data cards. Cross products and cumulative sums were then obtained in the standard way on multiplying punches and tabulators.

A few general remarks on the underlying rationale of this method of curve fitting and the choice of the type of curve are in order, as the situation about to be described is typical of that frequently encountered in tests of materials. The most elementary physical theory of the data would suggest that mean observed circumference should be directly proportional to the nominal diameter (which is actually defined to be one-third of the nominal circumference), and that observed weight and strength should then be directly proportional to the square of the observed circumference. This would ordinarily imply that the mean values of circumference, weight, and strength, as functions of nominal diameter, could be most appropriately estimated by fitting linear trends by the classical least squares method to the observed values, respectively, of circumference, the square root of weight, and the square root of strength.

Unfortunately, as is so often the case, the data for all of these variables reveal an unmistakable tendency for the dispersion of the readings (measured, say, by their standard deviation) to increase with their mean. This would necessitate the use of a weighted least squares solution. The simple unweighted least squares solution would give an inefficient estimate of the mean and would not yield any over-all estimates at all for the variances within nominal diameter groups. But the difficulty of determining *a posteriori* the proper individual weights to use in such cases has led in recent years to the widespread use of transformations of the scale, such as the logarithmic transformation here used, to effect, at least theoretically, a stabilization of variance over the whole range of values of the mean. Such transformations under certain circumstances have the additional property of rendering the distribution of the transformed variable more nearly normal or Gaussian.

In the present case, as far as could be determined from the data, the standard deviation of the observed circumference seemed to be roughly a linear function of the mean. The transformation ordinarily employed in that event is a logarithmic transformation [5]. Preliminary exploration revealed that this transformation indeed seemed to stabilize the variance of the circumference measurements. It also seemed to stabilize the variance of the weight and strength measurements. This would follow mathematically if the transformation really did stabilize the circumference variance

[2] It is the *geometric mean* of Y, however.

and if mean weight and strength really were directly proportional to some power of the circumference. Thus additional evidence was furnished thereby as to the correctness of the choice of the logarithmic transformation for the circumference data.

As for the choice of the curve, it is natural to choose a type that contains as few parameters as possible and that can easily be handled in conjunction with the logarithm transformation. Stang and Stickenberg [1] chose to use a one-parameter curve of the form

$$\overline{Y}=k\ X\ (X+1)=k\ X^2+k\ X,$$

to represent the strength-diameter relationship. Although this equation is readily adaptable to the logarithmic least squares approach (it seems to have been fitted empirically in [1]), nevertheless the first degree term is not easy to explain in terms of the physical theory. Exponential equations of the type (1), on the other hand, not only can be conveniently handled after a logarithmic transformation, but also accord very well with a slight extension of the simplest physical theory of the tests. They imply that weights and strengths of a series of ropes of different sizes whose successive nominal diameters are in a constant ratio will themselves be in a constant ratio.

As a check on the adequacy of (1), three-parameter curves of the type

$$\overline{Y}=C_1+C_2\ X+C_3\ X^2,$$

were actually fitted to the weight-diameter relations, and in spite of the additional parameter, the results obtained were approximately equivalent to those obtained with (1).

IV. Results and Discussion

The various equations for mean values, obtained as described in section III, together with the corresponding values of the regression constants a, b, and s associated with eq 2 of section III are all given in table 2.

In interpreting the equations, it should be understood that they give the estimated mean values of the dependent variable for each fixed, predetermined value of the independent variable. Thus the last equation, which gives the estimated mean of S as a function of W, cannot be obtained by merely eliminating D between the second and third equations, because the distribution of values of S corresponding to a fixed D, say $D=D_0$, and the distribution of values of S corresponding to a fixed W, are not in general quite the same, even if the fixed W was determined by setting $D=D_0$ in the second equation. (Actually the two methods of deriving the fourth equation in table 2 happen to agree to two significant figures in the exponent and three in the constant factor, owing to the relatively small scatter of the data about the various curves.)

The standard errors s_a and s_b of a and b are also presented in table 2. It will be noted that these standard errors turn out to be exceedingly small. This is partly due to the large number of items entering into the sample, and partly due to the relatively small size of s in each case. Statistical theory would state that if the sampling had been truly random and if curves of the type used exactly described the mean relationships in the sampled universe, then ranges of $a\pm3s_a$ and $b\pm3s_b$ would, with high probability, contain the corresponding "true" values of a and b; that is, the values for the universe. Due mainly to the

TABLE 2.—*Regression equations and statistics of distributions of circumferences, weights, and strengths of 3-strand manila rope*

Dependent variable			Independent variable			Equation of means	Regression statistics [a]				
Meaning	Symbol	Unit	Meaning	Symbol	Unit		a	b	s	s_a	s_b
Circumference	C	1/16 in	Nominal diameter	D	1/16 in	$C=3.119D$	0.49353	(b)	0.02026	0.00069	
Weight	W	lb/ft	Nominal diameter	D	1/16 in	$W=0.001447\ D^{1.9827}$	−2.84023	1.98268	.02541	.0038	0.0033
Strength	S	lb	Nominal diameter	D	1/16 in	$S=70.481\ D^{1.8910}$	1.845079	1.828193	.042619	.0064	.0055
Strength	S	lb	Weight	W	lb/ft	$S=40278\ W^{0.9994}$	4.602511	0.999040	.047059	.0028	.0024

[a] For explanation of a, b, and s, see discussion of eq. 2 in sec. III. The symbols s_a and s_b denote the standard errors of a and b, computed under the assumption that for each value of D, the data constitute a random sample from a universe of such data. (See sec IV.)

[b] Not adjusted to data.

fact that the method of sampling was not rigorously random, such a statistical interpretation of s_a and s_b is apparently unwarranted. It is believed, however, that these standard errors afford ample basis for the following important general statements about the coefficients and exponents in the equations in table 2:

(1) In the case of the circumference-diameter relationship, the coefficient of D is significantly larger than 3, which is the value suggested by the definition of nominal diameter.

(2) In the weight-diameter and strength-diameter relationships, the exponent of D is significantly less than the value 2 suggested by the simplest physical theory.

(3) In the strength-weight relationship, the exponent of W is significantly different from unity.

If "true" values of a and b may be postulated, then it follows that there exists a "true" value of the ordinate of the equation of the mean for each given value of the independent variable. Investigation of the appropriate standard errors reveals that theoretically with high probability the mean values of C, W, and S do not deviate from the corresponding "true" values by more than 2 percent in the case of C and W, and 4 percent in the case of S. But this statement must be interpreted with much caution, not only because of the nonrandomness of the sampling, but also because even if the curves had been fitted in some analogous manner to the *universe* instead of to the sample, it is possible that deviations of this order from the actual true means of the universe might be observed, because of the fact that the simple type of curve chosen for fitting may not accurately describe the real functional relation between the true means and the independent variables.

The preceding discussion of standard errors may be summarized by stating that from the viewpoint of theoretical statistical analysis, the curves have been fitted with a considerable amount of precision; but in default of exact knowledge as to the mechanism of the sampling method, the real accuracy of the curves as a description of the rational manila rope technological situation during the data period must be taken largely on faith.

The information in table 2 has been tabulated numerically in table 3, and represented graphically in figures 1, 2, 3, and 4. The "Estimates of Mean" columns in table 3 and the central curves in all of the graphs were obtained by straightforward substitution into the equations in table 2. The small circles that appear on the graphs represent the means of the observations for the respective indicated values of the independent variable.

The information as to dispersion of *individual observations* about the curve of means is presented in table 2 in the form of the standard error of estimate s. For convenience in the applications, this dispersion information is presented in table 3 in terms of tolerance limits obtained in the following manner:

Reverting to the notation of equation 2 of section III, if it be assumed that the value of log Y given by eq 2 is the true mean of values of log Y for each value of X, and s is the true standard deviation, then the interval [log $Y-ts$, log $Y+ts$] will bracket a fixed proportion p (t) of the underlying distribution, the proportion being dependent only on the value of t. (The trivially small size of all standard errors involved in the present case makes these assumptions entirely tenable from the theoretical point of view.) In the present case, the value of t was so chosen that if the distribution of individual value of log Y were normal or Gaussian, the value of p (t) would be 0.95. Specifically, this value of t to 6 decimal places is 1.959964. Thus the formulas for the tolerance limits appearing in table 3 were:

$$\text{Lower tolerance limit} = 10^{-1.959964s}\ Y$$
$$\text{Upper tolerance limit} = 10^{1.959964s}\ Y$$

In tabulating the numerical value of the tolerance limits given by these formulas, the general practice was to round off to the number of significant figures appearing in the raw data. However, a number of exceptions were made, chiefly in the direction of retaining one extra significant figure, to conform with the conventions of tabulation. Ambiguous cases were always rounded *outwards*.

The tolerance limits are plotted on the graphs as the outer curves. It should be emphasized that *these outer curves pertain to individual measurements, and not to means, such as those represented by the circles on the graphs*

In general, the analytic representation of the 863 observations is remarkably faithful, as can be seen from a glance at the figures. (In interpreting deviations of the circles from the central line, the varying number of observations represented by

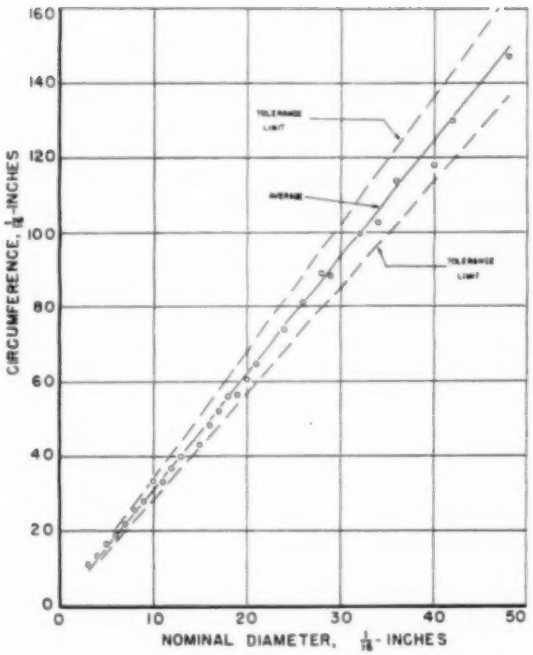

FIGURE 1.—*Circumference as a function of nominal diameter*

The central curve is that of the first equation in table 2.

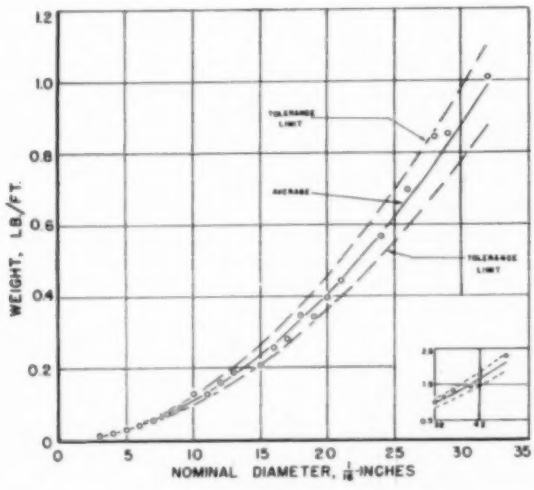

FIGURE 2.—*Weight as a function of nominal diameter*

The central curve is that of the second equation in table 2.

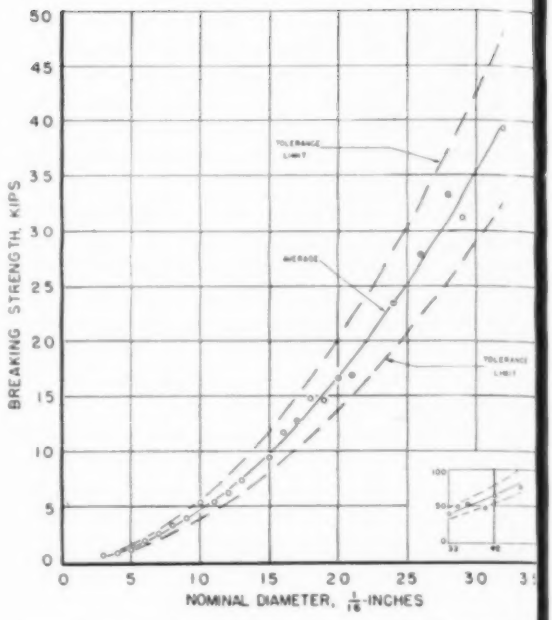

FIGURE 3.—*Breaking strength as a function of nominal diameter.*

The central curve is that of the third equation in table 2.

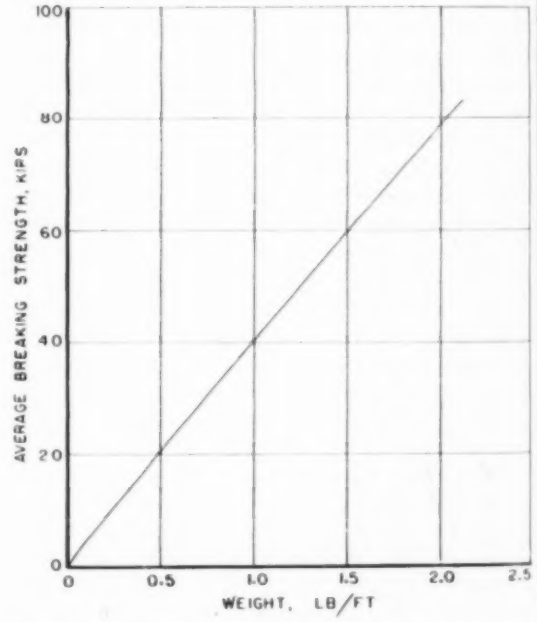

FIGURE 4.—*Breaking strength as a function of weight.*

The curve is that of the fourth equation in table 2.

TABLE 3.—*Circumference, weight, and strength of 3-strand manila rope*

Nominal diameter		Number of ropes tested	Circumference			Weight			Strength			Nominal diameter	
			Estimate of mean	Tolerance limits for individual ropes		Estimate of mean	Tolerance limits for individual ropes		Estimate of mean	Tolerance limits for individual ropes			
in.	1/16 in.		1/16 in.	1/16 in.		lb/ft	lb/ft		lb	lb		in.	1/16 in.
3/16	3	6	[a] 9.4	[a] 9	[a] 10	[a] 0.0114	[a] 0.010	[a] 0.013	525	430	630	3/16	3
1/4	4	47	12.5	11	14	.0197	.017	.022	889	730	1,070	1/4	4
5/16	5	21	15.6	14	17	.0300	.027	.034	1,336	1,100	1,610	5/16	5
3/8	6	60	18.7	17	21	.0422	.038	.047	1,865	1,530	2,250	3/8	6
7/16	7	3	21.8	20	24	.0564	.050	.063	2,472	2,030	2,980	7/16	7
1/2	8	106	25.0	23	27	.0726	.065	.081	3,156	2,590	3,810	1/2	8
9/16	9	5	28.1	26	31	.0906	.081	.101	3,914	3,210	4,720	9/16	9
5/8	10	19	31.2	28	34	.1104	.098	.124	4,745	3,900	5,720	5/8	10
11/16	11	18	34.3	31	38	.1322	.118	.148	5,648	4,640	6,810	11/16	11
3/4	12	106	37.4	34	41	.1557	.139	.174	6,622	5,440	7,990	3/4	12
13/16	13	8	40.5	37	44	.1810	.161	.203	7,666	6,290	9,250	13/16	13
7/8	14	.....	43.7	40	48	.2081	.185	.233	8,778	7,210	10,590	7/8	14
15/16	15	5	46.8	43	51	.2370	.211	.265	9,958	8,180	12,010	15/16	15
1	16	104	49.9	45	55	.2676	.238	.300	11,210	9,200	13,520	1	16
1 1/16	17	4	53.0	48	58	.3000	.267	.336	12,520	10,280	15,100	1 1/16	17
1 1/8	18	8	56.1	51	61	.3340	.297	.374	13,900	11,410	16,770	1 1/8	18
1 3/16	19	11	59.3	54	65	.3698	.329	.414	15,340	12,600	18,500	1 3/16	19
1 1/4	20	112	62.4	57	68	.4073	.363	.456	16,850	13,830	20,330	1 1/4	20
1 5/16	21	7	65.5	60	72	.4465	.397	.500	18,420	15,120	22,220	1 5/16	21
1 3/8	22	.....	68.6	62	75	.4874	.434	.546	20,060	16,470	24,200	1 3/8	22
1 7/16	23	.....	71.7	65	79	.5299	.472	.593	21,760	17,870	26,250	1 7/16	23
1 1/2	24	110	74.9	68	82	.5741	.511	.643	23,520	19,310	28,370	1 1/2	24
1 9/16	25	.....	78.0	71	85	.6200	.552	.694	25,340	20,810	30,570	1 9/16	25
1 5/8	26	10	81.1	74	89	.6675	.594	.747	27,220	22,350	32,840	1 5/8	26
1 11/16	27	.....	84.2	77	92	.7167	.638	.802	29,170	23,950	35,190	1 11/16	27
1 3/4	28	9	87.3	80	96	.7675	.683	.859	31,170	25,590	37,600	1 3/4	28
1 13/16	29	13	90.4	82	99	.8193	.729	.917	33,240	27,290	40,100	1 13/16	29
1 7/8	30	.....	93.6	85	103	.8739	.778	.978	35,360	29,030	42,650	1 7/8	30
1 15/16	31	.....	96.7	88	106	.9295	.827	1.041	37,550	30,830	45,300	1 15/16	31
2	32	50	99.8	91	109	.9868	.878	1.105	39,790	32,670	48,000	2	32
2 1/16	33	.....	102.9	94	113	1.0456	.931	1.171	42,080	34,560	50,770	2 1/16	33
2 1/8	34	1	106.0	97	116	1.1061	.985	1.238	44,450	36,500	53,620	2 1/8	34
2 3/16	35	.....	109.2	99	120	1.1682	1.040	1.308	46,870	38,480	56,540	2 3/16	35
2 1/4	36	13	112.3	102	123	1.2318	1.097	1.379	49,350	40,520	59,530	2 1/4	36
2 5/16	37	.....	115.4	105	126	1.2970	1.154	1.452	51,890	42,600	62,590	2 5/16	37
2 3/8	38	.....	118.5	108	130	1.3669	1.217	1.530	54,480	44,730	65,720	2 3/8	38
2 7/16	39	.....	121.6	111	133	1.4321	1.275	1.603	57,130	46,910	68,920	2 7/16	39
2 1/2	40	1	124.8	114	137	1.5020	1.337	1.682	59,830	49,120	72,170	2 1/2	40
2 9/16	41	.....	127.9	117	140	1.5735	1.401	1.762	62,600	51,400	75,510	2 9/16	41
2 5/8	42	4	131.0	119	143	1.6466	1.466	1.844	65,420	53,710	78,920	2 5/8	42
2 11/16	43	.....	134.1	122	147	1.7211	1.532	1.927	68,290	56,070	82,380	2 11/16	43
2 3/4	44	.....	137.2	125	150	1.7972	1.600	2.012	71,220	58,480	85,910	2 3/4	44
2 13/16	45	.....	140.4	128	154	1.8749	1.669	2.099	74,210	60,930	89,520	2 13/16	45
2 7/8	46	.....	143.5	131	157	1.9542	1.739	2.188	77,250	63,430	93,190	2 7/8	46
2 15/16	47	.....	146.6	134	161	2.0349	1.811	2.278	80,350	65,970	96,930	2 15/16	47
3	48	2	149.7	136	164	2.1172	1.885	2.370	83,500	68,560	100,700	3	48

[a] See table 4.

each circle must be taken into account.) The representation of dispersion is apparently as successful as that of the mean values. As a partial check it might be noted that, for example, 34 observations on S fell outside the tolerance limits for S given in table 3; this is 4 percent of the total number of observations on S, a proportion that compares favorably with the specified theoretical value of 5 percent. The fact that the number of observations that were too high was about equal to the number out on the low side gives added credence to the validity of the logarithmic transformation. Similar situations obtain in the cases of W and C.

The following irregularities in the data should be explicitly noted:

(1) The observed distributions of C, W, and S for nominal diameters of $\frac{5}{8}$ in., $1\frac{1}{8}$ in., and $1\frac{3}{4}$ in., not found in the Federal Specification [2], were very similar to the corresponding distributions for the nominal diameters of $1\frac{1}{16}$ in., $1\frac{3}{16}$ in., and $1\frac{13}{16}$ in., respectively. In each case, the means and tolerance limits given in table 2 for the larger size represented the mean and range of the observation for the smaller size (as well as for the larger size) much better than the mean and tolerance limits given in table 2 for the smaller size. Apparently, rope of the appropriate one of the three larger sizes is supplied whenever one of the three smaller sizes is stipulated in a purchase.

(2) The observed values of C, W, and S for a fixed value of D exhibited some tendency to occur in clusters having smaller individual dispersion than that represented by the values of s in table 2 or the tolerance limits in table 3. This phenomenon was undoubtedly due in part to nonrandom sampling.

The chief result of misclassification such as noted in (1) above, and of the clustering noted in (2), is to increase the values of s (and thus increase the spread of the tolerance limits) over the values that would have been obtained if such irregularities had been absent.

(3) In the case of the $\frac{3}{16}$ in. nominal diameter, the observed circumference and weights of the six ropes tested were not properly represented by the analytical expression. In view of the various testing, rounding off, sampling, and classification errors involved in the measurements, it may well be that extrapolation from the analytic representation based on over 800 measurements should furnish more reliable information than a sample of six possibly anomolous observations. However, for completeness, the means and ranges of the C and W observations for $D=\frac{3}{16}$ are given in table 4.

TABLE 4.—*Summary of observed circumferences and weights for $\frac{3}{16}$ in. 3-strand manila rope*

[Based on 6 observations on each variable]

	Circumference	Weight
	$\frac{1}{16}$ *in.*	*lb/ft*
Arithmetic mean	11.2	0.01
Minimum	10	.01
Maximum	12	.01

Figure 5 exhibits a comparison between the results on mean strength obtained in the present paper, and the curve fitted by Stang and Strickenberg [1] to the data on strength which they obtained in 1921. An examination of the closeness of fit of Stang and Strickenberg's curve and of the

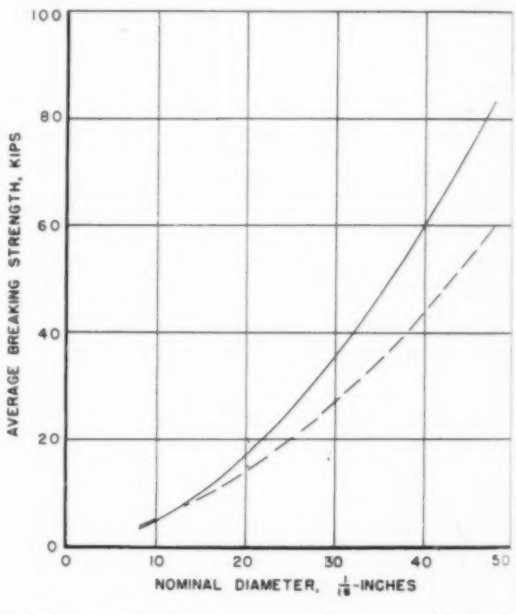

FIGURE 5.—*Comparison of present sample with that of reference [1]*

The solid line is the present sample. The broken line is the sample of reference [1]

spersion of their data, indicates that the theoetical accuracy of their curve should be roughly mparable with that of the corresponding curve the present paper when due allowance is made r the fact that their curve is based on only bout one-half as many observations. It follows at for sizes of 1 in. diameter and greater, the verage breaking strength of rope in 1921 as presented by Stang and Strickenberg's curve is nificantly lower than that of the rope discussed the present paper.

V. References

[1] A. H. Stang and L. R. Strickenberg, Techn. Pap. BS (1921) T198.

[2] Federal Standard Stock Catalog Section IV (Part 5), Federal Specification for Rope; Manila, T–R–601a, and amendments 1 and 2 (November 26, 1935).

[3] H. L. Whittemore, Commercial Standards Monthly **8**, No. 2, 57 (1931).

[4] Unpublished data.

[5] J. H. Curtiss, Annals of Math. Statistics **14**, 107 (1943).

WASHINGTON, May 26, 1947.

U. S. Department of Commerce
National Bureau of Standards

Research Paper RP1848
Volume 39, December 1947

Part of the Journal of Research of the National Bureau of Standards

Voltage Anomalies of the Glass Electrode and the Chemical Durability of the Glass

By Donald Hubbard and Gerald F. Rynders

Additional work has been done on the correspondence between voltage departures (errors) of electrodes prepared from Corning 015 glass and the change in the chemical durability of the glass. The results confirm and extend the earlier findings that voltage departures of the electrode are accompanied by durability changes of the glass. The pronounced voltage departures in the alkaline region and in hydrofluoric acid solutions are accompanied by conspicuous attack of the glass. Dilute solutions of acids that do not form soluble compounds of silica cause swelling of the glass. This swelling is repressed as the concentration of the solutions is increased. As is to be expected from the distribution law and Donnan membrane considerations, this repression of swelling was also brought about by high concentrations of organic acids and salts as well as by the so-called "strong" acids. The attack of Corning 015 glass by alkaline solutions of different ions was found to be in the order, $Na^+ > Li^+ > K^+ > Ba^{++} > NH_4^+$, which is the same order dictated for these ions by the voltage departure data.

I. Introduction

The ability of a glass to function satisfactorily as an indicator of the hydrogen ion activity of aqueous solutions appears to be determined largely by two properties of the glass, namely, the hygroscopicity (water sorption) and the uniformity of the chemical durability over an extended pH range. Glasses of inadequate hygroscopicity produce electrodes of high resistance whose pH responses fall appreciably below the theoretical dictates of the Nernst equation:

$$\Delta E = 0.000198 T \Delta \text{pH}$$ [1, p. 78, 2, 3].[1]

On the other hand, solutions that cause detectable change in attack of the glass [4] also bring about voltage departures (errors) from the straight-line relation of the Nernst equation [1, 5, 6].

The glass whose hygroscopicity and durability characteristics have most nearly fulfilled the requirements for pH measurements is one of composition SiO_2 72 percent, Na_2O 22 percent, CaO 6 percent (Corning 015) [1, 7]. Although this glass combines the two necessary properties of adequate hygroscopicity and uniform durability to a considerable degree, electrodes prepared from it exhibit voltage departures in the "super acid" range [5] and even more conspicuous errors in alkaline solutions above pH 9 [1]. Such voltage departures in alkaline solutions covering a limited range of conditions and pH values have been reported as being roughly directly proportional to the amount of attack [8, 9].

The present investigation was undertaken to ascertain if electrodes prepared from Corning 015 glass always have voltage departures accompanying changes in the chemical durability of the glass and also to determine to what extent the magnitude of these voltage departures is directly proportional to the change in the attack of the glass by the solutions.

II. Experimental Procedure

The glass electrodes were prepared by blowing a thin bulb of Corning 015 glass on the end of

[1] Figures in brackets indicate the literature references at the end of this paper.

soft glass tubing. The inner electrical connection was made by filling the bulb and tube with mercury [10]. Such metal-filled electrodes are simple to prepare and have the advantage that an electrode broken in service does not seriously contaminate or alter the pH of the solution under observation. All voltage and pH measurements were obtained at room temperature by means of a Beckman pH meter, laboratory model G. Unless otherwise stated, the hydrogen electrode was used as the reference electrode, and the value in 0.02 N hydrochloric acid as the zero reference voltage. This solution was chosen to avoid the uncertainty of the equilibrium between the hydrogen electrode and M/20 acid potassium phthalate [11]. Further, the acid solution served to restore the glass electrode after severe abuse to its initial condition [12].

The chemical durability (reported as attack) of the glass was determined by the interferometer method [4, 13]. This procedure offered a rapid means of determining the amount of solution or swelling of the glass over a wide range of conditions under circumstances in which the conventional analytical methods would be time-consuming, unreliable, or even impossible. [2] In this method the magnitude of the attack was determined by observing the displacement of the interference fringes when the specimen was placed under an optical flat. The optical flat of fused silica or other glass must have both surfaces polished "true plane" and adjusted to make an angle of 20′ with each other so that interference bands will not be formed by reflection between the upper and lower surfaces.

The specimens of glass for chemical durability measurements were small rectangular strips approximately 3 cm long with one surface pitch-polished, and were sufficiently flat to show interference bands when placed under an optical flat. The exposures were made by immersing these specimens to approximately one-third of their length in the desired solution. The surface of the solution in most instances was covered throughout the test period by a thin layer of liquid petrolatum to prevent evaporation. For the experiments with high percentages of ethanol (C_2H_5OH), the density of the solutions was too low to float the oil layer. In these experiments it was necessary to make the exposures in a closed system by suspending the specimen from the cork stopper of an Erlenmeyer flask.[3]

The desired temperatures were maintained constant to $\pm 0.2°$ C by means of an electrically heated thermostated water bath. All chemical durability data were obtained at 80° C except for the ethanol and hydrofluoric acid solutions. For the ethanol solutions the temperature was lowered to 78° C to insure that the surface remained undisturbed by boiling during the period of exposure. In the hydrofluoric acid solutions it was necessary to make the durability exposures at room temperature because of the vigorous attack on the glass.

As the purpose of the investigation was to furnish a comparison between the voltage departure of the glass electrode and the chemical durability of the glass, the solutions were adjusted to approximate concentrations only. Whenever possible the voltage departure of the glass electrode was observed for a given solution, followed immediately by a determination of the durability of the glass in the same solution.

III. Voltage Departures (Errors) of the Glass Electrode and the Chemical Durability of the Glass

1. Sodium Hydroxide Solutions

One of the most conspicuous voltage departures for the glass electrode occurs in the alkaline range beginning near pH 9 and increasing rapidly with increased alkalinity [1]. It has been shown that this region of voltage departure is accompanied by changing chemical durability of the electrode glass, the rate of attack increasing with increasing pH [4]. Published data covering a limited range of conditions indicate that this relation is linear [8, 9]. To check this observation further and to make as simple an experiment as possible, an aqueous solution of 1.0 N NaOH was prepared from which a series of solutions was obtained ranging in concentration from 0.015 N to 1.0 N, with each successive member of the series doubling

[2] An attack of less than 0.1 of an interference fringe can be readily detected. For a glass of density 2.5, an attack of 0.1 fringe (filtered helium source) amounts to approximately:

$$0.1 \times \frac{0.587 \times 10^{-4}}{2} \times (1)^2 \times 2.5 = 0.073 \times 10^{-4} \text{g or } 0.0073 \text{ mg/cm}^2.$$

[3] The use of a closed system was tried at the suggestion of A. W. Helz, of the Portland Cement Association Fellowship. It proved very effective and greatly increases the range of usefulness of the interferometer method for durability measurements.

n concentration. No additional buffer ions were added to these solutions.

The results, listed in section A of table 1 and plotted as curve A of figure 1, indicate a linear

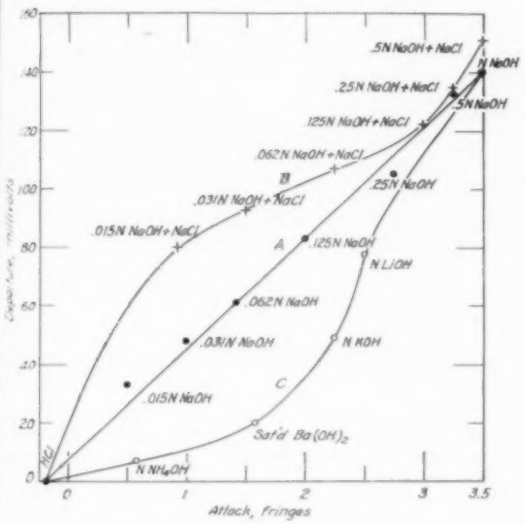

FIGURE 1.—*Comparison of the voltage departures of the glass electrode with the chemical durability of the glass in different solutions.*

A, NaOH solutions; *B*, NaOH+NaCl; *C*, NH_4OH, $Ba(OH)_2$, KOH, LiOH and NaOH. Durability exposure 6 hours at 80° C.

relation between voltage departure and attack within reasonable limits. The emf data were taken in order beginning with the weakest solution. The individual readings were usually steady; however, in accordance with published data, the reproducibility was found to depend greatly on the immediate previous history of the electrode [8, 9, 12]. Nevertheless, the data are sufficiently reliable to support the trends indicated by the curves.

2. Sodium Hydroxide Solutions Plus Sodium Chloride

It is known that the voltage departures of the glass electrode in alkaline solutions are increased by the addition of neutral sodium salts such as NaCl [1 p. 129, 14, 15, 16]. Chemical durability data have shown qualitatively that an increase in attack on the glass also accompanied this increased voltage departure [13]. To obtain quantitative data on this point, the same NaOH series as described in the previous section was prepared and sufficient NaCl added to make all of these solutions normal with respect to Na^+ ions. Once again the individual emf readings were steady. The results obtained are listed in section B of table 1 and plotted as curve B of figure 1. A pronounced increase in both voltage departure and attack was brought about by the increased $[Na^+]$. However, the voltage departure exhibited a greater increase than did the attack, and the data do not coincide with the previous straight line A. From this it is evident that factors other than the durability shift of the glass contribute to the voltage departure of the electrode.

3. Solutions Containing Na^+, Li^+, K^+, Ba^{++}, and NH_4^+ ions

The magnitude of the voltage departure in alkaline solutions is different for different ions [1, p. 130]; for example, the departures caused by cations are in the order, $Na^+ > Li^+ > K^+ > Ba^{++} > NH_4^+$. Earlier work suggested that this was the order

TABLE 1.—*Comparison of the voltage departures (errors) of the glass electrode with the chemical durability of the glass in solution of* NaOH, NaOH plus NaCl, *and other hydroxides*

Durability exposure 6 hours at 80° C

A			B			C		
Solution	Departure	Attack (fringes)	Solution	Departure	Attack (fringes)	Solution	Departure	Attack (fringes)
	mv			*mv*			*mv*	
Dilute HCl	0	<3/10 (swelling)	Dilute HCl	0	<3/10 (swelling)	Dilute HCl	0	<3/10 (swelling)
0.015 N NaOH	33	1/2 (attack)	0.015 N NaOH+NaCl	80	<1 (attack)	N NH_4OH	7	>1/2 (attack)
.031 N do	48	1 do	.031 N do	93	1 1/2 do	$Ba(OH)_2$ saturated.	20	>1 1/2 do
.062 N do	61	<1 1/2 do	.062 N do	107	2 1/4 do	N KOH	49	2 1/4 do
.125 N do	83	2 do	.125 N do	122	3 do	N LiOH	78	2 1/2 do
.25 N do	105	2 3/4 do	.25 N do	135	3 1/4 do	N NaOH	140	3 1/2 do
.50 N do	133	3 1/4 do	.50 N do	151	3 1/2 do			
1.0 N do	140	3 1/2 do						

of decreasing attack on the electrode glass by these ions [4, 13]. To check this point, normal solutions were prepared for each of these hydroxides except $Ba(OH)_2$. For $Ba(OH)_2$ a saturated solution was used. The voltage departure of the glass electrode was determined in each of these solutions, followed by a durability test of the glass. As the concentration of saturated $Ba(OH)_2$ at room temperature is less than 1 N, and at 80° C is greater than 1 N, the voltage departure value obtained is probably too low and the attack value is too high. The results given in section C of table 1 and plotted as curve C in figure 1 show that the relative attack on the glass by these solutions is in the same order as for the voltage departure, but the two properties do not plot as straight line nor does the resulting curve C coincide with either curve A or curve B. These results again indicate that some factor other than durability shift of the glass contributes to the errors of the glass electrode. However, before one accepts these data as an indication of a specific equilibrative response of the glass electrode to these ions, it must be emphasized that the glass electrode gives little or no specific response to any of them except under conditions of changing durability of the glass.

4. Buffer Solutions Containing NH_4^+ ions

The voltage departures of the glass electrodes are much less in alkaline buffer solutions containing NH_4^+ ions than in basic solutions prepared with Na^+ ions [17]. A typical set of data illustrating this point and making a comparison of voltage departure and chemical durability is given in table 2 and plotted in figure 2. The voltage departures were obtained on buffer solutions prepared from the Britton-Robinson universal buffer mixture [18] in which ammonia was substituted for the NaOH to obtain the desired pH range, the highest pH value being that of full strength ammonia solution.[4]

Most of the voltage results are qualitatively similar to those for buffers containing Na^+ ions, the departure remaining nearly constant in the acid range, then increasing with increasing alkalinity beyond pH 8. However, at the higher alkalinities beyond pH 11, the rate of departure

[4] In the durability tests no difficulty was encountered from loss of NH_3 through the oil layer except at pH 12.3 and for the full strength solution.

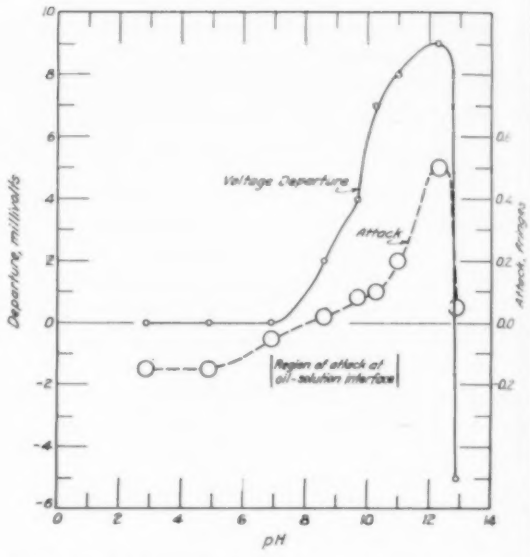

FIGURE 2.—*Comparison of the voltage departures of the glass electrode with the chemical durability of the glass in buffer solutions containing* NH_4^+ *ions.*

Durability exposure 6 hours at 80° C. In this and other figures the size of the circles does not indicate the probable error of the individual points for durability, but merely emphasize that the data must not be considered highly precise nor accurate.

TABLE 2.—*Comparison of the voltage departures (errors) of the glass electrode with the chemical durability of the glass in buffer solutions containing* NH_4^+ *ions*

[Durability exposure 6 hours at 80° C]

pH	Departure	Attack (fringes)	Surface cut at oil-solution interface
2.9	0	<1/10 Swelling	None
4.9	0	<1/10 Swelling	Do.
6.9	0	?	Detectable
8.6	2	?	1/10.
9.7	4	<1/10 Attack	1/10.
10.3	7	1/10 Attack	1/2.
11.0	8	3/10 Attack	3/4.
12.3	9	1/2 Attack [1]	None.
12.9 full strength NH_3	2-5 to 0	Detectable [1]	Slight.

[1] NH_3 escaped through the oil layer during the early minutes of the attack period.

[2] The temperature of the full-strength NH_3 fell sharply upon bubbling hydrogen through the solution.

falls off and goes through a reversal for full strength NH_3, even yielding a negative value in the latter case. This negative value for full strength NH_3 has been previously reported [4] but not adequately investigated. The hydrogen stream bubbling through the full strength am-

monia causes a large drop in the temperature of the solution. When adequate precautions were taken to minimize this temperature change, the voltage departure for the glass electrode approximated zero.

The trend of the departure curve over the pH range investigated was in complete accord with the durability curve for the glass in these same buffers. In the acid range the glass exhibited a slight swelling, and between pH 6.9 and pH 11.0 excessive surface cuts appeared at the oil-solution interface, similar to the results reported for buffer solutions containing Na^+ ions [4]. An increase in pH at the oil-solution interface brought about by preferential orientation of ions could account for the surface cuts in this pH range. In full-strength NH_3, the durability of the glass improved in accordance with that indicated by the voltage departure shift.

5. Electrode Prepared from a Glass of Low Hygroscopicity

The voltage departures for Corning 015 glass electrodes that appear under conditions of changing chemical durability of the glass [4] must not be confused with the voltage errors that are exhibited by electrodes prepared from glasses of low hygroscopicity [1, 2, 3,]. In the latter, departures appear over the entire pH range, with any departures accompanying a change in durability being merely superimposed on the general departure curve [3]. A typical example of the behavior of electrodes prepared from glasses of low and high hygroscopicity, Pyrex and Corning 015, respectively, is illustrated in table 3 and figure 3. These data were obtained in Britton-Robinson universal buffers over a pH range in which both glasses exhibit uniform durability [13], in order to eliminate any voltage effects attributable to change in the durability of either glass.

TABLE 3.—*Comparison of the voltage departure of an electrode prepared from a glass of low hygroscopicity, Pyrex, with the departure of an electrode of Corning 015 glass, using the hydrogen electrode as reference electrode*

pH	Departure	
	Pyrex	Corning 015
	mv	*mv*
1.9	0	0
2.7	+27	0
3.1	+120	1
7.8	+266	1
Water sorbed, mg/cm²	[1] 1.8	[1] 358

[1] Values taken from Fig. 6, RP1706 (J. Research NBS **36**, 365 (1946)).

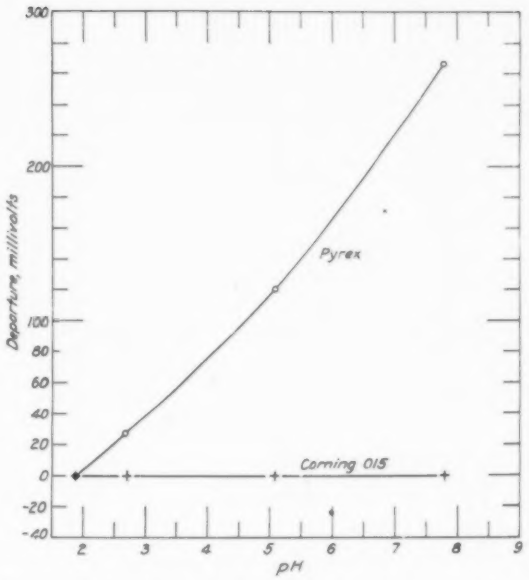

FIGURE 3.—*Comparison of the voltage departure of an electrode prepared from a glass of low hygroscopicity (Pyrex) with the departure of an electrode of Corning 015 glass.*

These data were taken over a pH range for which both glasses exhibit uniform durability.

6. Hydrofluoric Acid Solutions

Electrodes of Corning 015 glass exhibit very pronounced voltage departures in hydrofluoric acid (HF) solutions, the departures increasing with increased concentration [4, 16]. The data given in table 4 and plotted in figure 4 show that these increased voltage departures are accompanied by increased attack on the glass. However, the relation between voltage departure and attack is not a straight line. Although the attack on the glass was very severe, the emf readings were surprisingly steady. The attack was so rapid that to keep the durability measurements within the range of the interferometer, the time of exposure had to be reduced to 5 minutes at room temperature and further shortened to 1 minute, 30 seconds, and 10 seconds for the 2.0 N, 3.0 N and 5.0 N solutions, respectively. Hence, the results shown in figure 4 are only qualitative, but obviously the general shape of the curve will

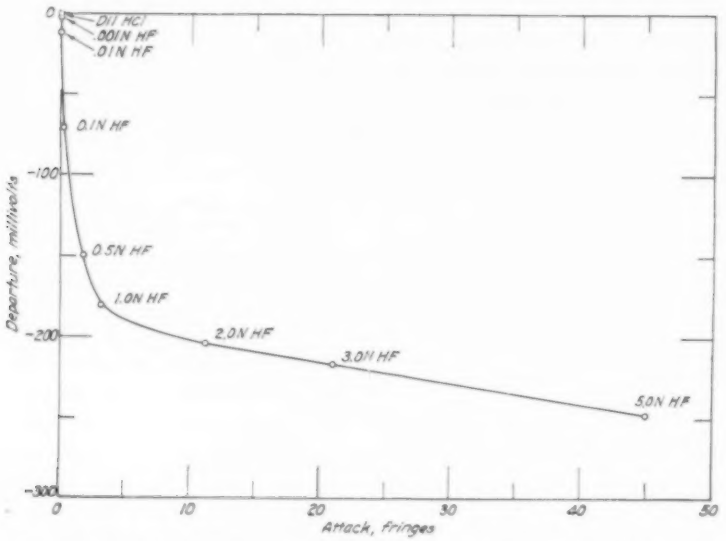

FIGURE 4.—*Comparison of the voltage departures of the glass electrode with the chemical durability of the glass in aqueous solutions of hydrofluoric acid.*

Durability exposure 5 minutes at room temperature.

not be altered even though the individual values may possess large cumulative errors.

TABLE 4.—*Comparison of the voltage departures (errors) of the glass electrode with the chemical durability of Corning 015 glass in aqueous solutions of hydrofluoric acid*

[Attack reported for 5 minutes exposure at room temperature]

Solution	Departure	Attack (fringes)
	mv	
Dilute HCl	0	Not detectable.
0.001 N HF	−3	Do.
.01 N HF	−12	Detectable.
.10 N HF	−71	>¼.
.5 N HF	−150	<2.
1.0 N HF	−181	>3¼.
2.0 N HF	−204	[1] 11¼.
3.0 N HF	−218	[1] 21.
5.0 N HF	−248	[1] 45.

[1] Values based on attacks observed for 1 minute, 30 seconds, and 10 seconds for concentrations 2 N, 3 N, and 5 N, respectively.

7. Ethanol and Acid Solutions

The voltage departures of the glass electrode that appear in nonaqueous solutions such as ethanol (C_2H_5OH) are often compared with the characteristic departures in strong acid solutions [1, 5, 19, 20, 21]. The increasing negative departure of the glass electrode in acid solutions of increasing concentration is accompanied by a repression of swelling of the glass [4]. Similar durability experiments carried out for ethanol solutions indicated that a repression of swelling with increased ehtanol concentration also accompanied the negative voltage departure. However, the latter data had not been convincing because of the difficulty of applying the interferometer procedure for durability, as the low density of the ethanol solutions prevented the floating of the oil layer. To obtain more conclusive data demonstrating that a durability shift of the glass does accompany the voltage departure in ethanol solutions, durability exposures were made in a closed system that eliminates the need for a layer of oil.

Table 5 and figure 5 give the results obtained for the repression of swelling of Corning 015 glass and the accompanying voltage departures of the glass electrode in water-ethanol solutions buffered at pH 4 with Britton-Robinson universal buffer mixtures [18]. The performance of this glass in ethanol appears to be similar to its performance in strong acid and salt solutions. This can be seen from inspection of table 5 and figures 6, 7, 8, and 9, which give similar data for sulfuric [5], formic, and acetic acids [21] and magnesium sulfate [22]. All of these have been plotted on a

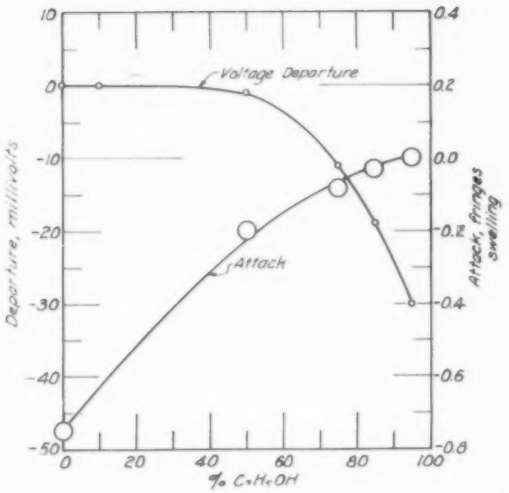

FIGURE 5.—*Comparison of the voltage departures of the glass electrode with the chemical durability of the glass (repression of swelling) in acid solutions* (pH 4) *of increased ethanol* (C_2H_5OH) *content.*

Durability exposure 48 hours at 78° C.

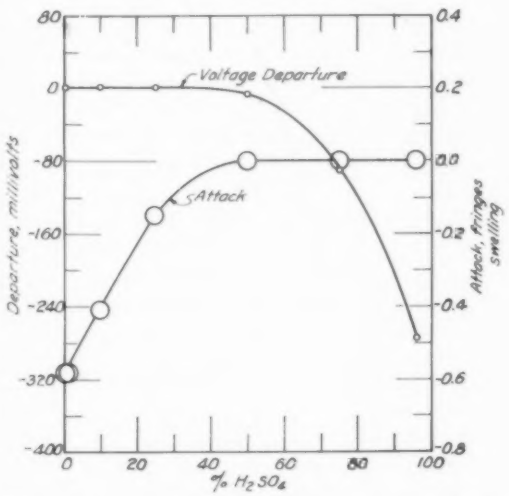

FIGURE 6.—*Comparison of the voltage departures of the glass electrode with the chemical durability of the glass (repression of swelling) in acid solutions of increased* H_2SO_4 *content.*

Durability exposure 48 hours at 80° C.

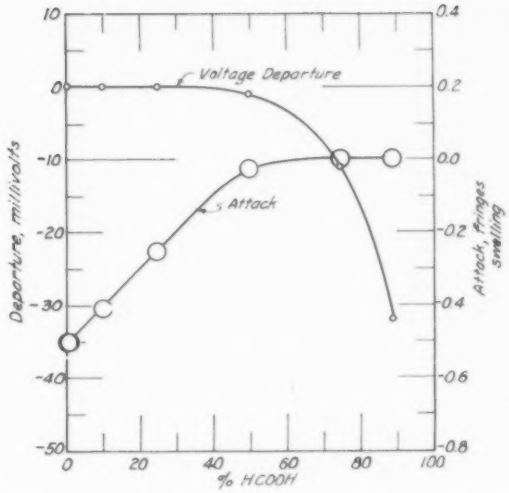

FIGURE 7.—*Comparison of the voltage departures of the glass electrode with the chemical durability of the glass (repression of swelling) in acid solutions of increased* HCOOH *content.*

Durability exposure 48 hours at 80° C.

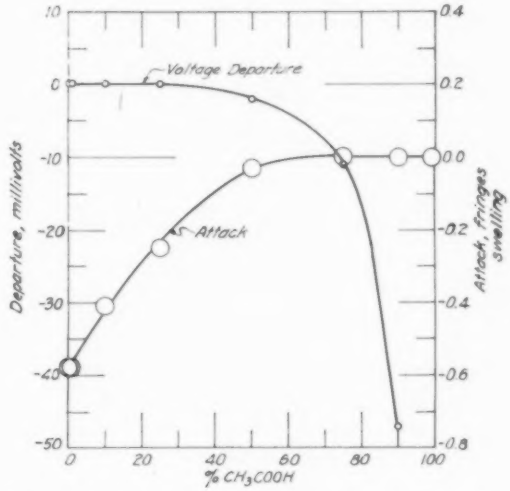

FIGURE 8.—*Comparison of the voltage departures of the glass electrode with the chemical durability of the glass (repression of swelling) in acid solutions of increased* CH_3COOH *content.*

Durability exposure 48 hours at 80° C.

percentage basis in order to make an easy intercomparison and also to avoid the confusion of thought caused by the abnormally large activities for high concentrations of strong acids [23].

TABLE 5.—*Comparison of the voltage departure of the glass electrode with the chemical durability of Corning 015 glass in solutions of* C_2H_5OH, H_2SO_4, HCOOH, CH_3COOH *and* $MgSO_4$

Solution	Departure	Attack (swelling)
	C_2H_5OH	
Percent	*mv*	*Fringes*
0 pH 4	0	¾.
10	0	
50	−1	2/10.
75	−11	<1/10.
85	−19	Detectable.
95	−30	Not detectable.
	H_2SO_4	
0.1	0	½
1.	0	½.
10.	0	<½.
25.	−1	1/10.
50.	−7	Not detectable.
75.	−91	Do.
96.	−277 drift	Do.
	HCOOH	
0.1	0	½.
1.	0	½.
10.	0	<½.
25.	0	¾.
50.	−1	Detectable.
75.	−11	Not detectable.
89.	−32	Do.
	CH_3COOH	
0.1	0	>½.
1.0	0	>½.
10.	0	<½.
25.	0	¾.
50.	−2	Detectable.
75.	−11	Not detectable.
90.	−47	Do.
99.	−159	Do.
	$MgSO_4$	
0.1	0	>½.
1.	0	>½.
10.	0	½.
[1] 27	−2	¾.
[2] 37	....	¾.

[1] Saturated at 25° C.
[2] Saturated at 80° C.

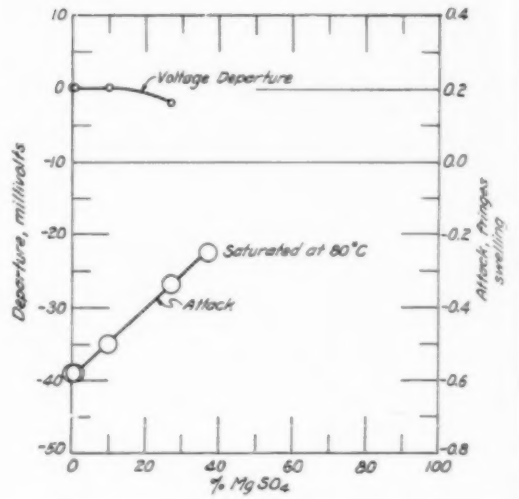

FIGURE 9.—*Comparison of the voltage departure of the glass electrode with the chemical durability of the glass (repression of swelling) in acid solutions of increased* $MgSO_4$ *content.*

Durability exposure 48 hours at 80° C

The repression of swelling by the higher concentrations of organic and inorganic acids, as well as for the magnesium sulphate [5] is readily predictable from Donnan membrane considerations and the distribution law [24]. The accompanying voltage departure can be attributed to the chemical change of the exposed glass surface [4], to a reduction of the water activity of the solution [1, 19, 20], or to a loss of electrode function because of induced decrease in water content of the glass [1, 2, 3]. Dehydration of the glass appears to be the most likely cause, as the major voltage departure is taking place over a concentration range in which no further detectable change in durability occurs.

For alkaline solutions of ethanol, the data obtained were far from satisfactory or conclusive, table 6 and [1 p. 81, 25]. Solutions of increased C_2H_5OH content, when prepared immediately before use, gave voltage departures that plotted as a straight line for 0.1 N and 0.01 N NaOH, curves A and B, figure 10. However, after the attack data, curves C and D, were obtained, the voltage-departure curves E and F for these same solutions were entirely different from curves A and B. The response of the hydrogen-glass electrode cell was sluggish, giving the impression

[5] A drop of H_2SO_4 was added to the $MgSO_4$ solutions to insure that they remain in the acid pH range.

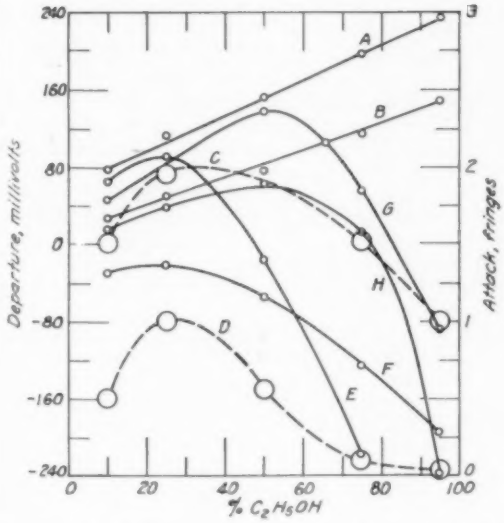

FIGURE 10.—*Comparison of the voltage departures with the chemical durability of the glass for 0.1 N and 0.01 N* NaOH *solutions of increased ethanol content.*

A, B, Voltage departure in 0.1 N and 0.01 N NaOH for freshly prepared solutions; *C, D,* chemical durability in solutions used for *A* and *B* 6 hours at 80° C; *E, F,* voltage departures in solutions *A* and *B* after the durability tests; *G, H,* voltage departures obtained for 0.1 N and 0.01 N NaOH prepared from stock solutions.

TABLE 6.—*Comparison of the voltage departure of the glass electrode with the chemical durability of Corning 015 glass in aqueous solutions of* NaOH *of various* C_2H_5OH *contents*

Solution	Voltage departure, millivolts, percent C_2H_5OH				
	10	25	50	75	95
0.1 N NaOH					
Fresh	A, +79	+113	+152	+196	+234
After 6 hr, 80° C	E, +64	+92	−16	−218	.....
Prepared from stock solution	G, +45	.....	+138	+56	−87
0.01 N NaOH					
Fresh	B, +26	+49	+77	+115	+149
After 6 hr, 80° C	F, −30	−22	−55	−125	−194
Prepared from stock solution	H, +15	+38	+61	+14	−237
	Attack, fringes				
0.1 N NaOH					
6 hr, 80° C	C, 1½	<2	.....	>1½	1
0.01 N NaOH					
6 hr, 80° C	D, ½	1	>½	1/10	[1] D

[1] Detectable.

that the hydrogen electrode was poisoned. However, checking the combination in the dilute HCl solution used to establish the zero reference potential showed that the initial voltage was duplicated to within 2 mv. This indicated that the electrodes had not been affected permanently and that some alteration had taken place in the solutions during the 6-hour period at the high temperature. Further data taken on 0.1 N and 0.01 N NaOH solutions prepared from a stock solution of NaOH in C_2H_5OH gave the departure curves G and H, respectively. The latter curves might be rationalized as compatible with the durability curves C and D, but it seems unlikely that any of the emf values are reliable. At least, it seems improbable that all of the voltage anomalies observed can be accredited to the glass electrode. However, it must be borne in mind that the glass is being vigorously attacked by some of these solutions, so that reliable performance of the glass electrode is not to be expected.

IV. Conclusions

Voltage departures in alkaline solutions of electrodes prepared from Corning 015 glass are accompanied by changes in the chemical durability of the glass. The positions in a voltage departure series occupied by different metal ions are in the same order as the attack on the electrode glass by these same ions. However, the previous suggestion that the magnitude of all voltage departures might be directly proportional to the extent of the change in attack on the electrode glass is not universally true; in fact, the data obtained show that such linear relations occur for only a limited number of conditions. Furthermore, in acid solutions of high concentration (with the exception of HF), ethanol, and also salts of high ionic strength; dehydration of the glass is probably responsible for voltage departures.

V. References

[1] Malcolm Dole, Glass electrode (John Wiley & Sons, Inc., New York, N. Y., 1941).

[2] Donald Hubbard, J. Research NBS **36**, 365 (1946) RP1706.

[3] Donald Hubbard, J. Research NBS **36**, 511 (1946) RP1719.
[4] Donald Hubbard, Edgar H. Hamilton, and Alfred N. Finn, J. Research NBS **22**, 339 (1939) RP1187.
[5] D. A. MacInnes and D. Belcher, J. Am. Chem. Soc. **53**, 3315 (1931).
[6] G. Buchbock, Z. physik. Chem. **156A**, 232 (1931).
[7] D. A. MacInnes and M. Dole, J. Am. Chem. Soc. **52**, 29 (1930).
[8] Edgar H. Hamilton and Donald Hubbard, J. Research NBS **27**, 27 (1941) RP1400.
[9] Donald Hubbard, J. Research NBS **37**, 223 (1946) RP1743.
[10] M. R. Thompson, BS J. Research **9**, 833 (1932) RP511.
[11] Walter J. Hamer and S. F. Acree, J. Research NBS **33**, 87 (1944) RP1598.
[12] H. F. Launer, J. Research NBS **22**, 553 (1939) RP1205.
[13] Donald Hubbard and Edgar H. Hamilton, J. Research NBS **27**, 143 (1941) RP1409.
[14] Malcolm Dole, J. Am. Chem. Soc. **53**, 4260 (1931).
[15] Malcolm Dole and B. Z. Wiener, Trans. Electrochem. Soc. **72**, 107 (1937).
[16] Malcolm Dole, R. M. Roberts, and C. E. Holley, Jr., J. Am. Chem. Soc. **63**, 725 (1941).
[17] S. E. Hill, J. Gen. Phys. **12**, 813 (1929).
[18] H. T. S. Britton, Hydrogen ions, 2d ed., table 57 (c), p. 225 (D. Van Nostrand and Co., Inc., New York, N. Y., 1932).
[19] Malcolm Dole, J. Am. Chem. Soc. **54**, 2120 (1932).
[20] Malcolm Dole, J. Am. Chem. Soc. **54**, 3095 (1932).
[21] J. A. Cranston and H. F. Brown, J. Roy. Tech. Coll. (Glasgow) **4**, 32 (1937).
[22] E. S. Amis and J. L. Gabbard, J. Am. Chem. Soc. **59**, 557 (1937).
[23] G. N. Lewis and M. Randall, Thermodynamics, table 4, p. 336, and table 9, p. 357 (McGraw-Hill Book Co., New York, N. Y., 1923).
[24] F. G. Donnan, Z. fur Elektrochemie **17**, 572 (1911).
[25] Norio Yui, Bul. Inst. Phys. Chem. Research (Tokyo) **19**, 1353 (1940).

WASHINGTON, August 26, 1947.

U. S. Department of Commerce
National Bureau of Standards

Research Paper RP1849
Volume 39, December 1947

Part of the Journal of Research of the National Bureau of Standards

Instability of Simply Supported Square Plate With Reinforced Circular Hole in Edge Compression

By Samuel Levy, Ruth M. Woolley, and Wilhelmina D. Kroll

A method is presented for computing the compressive buckling load of a simply supported elastic rectangular plate having a central circular hole reinforced by a circular doubler plate. Numerical results are presented for six square plates having hole diameters up to one-half of the plate length. Comparison of these results with those computed for plates without holes shows that an unreinforced circular hole causes a relatively small reduction in buckling load, and reinforcement of a circular hole by a doubler plate causes a substantial increase in buckling load.

I. Introduction

The stressed skin cover of airplane wings and fuselages has to be perforated by holes at a number of places to give access to the interior of the wing or fuselage. These holes must be reinforced to prevent weakening of the entire structure by the hole.

An ideal reinforcement would be one that confines the disturbance in the stress flow to the immediate neighborhood of the hole and which, at the same time, adds minimum weight to the structure.

Too little is known about reinforcements to approximate this ideal in practice. In the absence of a rational design procedure, it has been customary to reinforce holes by circular doubler plates riveted to one side of the sheet, thereby increasing the effective thickness and rigidity of the sheet at the edge of the hole.

The Bureau of Aeronautics, Navy Department, initiated a study of reinforcements around holes at the National Bureau of Standards to provide a better understanding of reinforcements and to indicate practical improvements in their design. The first phase of this investigation was a plane stress analysis of a doubler plate reinforcement around a circular hole in an infinite sheet under uniform compression in one direction or under shear.

The second phase of this investigation consisted of a check of the theoretical analysis by tests on plates having reinforced circular holes. It was found that the analysis gave an adequate description of the stresses and displacements provided that the doubler plate was fastened to the sheet by at least two concentric rows of rivets.

The third phase of this investigation is described in this paper. An analysis is given for the stabilizing effect of the doubler plate for square plates with central circular holes when the plates are subjected to edge compression in one direction.

II. Method of Analysis

An energy method for determining the buckling load of rectangular plates of constant thickness under compressive loads is presented by Timoshenko.[1] A review of this derivation shows that the method is also applicable to plates of variable thickness. In this case, Timoshenko's integrals I_1 and I_2 are

[1] S. Timoshenko, Theory of elastic stability pp. 307 to 326 (McGraw-Hill Book Co., New York, N. Y., 1936).

$$I_1 = \iint_{\text{surface}} D \left\{ \left(\frac{\partial^2 w}{\partial x^2} + \frac{\partial^2 w}{\partial y^2} \right)^2 - 2(1-\mu) \left[\frac{\partial^2 w}{\partial x^2} \frac{\partial^2 w}{\partial y^2} - \left(\frac{\partial^2 w}{\partial x \partial y} \right)^2 \right] \right\} dx\, dy$$

$$I_2 = \iint_{\text{surface}} h \left[\frac{\sigma_x}{S} \left(\frac{\partial w}{\partial x} \right)^2 + \frac{\sigma_y}{S} \left(\frac{\partial w}{\partial y} \right)^2 + 2 \frac{\tau_{xy}}{S} \frac{\partial w}{\partial x} \frac{\partial w}{\partial y} \right] dx\, dy \qquad (1)$$

where

h = plate thickness (function of x and y).

x, y = rectangular coordinates with origin at center of plate and x-axis in direction of load.

w = lateral deflection of plate.

$D = Eh^3/12(1-\mu^2)$, flexural rigidity of plate (function of x and y).

$\mu = 0.3$, Poisson's ratio.

σ_x = tensile stress in x direction.

σ_y = tensile stress in y direction.

τ_{xy} = shear stress.

S = tensile stress in x direction far from hole.

The stress ratios σ_x/S, σ_y/S, and τ_{xy}/S just prior to buckling may be obtained as shown by Gurney.[2] The stresses σ_r, σ_θ, and $\tau_{r\theta}$ referred to polar coordinates r, θ are given, with some change in notation, as

$$\left.\begin{aligned} \sigma_r &= S\{F + KR^2/r^2 - (A + 3CR^4/r^4 + 2DR^2/r^2)\cos 2\theta\} \\ \sigma_\theta &= S\{F - KR^2/r^2 + (A + 6Br^2/R^2 + 3CR^4/r^4)\cos 2\theta\} \\ \tau_{r\theta} &= S\{(A + 3Br^2/R^2 - 3CR^4/r^4 - DR^2/r^2)\sin 2\theta\} \end{aligned}\right\} \qquad (2)$$

where

r, θ = polar coordinates with origin at center of hole,

θ = angle between radius r to point and direction of load,

R = radius of hole.

F, K, A, B, C, D = coefficients with different values in sheet and in doubler plate.

The values of F, K, A, B, C, and D may be determined from the dimensions for a particular doubler plate by using figure 1. The coefficients from "1" region, figure 1, are used in eq 2 when computing the stresses in the unreinforced sheet; the coefficients from "2" region are correspondingly used when computing stresses in the r in- forced sheet. The abscissa in figure 1, $(T/-1)(b^2/a^2-1)$, is the ratio of the volume of material i the reinforcement to the volume of materia removed from the sheet to make the hole.

The stresses in rectangular coordinates may b computed from the stresses in polar coordinate as given in eq 2 by using the conversion formulas

$$\left.\begin{aligned} \sigma_x &= \sigma_r \cos^2\theta + \sigma_\theta \sin^2\theta - \tau_{r\theta} \sin 2\theta \\ \sigma_y &= \sigma_r \sin^2\theta + \sigma_\theta \cos^2\theta + \tau_{r\theta} \sin 2\theta \\ \tau_{xy} &= \left(\frac{\sigma_r - \sigma_\theta}{2} \right) \sin 2\theta + \tau_{r\theta} \cos 2\theta. \end{aligned}\right\} \qquad (3)$$

The lateral deflection w of a simply supported rectangular plate of length a and width b will b approximated by the first terms in the trigonometric series

$$w = a_{11} \cos \frac{\pi x}{a} \cos \frac{\pi y}{b} + a_{13} \cos \frac{\pi x}{a} \cos \frac{3\pi y}{b} + a_{31} \cos \frac{3\pi x}{a} \cos \frac{\pi y}{b} + a_{33} \cos \frac{3\pi x}{a} \cos \frac{3\pi y}{b} + \ldots \qquad (4$$

Substitution of eq 4 in eq 1 and integration (see next section for method of numerical integration) reduces integrals I_1 and I_2 to quadratic expressions in the coefficients a_{11}, a_{13} . . . . . The critical value of S at which buckling of the plate occurs is obtained from these expressions according to Timoshenko, as that value of S which reduces to zero the determinant of the coefficients of a_{11}, a_{13}, etc. in the set of simultaneous equations,

$$\left.\begin{aligned} \frac{\partial I_1}{\partial a_{11}} + S \frac{\partial I_2}{\partial a_{11}} &= 0 \\ \frac{\partial I_1}{\partial a_{13}} + S \frac{\partial I_2}{\partial a_{13}} &= 0. \\ \cdots\cdots\cdots & \\ \cdots\cdots\cdots & \end{aligned}\right\} \qquad (5)$$

The sign before S in eq 5 is plus, and that before γ in the corresponding eq 212 given by Timoshenko[4] is minus. Where S is considered positive for tensile stress, as is done in this report, the signs in eq 5 are correct.

[2] G. Gurney, Brit. Rep. Memo. No. 1834 (Feb. 1938).

[4] S. Timoshenko, Theory of elastic stability (McGraw-Hill Book Co., New York, N. Y., 1936).

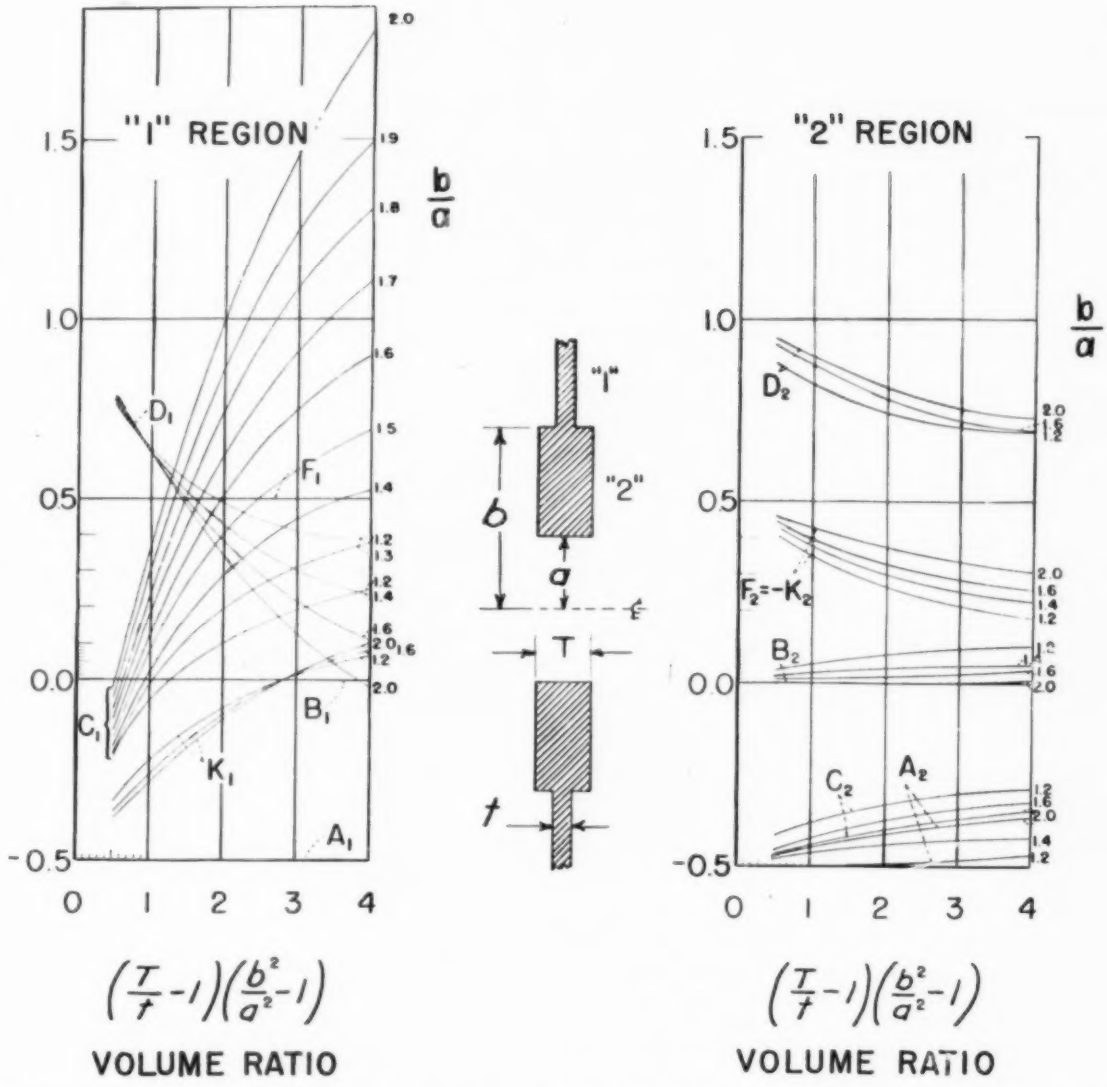

FIGURE 1.—*Values of coefficients F, K, A, B, C, and D to be used in eq 2 for computing the stress distribution in the sheet and reinforcement.*

III. Numerical Integration

The evaluation of the integrals in eq 1 over the surface of the plate is made difficult by having a circular inner and a rectangular outer boundary and by involving a stress that is a complicated function when expressed in rectangular coordinates.

The integral I_1, eq 1, was evaluated as the resultant of three integrations:

$$I_1 = I_{1a} + I_{1b} - I_{1c} \tag{6}$$

where

I_{1a} = The integral I_1 for the surface enclosed by the outer rectangular boundary of the plate taking $D = D_1$, the value of D in the unreinforced portion of the plate.

I_{1b} = The integral I_1 for the surface enclosed by the outer circular boundary of the reinforcement taking $D = D_2 - D_1$, where D_2 is the value of D in the reinforcement.

I_{1c} = The integral I_1 for the surface enclosed by the circular boundary of the hole taking $D = D_2$.

The double integration necessary to evaluate I_{1a} could in every case be done directly. However, this was not possible in evaluating I_{1b} and I_{1c}. The integrals I_{1b} and I_{1c} were obtained by integrating directly in respect to one variable and using Gauss' method of numerical integration,[4] for integration with respect to the other variable. In each case where numerical integration was used to evaluate I_1, the number of Gauss points was increased to the place where the addition of another point caused less than 1 percent change in the integral. In general, five Gauss points were enough for this purpose.

The integral I_2 was evaluated by considering the surface of the plate in three portions. The first portion, A, figure 2, was taken as the circular disk of the reinforced area; the second portion, B, figure 2, was taken as the circular disk between the outer edge of the reinforcement and the largest inscribed circle in the plate; and the third portion, C, figure 2, was taken as the remainder of the plate. The integral for each circular portion was determined, using Gauss' method of numerical integration, by first integrating numerically in a circumferential direction and then integrating numerically in a radial direction. The integral for the remainer of the plate was obtained also by using Gauss' method, first integrating numerically in the direction of the load and then at right angles to the direction of the load. Only one quadrant of the plate had to be considered because of symmetry. In each case, a sufficient number of Gauss points was used to reduce the estimated error to less than 1 percent. Twenty-three points in each quadrant were used for cases 1, 3, 4, and 5, table 1, thirty-three points for case 2, and twenty-eight points for case 6.

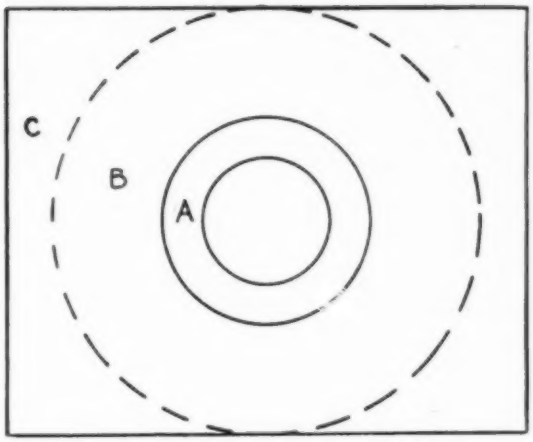

FIGURE 2.—*Subdivision of plate into three portions A, B, C, in evaluating I_2.*

TABLE 1.—*Dimensions for plates investigated*

Case	Width		Radius of hole, R	Outer radius of reinforcement	Thickness	
	Direction of load	Transverse to load			Reinforced region	Unreinforced region
1	a	a	0.125a	(1)	(1)	h
2	a	a	.0625a	(1)	(1)	h
3	a	a	.25a	(1)	(1)	h
4	a	a	.125a	0.25a	2.0h	h
5	a	a	.125a	.25a	1.5h	h
6	a	a	.125a	.1875a	3.4h	h

[1] Hole in plate not reinforced.

A typical distribution of Gauss points for computing I_2 is shown in figure 3 for one quadrant of a square plate with a central hole. For this distribution, the integral of a function F over the plate surface is

[4] E. T. Whittaker and G. Robinson, Calculus of observations, p. 159 (Blackie and Son, Ltd., London, 1944).

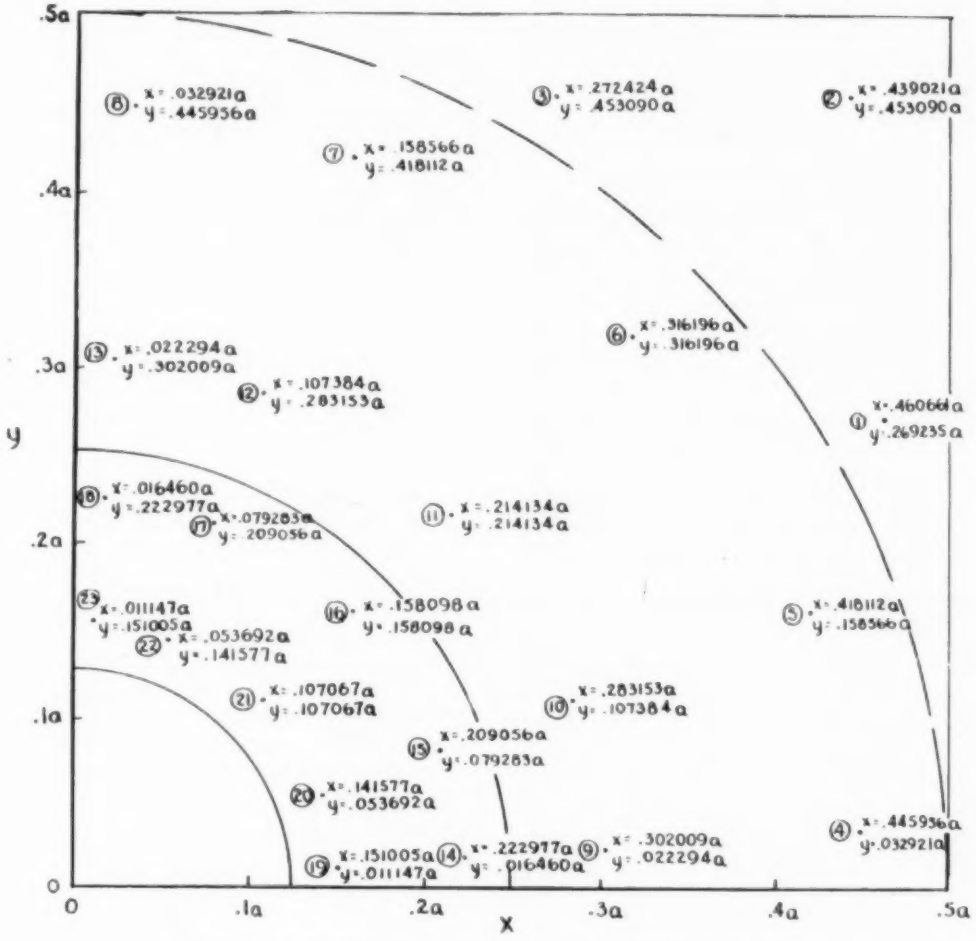

FIGURE 3.—*Distribution of Gauss points for computing I_2 in case 4.*

$$\iint_{\text{surface}} F dA = a^2[0.075316F_1 + 0.068366F_2 + 0.068366F_3 + 0.041605F_4 + 0.084048F_5 + 0.099898F_6 + 0.084048F_7 + 0.041605F_8 + 0.028176F_9 + 0.056919F_{10} + 0.067653F_{11} + 0.056919F_{12} + 0.028176F_{13} + 0.010401F_{14} + 0.021012F_{15} + 0.024975F_{16} + 0.021012F_{17} + 0.010401F_{18} + 0.007044F_{19} + 0.014230F_{20} + 0.016913F_{21} + 0.014230F_{22} + 0.007044F_{23}] \quad (7)$$

where F_1, F_2 . . . F_{23} are the values of the function F at the positions indicated in figure 3.

An approximate check on the over-all adequacy of the numerical integration methods used was obtained by determining the buckling load of a square plate with no hole both by the exact method,[5] and by numerical integration with 23 points for I_2. The results differed by only 0.7 percent. In the case of a plate with a reinforced hole, it is likley that the more complicated stress distribution and the greater prominence of higher order terms in the series used for the deflection causes the error to be somewhat higher.

IV. Convergence of Deflection Function

The correct value of S for buckling of the plate would be that value of S which reduces the determinant of the coefficients of a_{11}, a_{13}, . . . in the infinite set of eq 5 to zero. In order to limit the work of computing S to a finite amount, preliminary computations were made to see which terms in the deflection function, eq 4, were most important in determining the value of S for buckling. These computations were made for the square plate of case 4, table 1. The compressive stress $(-S)$ was $10.33\ Eh^2/a^2$ using only the first term of eq 4,

$$w = a_{11} \cos \frac{\pi x}{a} \cos \frac{\pi y}{b}$$

Using only terms 1 and 2 of eq 4,

$$w = a_{11} \cos \frac{\pi x}{a} \cos \frac{\pi y}{b} + a_{13} \cos \frac{\pi x}{a} \cos \frac{3\pi y}{b},$$

$(-S)$ was $9.43\ Eh^2/a^2$, a decrease of 8.6 percent. Using only terms 1 and 3,

$$w = a_{11} \cos \frac{\pi x}{a} \cos \frac{\pi y}{b} + a_{31} \cos \frac{3\pi x}{a} \cos \frac{\pi y}{b},$$

$(-S)$ was $8.80\ Eh^2/a^2$, a decrease of 14.7 percent. Using only terms 1 and 4,

$$w = a_{11} \cos \frac{\pi x}{a} \cos \frac{\pi y}{b} + a_{33} \cos \frac{3\pi x}{a} \cos \frac{3\pi y}{b},$$

$(-S)$ was $10.32\ Eh^2/a^2$, a decrease of 0.1 percent. Had additional terms of the trigonometric series been used with term 1, the decrease in the buckling stress would probably have been proportionately smaller. It is believed, on this basis, that the first three terms of eq 4 approximated the lateral deflection of the square plates with simply supported edges with sufficient accuracy to give the buckling stresses within 5 percent. Accordingly, only the terms

$$w = a_{11} \cos \frac{\pi x}{a} \cos \frac{\pi y}{b} + a_{13} \cos \frac{\pi x}{a} \cos \frac{3\pi y}{b} + a_{31} \cos \frac{3\pi x}{a} \cos \frac{\pi y}{b}$$

were used in the remaining computations for square plates.

V. Results

The compressive buckling load was computed for six square plates with reinforced and unreinforced holes, figure 4. The dimensions for the plates are given in table 1.

The analysis gave the compressive buckling stress $(-S)$ far from the hole corresponding to the stress distribution derived in reference [2]. Values of $(-S)$ are given in table 2. The compressive stress $(-S)$ is somewhat larger than the average stress in the direction of the load along the edge of the plate. A better value of the average buckling stress σ_{cr} along the edge of the plate was obtained from

$$\sigma_{cr} = \frac{\sigma_1 + \sigma_2}{2} \quad (8)$$

where σ_1 is the average compressive stress on the loaded edge of the plate and σ_2 the average compressive stress on the center cross section, obtained by dividing the load on that section by ah. The value of σ_1 was obtained by numerical integration and the value of σ_2 by direct integration of the stresses σ_x given by eq 3. Values of $(-S)$, σ_1, σ_2, and σ_{cr} are given in table 2. The average stresses

[5] S. Timoshenko, Theory of elastic stability, p. 331 (McGraw-Hill Book Co., New York, N. Y., 1936).

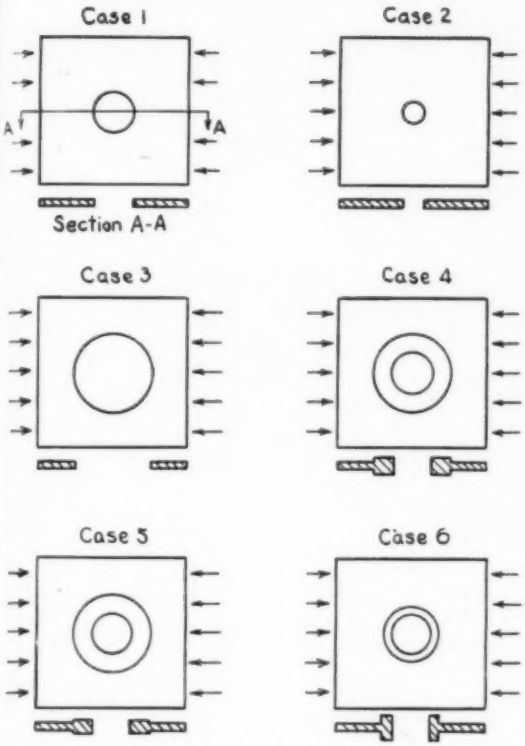

FIGURE 4.—*Loading of square plates with simply supported edges.*

Dimensions in table 1.

σ_1 and σ_2 differed from each other by less than 3 percent, indicating that the equilibrium condition is substantially satisfied.

TABLE 2.—*Critical compressive stress for plates investigated*

Case	Stress (−S) far from hole	Average stress σ_1 at $x=\frac{a}{2}, -\frac{a}{2}<y<\frac{a}{2}$	Average stress σ_2 corresponding to load at $x=0$ divided by ah	Buckling stress, σ_{cr}, average of σ_1 and σ
1	3.611 Eh^2/a^2	3.454 Eh^2/a^2	3.490 Eh^2/a^2	3.472 Eh^2/a^2
2	3.620 Eh^2/a^2	3.578 Eh^2/a^2	3.591 Eh^2/a^2	3.584 Eh^2/a^2
3	3.750 Eh^2/a^2	3.076 Eh^2/a^2	3.164 Eh^2/a^2	3.120 Eh^2/a^2
4	8.021 Eh^2/a^2	7.984 Eh^2/a^2	8.069 Eh^2/a^2	8.027 Eh^2/a^2
5	5.700 Eh^2/a^2	5.578 Eh^2/a^2	5.646 Eh^2/a^2	5.612 Eh^2/a^2
6	7.945 Eh^2/a^2	7.881 Eh^2/a^2	7.984 Eh^2/a^2	7.932 Eh^2/a^2

The buckling stress of a simply supported square plate of constant thickness without a hole is given on p. 331 of reference [3] (taking Poisson's ratio as 0.3) as

$$\sigma_{cr}=3.615\ Eh^2/a^2. \qquad (9)$$

Comparison of this value with the values computed for cases 1 to 3 of table 2 shows that unreinforced central holes, having a diameter of ⅛, ¼ and ½ of the length of a side of a square plate, reduce its buckling load by only 1, 4, and 14 percent, respectively. Comparison of the value in eq 9 with the values for cases 4 to 6 of table 2 shows that the reinforcements increased the buckling stress over that for the plate without a hole by 55 to 122 percent.

The effect of the shape of the reinforcement on the buckling load is indicated by comparing cases 4 and 6, table 2. For these cases, the hole size and volume of reinforcing material are identical but the reinforcing material is concentrated nearer the edge of the hole in case 6 (see fig. 4). The computed buckling stresses are the same within 1.2 percent.

VI. Conclusions

A numerical procedure was developed for estimating the buckling stress of simply supported rectangular plates with circular holes and doubler plate reinforcement. The procedure provides a convenient method for solving the integrals for the energy stored in the plate.

The computations showed that the buckling stress of square plates is reduced only a small amount by the presence of unreinforced holes. For the cases considered, the greatest reduction, 14 percent, corresponded to case 3, a square plate with a hole diameter 0.5 times the length of the plate.

Reinforcements of the doubler-plate type are shown by the computations to cause marked increases in the buckling stress. For case 4 with reinforcement, the computed buckling stress was 2.3 times that for case 1 with no reinforcement.

The buckling stress seems to be insensitive to change in shape of reinforcements of given volume. The computed buckling stresses were the same within 1.2 percent for cases 4 and 6, which differed in having doubler plates of different thickness and radius, but of the same volume.

The authors thank the Bureau of Aeronautics, Navy Department, for their cooperation in carrying out this investigation and for permission to publish the results.

WASHINGTON, August 19, 1947.

INDEX TO VOLUME 39

A

Page

Abradant, constant, for testing textiles, RP1807 1
Abrasion, solution of problem of producing uniform, RP1807 1
Acceptance sampling by variables, RP1827 721
Acid base reactions in benzene and other organic solvents; the behavior of bromphthalein magenta with different classes of organic bases, RP1825 221
Activity coefficients of phosphates, RP1837 411
Adsorption of nitrogen and water vapor by textile fibers, RP1842 479
Aircraft engine cylinder wear, RP1819 155
Alkylcyclohexanes, purification, purity, and freezing points, RP1833 321
Alkylbenzenes in the C_9 fraction of petroleum, RP1839 425
Alkylcyclohexanes, thermodynamic properties of, RP1845 523
Alkylcyclopentanes, purification, purity, and freezing points, RP1833 321
Alkylcyclopentanes, thermodynamic properties of, RP1845 523
Alloys, copper, thermal expansion, RP1838 419
Alpha particles, operation for counting, RP1846 545
Aluminates, in chemistry of portland cement, RP1822 177
American Petroleum Institute-National Bureau of Standards hydrocarbons, RP1833 321
American Petroleum Institute-Standard hydrocarbons, RP1833 321
Aromatic hydrocarbons, analysis, in products from catalytic petroleum refining processes, RP1830 203
Atmosphere, influence on precision of telescope pointing, RP1829 297
Austenite grain size of boron steels, RP1815 67

B

Bases, organic, relative strengths, RP1825 221
Bates, Roger G., Activity coefficients in aqueous mixtures of phosphates with sodium chloride, sodium bromide, and sodium iodide, and the pH of phosphate buffer solutions, RP1837 411
Beckett, Charles W., John E. Kilpatrick, Helene G. Werner, Kenneth S. Pitzer, Frederick D. Rossini, Heats, equilibrium constants, and free energies of formation of the alkylcyclopentanes and alkylcyclohexanes, RP1845 523
Benzene, acid-base reactions, in, RP1825 221
Bhine, R. L., John W. Rowen, Sorption of nitrogen and water vapor on textile fibers, RP1842 479
Bogue, Robert H., Some recent advances in our understanding of the chemistry of portland cement, RP1822 177
Brasses, thermal expansion, RP1838 419
Breit, G., F. L. Friedman, Calculations on countercurrent electromigration, RP1836 397
Brenner, Abner, Grace Riddell, Deposition of nickel and cobalt by chemical reactions, RP1834 385
, Polly Burkhead, Emma Seegmiller, Electrodeposition of tungsten alloys containing iron, nickel, and cobalt, RP1834 351
Bromphthalein magenta, reactions with amines, RP1825 221
Bronzes, thermal expansion, RP1838 419
Buckling, in compression, square plate with reinforced circular hole, RP1849 571
Burkhead, Polly, Abner Brenner, Emma Seegmiller, Electrodeposition of tungsten alloys containing iron, nickel, and cobalt, RP1834 351
Butadiene, determination of, RP1841 453
1,2-Butadiene, purification, purity, and freezing points, RP1833 321
Butadiene, 1,3, thermodynamic properties of, RP1844 507
2-Butyne, purfication, purity, and freezing points, RP1833 321

C

C_9 alkylbenzenes, analysis, in products from catalytic petroleum refining processes, RP1830 203
CS_2, infrared spectra, RP1814 59
Calculations on countercurrent electromigration, RP1838 419
Catalytic petroleum refining processes, analysis of C_9 alkylbenzenes, RP1830 203
Cellulose chemistry, RP1816 133
Cement compounds, RP1822 177
Charpy impact tests of boron treated steels, RP1815 67
Chemical reduction of cobalt and nickel, RP1835 385
Cheney, Ruth K., Paul F. Wacker, Specific heat, enthalpy, and entropy of uranyl fluoride, RP1832 317
Cobalt deposition without current, RP1835 385
Cobalt, freezing point of, RP1828 291
Cobalt-tungsten alloy, RP1834 351
Cold starting abilities of fuels, RP1811 39
Combustion of the C_9H_{18} alkylcyclohexanes, heats of, RP1812 49
Conjugated dienes, determination of, RP1840 435
Corruccini, Robert J., Defoe C. Ginnings, Heat capacities at high temperatures of uranium, uranium trichloride, and uranium tetrachloride, RP1831 309
Cosine-fourth-power law, validity of, RP1824 213
Cragoe, Carl S., Cyril H. Meyers, Eugene F. Mueller, Table and Mollier chart of the thermodynamic properties of 1,3-butadiene, RP1844 507
Critical compressive stress, square plate with circular reinforced hole, RP1849 571
Cryoscopic constants of hydrocarbons, RP1833 321
Current efficiency, solutions of uranyl chloride, RP1817 141
Curtiss *John H.*, Acceptance sampling by variables, with special reference to the case in which quality is measured by average or dispersion, RP1827 721
—, *Sanford B. Newman*, A statistical analysis of some mechanical properties of manila rope, RP1847 551
Cyclohexane, thermodynamic properties of, RP1845 523
Cyclohexanes, alkyl, heats of formation and isomerization, RP1821 173
Cyclohexanes, heats of combustion and isomerization of, RP1812 49
Cycloparaffin hydrocarbons, purification, purity, and freezing points, RP1833 321
Cyclopentane, thermodynamic properties of, RP1845 523

D

Dahl, Andrew I., Milton S. VanDusen, Freezing points of cobalt and nickel, RP1828 291
—, —, Resistance-temperature relation and thermoelectric properties of uranium, RP1813 53
Davis, F. J., Factors affecting operation of apparatus for counting alpha particles in an ion counting chamber, RP1846 545
Davis, Marion Maclean, Priscilla J. Schuhmann, Acid-base reactions in benzene and other organic solvents: Behavior of bromphthalein magenta with different classes or organic basis, RP1825 221
n-Decane, purification, purity and freezing points, RP1833 321
Dibeler, Vernon H., Fred L. Mohler, Analysis by the mass spectrometer of a liquefied hydrocarbon mixture containing C_3–C_5 paraffins and olefins, RP1818 149
—, *Marlin Shepherd, Richard Thomas, Shufford Schumann*, Experimental study of the Koppers-Hinckley-Podbielniak apparatus and method for the determination of conjugated dienes, RP1840 435
Digges, Thomas G., Fred M. Reinhart, Influence of boron on some properties of experimental and commercial steels, RP1815 67
Dimethylcyclohexanes, heats of formation and isomerization, RP1821 173
Dimethylcyclohexanes, thermodynamic properties of RP1845 523
Distortion of photographic objective, effect on variation of illumination of image, RP1824 213
Douglas, Florence Leach, Geraldine Walker Haupt, Chromaticities of Lovibond glasses, RP1808 11

E

Page

End-quench test of boron steels, RP1815 67
Electrode, glass, voltage anomalies of, RP1848 561
Electrodeposition of alloys, RP1834 351
Electroless deposition, cobalt and nickel, RP1835 385
Electrolysis of uranyl chloride, RP1817 141
Electromigration, calculations on countercurrent, RP1838 419
Entropies of alkylcyclopentanes and alkylcyclohexanes, RP1845 523
Equilibrium constants of formation of alkylcyclopentanes and alkylcyclohexanes, RP1845 523
Ethylbenzene, analysis, in mixtures with other C_8 alkylbenzenes, RP1830 203
Ethylcyclohexane, heats of formation and isomerization, RP1821 173
Ethylcyclopentane, thermodynamic properties of, RP1845 523
Ethylcyclohexane, thermodynamic properties of, RP1845 523
Expansion, thermal, of copper alloys, RP1838 419

F

Filter papers, analytical, standards for, RP1809 21
Forziati, A. F., Frederick D. Rossini, Alkylbenzenes in the C_9 fraction from seven representative crude petroleums, RP1839 425
Free energies of formation of alkylcyclopentanes and alkylcyclohexanes, RP1845 523
Freezing points of American Petroleum Institute-Standard and National Bureau of Standards hydrocarbons, RP1833 321
Friedman, F. L., G. Breit, Calculations on countercurrent electromigration, RP1836 397
Fuels, motor, substitute, RP1811 39

G

Gardner, Irvine C., Validity of the cosine-fourth-power law of illumination, RP1824 213
Gels, strength of, RP1810 29
Ginnings, Defoe C., Nathan S. Osborne, Measurements of heat of vaporization and heat capacity of a number of hydrocarbons, RP1841 453
—, *Robert J. Corruccini*, Heat capacities at high temperatures of uranium, uranium trichloride, and uranium tetrachloride, RP1831 309
Glass, chemical durability of, RP1848 561
Glass, electrode function of, RP1848 561
Glasses, Lovibond, RP1808 11
Grain size of magnesium castings, RP1826 265

H

Hamer, Walter J., An improved method for measurement of gel strength and data on starch gels, RP1810 29
—, Anodic current efficiency in the counterflow electrolysis of uranyl chloride solutions, RP1817 141
Haupt, Geraldine Walker, Florence Leech Douglas, Chromaticities of Lovibond glasses, RP1808 11
Heat capacity for specific heat of uranyl fluoride, RP1832 317
Heat capacity, 12 hydrocarbons, RP1841 453
Heat content for specific enthalpy of uranyl fluoride, RP1832 317
Heat of vaporization, 59 hydrocarbons, RP1841 453
Heats of formation and isomerization of alkylcyclohexanes, RP1821 173
Heats of formation of alkylcyclopentanes and alkylcyclohexanes, RP1845 523
Hidnert, Peter, Harrison S. Krider, Thermal expansion of some copper alloys, RP1838 419
Holm, Vernon C. F., Alexander I. Krynitsky, Observations on the control of grain size in magnesium casting alloys, RP1826 265
Hubbard, Donald, Gerald F. Rynders, Voltage anomalies of the glass, electrode and the chemical durability of the glass, RP1848 561
Humphreys, Curtis J., Earle K. Plyler, Infrared absorption spectrum of carbon disulfide, RP1814 59
Hunt, Charles M., John W. Rowen, Earle K. Plyler, Absorption spectra in the detection of chemical changes in cellulose and cellulose derivatives, RP1816 133
Hydrocarbons, heat capacity and heat of vaporization, RP1841 453
Hydrocarbons, purification, purity and freezing points of the American Petroleum Institute-Standard and the American Petroleum Institute-National Bureau of Standards series, RP1833 321
Hypophosphite, use of, for cobalt and nickel reduction, RP1835 385

I

Identification method for measuring wear, RP1819 155
Indicators, acid-base, for organic media, RP1825 221
Inductors, for surge current measurement, RP1823 1
Infrared absorption spectrum of CS_2, RP1814 59
Infrared spectrum of cellulose, RP1816 133
Ion counting chamber, RP1846 537
Iron-tungsten alloy, RP1834 351
Isomerization of the C_8H_{16} alkylcyclohexanes, heats of, RP1812 9
Isopropylbenzene in petroleum, RP1839 425
Isotope separation, calculations on electromigration method for, RP1838 419

J

Johnson, Walter H., Edward J. Prosen, Frederick D. Rossini, Heats of combustion and isomerization of the eight C_8H_{16} alkylcyclohexanes, RP1812 9
—, —, —, Heats of formation and isomerization of the eight C_8H_{12} alkylcyclohexanes in the liquid and gaseous states, RP1821 173

K

Kilpatrick, John E., Helene G. Werner, Charles W. Beckett, Kenneth S. Pitzer, Frederick D. Rossini, Heats, equilibrium constants, and free energies of formation of the alkylcyclopentanes and alkylcyclohexanes, RP1845 523
Koppers-Hinckley method for determination of conjugated dienes, RP1840 481
Kroll, Wilhelmina D., Samuel Levy, Ruth M. Woolley, Instability of simply supported square plate with reinforced circular hold in edge compression, RP1849 577
Krider, Harrison S., Peter Hidnert, Thermal expansion of some copper alloys, RP1838 419
Krynitsky, Alexander I., Vernon C. F. Holm, Observations on the control of grain size in magnesium casting alloys, RP1826 265

L

Levy, Samuel, Ruth M. Woolley, Wilhelmina D. Kroll, Instability of simply supported square plate with reinforced circular hole in edge compression, RP1849 577
Liquefied hydrocarbon mixture containing C_3–H_3 paraffins and olefins, RP1818 147
Lovibond color system, and glasses, RP1808 11

M

Magnesium alloy castings, RP1826 265
Magnification, effect on precision of indoor telescope pointing, RP1820 181
Manila rope, statistical analysis of some mechanical properties, RP1847 557
Mass spectrometer, analysis of, RP1818 147
McKee, Samuel A., An indentation method for measuring wear, RP1819 155
McQuaid-Ehn grain size of boron steels, RP1815 67
Metal powders, sieve tests of, RP1843 489
1-Methyl-2-ethylbenzene in petroleum, RP1839 425
Methylcyclohexane, thermodynamic properties of, RP1845 523
Meyers, Cyril H., Carl S. Cragoe, Eugene F. Mueller, Table and Mollier chart of the thermodynamic properties of 1,3-butadiene, RP1844 505
Mohler, Fred L., Vernon H. Dibeler, Analysis by the mass spectrometer of a liquified hydrocarbon mixture containing C_3–C_5 paraffins and olefins, RP1818 147
Mollier chart and table for 1,3-butadiene, RP1844 505
Monoolefins, purification, purity, and freezing points, RP1833 321
Mueller, Eugene F., Cyril H. Meyers, Carl S. Cragoe, Table and Mollier chart of the thermodynamic properties of 1,3-butadiene, RP1844 505
Murphy, Evelyn T., Anton J. Streiff, Janice C. Zimmerman, Laurel F. Soule, Vincent A. Sedlak, Charles B. Willingham, Frederick D. Rossini, Purification, purity, and freezing points of *n*-decane, 4 alkylcyclopentanes, 8 alkylcyclohexanes, 2 monoolefins, 1,2-butadiene and 2-butyne of the American Petroleum Institute-Standard and American Petroleum Institute-National Bureau of Standards series, RP1833 321

N

Newman, Sanford B., J. H. Curtiss, A statistical analysis of some mechanical properties of manila rope, RP1847 557
Nickel deposition without current, RP1835 385
Nickel, freezing point of, RP1828 281
Nickel-tungsten alloy, RP1834 351

O

Osborne, Nathan S., Defoe C. Ginnings, Measurements of heat of vaporization and heat capacity of a number of hydrocarbons, RP1841 453

P

Page

Papers, filter, analytical, standards for, RP1809 ... 21
Park, John H., Shunts and inductors for surge current measurements, RP1823 ... 191
Particle size distribution of metal powders, RP1843 ... 487
Petroleum, alkylbenzenes in C_9 fraction, RP1839 ... 425
pH of phosphate buffer solutions, RP1837 ... 411
Phosphate buffer solutions, pH and activity coefficients of, RP1837 ... 411
Photographic objective, variation of illumination of image formed by, RP1824 ... 213
Pitzer, Kenneth S., John E. Kilpatrick, Helene G. Werner, Charles W. Beckett, Frederick D. Rossini, Heats, equilibrium constants, and free energies of formation of the alkylcyclopentanes and alkylcyclohexanes, RP1845 ... 523
Planck's constant C_5, RP1828 ... 291
Plyler, Earle K., Curtiss J. Humphreys, Infrared absorption spectrum of carbon disulfide, RP1814 ... 59
—, *John W. Rowen, Charles M. Hunt*, Absorption spectra in the detection of chemical changes in cellulose and cellulose derivatives, RP1816 ... 133
Pollard, Rolla E., Sieve tests of metal powders, RP1843 ... 487
Portland cement, recent advances in chemistry of, RP1822 ... 177
Precision of indoor telescope pointing, the effect of magnification on, RP1820 ... 163
Precision of telescope pointing, influence of atmosphere upon, RP1829 ... 297
n-Propylbenzene in petroleum, RP1839 ... 425
n-Propylcyclohexane, thermodynamic properties of, RP1845 ... 523
n-Propylcyclopentane, thermodynamic properties of, RP1845 ... 523
Prosen, Edward J., Walter H. Johnson, Frederick D. Rossini, Heats of combustion and isomerization of the eight C_8H_{16} alkylcyclohexanes, RP1812 ... 173
—, —, —, Heats of formation and isomerization of the eight C_8H_{12} alkylcyclohexanes in the liquid and gaseous states, RP1821 ... 173
Purification of the American Petroleum Institute-Standard and the American Petroleum Institute-National Bureau of Standards hydrocarbons, RP1833 ... 321

Q

Quality control, acceptance sampling, RP1827 ... 721

R

Refinement of grain in magnesium casting alloys, RP1826 ... 265
Reinforced circular hole, critical compressive stress of plate with, RP1849 ... 571
Reinhart, Fred M., Thomas G. Digges, Influence of boron on some properties of experimental and commercial steels, RP1815 ... 67
Reproducibility of sieve tests, RP1843 ... 487
Resistance-temperature relation of uranium, RP1813 ... 53
Riddell, Grace, Abner Brenner, Deposition of nickel and cobalt by chemical reduction, RP1835 ... 385
Rope, manila, some mechanical properties, RP1847 ... 551
Rossini, Frederick D., Anton J. Streiff, Alkylbenzenes in the C_9 fraction from five different catalytic petroleum refining processes, RP1830 ... 203
—, —, *Evelyn T. Murphy, Janice C. Zimmerman, Laurel F. Soule, Vincent A. Sedlak, Charles P. Willingham*, Purification, purity, and freezing points of *n*-decane, 4 alkylcyclopentanes, 8 alkylcyclohexanes, 2 monoolefins, 1,2-butadiene, and 2-butyne of the American Petroleum Institute-Standard and American Petroleum Institute-National Bureau of Standards series, RP1833 ... 321
—, *Edward J. Prosen, Walter H. Johnson*, Heats of formation and isomerization of the eight C_8H_{12} alkylcyclohexanes in the liquid and gaseous states, RP1821 ... 173
—, *A. F. Forziati*, Alkylbenzenes in the C_9 fraction from seven representative crude petroleums, RP1839 ... 419
—, *John E. Kilpatrick, Helene G. Werner, Charles W. Beckett, Kenneth S. Pitzer*, Heats, equilibrium constants, and free energies of formation of the alkylcyclopentanes and alkylcyclohexanes, RP1845 ... 523
—, *Walter H. Johnson, Edward J. Prosen*, Heats of combustion and isomerization of the eight C_8H_{16} alkylcyclohexanes, RP1812 ... 49
Rowen, John W., Charles M. Hunt, Earle K. Plyler, Absorption spectra in the detection of chemical changes in cellulose and cellulose derivatives, RP1816 ... 133
—, *R. L. Plaine*, Sorption of nitrogen and water vapor on textile fibers, RP1842 ... 479
Rynders, Gerald F., Donald Hubbard, Voltage anomalies of the glass electrode and the chemical durability of the glass, RP1848 ... 561

S

Schiefer, Herbert F., Solution of problem of producing uniform abrasion and its application to the testing of textiles, RP1807 ... 1
Schuhmann, Priscilla J., Marion Maclean Davis, Acid-base reactions in benzene and other orgsaic solvents. Behavior of bromphthalein magenta with different classes of organic basis, RP1825 ... 221
Schuhmann, Shuford, Martin Shepherd, Richard Thomas, Vernon H. Dibeler, Experimental study of the Koppers-Hinckley-Podbielniak apparatus and method for the determination of conjugated dienes, RP1840 ... 435
Scott, Leo W., Francis E. Washer, Influence of the atmosphere upon the precision of telescope pointing, RP1829 ... 297
Scribner, Pourdon W., William K. Wilson, Development of standards for analytical filter papers, RP1809 ... 21
Sedlak, Vincent A., Anton J. Streiff, Evelyn T. Murphy, Janice C. Zimmerman, Charles P. Willingham, Frederick D. Rossini, Purification, purity, and freezing points of *n*-decane, 4 alkylcyclopentanes, 8 alkylcyclohexanes, 2 monoolefins, 1,2-butadiene, and 2-butyne of the American Petroleum Institute-Standard and American Petroleum Institute-National Bureau of Standards series, RP1833 ... 321
Seegmiller, Emma, Abner Brenner, Polly Purkhead, Electrodeposition of tungsten alloys containing iron, nickel, and cobalt, RP1834 ... 351
Shepherd, Martin, Richard Thomas, Shuford Schuhmann, Vernon H. Dibeler, Experimental study of the Koppers-Hinckley-Podbielniak apparatus and method for the determination of conjugated dienes, RP1840 ... 435
Sieve tests of metal powders, RP1843 ... 487
Silicates, in chemistry of portland cement, RP1822 ... 177
Shunts, for surge current measurement, RP1823 ... 191
Silver-silver bromide chloride and iodide electrodes, use in phosphate-chloride mixtures, RP1837 ... 411
Soule, Laurel F., Anton J. Streiff, Evelyn T. Murphy, Janice C. Zimmerman, Vincent A. Sedlak, Charles P. Willingham, Frederick D. Rossini, Purification, purity, and freezing points of *n*-decane, 4 alkylcyclopentanes, 8 alkylcyclohexanes, 2 monoolefins, 1,2-butadiene, and 2-butyne of the American Petroleum Institute-Standard and American Petroleum Institute-National Bureau of Standards series, RP1833 ... 321
Spectra, infrared CS_2, RP1814 ... 59
Spectrophotometric studies of acid-base reactions in organic solvents, RP1825 ... 221
Standards for analytical filter papers, RP1809 ... 21
Starch, strength of gels, RP1810 ... 29
Starting and warm-up with ethyl alcohol blends at sea level and altitude, RP1811 ... 39
Statistical sampling plans, RP1827 ... 721
Streets, Ronald E., Cold-starting abilities of various substitute motor fuels, RP1811 ... 39
Streiff, Anton J., Evelyn T. Murphy, Janice C. Zimmerman, Laurel F. Soule, Vincent A. Sedlak, Charles P. Willingham, Frederick D. Rossini, Purification, purity, and freezing points of *n*-decane, 4 alkylcyclopentanes, 8 alkylcyclohexanes, 2 monoolefins, 1, 2-butadiene, and 2-butyne of the American Petroleum Institute-Standard and American Petroleum Institute-National Bureau of Standards series, RP1833 ... 321
—, *Frederick D. Rossini*, Alkylbenzenes in the C_9 fraction from five different catalytic petroleum refining processes, RP1830 ... 203
Substitute motor fuels, RP1811 ... 39

T

Telescope, effect of magnification on the precision of indoor pointing, RP1820 ... 163
Telescope, influence of atmosphere upon precision pointing, RP1829 ... 297
Textiles, solution of problem of producing uniform abrasion, RP1807 ... 1
Textiles, sorption of nitrogen and water vapor, RP1842 ... 479

Page

Thermochemistry of alkylcyclohexanes, RP1821 173
Thermodynamic properties of 1,3-butadiene, RP1843 487
Thomas, Richard, Martin Shepherd, Shuford Schuhmann, Vernon H. Dibeler, Experimental study of the Koppers-Hinckley-Podbielniak apparatus and method for the determination of conjugated dienes, RP1840 435
1,2,4-Trimethylbenzene in petroleum, RP1839 425
1,3,5-Trimethylbenzene in petroleum, RP1839 425
Tungsten alloys, RP1834 351

U

Ultraviolet spectrum of cellulose, RP1816 133
Uranium chloride, electrolysis of, RP1817 141
Uranium, heat capacity, RP1831 309
Uranium, resistance-temperature relation of, RP1813 53
Uranium tetrachloride, heat capacity, RP1831 309
Uranium, thermoelectric properties of, RP1813 53
Uranium trichloride, heat capacity, RP1831 309
Uranium, transformation temperatures of, RP1813 53
Uranyl fluoride, RP1832 317

V

VanDusen, Milton S., Andrew I. Dahl, Freezing points of cobalt and nickel, RP1828 291
—, —, Resistance-temperature relation and thermoelectric properties of uranium, RP1813 53
Variables, acceptance sampling by, RP1827 721

W

Wacker, Paul F., Ruth K. Cheney, Specific heat, enthalpy, and entropy of uranyl fluoride, RP1832 317
Washer, Francis E., Effect of magnification on the precision of indoor telescope pointing, RP1820 163
—, *Leo W. Scott*, Influence of the atmosphere upon the precision of telescope pointing, RP1829 20
Wear measurements of engine cylinders, RP1819 1
Werner, Helene G., John E. Kilpatrick, Charles W. Beckett, Kenneth S. Pitzer, Frederick D. Rossini, Heats, equilibrium constants, and free energies of formation of the alkylcyclopentanes and alkylcyclohexanes, RP1845 5
Wide-angle photographic objective, negative distortion corresponding to even illumination of field, RP1824 2
Willingham, Charles B., Anton J. Streiff, Evelyn T. Murphy, Janice C. Zimmerman, Laurel F. Soule, Vincent A. Sedlak, Frederick D. Rossini, Purification, purity, and freezing points of *n*-decane, 4 alkylcyclopentanes, 8 alkylcyclohexanes, 2 monoolefins, 1,2-butadiene, and 2-butyne of the American Petroleum Institute-Standard and American Petroleum Institute-National Bureau of Standards series, RP1833 2
Wilson, William K., Hourdon W. Scribner, Development of standards for analytical filter papers, RP1809 2
Woolley, Ruth M., Samuel Levy, Wilhelmina D. Kroll, Instability of simply supported square plate with reinforced circular hole in edge compression, RP1849 57

X

m-Xylene, analysis, in mixtures with other C_8 alkylbenzenes, RP1830 2
o-Xylene, analysis, in mixtures with other C_8 alkylbenzenes, RP1830 2
p-Xylene, analysis, in mixtures with other C_8 alkylbenzenes, RP1830 2

Z

Zimmerman, Janice C., Anton J. Streiff, Evelyn T. Murphy, Laurel F. Soule, Vincent A. Sedlak, Charles B. Willingham, Frederick D. Rossini, Purification, purity, and freezing points of *n*-decane, 4 alkylcyclopentanes, 8 alkylcyclohexanes, 2 monoolefins, 1,2-butadiene, and 2-butyne of the American Petroleum Institute-Standard and American Petroleum Institute-National Bureau of Standards series, RP1833 3

Engineering Library

Journal of Research

of the

National Bureau of Standards

DECEMBER 1947

VOLUME 39 NUMBER 6

PERIODICALS OF THE NATIONAL BUREAU OF STANDARDS

Journal of Research

The National Bureau of Standards is the principal agency of the Federal Government for fundamental research in physics, chemistry, and engineering. It has the custody of the national standards of physical measurement in terms of which all working standards in research laboratories and industry are calibrated, and carries on necessary research leading to improvement in such standards and methods of measurement. It also has a general responsibility for basic research in physics, chemistry, and engineering, and for development of improved methods for testing materials and equipment. It determines physical constants and properties of materials, tests and calibrates standard measuring apparatus and reference standards, and studies technical processes. The results of the Bureau's research and investigations are published in the JOURNAL OF RESEARCH.

Research Papers

Reprints of individual articles appearing in the JOURNAL OF RESEARCH. They are made available to serve the needs of research workers, technical groups, and others for the separate papers relating to the special subjects in which they are interested.

Technical News Bulletin

Contains short but complete summaries of research, development, and testing in progress at the Bureau, accounts of the Bureau's national and international activities, scientific and technical announcements of new plans and programs, and a list of publications by members of the staff. It is a prompt and reliable source of official information of value to those who desire to keep in touch with the general activities of the Bureau.

Basic Radio Propagation Predictions

The CRPL series D, Basic Radio Propagation Predictions, is issued as a monthly publication for those concerned with radio communication in determining the best sky-wave frequencies over any path at any time of day for average conditions for the month of prediction, which is made 3 months in advance. Charts of extraordinary-wave critical frequency for the F2 layer, of maximum usable frequency for a transmission distance of 4,000 km, and of percentage of time occurrence for transmission by sporadic E in excess of 15 Mc, for a distance of 2,000 km, are included.

ANNUAL SUBSCRIPTION Send order, with remittance, to Superintendent of Documents, U. S. Government Printing Office, Washington 25, D. C.	United States, Canada, Cuba, Mexico, Newfoundland, Republic of Panama	Other countries
JOURNAL OF RESEARCH of the National Bureau of Standards:		
12 monthly issues (2 volumes), paper covers	$4.50	$5.50
Bound volume (½ year, 1 volume), blue buckram	3.00	3.50
RESEARCH PAPERS	(*)	(*)
TECHNICAL NEWS BULLETIN, 12 monthly issues	1.00	1.38
BASIC RADIO PROPAGATION PREDICTIONS, 12 monthly issues	1.00	1.25

*The prices of the separate Research Papers appearing in this JOURNAL are given in the Contents. A 100 or more copies of any separate are ordered, a discount of 25 percent is allowed. Those who desire copies of separate Research Papers should send their orders and remittances without delay to the Superintendent of Documents, U. S. Government Printing Office, Washington 25, D. C. This will aid him to determine the number of copies to be printed for sale. Research Papers are not printed from electrotypes and usually no more reprints can be had when the first and only printing is exhausted.

Published with approval of Bureau of the Budget